Plasmid-mediated β-lactam resistance in *Neisseria gonorrhoeae*

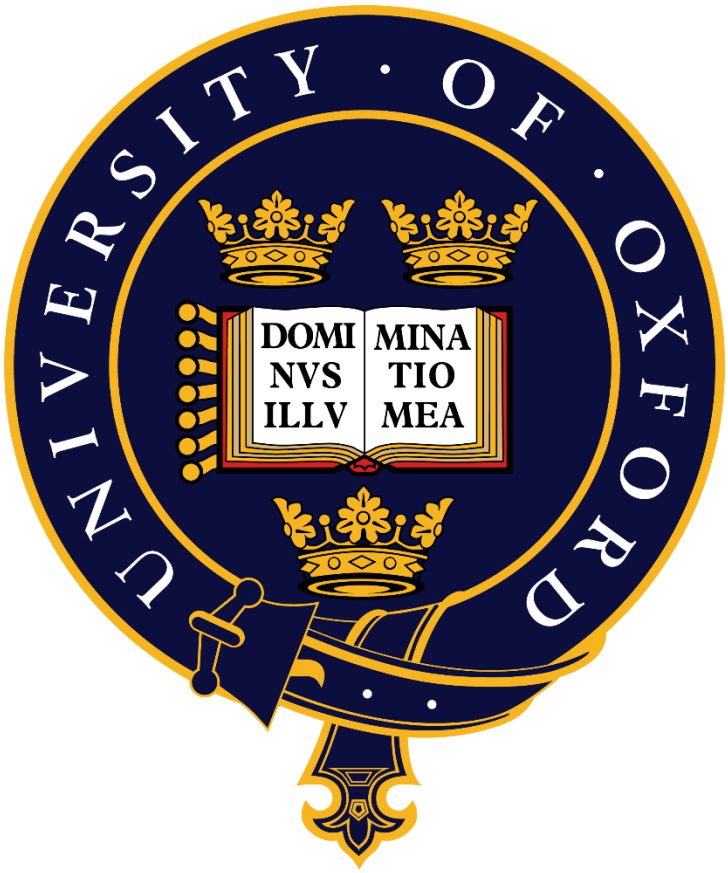

Tabea Anna Elsener

Sir William Dunn School of Pathology

Jesus College

University of Oxford

A thesis submitted for the degree of

Doctor of Philosophy

Trinity Term 2025

Plasmid-mediated β-lactam resistance in *Neisseria gonorrhoeae*

Tabea Anna Elsener, DPhil in Molecular Cell Biology in Health and Disease, Trinity Term 2025, Jesus College

Abstract

Plasmids are diverse extrachromosomal elements that play a pivotal role in the rapid dissemination of antimicrobial resistance (AMR). While broad host range plasmids have been extensively studied, host-restricted plasmids remain underexplored, despite their significant impact on treatment options of clinically relevant bacteria. This thesis investigates plasmid-mediated resistance in the sexually transmitted infection (STI) pathogen *Neisseria gonorrhoeae* (the gonococcus), a leading cause of pelvic inflammatory disease, infertility and ectopic pregnancy, and a WHO priority pathogen due to escalating resistance to all previously recommended antibiotics. Two narrow host range resistance plasmids are found in the gonococcus: the conjugative plasmid pConj and the β-lactamase plasmid p*bla*, conferring resistance to tetracycline and penicillin antibiotics, respectively. With the p*bla*-encoded β-lactamase only differing in a few amino acids from extended spectrum β-lactamases and current treatment relying on third-generation cephalosporins, and the recent implementation of doxycycline (a tetracycline antibiotic) post-exposure prophylaxis (Doxy-PEP), understanding plasmid-mediated resistance in *N. gonorrhoeae* is of urgent public health importance.

This thesis focuses on three aspects of plasmid-mediated resistance in *N. gonorrhoeae*: i) the evolution and epidemiology of p*bla* in gonococci; ii) the molecular characteristics of p*bla* variants, including resistance, fitness costs and mobility; and iii) the influence of restriction-modification systems (RMSs) on plasmid transfer, using a combination of bioinformatic and molecular genetics

approaches. Phylogenetic and comparative analyses suggest that p*bla* originated from *Haemophilus ducreyi*, another cause of STI, and has adapted to the gonococcus through gene loss and changes in the bla_{TEM} resistance determinant. Development and implementation of a p*bla* typing scheme revealed that there are three major variants in gonococci, which show distinct global distributions and are associated with specific lineages. Functional assays demonstrated these p*bla* variants differ in their resistance, fitness costs and mobilisation potential, with interactions with pConj driving the transfer of p*bla*. Furthermore, characterisation of gonococcal RMS indicated minimal impact on plasmid dissemination within the *N. gonorrhoeae* population.

Together, this thesis enhances understanding of plasmid-mediated β-lactam resistance in *N. gonorrhoeae*, with implications for surveillance, treatment, and prevention strategies, including the deployment of Doxy-PEP. Furthermore, my work underscores the value of integrating computational and experimental approaches to uncover novel insights into plasmid biology and the evolution and spread of AMR.

Acknowledgements

I would like to express my deepest gratitude to my supervisors - **Prof. Chris Tang**, **Prof. Martin Maiden** and **Dr Ana Cehovin** - for their support and guidance throughout my DPhil journey.

To **Chris** - thank you for always having an open door to discuss yet another idea I had, and for consistently identifying areas where I could improve, while never forgetting to acknowledge progress made. I'm especially grateful for all the time you invested not only in my science but also in shaping me as a person and scientist.

To **Martin** - thank you for your wisdom and encouragement, and for offering perspective on both my science and career.

To **Ana** - thank you for teaching me how not to kill *N. gonorrhoeae* and making me fall in love with gonococcal plasmids in the first place. I am deeply grateful for your honest advice, emotional support, and for inspiring me to aim higher.

I am also grateful to **Dr Wearn-Xin Yee** for her help with all things plasmid-related, and to **Dr Rebekah Jones** for patiently teaching me Western blots and helping troubleshoot my many failed cloning attempts and colony PCRs.

A heartfelt thank you to **Dr Samantha McKeand**, for generously giving me access to her strain collection, which not only completed my collection of p*bla* variants but was also integral to exploring the relationship between p*bla* and its bacterial host.

To all the **members of the Tang lab**—thank you for your collegiality, shared laughter, and post-lab runs. Special thanks to **Dr Kacper Kurzyp**, for coming in on a weekend to save my experiment when I got knocked out by the flu and for keeping me company during the early hours in the lab, and to

Dr Rene Baerentsen, for his help with characterising NEIS2964 and reminding me of that elusive concept called 'work-life balance'.

To **Dr Anastasia Unitt** - thank you for the many hours spent discussing *Neisseria* genomics and for a truly memorable conference in Boston.

I am grateful to **Dr Odile Harrison** and **Dr Keith Jolley** for their help with PubMLST; to **Prof. Stanley Spinola** and **Kate Fortney** for a fruitful collaboration on plasmid-mediated β-lactam resistance in *H. ducreyi;* and to **Dr Sam Palmer** and **Dr Aden Forrow** for their contributions to the project on the impact of RMSs on the spread of plasmids in *N. gonorrhoeae*.

I would like to acknowledge my examiners throughout the different stages of my DPhil - **Prof. Craig McLean** and **Prof. Samuel Sheppard** (Transfer of Status), **Prof. Syma Khalid** and **Prof. Daniel Wilson** (Confirmation of Status), and **Dr James Hall** and **Prof. Craig McLean** (*Viva Voce*) - for their time, feedback, and thoughtful engagement with my work.

This work would not have been possible without the generous support of the **Oxford Hoffman Scholarship** and the **Sir William Dunn School of Pathology**.

To **my family** – thank you for trusting me to find my path and for always having my back.

And finally, to **Dr Laura de Nies** - for the many rounds around Uni Parks discussing experiments and plans, for celebrating achievements together, and supporting me with all my decisions - even if it meant walking through the desert with me.

Table of Contents

List of Figures

List of Tables

Abbreviations

2-DOG	2-deoxy-galactose
AMR	Antimicrobial resistance
ANOVA	Analysis of variance
APBS	Adaptive Poisson-Boltzmann Solver
BLAST	Basic Local Alignment Search Tool
bp	Base pair
carb	Carbenicillin
CFU	Colony forming unit
cgMLST	Core genome multi-locus sequence typing
ddPCR	Digital droplet PCR
DNA	Deoxyribonucleic acid
dsDNA	Double-stranded DNA
DTR	DNA transfer and replication region
DUS	DNA uptake sequence
EDTA	Ethylenediaminetetraacetic acid
ery	Erythromycin
ESBL	Extended-spectrum β-lactamase
FB	Fastidious broth
FlaGs	Flanking genes analysis
GCB	Gonococcal base agar
GCBL	Liquid gonococcal media (GCB without agar)
GGI	Gonococcal Genetic Island
HGT	Horizontal gene transfer
HIC	High-income country
HIV	Human immunodeficiency virus
HsdM	Type I RMS methyltransferase subunit
HsdR	Type I RMS restriction endonuclease subunit
HsdS	Type I RMS specificity subunit

ICE	Integrative conjugative element
Inc	Plasmid incompatibility group
IS	Insertion sequence
kan	Kanamycin
kb	Kilobase
L.O.D.	Limit of detection
LB	Luria Bertani media
LIN code	Life Identification Number codes
LMIC	Low and middle-income country
LOS	Lipooligosaccharide
mb	Megabase
MEase	Methyltransferase
MGE	Mobile genetic element
MIC	Minimum inhibitory concentration
Mod	Type III RMS methyltransferase subunit
MPF	Mating pair formation region
MSM	Men who have sex with men
NCBI	National Center for Biotechnology Information
Ng_cp	*N. gonorrhoeae* pConj core gene plasmid typing scheme
NmUC	*N. meningitidis* urogenital clade
OD_{600}	Optical density measured at absorbance of 600 nm
Opa	Opacity protein
OR	Odds ratio
ORF	Open reading frame
ori	Origin of replication
oriT	Origin of transfer
p*bla*	Gonococcal β-lactamase plasmid
PCR	Polymerase chain reaction
PBP	Penicillin-binding protein
PBS	Phosphate-buffered saline
pConj	Gonococcal conjugative plasmid

PCR	Polymerase chain reaction
pCryp	Cryptic plasmid in *N. gonorrhoeae*
PDB	Protein data bank
r.p.m.	Revolutions per minute
RAF	Relaxase-accessory factor
REase	Restriction endonuclease
Rep	Plasmid replication initiation protein
Res	Type III RMS restriction endonuclease subunit
rMLST	Ribosomal multilocus sequence type
RMS	Restriction modification system
RNA	Ribonucleic acid
RT-ddPCR	Reverse transcriptase digital droplet PCR
SD	Standard deviation
SDS-PAGE	Sodium dodecyl sulfate–polyacrylamide gel electrophoresis
spp.	Species
ssDNA	Single-stranded DNA
STI	Sexually transmitted infection
T4CP	Type IV secretion system coupling protein
T4P	Type IV pili
T4SS	Type IV secretion system
TA	Toxin-antitoxin
TAE	Tris acetate EDTA buffer
tet	Tetracycline
Tn	Transposon
WGS	Whole genome sequences
WHO	World Health Organization
WT	Wild type

1 Introduction

1.1 Plasmids are important vehicles for the spread of antimicrobial resistance

The global rise of antimicrobial resistance (AMR) is a major threat to modern medicine, undermining our ability to treat bacterial infection and jeopardising a wide range of medical advances and food production. Without effective antibiotics, medical procedures such as complex surgery, caesarean sections and cancer chemotherapy carry an increased risk of severe, potentially fatal infection. AMR also impacts food security by diminishing livestock productivity[15]. Alarmingly, recent projections estimate a 67.5% increase in annual deaths directly attributed to bacterial AMR - from 1.14 million in 2021 to 1.91 million in 2050 - as well as a 74.5% rise in AMR-associated deaths from 4.71 million in 2021 to 8.22 million in 2050[16].

Plasmids are a major driver of AMR due to their ability to rapidly disseminate resistance genes by horizontal gene transfer (HGT)[17]. Plasmids are self-replicating, usually double-stranded circular DNA molecules, although linear plasmids exist[18], that can vary from under 1 kb to over 1 mb in size[7]. The boundary between plasmids and other mobile genetic elements (MGEs) is not always clear. Hybrid forms such as phage-plasmids combine features of plasmids and bacteriophages, enabling them to transfer horizontally as phages, while also being transmitted vertically like plasmids[7,19-21]. Integrative conjugative elements (ICEs) are a class of MGEs that integrate into the host chromosome after conjugative transfer but retain the ability to excise and transfer themselves by conjugation[22].

Unlike the gradual process of adaptation through *de novo* mutations, plasmid-mediated HGT enables rapid acquisition of traits and allows bacteria to respond quickly to selection pressures

imposed by antibiotics. This accelerates microbial evolution, bypassing the need to evolve resistance independently, and allows for the rapid spread of resistance determinants across populations and environments[17,23].

1.1.1 Mechanisms of plasmid transfer

Different modes of transfer allow plasmid dissemination within and across bacterial populations. Conjugation, mobilisation, transduction and transformation all contribute to the HGT of plasmids, and understanding of these processes is essential to anticipate future trends in AMR.

1.1.1.1 Conjugation

Conjugative plasmids encode all the protein factors needed to transfer themselves from a donor to a recipient bacterium. Two genetic modules are central to conjugation: the mating pair formation (MPF) and the DNA transfer and replication (DTR) regions (Figure 1).

The MPF region of Gram-negative bacteria encodes the structural components of a Type IV Secretion System (T4SS), a macromolecular complex spanning both membranes of the bacterial cell wall, which mediates DNA transfer. The T4SS consists of a membrane-embedded secretion channel and an extracellular pilus apparatus, which is involved in establishing contact between donor and recipient cells[24,25].

The DTR encodes the proteins necessary to initiate DNA transfer and includes an origin of transfer (*oriT*), where DNA transfer is initiated. The DTR-encoded relaxase commences plasmid transfer by interacting with inverted repeats within the *oriT* and catalysing a site-specific cleavage at the *nic* site, creating a single-stranded DNA (ssDNA) intermediate[26-30]. The relaxase remains covalently attached to the 5' end of the cleaved strand, forming a nucleoprotein complex referred to as the relaxosome[26].

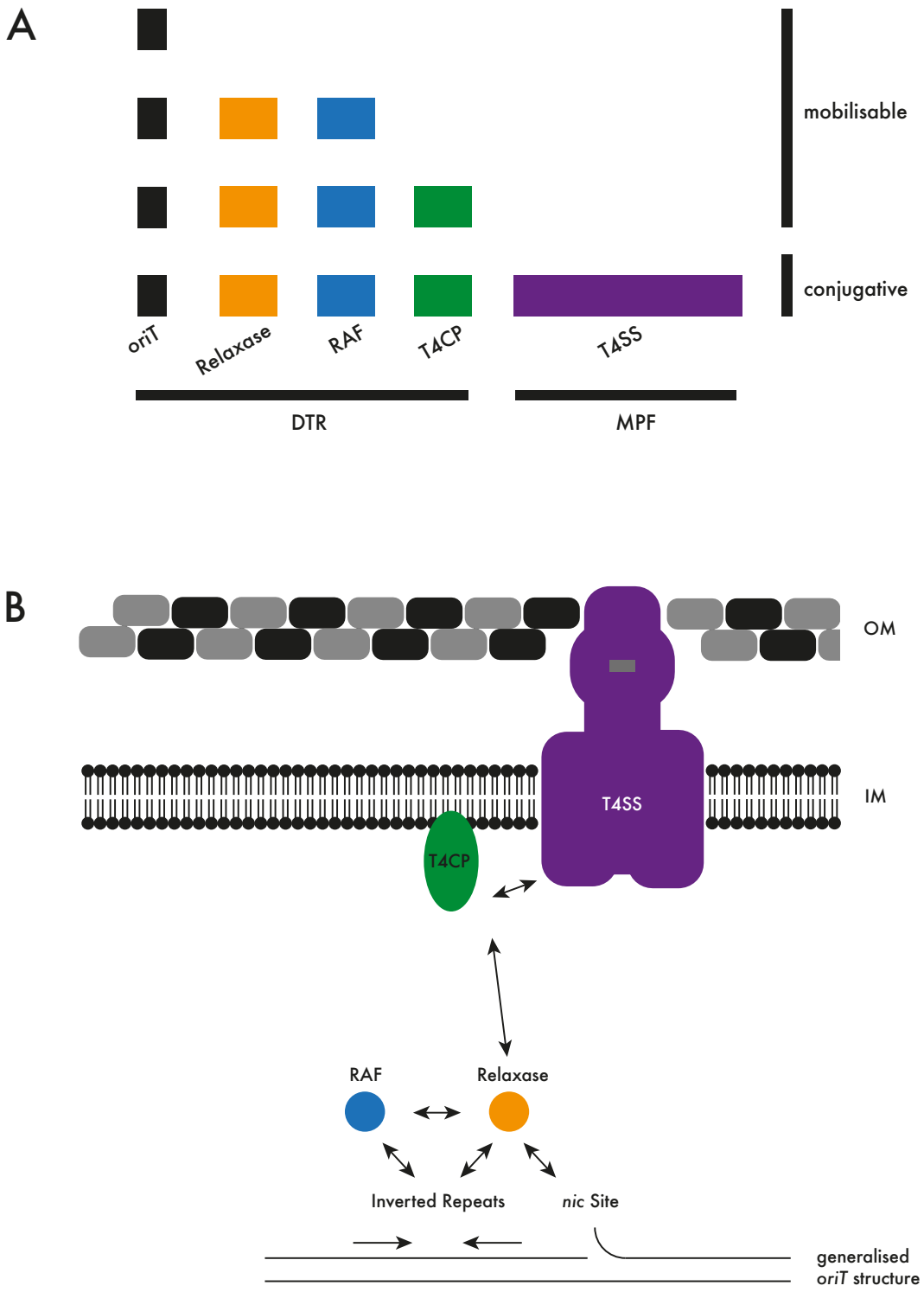

Figure 1: Genetic constitution of transmissible plasmids and the interactions between components facilitating the conjugative transfer of a plasmid.
(A) Schematic representation of the genetic elements carried by transmissible plasmids. Conjugative plasmids encode a T4SS as well as an *oriT*, relaxase, RAFs and a T4CP. Mobilisable plasmids only contain a DTR region of variable composition. (B) Specific interactions link the *oriT* to the T4SS. The relaxase (orange) nicks the plasmid at the *oriT nic* site. RAFs (blue) can increase the efficiency of nicking. The relaxosome interacts with the T4CP (green), which provides the energy for DNA transfer through the T4SS (purple). OM, outer membrane; IM, inner membrane. The figures were adapted from [6,7].

Assembly of the relaxosome can be facilitated by relaxase accessory factors (RAFs), which modulate local DNA topology, enhance sequence recognition, and stabilise protein-DNA interactions to optimise nicking efficiency[31].

The relaxosome subsequently interacts with the T4SS coupling protein (T4CP), a VirD4-like ATPase[32], which couples the relaxosome to the T4SS and provides energy for plasmid transfer[33,34]. The relaxase remains bound to the DNA during transfer and facilitates plasmid recircularisation in the recipient[35-37]. Rolling circle replication restores the plasmid to double-stranded DNA (dsDNA) in the donor and the recipient[38].

However, only approximately 25% of plasmids are conjugative; the remainder are either immobile or depend on cooperative interactions with other MGEs for their transfer[7,39].

1.1.1.2 Mobilisation

Mobilisable plasmids lack the MPF region but encode a relaxase and have an *oriT* (Figure 1); their relaxosome is transferred through the T4SS of a co-resident conjugative plasmid or ICE[6,7]. The ability of a plasmid to be mobilised depends on the interaction between its relaxosome with the T4SS of the conjugative plasmid *via* the T4CP. At the interface between T4SS and relaxosome, T4CP coupling is key to substrate specificity[40,41]; some mobilisable plasmids encode their own T4CP[5,17]. Approximately 25% of plasmids are mobilisable[7]; however, some plasmids lack a relaxase entirely, yet contain an *oriT* that is recognised by another plasmid's relaxase[42-45], highlighting the modularity of plasmid transfer[39,46].

Relaxases and rolling circle replication initiation proteins have been suggested to have evolved from a common ancestor and perform related molecular functions[6]. As such, some small rolling circle replicating plasmids can be mobilised by co-resident ICEs[47].

Mobilisation provides a low-cost strategy for plasmids to transfer within and between bacterial populations without the burden of expressing an energetically expensive conjugation system[48]. However, the competition between the mobilisable and the conjugative plasmid for a common pool of resources can impede the fitness of the latter, reducing the transfer rates of the conjugative plasmid[49]. This can result in a dead end for the mobilisable plasmid in a host without a helper plasmid. However, some mobilisable plasmids can interact with multiple types of conjugative systems by carrying multiple *oriT*s or encoding a T4CP, expanding the range of potential helper plasmids[41,50,51]. As such, many of the plasmids with the broadest host ranges (*e.g.* RSF1010[52], pLS1[53] and pBI143[54]) are mobilisable.

1.1.1.3 Other modes of plasmid transfer

While conjugation and mobilisation account for a large fraction of plasmid dissemination events, additional mechanisms such as transduction and transformation also contribute to the spread of plasmids.

Phage-mediated transduction occurs when plasmid DNA is packaged into phage particles[55-57], leading to the transfer of plasmid instead of phage DNA. Distinct from conjugation, transduction does not depend on direct contact between a donor and recipient, and phage particles can persist in the environment[58], protecting plasmid DNA from degradation. However, due to size limitations of phage capsids, this mode of transfer is more applicable to small plasmids[59].

The uptake of DNA from the environment through transformation is another route of plasmid transfer[60]. Many human pathogens, including *Campylobacter*, *Helicobacter*, *Haemophilus*, *Neisseria*, *Pseudomonas*, *Staphylococcus* and *Streptococcus* spp. are naturally transformable[61], *i.e.* they can take up DNA from their environment and integrate it into their genome or convert it into extra-chromosomal elements such as plasmids. In Gram-negative bacteria, type IV pili interact with

external DNA and pull it into the periplasm through secretin pores in the outer membrane[62]. Subsequently, ssDNA is translocated through *rec2* or *comEC*-encoded pores into the cytoplasm[63,64], where RecA-mediated recombination integrates homologous sequences into the chromosome or reconstitutes plasmids. However, due to the conversion to linear ssDNA during translocation and the need for subsequent recircularisation, transformation of circular plasmid DNA is generally less efficient than for linear DNA fragments[65]. Nevertheless, transformation can contribute to plasmid transfer in specific environments such as biofilms[66].

1.1.2 Barriers to plasmid transfer

While HGT can provide bacteria with new traits, it is a double-edged sword as newly acquired MGEs may be costly or lethal in the case of phage infection[67]. Therefore, bacteria have evolved a diverse set of defence strategies against incoming DNA[68].

Restriction modification systems (RMSs) are the most abundant bacterial defence systems, with >80% of bacterial genomes harbouring at least one RMS[69], and are based on restriction and methylation. Restriction endonucleases (REases) target unmethylated dsDNA sequences on incoming DNA, while the methyltransferases (MTases) protect the host DNA by adding methyl groups to specific adenine or cytosine residues. Bacterial RMSs can be grouped into four types[70], with type II RMSs being the most abundant[69]. Type I RMSs are multi-enzyme complexes of MTase subunits (HsdM), REase subunits (HsdR) and a specificity subunit (HsdS), which must be active for the system to be functional (Figure 2)[70]. Two HsdM and a HsdS form the methylase complex (M_2S_1). The addition of two HsdR to M_2S_1 results in the functional restriction complex ($R_2M_2S_1$); DNA restriction by type I RMSs occurs at variable positions distant from the recognition site[71]. Type II RMSs consist of individual MTase and REase; the REase cuts at a constant position at or close to the RMS's recognition sequence (Figure 2). Type III RMSs consist of DNA recognition and modification (Mod) and restriction (Res) subunits. A complex of Mod and Res interacts with two inversely

oriented non-palindromic sequences and cuts the DNA at a specific distance away from the recognition sequences (Figure 2). Mod subunits can modify DNA independently of Res, resulting in hemi-methylated DNA, different from types I and II, which preferentially modify hemi-methylated DNA to fully methylated DNA[70]. Type IV RMSs do not possess any methyltransferase activity and cleave only modified DNA[70]. Of note, most literature on RMSs dates back to the last century, and only a few recent studies provide structural insights into the function of RMSs[72].

While the presence of RMS in recipients can reduce plasmid transfer[73-76], restriction efficiency depends on the combination of RMS and plasmid[77]. The number and location of restriction modification sites on the plasmid[74,78] and anti-restriction functions expressed by the plasmid, as well as the type of RMS[77] all impact the restriction efficiency. Generally, the effect of RMSs on conjugation is lower than on transformation[79], although the reason for this remains poorly understood. Nevertheless, RMSs play an important role in shaping the evolution and distribution of plasmids[80], with small plasmids adapting to RMSs through target avoidance and larger plasmids by acquiring anti-restriction systems.

In recent years, a host of novel bacterial defence systems with diverse modes of activity have been discovered[68,81]. Systems such as CRISPR-Cas[82], BREX[83] or CBASS[84] have primarily been explored in the context of phage infection, but could also hinder plasmid transfer. Indeed, the presence of plasmid sequences in CRISPR arrays indicates a broader role in bacterial immunity against MGEs[85].

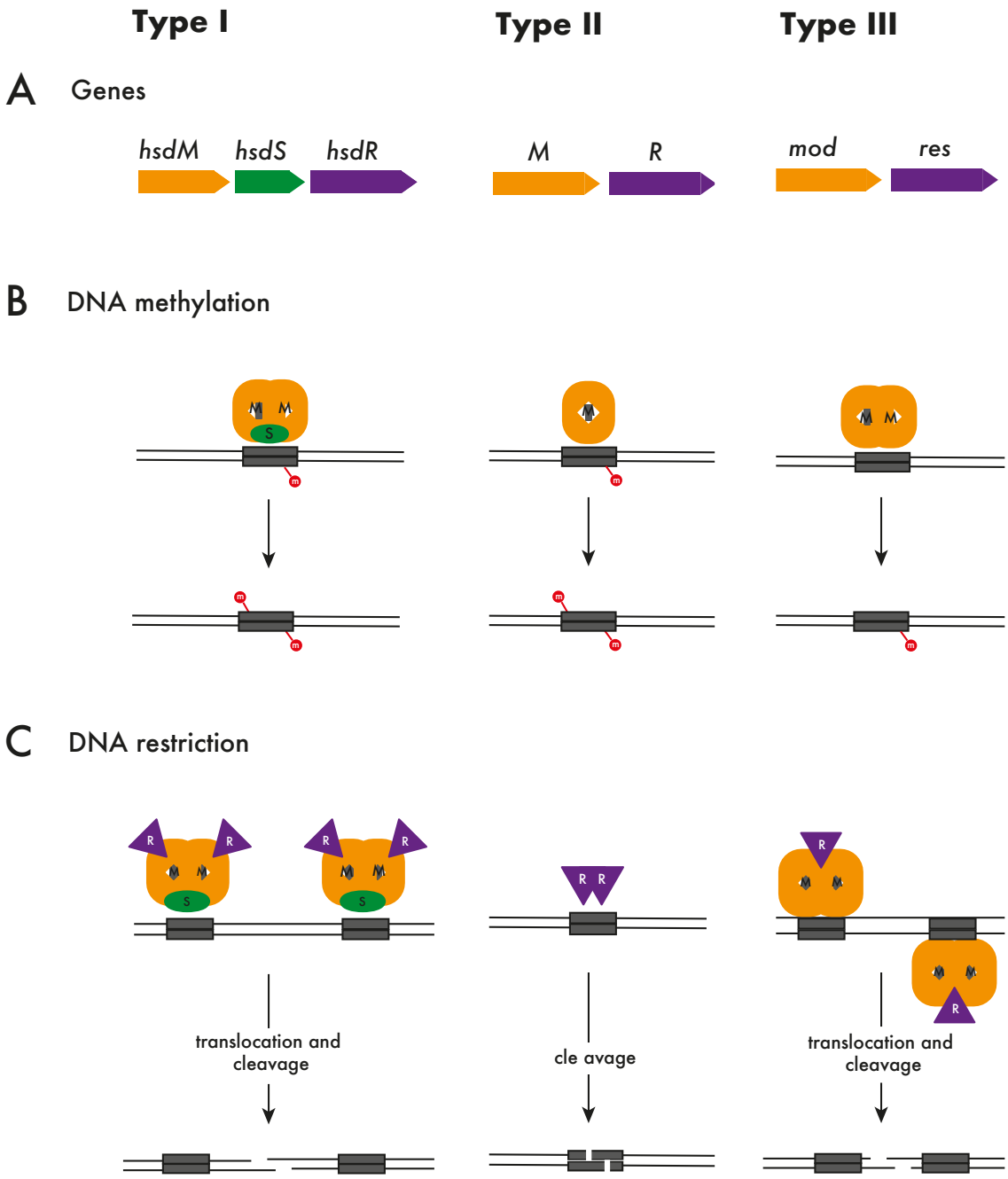

Figure 2: Organisation of Type I - III RMSs.
(A) Gene organisation of the different RMS types. *hsdM*, *M* and *mod*, methylase genes (orange); *hsdR*, *R* and *res*, endonuclease genes (purple); *hsdS* encodes for the type I specificity subunit (green). (B) DNA methylation complex composition; M, methylase; S, specificity subunit; the RM recognition sequence is indicated as a grey box, methyl groups as red circles. Type I and II RMSs preferentially methylate hemi-methylated DNA, resulting in fully methylated DNA. Type III RMSs result in hemi-methylation. (C) Composition of the DNA restriction complex. Type I and III RMSs cut distant from the site, whereas type II RMSs cut directly at the sequence. The figure was adapted from [13].

Besides bacterial defence systems, interactions with other mobile genetic elements can limit the spread of a plasmid. Surface and entry exclusion mechanisms are widespread among conjugative plasmids[86] and prevent plasmid uptake by a cell already harbouring a related plasmid[86-88]. Most surface exclusion factors characterised to date are associated with the outer membrane, where they prevent cell to cell contact and destabilise the MPF[89-93]. In contrast, entry exclusion proteins are in the cytoplasmic membrane and block DNA translocation into the cell. Of note, surface and entry exclusion are specific to the mating pair rather than the type of DNA. As such, they also affect co-transferred plasmids, preventing their entry into cells that already harbour their helper plasmid[94].

Finally, plasmid incompatibility poses a post-entry barrier to plasmid maintenance. Plasmids that share similar replication or partitioning systems fail to stably co-exist due to competition for shared replication mechanisms or interference with control of replication or partitioning systems[95]. Therefore, they are considered incompatible, and plasmids have been categorised into incompatibility (Inc) groups based on their replication systems[96,97]. However, more recent work suggests that especially higher copy number plasmids co-exist despite shared replication strategies[98].

1.1.3 Plasmid fitness costs

Plasmid carriage can impose a burden on bacteria, resulting in plasmid loss from a population due to purifying selection. Plasmid fitness costs are evident under conditions lacking selective pressure for plasmid-encoded traits, in which plasmid-carrying isolates show slower growth and diminished competitiveness compared to plasmid-free isolates[99,100].

A variety of mechanisms lead to plasmid fitness costs[67]. Initial plasmid acquisition costs[101] result from the activation of the host's SOS response upon the conjugative transfer of ssDNA[102] and the

transient overexpression of plasmid genes due to disrupted negative feedback loops[103,104]. Of note, while plasmid acquisition costs reduce vertical transmission of plasmids, this may be counterbalanced by derepression of the conjugation machinery, leading to increased horizontal transmission[103].

Plasmid replication can be costly due to pleiotropic effects of the plasmid-encoded replication initiation (Rep) proteins[105,106]. To replicate plasmid DNA, plasmid Rep proteins interact with host DNA polymerases and helicases[106,107]. Overexpression of Rep genes, particularly by high copy number plasmids, can lead to sequestration of the cellular replication machinery and impair chromosomal replication, activating the cellular SOS response and inhibiting cell division[105,106].

The misalignment between plasmid gene expression and the host's ability to support protein synthesis contributes to plasmid fitness costs[81]. High levels of plasmid-derived mRNA may exceed the availability of tRNAs or ribosomes, resulting in codon usage imbalances, depletion of amino acids, and competition for ribosomes[108-110]. Additionally, plasmid-encoded proteins can interfere with regulatory or metabolic networks or cause toxicity due to deleterious interactions with host proteins[105,106,111,112].

Conjugative plasmids can impose additional fitness costs due to the ATP requirement for plasmid conjugation. Furthermore, conjugative pili can act as the receptor for certain bacteriophages[113,114], rendering plasmid-carrying cells vulnerable to phage infection. Consequently, many conjugative plasmids tightly control the expression of their conjugative machinery, with only a subset of cells expressing a T4SS[103,115-117].

1.1.4 Plasmid stability

Given the cost of plasmid carriage and the stochastic emergence of plasmid-free daughter cells, non-beneficial plasmids should be lost from a population due to the competitive advantage of

plasmid-free cells[118-120]. Despite this, plasmids are maintained in bacterial populations over time, a phenomenon often referred to as 'the plasmid paradox'[119], and several mechanisms have been explored to explain the prevalence and persistence of plasmids[121].

Many large and low copy number plasmids encode maintenance systems, such as multimer resolution and partitioning systems, to ensure their stable inheritance during cell division[122]. The former resolves plasmid multimers *via* site-specific recombination[123], resulting in individual plasmids that can segregate into daughter cells[124]. Plasmid partitioning systems (encoded by the *par* locus) consist of a *cis*-acting centromere-like site and two trans-acting proteins: a sequence-specific DNA-binding protein recognises the centromere-like site, and a nucleotide hydrolase (ATPase or GTPase) capable of forming dynamic filaments[125]. Association of the DNA-binding protein with its target site forms a partitioning complex, and plasmids are pushed to the cell poles by the polymerising ATPase/GTPase filaments[126].

In addition, many plasmids encode toxin-antitoxin (TA) systems, leading to postsegregational killing of plasmid-free daughter cells[127]. TA systems consist of a stable toxin and a labile cognate antitoxin. If the TA encoding plasmid is lost during cell division, the daughter cell is killed by the more stable toxin that is no longer counteracted by the antitoxin. TA systems are divided into eight types based on the nature of their antitoxin (RNA molecule *vs.* protein) and mechanism of inactivation of the toxin (*e.g.* direct binding to the toxin in type II systems, degradation of toxin mRNA in type V systems or toxin modification in type VII systems)[128]. Smaller plasmids rarely encode active maintenance systems, instead, they rely on a high copy number to minimise segregational loss[129].

Beyond vertical inheritance, HGT can counteract plasmid loss. However, conjugation rates observed in nature are often too low to compensate for plasmid loss, and conjugation itself can impose fitness costs[118,130]. Nevertheless, conjugation rates and plasmid fitness costs can vary significantly between bacteria and plasmids[131-135], and depend on the environment of a plasmid-

carrying strain[136]. Modelling has shown that variability in plasmid fitness cost can improve stability of low-cost plasmids in a population but does not explain the persistence of high-cost plasmids[132]. In addition to the host genetic background, interactions between plasmids can further modify fitness costs, and synergistic epistasis can reduce fitness costs of co-infecting plasmids[137-140], favouring plasmid co-existence[39,141]. In line with this, plasmids co-occur in bacterial isolates more frequently than expected by chance alone[137].

Plasmid fitness costs can be reduced by compensatory mutations in the plasmid and/or host chromosome[141,142]; chromosomal compensatory mutations frequently occur in genes associated with the SOS response or DNA helicase and resolve genetic conflicts between the plasmid and its host[111,112,141,143]. Compensatory mutations emerge rapidly in transconjugants[144], with the probability of such mutations emerging increasing with the population size of plasmid-carrying isolates. Therefore, selection for plasmid-encoded traits leading to clonal expansion of plasmid-carrying isolates also increases the probability of the emergence of compensatory mutations that stabilise the plasmid[141].

Even in the absence of plasmid fitness cost, theory predicts that beneficial genes should relocate onto the chromosome, making plasmid carriage redundant[118]. However, the location of resistance genes on multi-copy plasmids may not only facilitate their spread, but can also accelerate resistance evolution by increasing the rate of emergence of resistance-increasing mutations and amplifying resistance levels due to increased gene dosage[145]. Additionally, heterogeneity in plasmid copy number generates phenotypic variability, allowing rapid adaptation of gene dosage, which is beneficial under fluctuating selection[146].

1.2 *Neisseria gonorrhoeae*

1.2.1 *Neisseria* spp.

Neisseria spp. are Gram-negative, coccoid or rod-shaped bacteria that typically colonise mucosal surfaces of humans or animals[147]. Most *Neisseria* spp. are non-pathogenic and part of the healthy human oropharyngeal and nasal flora[148]. However, individual reports indicate that some *Neisseria* spp. can cause disease in immunocompromised hosts[149]. In contrast, *N. gonorrhoeae* and *Neisseria meningitidis* are human pathogens with significant clinical relevance. *N. gonorrhoeae* causes the sexually transmitted infection (STI) gonorrhoea. *N. meningitidis* is carried by 10 - 15% of the general population as a commensal[150]; however, under certain conditions, the bacterium can breach mucosal barriers and enter the bloodstream, causing meningococcal septicaemia, or cross the blood-brain barrier to result in bacterial meningitis. Recent epidemiological studies have identified an *N. meningitidis* urogenital clade (NmUC), which has adapted to the urogenital tract through the acquisition of genetic material from *N. gonorrhoeae*[151,152]. Like *N. gonorrhoeae*, NmUC is transmitted *via* sexual contact and has been associated with urethritis in males.

Members of *Neisseria* spp. are characterised by remarkable genetic plasticity, facilitated by competence for DNA uptake, frequent horizontal gene transfer and high rates of homologous recombination[8]. This genome fluidity enables rapid adaptation to new ecological niches and contributes to the development of antimicrobial resistance[153].

1.2.2 Gonococcal disease

Among the diverse species of *Neisseria*, *N. gonorrhoeae* presents a significant public health challenge, particularly due to increasing levels of antimicrobial resistance[154,155]. *N. gonorrhoeae* primarily infects the mucosal tissues of the urethra and uterine cervix, causing the STI gonorrhoea.

The bacterium can also infect the pharynx and rectum. Pathology is largely driven by inflammation at the infection site, typically manifesting as cervicitis and urethritis[156]. An array of phase-variable adhesins and surface factors facilitates gonococcal infection of distinct niches. Type IV pili and opacity proteins (Opas) are essential for initial adhesion and colonisation of mucosal epithelia[157-162]. Abundant surface molecules include the porin PorB, Opas, RmpM, lipooligosaccharide (LOS) and iron-acquisition proteins[156]. However, due to extensive antigenic and phase variation[160,163,164] and immune evasion mechanisms[165-169], infected individuals do not develop protective immunity following infection[170,171].

N. gonorrhoeae is an exclusively human pathogen, and asymptomatic individuals constitute a major reservoir for continued transmission. Among infected women, 30 - 50% do not exhibit symptoms, while only 5 - 10% of infected men are asymptomatic[147]. Rectal and pharyngeal infections are also often asymptomatic[172]. Notably, pharyngeal infections provide an opportunity for genetic exchange with commensal *Neisseria* spp., which has been linked to the development of AMR[173].

Untreated gonococcal infection can lead to serious complications, including pelvic inflammatory disease, infertility, ectopic pregnancy and disseminated gonococcal infection, which has been associated with arthritis and endocarditis[174]. Mother-to-child transmission during birth can result in ophthalmia neonatorum, a major cause of neonatal blindness in low- and middle-income countries (LMICs)[175]. In addition, co-infection with other STIs, most notably *Chlamydia trachomatis* and HIV, is common, and *N. gonorrhoeae* increases the risk of acquisition and transmission of HIV[176].

1.2.3 *N. gonorrhoeae* epidemiology and population structure

The World Health Organisation estimated there were 82.4 million new cases of gonorrhoea in 2020[177]. Incidence varies significantly in different geographical regions and among populations with

different sexual behaviour, socioeconomic status, and ethnic background[178]. The highest rates of gonorrhoea have been reported in the WHO African and Western Pacific Regions (Figure 3A)[172]. These geographic disparities are influenced by access to healthcare, sexual education, and social factors such as stigma. In high-resource settings, increased travel, sexual networks, and changes in sexual behaviour - partly driven by the availability of antiretroviral therapy and pre-exposure prophylaxis for HIV[179,180] - have contributed to rising gonorrhoea incidence[178]. Certain groups, including men who have sex with men (MSM), migrants, young people, and sex workers, are disproportionately affected by gonococcal disease[172].

The *N. gonorrhoeae* population structure is shaped by high rates of both intra- and interspecies HGT, resulting in extensive genetic diversification and weak clonal structure[181-183]. Multiple molecular typing schemes, such as MLST[184], NG-MAST[185], NG-STAR[186] and cgMLST[2], have been employed to classify gonococcal isolates. However, MLST, NG_MAST and NG-STAR rely on a few loci for typing and poorly resolve the population structure due to HGT of the respective genes[187]. In contrast, whole genome approaches like core genome multi-locus sequence typing (cgMLST) allow for more robust classification. cgMLST clusters isolates using 1 668 loci core to the gonococcus (*i.e.* present in >95% of gonococci). Using single linkage clustering with a cut-off of 400 allelic differences, isolates can be grouped into *N. gonorrhoeae* core genome clusters (Ng_cgc_{400}), which persist over time and correlate with AMR phenotypes[2] (Figure 3B).

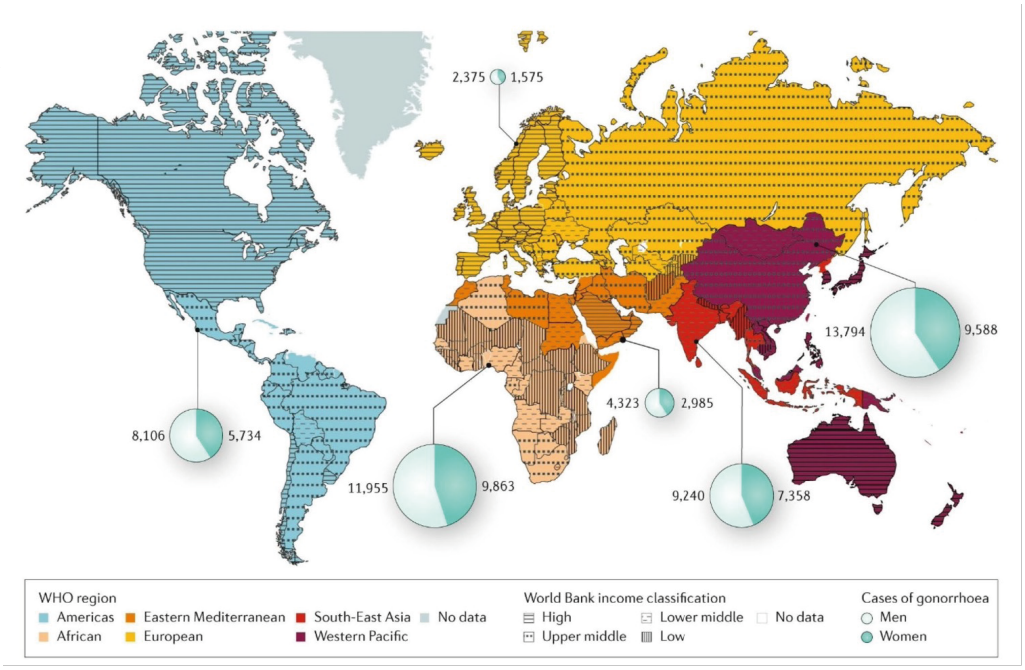

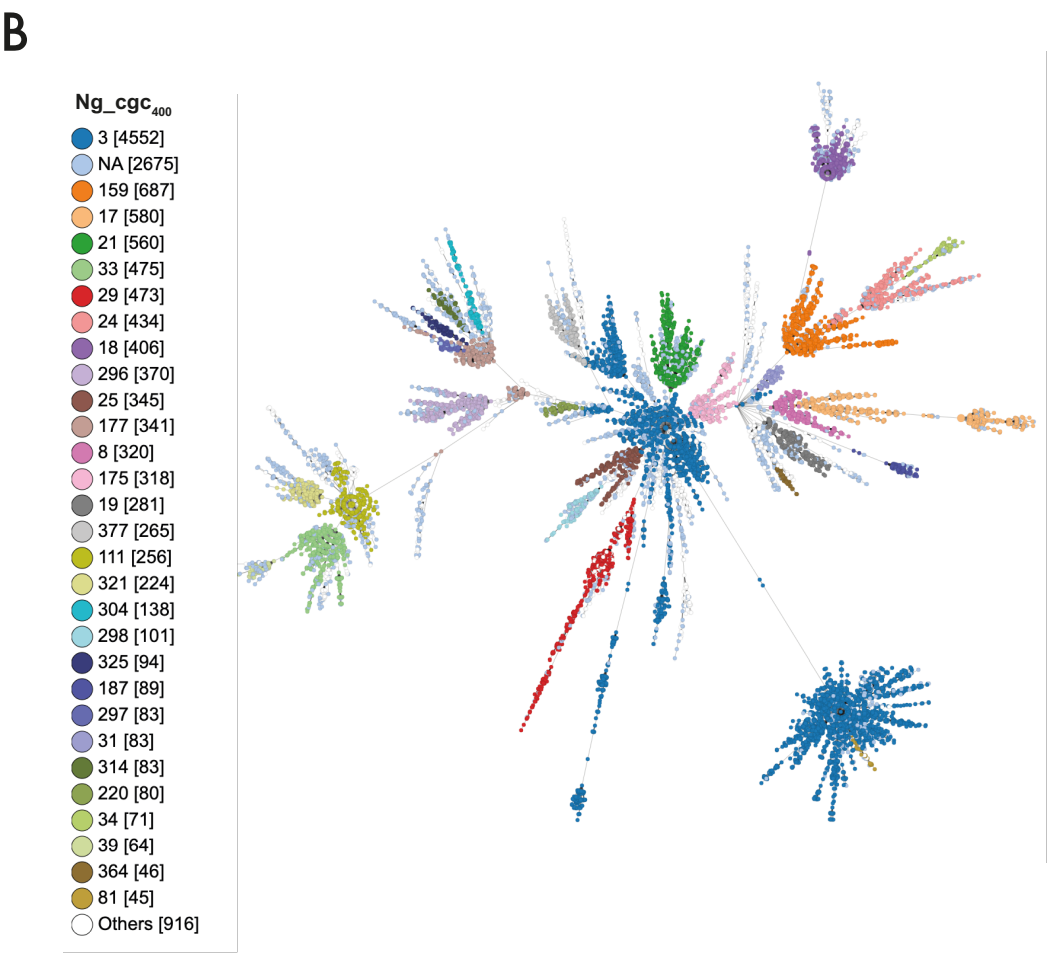

Figure 3: Epidemiology and population structure of *N. gonorrhoeae.*
(A) Estimated global incidence of gonorrhoea; numbers (in millions) of cases by WHO region and gender. Figure from [1]. (B) Minimum spanning tree of 15 532 *N. gonorrhoeae* isolates clustered by *N. gonorrhoeae* cgMLST v1[2]. Dots represent individual isolates and are coloured according to their core genome cluster (Ng_cgc_{400}).

1.2.4 The genetics of *N. gonorrhoeae*

N. gonorrhoeae is polyploid with each coccus harbouring on average three copies of its 2.2 Mb chromosome[188]. However, despite its polyploidy, cells usually lack allelic diversity at specific loci[189]. Gonococcal genomes contain many repetitive elements, insertion sequences (IS) and phage elements, all contributing to genomic plasticity[190]. The most frequent repetitive element is the *N. gonorrhoeae* DNA uptake sequence (DUS) 5'-ATGCCGTCTGAA-3' (underlined bases are semi-conserved between strains), which is critical for species-specific transformation[191,192]. DUS sequences are present at a frequency of approximately one per kb, although DUSs are overrepresented around genome maintenance genes[193,194]. There are between 10 to 50 IS sequences per genome, consisting of genes required for transposition flanked by inverted repeats[193]. Additional mobile elements include minimal mobile elements, cassettes with varying contents that can be exchanged and incorporated by homologous recombination in the conserved flanking regions[195], and Correia Elements[196]. The Gonococcal Genetic Island (GGI) is present in approximately 80% of strains and encodes a T4SS that secretes single-stranded DNA, likely facilitating transformation[197,198].

Bacteriophage elements in *Neisseria* are limited to a few double-stranded DNA and M13-like filamentous phages[199-201], with no described lytic or transducing phages[8,202]. However, the *N. gonorrhoeae* phagemid Ngoϕ6 displays a broad host range including *E. coli*, *H. influenzae* and *Pseudomonas* spp.[203].

1.2.4.1 Phase and antigenic variation

Phase and antigenic variation are central to the ability of the gonococcus to evade immune surveillance, generating phenotypic heterogeneity in surface structures and virulence factors, which allows rapid adaptation to different niches in the host.

Phase variation is the reversible ON : OFF switching of gene expression resulting from DNA inversions, differential methylation, and changes in the length of homopolymeric tracts or microsatellites[204]. In *Neisseria*, the major mechanism of phase variation is slipped-strand mispairing during DNA replication[205], leading to the expansion or contraction of homopolymeric tracts. Alterations in the length of tracts within coding sequences can result in frameshift mutants and ON : OFF switching of gene activity; changes in non-coding regions can modify the spacing of -10 and -35 elements and modulate transcription (Figure 4). The rate of phase variation differs between genes, ranging from 10^{-2} to 10^{-6} per cell per generation[206,207]. Over 100 genes in *N. gonorrhoeae* are phase-variable, including those encoding major surface components like LOS and Opas[208,209].

Antigenic variation refers to changes to the antigenic structure rather than the expression level. The classic example of antigenic variation in *N. gonorrhoeae* is PilE, the major component of the type IV pili. *pilE* sequences are varied through gene conversion, where sequences from non-expressed *pilS* loci, scattered throughout the chromosome, recombine with the expressed *pilE* locus without altering the donor *pilS* locus (Figure 4)[163,210-212].

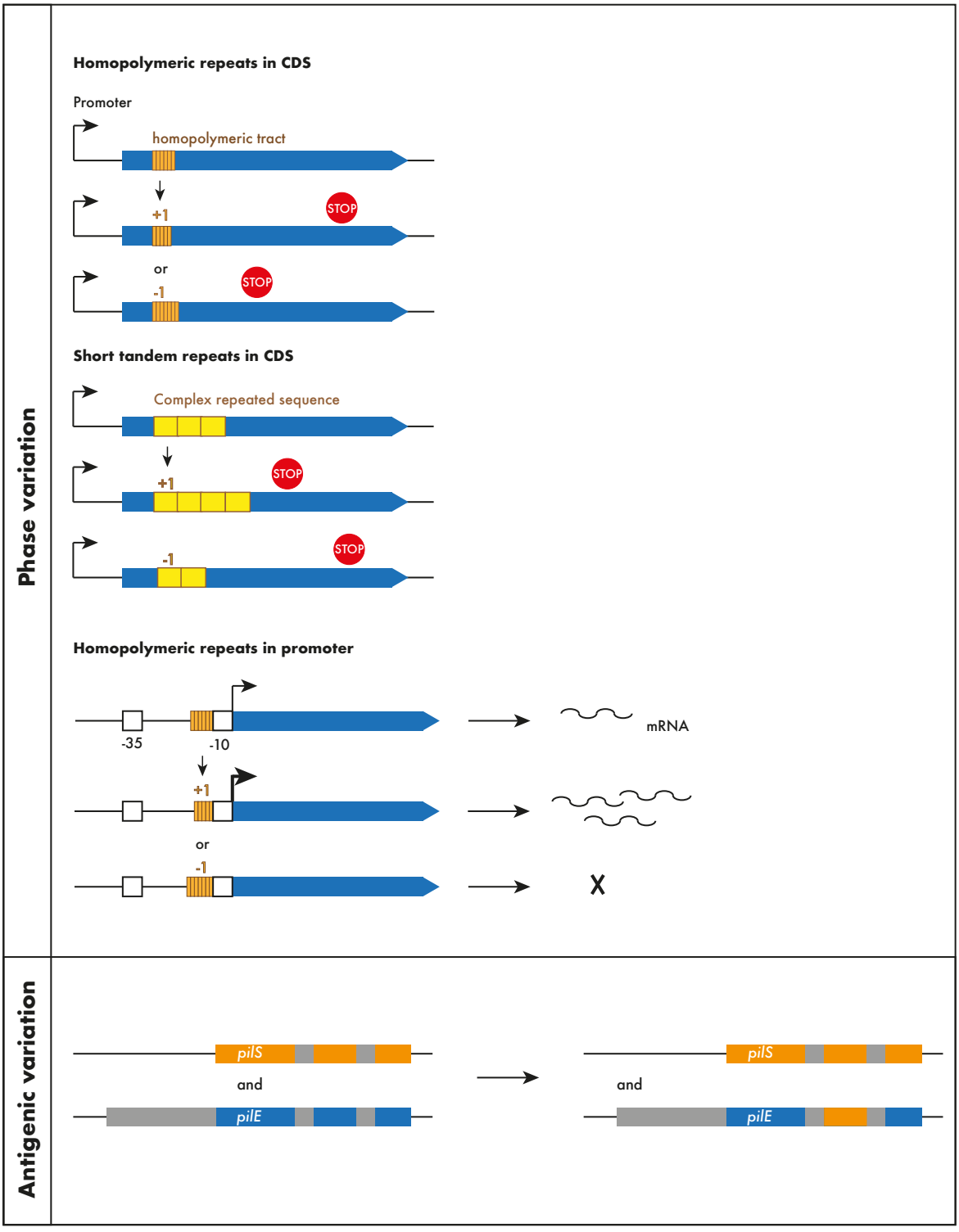

Figure 4: Phase and antigenic variation generate phenotypic heterogeneity.
The types of phase variation are shown on top. The blue arrow indicates the CDS with orange rectangles and yellow squares representing homopolymeric repeats and short tandem repeats, respectively. Changes in the length of the homopolymeric tracts and repeat sequences lead to ON : OFF switching of the gene, whereas alterations in tracts in the promoter region affect the transcription levels by varying the spacing between the -10 and -35 RNA polymerase recognition sequences. A schematic of antigenic variation of PilE is shown at the bottom. *pilE* and *pilS* loci have regions of sequence microhomology (grey) and variable sequences (in colour). Recombination between the expressed *pilE* and silent *pilS* copies results in diversification of the *pilE* locus while the *pilS* copies remain unaltered. Figures were adapted from [8] and [14].

1.2.4.2 Transformation

N. gonorrhoeae is naturally competent throughout its life cycle, so is transformable throughout all growth phases[213,214]. Transformation facilitates the acquisition of resistance genes and can serve as a mechanism for DNA repair[214,215]. Gonococcal transformation depends on type IV pili, which bind ssDNA and dsDNA[213,214]. Type IV pili are filamentous cell appendages made up of the major pilin PilE and a variety of minor pilin subunits, including ComP, which specifically recognises gonococcal DUS, increasing the efficiency of DNA uptake[216]. Different 'dialects' of DUS exist within *Neisseria* spp.[192], and 76% *of N. gonorrhoeae* DUS have two nucleotides in addition to the prototypic 10 bp sequence, which slightly increase transformation efficiency[217].

DNA enters the cell as ssDNA[63] and is integrated into the chromosome by homologous recombination. While *N. gonorrhoeae* has multiple recombination systems, *recA* is the only gene which is essential for homologous recombination; *recBCD* mutations decrease the frequency of recombination[218,219]. Furthermore, the efficiency of homologous recombination is influenced by the sequence identity between donor and recipient DNA.

1.2.4.3 RMS in *N. gonorrhoeae*

Like other naturally competent bacteria, *N. gonorrhoeae* has a disproportionately high number of RMSs[220]. *N. gonorrhoeae* isolates can harbour up to 16 distinct RMSs[221], many of which are phase-variable, leading to ON : OFF switching or changes in the recognition sequence[222]. DNA methylation is crucial for DNA acquisition through transformation and conjugation; however, larger effects have been observed for transformation than for conjugation[76,79].

Some gonococcal RMS also have regulatory roles in the pathogenic *Neisseria* spp.. Differences in the DNA recognition domain of the type III RMS methylases ModA and ModB alter their methylation sequence, while phase-variation of *mod* modifies methylation activity[223]. Changes in

Mod-mediated methylation modify global gene expression, a phenomenon referred to as a 'phasevarion'[223-226]. The ModA-corresponding restriction endonuclease appears to be inactive, suggesting the restriction function has been lost and ModA is dedicated to gene regulation[223]. Similarly, phase-variation of the type I RMS NgoAV *hsdS*, modifiesies the activity and specificity of the system[227], and results in transcriptional changes that alter biofilm formation, AMR, and invasion of human epithelial cells[228].

Despite their abundance and diverse roles in *N. gonorrhoeae*, the distribution of different RMSs within the population and their impact on plasmid transfer are poorly understood.

1.2.5 Antimicrobial resistance in *N. gonorrhoeae*

1.2.5.1 Treatment of gonococcal disease and resistance development

Management of gonococcal disease relies on antimicrobial treatment of cases and their contacts. However, treatment has become increasingly challenging due to the bacterium's remarkable ability to acquire, spread and maintain resistance determinants[1].

Sulphonamides were the first antibiotics introduced for gonorrhoea in the mid-1930s (Figure 5)[229]. However, by the mid-1940s, resistance was already widespread[230]. In 1943, benzylpenicillin was introduced for the treatment of gonorrhoea and was initially highly effective[231]. However, within 10 to 15 years, escalating doses were required due to the gradual accumulation of chromosomal resistance mutations[232]. The emergence of the gonococcal β-lactamase plasmid p*bla* in 1976 led to high-level penicillin resistance[4,233], and penicillin treatment ceased in mid-1980[234]. In the early 1950s, alternative antibiotics such as aminoglycosides, macrolides and tetracycline were introduced. However, resistance to these antibiotics emerged rapidly, driven by chromosomal mutations and the acquisition of the conjugative plasmid pConj, carrying the tetracycline resistance gene *tetM*[235].

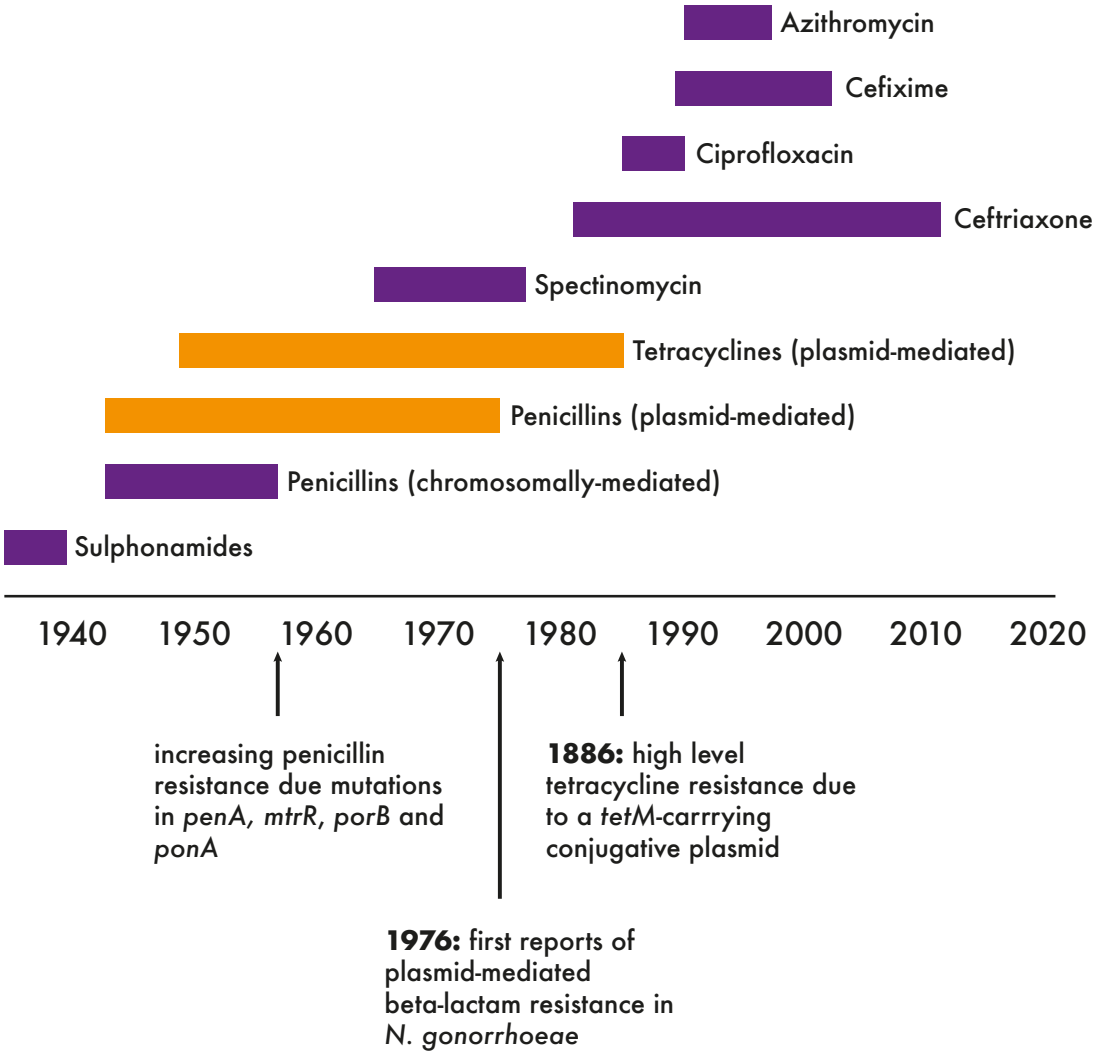

Figure 5: Timeline of treatment recommendations for gonococcal disease and the emergence of resistance. Bars indicate the time between the introduction of an antibiotic and the emergence of resistance. Purple bars represent chromosomally encoded resistance mechanisms; plasmid-mediated resistance is shown in orange. The figure was adapted from [11].

Fluoroquinolones including ciprofloxacin were employed until the mid-2000s, when the spread of mutations in *gyrAB* and *parC*[236,237] necessitated their withdrawal. Currently, high-dose monotherapy with the third-generation cephalosporin ceftriaxone is recommended in high-income countries[238,239]. In low resource settings, doxycycline remains a common syndromic treatment for STIs[240]. Doxycycline has also been proposed, and already implemented in some regions, as a post exposure prophylaxis in risk groups taken within 48 hours of unprotected intercourse[241,242]. However, strains resistant to ceftriaxone and doxycycline are already circulating in the population[154,240,243-247], threatening the efficacy of these interventions.

The WHO identified *N. gonorrhoeae* as a high-priority pathogen for the development of novel antibiotics due to its extensive resistance[248]. Efforts to develop novel treatments for gonorrhoea have resulted in the antibiotics zoliflodacin and gepotidacin[249-251], which selectively inhibit bacterial DNA replication *via* interactions with subunits of DNA gyrase and topoisomerase IV[252,253]. Pre-existing resistance to these novel antibiotics is rare[254,255]. However, resistance to zoliflodacin readily evolves in commensal *Neisseria* and might be transferred into gonococci by transformation[249,256,257].

The implementation of novel antibiotics like zoliflodacin and gepotidacin offers a promising alternative to existing therapies. However, lessons learned from the past highlight the capacity of *N. gonorrhoeae* to quickly acquire and spread resistance mechanisms. Therefore, continuous monitoring of resistance determinants in the population, paired with knowledge of the molecular mechanisms of their spread, are essential to ensure the sustained effectiveness of new therapeutic agents.

1.2.5.2 β-lactam resistance in *N. gonorrhoeae*

1.2.5.2.1 Resistance due to the stepwise acquisition of chromosomal resistance determinants

The gradual increase in penicillin resistance over almost four decades involved antibiotic target modifications and changes in antibiotic influx and efflux[215]. Polymorphisms in *penA*, *mtr* and *porB* additively increased resistance to penicillin, and affected susceptibility to other antimicrobials such as tetracyclines and macrolides[258].

Penicillin binds to bacterial transpeptidases (penicillin-binding proteins, PBPs), preventing peptidoglycan cross-linking in the bacterial cell wall[259]. In *N. gonorrhoeae*, the main target of penicillin is the *penA*-encoded PBP2. PBP2 catalyses the final transpeptidation step in peptidoglycan biosynthesis, crosslinking adjacent glycan strands. Penicillin mimics the D-Ala-D-Ala substrate of PBP2 and irreversibly acylates the PBP2 active site serine[260], inactivating the enzyme and stopping cell wall synthesis. An aspartic acid insertion at position 345 in the transpeptidase domain of PBP2 induces a conformational change that reduces penicillin binding affinity and preserves its transpeptidase activity even in the presence of the antibiotic[261,262].

Low-level penicillin resistance is enhanced by overexpression of the MtrCDE efflux pump, which exports antimicrobials from the periplasm. MtrCDE overexpression results from loss of function mutations in the gene encoding the transcriptional repressor MtrR or the promoter of the *mtrCDE* operon. Alterations in the outer membrane porin PorB further increase resistance[263,264], potentially by decreasing the influx of antibiotics across the outer membrane[263]. There are two major variants of PorB in gonococci, PorB1A and PorB1B, which differ in their surface-exposed portions and size[265]. PorB1B-producing gonococci are slightly less susceptible to penicillin[232]. Amino acid changes in the external loop 3 (G120K and A121D) further increase penicillin resistance of strains with PorB1B, and concomitantly result in porin-mediated tetracycline resistance[266]. High-level penicillin resistance requires further mutations in *ponA* and *penC* (also referred to as *pilQ*). An L421P

replacement in the *ponA*-encoded PBP1, decreases penicillin affinity, while an E666K change in PilQ reduces penicillin entry[267,268].

Transformation plays a key role in the evolution of *N. gonorrhoeae* AMR. Acquisition of DNA from commensal *Neisseria* spp. has led to mosaic genes, with mosaic *penA* variants resulting in PenA with up to 70 amino acid changes[182,269]. Some mosaic PenA variants have reduced affinity for β-lactam antibiotics, including 3rd generation cephalosporins[243,270]. However, resistance-increasing *penA* alleles *pen*A14 and *pen*A89 impose a fitness cost and require additional compensatory mutations to be successful in gonococcal populations[271].

1.2.5.2.2 Plasmid-borne resistance

In contrast to the gradual increase in penicillin resistance due to chromosomal mutations, the emergence of a plasmid-borne TEM β-lactamase resulted in high-level resistance in a single step.

β-lactamases hydrolyse β-lactam antibiotics. Based on sequence homology, they are classified into A - D. Class B are metallo-enzymes that use zinc ions to hydrolyse the β-lactam ring, whereas A, C and D rely on a catalytic serine[272]. The catalytic mechanism of class A β-lactamases includes acylation followed by deacylation (Figure 6A)[273]. In the first step, the catalytic Serin (S70) is activated by the removal of a proton and the S70 oxygen attacks the carbonyl group of the β-lactam forming an acyl intermediate[274,275]. Subsequently, an activated water molecule attacks the covalent bond of the acyl intermediate, hydrolysing the β-lactam antibiotic and regenerating the enzyme[276-278].

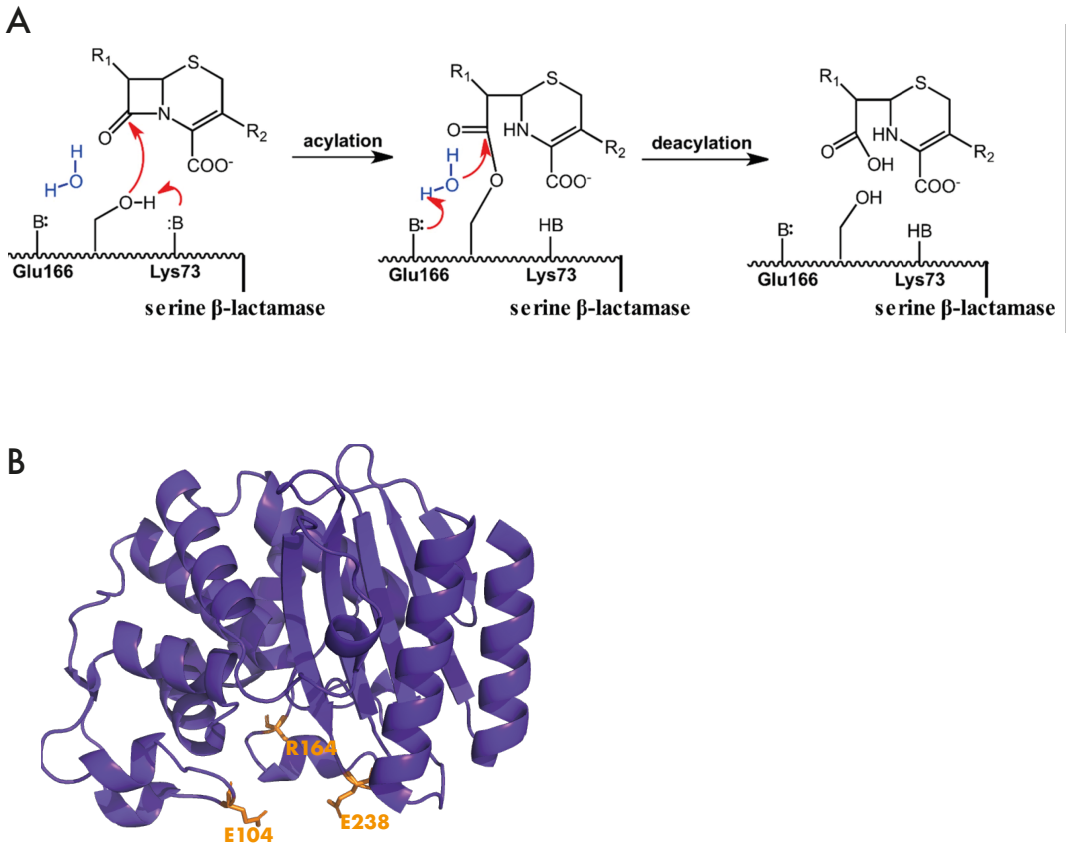

Figure 6: Catalytic mechanism and structure of TEM β-lactamases.
(A) The catalytic mechanism of Serine β-lactamases. The catalytic S70 is activated by the removal of a proton, and the S70 oxygen attacks the carbonyl group of the β-lactam, forming an acyl intermediate. Subsequently, a water molecule is activated to attack the covalent bond of the acyl intermediate structure, hydrolysing the β-lactam antibiotic and regenerating the enzyme. Figure from [10]. (B) TEM-1 β-lactamase with locations of common ESBL substitutions highlighted in orange.

TEM is a class A β-lactamase. Class A β-lactamases have a broad substrate profile including penicillins, cephalosporins and, for some enzymes, carbapenems[279,280]. TEM-1 is the most common plasmid-encoded β-lactamase in Gram-negative bacteria and efficiently hydrolyses penicillins, but not 3rd generation cephalosporins[281]. However, only a few amino acid substitutions are needed to convert TEM-1 into an extended-spectrum β-lactamase (ESBL)[282]. ESBL-conferring mutations mainly cluster around the active site, with common substitutions at positions 104 (E104K), 164 (R164S or R164H), 238 (E238S, Figure 6B)[282,283]. However, mutations increasing the thermodynamic stability of the enzyme, most prominently the M182T substitution found in TEM-135, frequently occur together with mutations in the active site[282]. Whilst not impacting the resistance levels and substrate spectrum, the M182 substitution is considered a 'stepping stone mutation', counterbalancing potential destabilising effects of changes in the active site[284,285]. Both TEM-1 and TEM-135 are expressed by plasmids in gonococci[286].

1.2.6 The narrow host range plasmids of *N. gonorrhoeae*

Plasmids are major drivers of AMR, and bacterial species often carry a wide variety of plasmids[287-289]. Strikingly, only three plasmids have been described in *N. gonorrhoeae* to date[202].

1.2.6.1 The cryptic plasmid, pCryp

Over 90% of all gonococci harbour the 4.2 kb cryptic plasmid pCryp[290,291]. This plasmid has ten open reading frames (ORFs), which encode a replicase (*repA*), the VapDX TA system, the mobilisation proteins MobB and MobC, and four proteins of unknown function[290]. Early studies suggest pCryp has a high copy number ranging between 24 and 32 plasmids per chromosome copy[292], which, together with its TA system, could explain the stability of pCryp in gonococci. Despite its prevalence, little is known about the function or origin of this plasmid. However, the earliest gonococcal isolate on the PubMLST database from 1928 harbours pCryp, and the presence of pCryp increases the

transfer of the gonococcal conjugative plasmid pConj from *N. gonorrhoeae* into *E. coli*, potentially due to the neutralisation of the pConj-encoded VapD orphan toxin by the pCryp VapX antitoxin[293,294].

1.2.6.2 The conjugative plasmid, pConj

The gonococcal conjugative plasmid pConj (39 - 42 kb) is present in around one-third of gonococci, and its ability to spread horizontally is reflected by its presence in different gonococcal lineages[290]. pConj is an IncP1 plasmid[293]. Like other IncP1 plasmids, the pConj backbone contains genes for replication initiation (*ssb* and *trfA*), conjugative transfer (*tra*) and mating pair formation (*trb*), as well as plasmid partitioning (*kor*, *kle*, *inc* and *kfr*)[293]. Between the *trb* and *tra* modules is the variable pConj genetic load region, which harbours an array of TA systems and *tetM*[293]. pConj encodes a ParAB partitioning system, two ε:ζ type II TA systems, as well as an orphan VapD toxin[293]; these systems act redundantly to maintain the plasmid with remarkably little loss in the laboratory[294].

pConj can be grouped into seven variants[290]; pConj variants 1 to 4 encode TetM, conferring resistance to tetracyclines, including doxycycline. TetM binds to the ribosome, preventing the binding of the antibiotic and maintaining protein synthesis[295]. In contrast, variants 5 to 7 are markerless. pConj variants further differ in their repertoire of TA systems and components of the T4SS. Of note, pConj variants 1, 3, 5 and 6 are found across the gonococcal population, whereas variants 2, 4 and 7 are restricted to particular lineages. This correlates with the high conjugation rates reported for pConj.1, while pConj.2 transfer is reduced due to changes in the T4SS component TrbL[296]. The transfer of the remaining pConj variants has not been examined to date.

pConj prevalence differs between geographical regions, with a negative correlation between a country's gross domestic product and the prevalence of *tetM*$^{+}$ pConj[290]. This correlation was not observed for markerless pConj, suggesting antibiotic use is a driver of pConj prevalence. Of note,

coinciding with a shift towards doxycycline treatment for chlamydia and the introduction of Doxy-PEP in the US[297], an increase in *tetM*$^{+}$ isolates has been reported, rising from below 10% in 2020 to over 35% in 2024[298].

1.2.6.3 The β-lactamase plasmid, p*bla*

Around one in ten gonococci carries the β-lactamase plasmid p*bla*[286], conferring high-level penicillin resistance[4,299]. Seven structurally related β-lactamase plasmids have been described and named according to their geographic site of origin (Figure 7): p*bla*.Af (Africa, 5.6 kb), p*bla*.As (Asia, 7.4 kb), p*bla*.Au (Australia, 3.2 kb), p*bla*.Jo (Johannesburg, South Africa, 5.4 kb), p*bla*.Ni (Nîmes, France, 6.8 kb), p*bla*.NZ (New Zealand, 9.3 kb) and p*bla*.Rio (Rio de Janeiro, Brasil, 5.1 kb)[300-302]. All these plasmids carry bla_{TEM} on a truncated Tn*2* transposon[303], with TEM-1 and TEM-135 the most prevalent TEM variants in gonococci[290]. TEM-1 is widely distributed in the population, whereas TEM-135 is associated with distinct lineages[286].

p*bla*.Af and p*bla*.As were described in 1976[4,299]. However, p*bla*.As was postulated as the ancestral p*bla*, from which all other variants emerged following deletion (p*bla*.Af, p*bla*.Rio and p*bla*.Au, Figure 7A) or insertion (p*bla*.Jo and p*bla*.Ni, Figure 7B)[300] events. Of note, the emergence of deletion variants has been observed following transformation of p*bla*.As into gonococci[304].

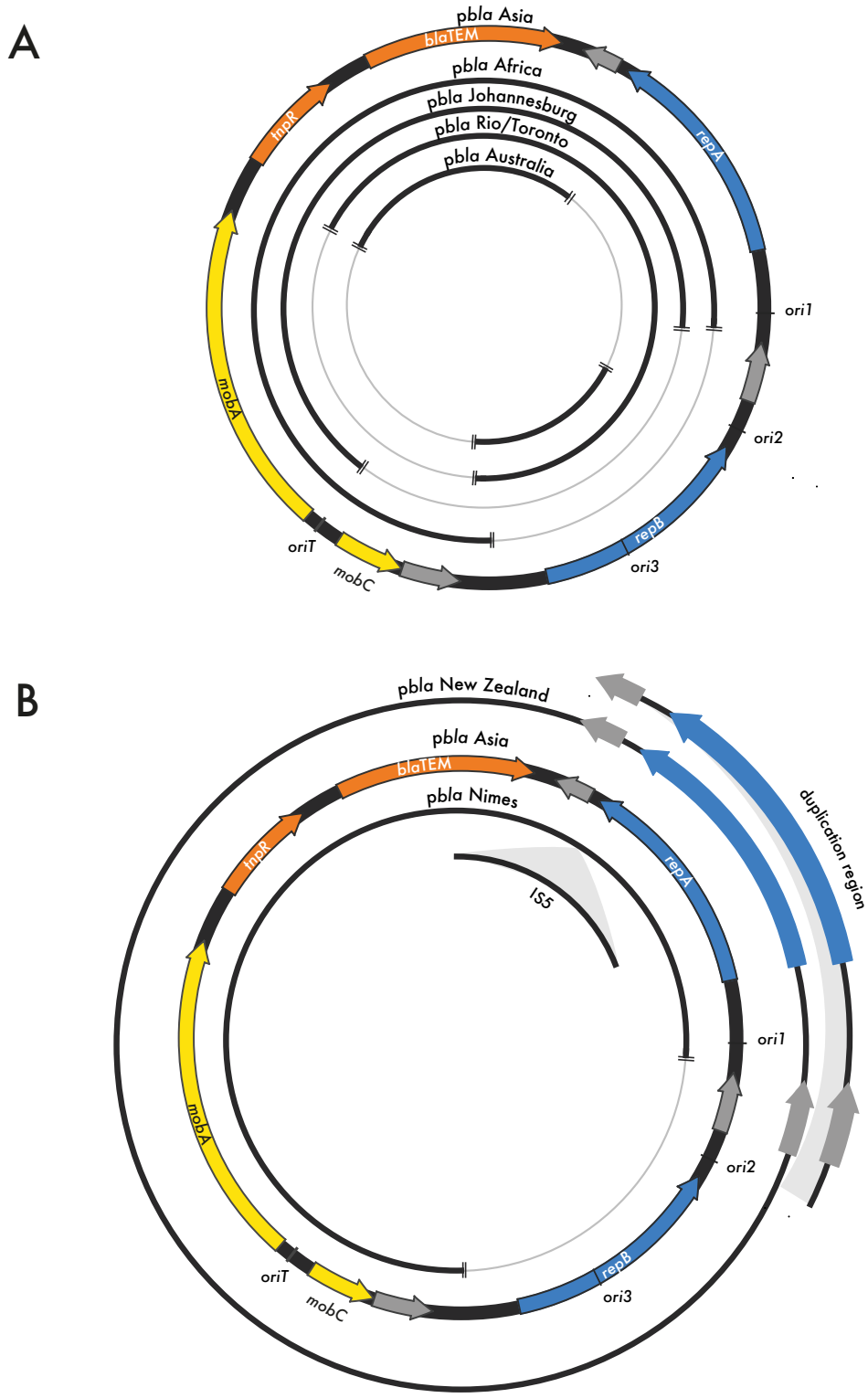

Figure 7: Schematic representation of the p*bla* deletion (A) and insertion variants (B).
Deleted regions (grey lines) and insertions/duplications relative to the Asia-type p*bla* are shown. ORFs are represented as arrows that are coloured according to gene products: yellow, mobilisation proteins; orange, Tn*2*-derived genes including bla_{TEM}; blue, replication initiation proteins; grey, undefined gene function.

p*bla*.As has three distinct origins of replication, *ori*1, *ori*2 and *ori*3, which can be utilised in different hosts[305,306]. In the laboratory, p*bla*.As can replicate in diverse bacteria, including different *Neisseria* spp., *E. coli*, *Salmonella typhimurium* var. Minnesota, *Haemophilus influenzae*, *Haemophilus parainfluenzae* and *Haemophilus ducreyi*[307]. p*bla oris* are iteron-based[306], with about half of the origin sequence consisting of an array of approximately 20 bp repeats (iterons) that serve as binding sites for the replication initiator proteins. Two replication initiation proteins, RepA and RepB, initiate replication at *ori*1 and *ori*2/*ori*3, respectively[306]. Replicon-based typing classified p*bla*.As as an IncW plasmid with an inactive IncFII replicon[306]. In *E. coli*, p*bla*.As preferentially replicates from *ori*2/*ori*3 using RepA and is incompatible with IncW plasmids. In contrast, p*bla* variants that lack *ori*2/*ori*3 and *repB* initiate replication from *ori*1 and fail to co-exist with IncFII plasmids[306].

p*bla* is not mobile on its own, but can be mobilised in *E. coli* by several conjugative plasmids, including IncP, IncFIV, IncFII and IncIα plasmids[307]. In *N. gonorrhoeae*, the presence of p*bla* is associated with the conjugative plasmid pConj, which can transfer p*bla*[290,308]. The 1.9 kb p*bla* mobilisation region contains *mobA* and *mobC*, separated by an intergenic *oriT*[309]. Functional characterisation in *E. coli* strain S17-1, which contains integrated *tra* genes of conjugative plasmid RP4[310], identified MobA as a relaxase that specifically recognises and nicks the p*bla oriT* sequence; MobC was not required for efficient plasmid transfer[309]. However, it is unclear if the results obtained for p*bla* mobilisation in *E. coli* are relevant for p*bla* transfer by pConj *N. gonorrhoeae*.

p*bla*.Af and p*bla*.As are structurally identical except for a 1 826 bp fragment spanning *repB* and *ori*2/*ori*3 that is missing in p*bla*.Af[286,300] (Figure 7A). p*bla*.Jo has a 2 560 bp deletion relative to p*bla*.Af that includes *repB* and *ori*2/*ori*3*,* but also *mobC* (Figure 7A)[311]. The p*bla*.Rio 2 270 bp deletion spans the *mob*/*oriT* region (Figure 7A), and there are conflicting reports about the mobility of this variant[312-314]. This is highly relevant as p*bla*.Rio is associated with the TEM-135[315], which is of particular concern due to its potential to evolve into an ESBL[316]. p*bla*.Au (3.2 kb) is the smallest

described p*bla* variant to date[302]. It resembles p*bla*.Rio with a deletion of 2 273 bp (including the *mob*/*oriT* region, Figure 7A) and its association with TEM-135, but has a further 1 885 bp deletion comprising *ori*1 and truncating *repA*[290,302].

p*bla*.NZ and p*bla*.Ni are variants with insertions downstream of bla_{TEM}[300]. p*bla*.NZ has an 1 183 bp duplication that includes *repA* (Figure 7B). p*bla*.Ni lacks *mobC* and *repB* and has an IS*5* insertion between bla_{TEM} and *repA* (Figure 7B).

To date, plasmid variants have been identified by restriction digestion and PCR-based assays[317-319]. Difficulties of assembling p*bla* from short read sequences[286,320], a result of several repeated sequences on the plasmid[300], have limited analysis of the prevalence and distribution of different p*bla* variants in gonococci, and their associations with TEM variants remain poorly understood.

1.3 Project aims

The objective of this thesis was to understand plasmid-mediated β-lactam resistance in *N. gonorrhoeae*. Specifically, I aimed to:

i) Develop a plasmid typing scheme that identifies p*bla* variants from short-read whole genome sequences. By applying the typing scheme, I aimed to assess the distribution of p*bla* variants in the gonococcal population.

ii) Elucidate the basis for the distribution of p*bla* variants in gonococci, characterising the mobilisation, resistance levels, and fitness costs of p*bla* variants.

iii) Examine the impact of RMSs on plasmid transfer within the *N. gonorrhoeae* population.

By complementing bioinformatic analyses with molecular biology approaches, the object of this thesis is to define the molecular determinants of plasmid mediated β-lactam resistance in gonococci.

2 Materials and Methods

2.1 Bioinformatic analysis

2.1.1 Whole genome sequences

Gonococcal whole genome sequences (WGS) in the PubMLST database (15 664 sequences, accessed 28th July 2022) were analysed on the BIGSdb platform[321]. Isolates with ambiguous ribosomal multilocus sequence type (rMLST, *e.g.* incorrect assignment of species)[322] and duplicated entries were discarded, resulting in a dataset of 15 532 isolates from 1928 to 2022, originating from 66 countries (Appendix, Supplementary Table S1).

2.1.2 Characterisation of p*bla*

The nucleotide sequence of pJD4 (Genbank accession NC_002098.1; representative p*bla* Asia variant)[323] was blasted (BLASTn with expect threshold: 0.05, word size: 28, match/mismatch scores: 1, -2, linear gap costs) against the NCBI nucleotide collection[324] to characterise the host range of p*bla*. The amino acid sequences of individual open reading frames (ORFs) were used for BLASTp search against the NCBI non-redundant protein sequence database[324] (expect threshold: 0.05, word size: 6, BLOSUM62 scoring matrix, gap costs: 11 existence, 1 extension). Furthermore, p*bla* RepA and RepB sequences were compared to RepA of the IncFII plasmid R1[325] and IncW plasmid R388[326] using ClustalW with default parameters[327].

2.1.3 Protein structure predictions

The structures of the NEIS2964 monomer, homodimers of NEIS2962 and RSF1010 MobC (GenBank accession: S96966.1) and NEIS2962 with the p*bla oriT* sequence[309] were predicted with

AlphaFold3[328] and visualised with PyMol v2.5.4[329]. Charge distributions were visualised with the Adaptive Poisson-Boltzmann Solver (APBS) electrostatics plugin[330].

Hydrophobicity plots of NEIS2964 were generated with ProtScale[331] using the Hydropath./Kyte and Doolittle scale. To identify conserved residues of NEIS2964, homologues were identified using BLASTp against the NCBI non-redundant protein database[324], followed by multiple sequence alignments with PROMALS[9]. The alignment was analysed to determine highly conserved residues based on sequence conservation scores, and key residues were mapped onto the predicted AlphaFold structure. Conserved genes flanking NEIS2964 were determined using WebFlaGs[12] with BLASTp against NCBI RefSeq database (updated 29th January 2021, e-value <$1e^{-10}$) and three jackhmmr iterations. Subsequently, hits of conserved neighbours (WP_140450222.1, WP_010904468.1 and WP_012881329.1) were queried as above to assess their co-occurrence with NEIS2964.

2.1.4 Typing of p*bla* variants

Published sequences of p*bla* deletion variants (Genbank accessions NZ_LT591905.1, p*bla*.1; DQ355980.1, p*bla*.3; HM756641.1, p*bla*.4; KJ842484, p*bla*.6) were mapped onto pJD4 (NC_002098.1, p*bla*.2) in Snapgene v6.1.1 (Insightful Science; available from snapgene.com) to identify variant-specific deletions and establish the gene presence/absence matrix for the p*bla* typing scheme. The published insertion/repeat sequences U20421 and U20422.1 were queried (BLASTn, word size: 11, match/mismatch scores: 2, -3, linear gap costs) against the isolate dataset (Appendix, Supplementary Table S1) in the PubMLST database[321]. Hits with an alignment length of >500 bp (IS*5* sequence U20421) or >50% (repeat sequence U20422.1) were assessed for their genomic context by extracting the relevant contig from the sequencing bin and identifying the adjacent ORFs. Additionally, the IS*5* sequence was blasted (BLASTn, word size: 28, match/mismatch scores: 1, -2, linear gap costs) against the NCBI nucleotide collection[324].

p*bla*-carrying gonococci in the dataset (n = 2 758) were identified by the presence of NEIS2960, which encodes a hypothetical protein that is present in all p*bla* variants[290]. Gene absence was confirmed by blasting available alleles against plasmid sequences using the sequence tag scan function on PubMLST (minimum identity: 97%, minimum alignment length: 50% and BLASTn word size: 20). Plasmids were typed according to the characteristic gene presence/absence patterns of variants, with incompletely assembled loci considered as present.

To check the accuracy of the typing scheme, short-read sequences of the p*bla*-containing WHO reference strains (WHO M, WHO N and WHO O), for which plasmid sequences have been characterised by hybrid assemblies of long and short-read sequences[320], were used. Additionally, 16 gonococcal isolates, from nine Ng_cgc$_{400}$ lineages, eight countries and isolated from 1986 to 2015, containing different p*bla* variants were randomly selected from the gonococcal dataset (Appendix, Supplementary Table S2) and typed using the scheme. p*bla*-containing contigs were then extracted from the sequence bin and aligned to pJD4 (NC_002098.1) to identify deleted regions and confirm the completeness of the remaining sequences. Sequencing quality was assessed by comparing sequencing parameters, such as the number of contigs, N50, L50, percentage of alleles designated, and percentage of loci tagged in isolates, which are accessible on PubMLST.

2.1.5 Analysis of the distribution of p*bla* variants

The *N. gonorrhoeae* population structure was resolved using core genome MLST (cgMLST v1, accessible on https://pubmlst.org/organisms/neisseria-spp[321]), which groups gonococcal isolates according to allelic designations in 1 668 loci, previously determined to be core to the gonococcus (*i.e.* present in >95% of gonococcal isolates)[2]. At every locus, each different allele is given a unique integer, and isolates are grouped into single-linkage clusters according to the number of allelic differences. A cut-off of 400 allelic differences resolves the population into

discrete *N. gonorrhoeae* core genome clusters (Ng_cgc_{400})[2]. A minimal spanning tree was generated with GrapeTree[332]. NEIS2220 (*trbM*) was used to detect the presence of pConj in individual isolates[286]. Previously, pConj variants had been assigned by clustering according to allelic differences in plasmid core genes with a cut-off of 5 allelic differences (Ng_cp_5)[286]. However, the expansion of the database resulted in the unification of Ng_cp_5s, and previously described Ng_cp_5 pConj variant assignments[286] no longer match. Therefore, pConj variants were assigned by clustering pConj sequences in the dataset together with previously characterised pConj variants[290] using pConj core genome loci[290] and GrapeTree[332].

2.1.6 Identification of p*bla* in *Haemophilus* spp. and *Neisseria* spp.

Tn*2* carrying isolates of *Haemophilus* spp. and *Neisseria* spp. were identified by blasting the sequence of Tn*2* (GenBank accession: LC091537.1) against the *Haemophilus* (accessed 24th July 2024, 6 896 isolates, 12 species) and *Neisseria* (accessed 24th July 2024, 41 158 isolates, 33 species) BIGSdb databases[321] (BLASTn search with word size: 11, scoring: reward: 2; penalty: -3; gap open: 5; gap extend: 2, sequence identity >97%, alignment length >50% of query length), the presence of the TnpA transposase was assessed independently in hits. p*bla*-like plasmids were identified by the presence of NEIS2960. Hits with a sequence identity >80% and alignment length >50% were further verified by assessing the presence of NEIS2358 (*repA*).

2.1.7 Characterisation of *H. ducreyi* p*bla*

DNA from *H. ducreyi* strains HD183 (PubMLST id: 16144) and DMC64 (PubMLST id: 16150) was provided by Prof. S. Spinola (Indiana University School of Medicine). Chromosomal plasmid integration was tested using primers TE45 and TE46, which bind to the flanking chromosomal regions of the plasmid insertion site, in combination with TE44 and TE42, respectively, which bind within the plasmid sequence. The primers were designed using the published genome assembly of

H. ducreyi DMC64 (GenBank accession: CP011230.1); all primers are available in Supplementary Table S3 in the Appendix.

The presence of p*bla* was verified using the primer pairs JDA/JDB and p*bla*_seq_10fw/ p*bla*_seq_2rv, generating overlapping PCR products only in the presence of circular p*bla* DNA. Plasmids were sequenced by Sanger sequencing using the p*bla*_seq primers.

2.1.8 Phylogenetic analysis of p*bla*

To detect phylogenetic relationships, a subset of the p*bla*-containing isolates on PubMLST[321] was selected. All p*bla*-containing isolates predating 2000 with available sequence data (n = 35) were included in the dataset. Isolates between 2000 and 2022 (n = 379) were randomly selected using the r sample function, conserving the ratio between variants in the population (70% p*bla*.1, 14% p*bla*.2, 16% p*bla*.3). This resulted in a dataset of 414 p*bla*-carrying isolates (Appendix, Supplementary Table S4). Plasmid reads were mapped onto the *H. ducreyi* DMC64 p*bla* with Snippy v4.6.0 (minimum coverage = 4, base quality = 25). Subsequently, multiple sequence alignments were generated with snippy-core v4.6.0 and snippy-clean v4.6.0. A maximum likelihood tree was generated using RaxML-ng v1.2.2[333]. The tree was rooted at *H. ducreyi* DMC64 p*bla* and visualised with the R libraries ape[334] and ggtree[335].

2.1.9 Methylation analysis of NgoAV strains

FA1090 strains with different *hsdS* (Table 1) were sequenced using Nanopore (v14 library prep chemistry, R10.4.1 flow cells, PlasmidSaurus). Reads were aligned to the FA1090 genome (PubMLST id: 2855) using Dorado[336], and the aligned files were sorted and indexed with Samtools[337]. Genome-wide base modifications and predicted motifs were called with Modkit[338] pileup and motif search.

2.2 Bacterial strains and growth conditions

Strains and plasmids used in this work are listed in Tables 1 and 2, respectively. *E. coli* DH5α was grown on Luria Bertani (LB) agar at 37°C or in liquid LB with shaking at 180 r.p.m.. *N. gonorrhoeae* strains were grown on Gonococcal Base Medium (GCB) agar or liquid medium (GCBL) supplemented with 1% Vitox (Oxoid) at 37°C, 5% CO_2; liquid cultures were shaken at 180 r.p.m.. For experiments requiring extended growth, *N. gonorrhoeae* was grown in fastidious broth (FB)[339].

Antibiotics were added at the following concentrations: for *E. coli*, carbenicillin (carb) 100 μg/ml; for *N. gonorrhoeae*, carbenicillin 2.5 μg/ml; erythromycin (ery) 1 μg/ml; kanamycin (kan) 50 μg/ml; tetracycline (tet) 2 μg/ml.

2.2.1 Strains used in this study

Table 1: Strains used in this study.

***N. gonorrhoeae* clinical and lab strains**	**Ng_cgc_400**	**PubMLST id**	**Reference**
FA1090 wt	286	2855	a kind gift from Prof. Ann Jerse
WHO M	3	31663	[320]
WHO N	54	31764	[320]
WHO F	316	31562	[320]
2086_K	21	31764	[240]
44569	34	36296	[240]
44593	364	36284	[240]
55496	34	36267	[240]

60755	21	36291	[240]
NG106	3	36305	a kind gift from Dr Samantha McKeand
NG102	296	36303	this study
NG028	321	127755	a kind gift from Dr Samantha McKeand
NG015	3	127742	a kind gift from Dr Samantha McKeand
NG064	29	127791	a kind gift from Dr Samantha McKeand
NG114	25	127838	a kind gift from Dr Samantha McKeand
NG149	377	127872	a kind gift from Dr Samantha McKeand
NG296	25	128011	a kind gift from Dr Samantha McKeand
***N. gonorrhoeae pilD::aph(3)* strains**		**Background**	**Reference**
FA1090 *pilD::aph(3)*		FA1090	[340]
FA1090 *pilD::aph(3)* pConj.1		FA1090	[340]
FA1090 *pilD::aph(3) ngoAV::44569*		FA1090	this study
FA1090 *pilD::aph(3) ngoAV::60755*		FA1090	this study
FA1090 *pilD::aph(3) ngoAV::ng102*		FA1090	this study
FA1090 *pilD::aph(3) nlaIV* ON		FA1090	this study

FA1090 *pilD::aph(3) nlaIV* OFF	FA1090	this study
FA1090 *pilD::aph(3)* NEIS2765 ON	FA1090	this study
FA1090 *pilD::aph(3)* NEIS2765 OFF	FA1090	this study
2086_K *pilD::aph(3)*	2086_K	this study
NG015 *pilD::aph(3)*	NG015	this study
NG064 *pilD::aph(3)*	NG064	this study
NG114 *pilD::aph(3)*	NG114	this study
NG149 *pilD::aph(3)*	NG149	this study
NG106 *pilD::aph(3)*	NG106	this study
***pilD::ermC* strains**	**Background**	**Reference**
FA1090 *pilD::ermC* p*bla*.1	FA1090	this study
FA1090 *pilD::ermC* p*bla*.2	FA1090	this study
FA1090 *pilD::ermC* p*bla*.3	FA1090	this study
FA1090 *pilD::ermC* p*bla*.2$^{\text{TEM-135}}$	FA1090	this study
FA1090 *pilD::ermC* p*bla*.2 TEM-1$^{\text{P14S}}$	FA1090	this study
FA1090 *pilD::ermC* p*bla*.2$^{\Delta\text{NEIS2961}}$ pConj.1	FA1090	this study
FA1090 *pilD::ermC* p*bla*.2$^{\Delta\text{NEIS2962}}$ pConj.1	FA1090	this study
FA1090 *pilD::ermC* p*bla*.2$^{\Delta\text{NEIS2964}}$ pConj.1	FA1090	this study

FA1090 *pilD::ermC* p*bla*.1 pConj.1	FA1090	this study
FA1090 *pilD::ermC* p*bla*.2 pConj.1	FA1090	this study
FA1090 *pilD::ermC* p*bla*.3 pConj.1	FA1090	this study
FA1090 *pilD::ermC* p*bla*.1 pConj.2	FA1090	this study
FA1090 *pilD::ermC* p*bla*.1 pConj.3	FA1090	this study
FA1090 *pilD::ermC* p*bla*.1 pConj.4	FA1090	this study
FA1090 *pilD::ermC* p*bla*.1 pConj.7^{tetM+}	FA1090	this study
2086_K *pilD::ermC* p*bla*.1 pConj.1	2086_K	this study
NG015 *pilD::ermC* p*bla*.1 pConj.1	NG015	this study
NG064 *pilD::ermC* p*bla*.1 pConj.3	NG064	this study
NG064 *pilD::ermC* p*bla*.1	NG064	this study
NG064 *pilD::ermC* p*bla*.2	NG064	this study
NG064 *pilD::ermC* p*bla*.3	NG064	this study
NG114 *pilD::ermC* p*bla*.1 pConj.1	NG114	this study
NG149 *pilD::ermC* p*bla*.1 pConj.1	NG149	this study
NG106 *pilD::ermC* p*bla*.1 pConj.1	NG106	this study
***N. gonorrhoeae* MIC strains**		
FA1090 p*bla*.1	FA1090	this study

FA1090 p*bla*.2	FA1090	this study
FA1090 p*bla*.3	FA1090	this study
FA1090 p*bla*.2$^{TEM\text{-}1\ P14S}$	FA1090	this study
FA1090 p*bla*.2$^{TEM\text{-}135}$	FA1090	this study
FA1090 p*bla*.3$^{TEM\text{-}1}$	FA1090	this study
2086_K p*bla*.1	2086_K	this study
2086_K p*bla*.2	2086_K	this study
2086_K p*bla*.3	2086_K	this study
NG015 p*bla*.1	NG015	this study
NG064 p*bla*.1 pConj.3	NG064	this study
NG114 p*bla*.1	NG114	this study

2.2.2 Plasmids used in this study

Table 2: Plasmids constructed and used in this study

Plasmid	Origin	Comment	Reference
p*bla*.1	WHO M	sequence confirmed by hybrid assembly from long and short read sequences	[320]
p*bla*.2	WHO N	sequence confirmed by hybrid assembly from long and short read sequences	[320]

p*bla*.3	NG296	WT p*bla*.3 with $bla_{\text{TEM-135}}$	this study
p*bla*.2$^{\text{TEM-1 P14S}}$		modification of p*bla*.2 from WHO N	this study
p*bla*.2$^{\text{TEM-135}}$		modification of p*bla*.2 from WHO N	this study
p*bla*.3$^{\text{TEM1}}$		modification of p*bla*.3 from NG296	this study
p*bla*.2$^{\Delta\text{NEIS2961}}$		modification of p*bla*.2 from WHO N	this study
p*bla*.2$^{\Delta\text{NEIS2962}}$		modification of p*bla*.2 from WHO N	this study
p*bla*.2$^{\Delta\text{NEIS2964}}$		modification of p*bla*.2 from WHO N	this study
pConj.1	60755	WT pConj.1	[340]
pConj.2	44359		[296]
pConj.3	WHO N		[320]
pConj.4	55496		this study
pConj.7	NG028		this study
pConj.7^{tetM+}		modification of pConj.7 from NG028	this study
pCR2.1-TOPO		template for *ermC*	

2.3 Genetic methods

2.3.1 DNA extraction

Genomic DNA was extracted using the Wizard Genomic DNA Purification Kit (Promega) according to the manufacturer's protocol with minor modifications. In brief, strains grown overnight on plates were harvested, resuspended in 600 μl nuclei lysis solution and incubated for 5 minutes at 80°C. RNase (3 μl) was added and the suspension incubated for 30 minutes at 37°C. Proteins were precipitated by the addition of 200 μl protein precipitation solution. After vortexing for 20 seconds, tubes were incubated on ice for 5 minutes, then spun at 14 000 x *g* for 10 minutes. Supernatants were collected and DNA precipitated by the addition of 600 μl isopropanol. DNA was pelleted, washed thrice with 70% ethanol and resuspended in elution buffer (Qiagen).

Plasmids were purified with the Miniprep Kit (Sigma) as per the manufacturer's instructions. *E. coli* was grown in liquid culture supplemented with antibiotics, harvested by centrifugation and bacterial pellets were resuspended in 200 μl resuspension solution. *N. gonorrhoeae* was collected from overnight growth on agar and directly resuspended in 200 μl resuspension solution. Subsequently, bacteria were lysed with 200 μl lysis solution, neutralised with 350 μl neutralisation solution, and the debris was pelleted by centrifugation. The supernatant was loaded onto columns, washed with wash solution, and DNA was eluted in 40 μl nuclease-free water.

2.3.2 Gibson assembly

Gibson Assembly was performed using the NEBuilder HiFi DNA Assembly Kit (NEB) according to the manufacturer's instructions. DNA fragments were amplified using primers that introduced 15 - 30 bp overlap sequences. A total of 0.002 - 0.5 pmol of fragments (in 10 μl) was mixed with the Gibson Assembly Master Mix, which contains 5' exonuclease (T5), DNA polymerase, DNA ligase and

deoxynucleoside triphosphates. The reaction was incubated at 50°C for 1 hour, and the assembled product was transformed into *E. coli* DH5α cells (NEB, protocol E2611).

2.3.3 Agarose gel electrophoresis and gel extraction

Agarose gels consisted of 0.8% (w/v) agarose (Invitrogen) in 1x TAE buffer (40 mM Tris, 20 mM acetic acid, 1 mM EDTA) with SYBR Safe DNA dye (0.01%, ThermoFisher) added to visualise DNA. Samples were mixed with loading dye (30% v/v glycerol, 0.25% w/v bromophenol blue, 0.25% w/v xylene cyanol FF) and loaded onto gels. HyperLadder (1 kb, Bioline) served as a size reference. Samples were separated by electrophoresis (110 V) and visualised on Biorad gel Doc XR+.

2.3.4 Bacterial transformation

2.3.4.1 Transformation of chemically competent *E. coli*

Plasmid DNA (100 ng) was transformed into 50 μl chemically competent *E. coli* DH5α. Bacteria were incubated on ice for 30 minutes before heat shock (42°C, 45 seconds). For recovery, bacteria were placed on ice for 90 seconds, after which, 1 ml of LB was added. Bacteria were incubated for 1 hour at 37°C, with shaking at 180 r.p.m.. Transformants were selected by plating on selective media.

2.3.4.2 Spot transformation of *N. gonorrhoeae*

PCR constructs were transformed into *N. gonorrhoeae* as described previously[341]: 1 μg of DNA in water was spotted onto GCB plates and allowed to dry. Bacteria grown on GCB agar for 16 - 18 hours were harvested with a sterile cotton swab and streaked over the dried spots. Plates were incubated for 8 hours, then bacteria were transferred onto selective media and incubated overnight. Transformants were re-streaked onto selective media, and constructs were confirmed by PCR and Sanger sequencing.

2.3.4.3 Electroporation of *N. gonorrhoeae*

For electroporation of *N. gonorrhoeae*, bacteria grown overnight on GCB agar were resuspended in sterile PBS (Sigma), and the bacterial density was adjusted to $5x\,10^7$ CFU/ml. Bacteria were washed three times with 20% glycerol / 1% MOPS (Sigma) v/v and resuspended in a final volume of 50 μl 20% glycerol / 1% MOPS. A maximum of 12 μl of DNA was electroporated using the following settings: 2.5 kV, 200 Ω, 25 mF. Cells were recovered in 1 ml of GCBL supplemented with 2% Vitox, pelleted, resuspended and plated on GCB agar. Plates were incubated for 3 hours, after which the cells were collected and transferred to selective media. Plates were incubated overnight, and individual transformants were re-streaked onto selective agar before analysis.

2.4 Strain construction

Regions of interest were amplified using Herculase II fusion (Agilent) or PrimeSTAR GXL DNA (Takara Bio) polymerase according to the manufacturer's instructions with primers listed in Supplementary Table S3 (Appendix). To enable integration of the fragments by homologous recombination, constructs included approximately 1 kb of sequence up- and downstream of the gene of interest. If constructs did not contain a gonococcal DUS[342], it was included at the 5' end of the primer.

2.4.1 *N. gonorrhoeae pilD* knockouts

FA1090 *pilD::aph(3)* was kindly provided by Dr Wearn-Xin Yee. To use erythromycin resistance, *aph(3)* was replaced with *ermC*. For this, flanking regions were amplified from FA1090 using primers TE25/TE28 and TE26/TE29; *ermC* was amplified from pCR2.1-TOPO with TE22/TE23. Resulting PCR fragments were joined by Gibson assembly. The *pilD::ermC* fragment was reamplified with TE28/TE29, gel extracted and transformed into *N. gonorrhoeae*.

2.4.2 RMS modifications

FA1090 *nlaIV* ON/OFF, NEIS2765 ON/OFF and NgoAV recipient strains were generated by Dr Ana Cehovin. Donor strains with different NgoAV *hsdS* sequences were constructed by markerless gene editing[340], which uses a positive-negative selection cassette to genetically modify *N. gonorrhoeae* strains without introducing additional DNA sequences. First, the *hsdS* locus was replaced with the *aph(3)-galK* cassette. For this, upstream and downstream regions of NgoAV *hsdS* (NEIS2362) were amplified with PrimeSTAR GXL polymerase (Takara Bio) and primer pairs Ngo_AV_UpF/NgoAV_POpa_R and NgoAV_Kan_F/NEIS2391_Down_R using FA1090 genomic DNA as template; the *aph(3)-galK* cassette was amplified from FA1090 *fetA::aph(3)-galK* genomic DNA[340] provided by Dr Ana Cehovin using TE134/TE135. Fragments were joined by Gibson assembly, reamplified with NgoAV_AV_UpF/NEIS2391_Down_R and transformed into FA1090. Transformants were selected on kan. Next, the cassette was exchanged for the *hsdS* sequences amplified from *N. gonorrhoeae* 60755, NG102 or 44569 using primers NgoAV_AV_UpF/NEIS2391_Down_R. Transformants were selected on GCB agar supplemented with 6.4% (w/v) 2-deoxy-galactose (2-DOG, Merck). In the presence of GalK, 2-DOG is phosphorylated into 2-deoxy-galactose-1-phosphate, which is toxic to the gonococcus, so only transformants in which *galK* had been replaced survived. The *hsdS* sequence was confirmed by PCR and Sanger Sequencing.

2.4.3 Generation of plasmid-carrying *N. gonorrhoeae* strains by conjugation

While strains with p*bla* without pConj were generated by electroporation, pConj with/without p*bla* was introduced by conjugation. For this, donor and recipient strains with *pilD::ermC* and *pilD::aph(3)*, respectively, grown overnight on GCB agar, were collected with a sterile cotton swab and mixed by plating onto GCB agar. Plates were incubated for 6 hours, then bacteria were collected and plated on selective media. Individual colonies were analysed by PCR, confirming the

presence of p*bla* (primers JDA/JDB), pConj (primers *tetM*_UF/*tetM*_AR). To confirm strain identity, *porB* was amplified with PorF/PorR and sent for sequencing.

2.5 Plasmid modifications

2.5.1 Isogenic p*bla* variants

Isogenic p*bla* variants (p*bla*^{iso}) were constructed from p*bla*.2. To generate linear templates for p*bla*.1^{iso} and p*bla*.3^{iso}, p*bla*.2 was cut with *Hin*dIII-HF (NEB, for p*bla*.1^{iso}) or *Pvu*II-HF (NEB, for p*bla*.3^{iso}). The sequence corresponding to p*bla*.1^{iso} was amplified from linearised p*bla*.2 with primers TE18/TE19 and PrimeSTAR GXL polymerase (Takara Bio). Overlap sequences for Gibson assembly were introduced in a subsequent PCR with primers TE20/TE21, using the diluted product of the first PCR as template. p*bla*.3^{iso} was amplified in two fragments with primers TE7/TE17 and TE9/TE16, producing products with overlapping regions. Isogenic plasmid variants were assembled using Gibson Hifi master mix (NEB) and transformed into chemically competent *E. coli* DHα following standard procedures (NEB, protocol E2611). Plasmids were confirmed by Sanger sequencing.

2.5.2 Generation of *mob* mutants

p*bla*.2 NEIS2961 and NEIS2962 deletion variants (p*bla*.2$^{\Delta NEIS2961}$ and p*bla*.2$^{\Delta NEIS2962}$) were generated using PrimeSTAR polymerase. p*bla*.2 sequences were amplified by PCR with primers TE54/TE53 (p*bla*.2$^{\Delta NEIS2961}$) or TE50/TE51 (p*bla*.2$^{\Delta NEIS2962}$). Next, overhangs were introduced by PCR (TE55/TE54, p*bla*.2$^{\Delta NEIS2961}$; TE50/TE52, p*bla*.2$^{\Delta NEIS2962}$). PCR products containing overhangs were transformed into chemically competent *E. coli* DH5α, and plasmid sequences were confirmed by Sanger Sequencing.

To delete both copies of NEIS2964 from p*bla*, the *repB* containing fragment was amplified from p*bla*.2 using primers TE47/TE48. The plasmid backbone was amplified from p*bla*.1^{iso} with primers TE47/TE59. Overhangs were added to the *repB* and plasmid backbone fragments using primers TE48/TE60 and TE59/TE49, respectively. PCR products were joined by Gibson assembly and transformed into *E. coli* DH5α.

2.5.3 Introduction of TEM variants in different p*bla* backbones

Point mutations in bla_{TEM} were introduced using the RAIR method[343]. In summary, PCRs with the respective primers (TE56/TE57, p*bla*.2$^{TEM\text{-}135}$; TE63/TE64, p*bla*.2$^{TEM\text{-}1\ P14S}$; TE65/TE66, p*bla*.3$^{TEM\text{-}1}$) were performed using Herculase II fusion polymerase (Agilent), with p*bla*.2 or p*bla*.3 as template. PCR products were purified (Promega Wizard SV Gel and PCR Clean-up system) and transformed into chemically competent *E. coli* DH5α. bla_{TEM} nucleotide sequences were confirmed by Sanger sequencing using primers p*bla*_seq_1fw/p*bla*_seq_2rv.

2.5.4 Construction of pConj.7^{tetM+}

pConj.7^{tetM+} was constructed by introducing *tetM* from pConj.3 (*tetM* allele 1) into the genetic load region of pConj.7. *tetM* was amplified from *N. gonorrhoeae* WHO N using primers TE34/TE35 and Herculase II fusion polymerase. Flanking regions were amplified from pConj.7 using primer pairs TE36/TE37 and TE38/TE39. PCR fragments were joined by Gibson assembly, then the resulting fragment was amplified with TE36/TE39. The construct was introduced into *N. gonorrhoeae* NG028 by electroporation. The insertion was confirmed by Sanger sequencing, and pConj.7^{tetM+} was transferred into *N. gonorrhoeae* FA1090 Δ*pilD*::*ermC* p*bla*.1 by conjugation.

2.6 Bacterial growth and competition assays

2.6.1 Growth curves

Bacterial growth curves were determined in GCBL/1% Vitox inoculated at OD_{600} 0.1. Liquid cultures (200 µl) were incubated at 37°C, 5% CO_2, shaking at 200 r.p.m., and OD_{600} measurements were acquired every 20 minutes using the FLUOstar Omega Microplate Reader (BMG Labtech). For each strain, readings were acquired in three technical replicates, on three occasions (biological replicates). The maximum growth rate (μ_{max}), maximum OD (OD_{max}) and AUC were determined with the R growthrates package[344].

2.6.2 Competition assays

To measure the fitness costs of p*bla*, plasmids were introduced into FA1090 Δ*pilD*::*ermC* and competed against FA1090 Δ*pilD*::*aph(3)*. Strains grown overnight on GCB agar were resuspended in PBS and adjusted to an OD_{600} of 1 (~ 10^9 CFU/ml). Strains were mixed in a 1:1 ratio, serially diluted to 10^5 CFU/ml in 200 µl FB and grown at 37°C, 5% CO_2, with shaking at 180 r.p.m.. After 24 hours, strains were enumerated by spotting on GCB/kan and GCB/ery. Fitness costs (w) were calculated as follows:

$$w = \frac{ln(N_f/N_i)}{ln(N_{f,pbla}/N_{i,pbla})}$$

where w is the relative fitness of the p*bla*-carrying isolate compared to the plasmid-free isolate. N_i and N_f are the number of cells of the p*bla*-free clone at the beginning and end of the competition, respectively, $N_{i,pbla}$ and $N_{f,pbla}$ the number of the p*bla*-carrying clone. To correct for fitness costs imposed by the resistance markers, FA1090 Δ*pilD*::*ermC* was competed against FA1090 Δ*pilD*::*aph(3)*. All competitions were performed on four separate occasions.

2.6.3 Mobilisation and conjugation assays

p*bla* mobilisation by pConj was assessed in isogenic matings as previously described[296] with minor modifications. Donor (*pilD*::*ermC*) and recipient (*pilD*::*aph(3)*) strains were grown overnight on GCB agar, then inoculated in 5 ml GCBL/1% Vitox at an OD_{600} of 0.1 and grown to OD_{600} 0.6 - 0.8. The bacterial density was adjusted to 10^8 CFU/ml, and donor and recipient strains were mixed in a 10:1 ratio. Bacteria (5 µl) were spotted onto GCB agar, incubated for 6 hours at 37°C, 5% CO_2, then harvested in 200 µl GCBL, serially diluted and spotted in triplicate onto GCB agar with antibiotics (ery for the donors, kan for the recipients, kan/tet for pConj transconjugants, kan/carb for p*bla* transconjugants). Conjugation and mobilisation frequencies were defined as the number of transconjugants per recipient, and each conjugation was performed on at least three occasions.

2.7 Antibiotic susceptibility testing

Benzylpenicillin minimal inhibitory concentrations (MICs) were measured by broth microdilution[345]. Microdilution 96-well plates were prepared using two-fold serial dilutions of penicillin in a total volume of 50 µl water. The last column contained only water and served as growth control. For the bacterial inoculum, strains were grown overnight on GCB agar, resuspended in PBS (Sigma), their OD_{600} adjusted to 1.0 (equivalent of 10^9 CFU/ml) and diluted in 2x FB/2% Vitox to 10^5 CFU/ml. Bacteria (50 µl) were added to each well. Plates were incubated for 24 hours before measuring the OD_{600}. The MIC was defined as the first well with a reduction of OD_{600} >50% compared to the antibiotic-free well of the respective strain.

2.8 SDS-PAGE and Western blot analysis

To assess cellular TEM levels, strains were grown overnight on GCB agar and sub-cultured in GCBL/1% Vitox to mid-exponential phase. Bacterial cell lysates were prepared by the addition of 2x SDS-PAGE loading buffer to an equal volume of bacteria in liquid culture. A 10 µl sample was subjected to electrophoresis on 12% SDS-polyacrylamide gels and transferred to Amersham Protan nitrocellulose membranes (GE Healthcare) for 30 minutes at 25 V using the Trans-Blot Turbo System (Bio-Rad). Subsequently, membranes were incubated overnight in blocking buffer (PBS/0.5% Tween-20/5% milk), washed thrice for 5 minutes with PBS-T (PBS/0.5% Tween-20) and incubated with the primary antibodies (Rabbit anti-RecA, Abcam, ab63797, final dilution of 1 : 5 000; Mouse anti-TEM, Abcam, 8A5.A10, final dilution of 1 : 1 000) in blocking buffer for 2 hours at room temperature. After three 10 minutes washes with PBS-T, membranes were incubated with fluorophore-conjugated secondary antibodies (LI-COR Biosciences, 925-68071 IRDye® 680RD Goat anti-Rabbit IgG and 925-32210 IRDye® 800CW Goat anti-Mouse IgG) at a final dilution of 1 : 10 000 for 1 hour at room temperature. Membranes were washed thrice with PBS-T and dried before imaging. Band intensities indicated in immunoblots were quantified using the Image Studio software (LI-COR Biosciences) and normalised to protein levels of the RecA loading control.

2.9 Plasmid copy number estimation

DNA was extracted from 1 ml of mid-exponential phase liquid culture using the Wizard Genomic DNA Purification Kit (Promega) according to the manufacturer's instructions. For each strain, DNA was isolated on three independent occasions. Gene copy numbers of the chromosomal *recA* and plasmid *tnpR* were quantified using the QX200 Droplet Digital PCR system (Bio-Rad) according to the manufacturer's instructions. ddPCRs contained 1x EvaGreen supermix (Bio-Rad), 100 nM of each primer (TE79 and TE80 for *recA*; TE81 and TE82 for *tnpR*). To optimise template

concentrations, DNA titrations were performed. A total DNA concentration of 2 pg/reaction yielded appropriate positive and negative droplet counts for both targets and was used in all subsequent reactions. Droplets were generated using the automated droplet generator (Bio-Rad) employing 20 µl of PCR mixture and 70 µl of Droplet Generation Oil for EvaGreen (Bio-Rad). Prepared droplet emulsions were transferred into 96-well PCR plates, covered with pierceable foil and heat-sealed using the PX1 PCR Plate Sealer (Bio-Rad). PCR targets were amplified with the following cycling conditions: enzyme activation at 95°C for 5 minutes, followed by 39 cycles of denaturation at 95°C for 30 seconds, annealing and extension at 60°C for 1 minute. Droplets were stabilised by cooling to 4°C for 10 minutes and heating to 90°C for 5 minutes, before holding at 4°C. For each step, a 2.5°C/second ramp rate was introduced to ensure each droplet reached the correct temperature. After thermal cycling, data were acquired and analysed using the QX200 Droplet Reader together with the Quanta Soft Analysis software (Bio-Rad). Each reaction was performed on three occasions. Plasmid copy number per chromosome was calculated as *tnpR* copies / *recA* copies.

2.10 TEM mRNA expression

To analyse TEM expression in different strain backgrounds, p*bla*.1$^{TEM\text{-}1}$ carrying isolates were sub-cultured to mid-exponential phase in 5 ml GCBL/1% Vitox, bacteria harvested from 1 ml of culture, and RNA was extracted using the Qiagen RNeasy Mini Kit together with the RNA protect Reagent (Qiagen, #76506) and on-column RNase-free DNase I treatment (Qiagen, #79254, protocol RY28). RNA was subsequently reverse transcribed to cDNA using the LunaScript RT SuperMix Kit (NEB, #E3010). The cDNA was used in ddPCRs as described above with primers TE79/TE80 (*recA*) and TE97/TE98 (bla_{TEM}). No-RT and no-template reactions served as negative controls.

2.11 Statistical analyses

Data manipulation and analysis were performed in R version 4.1.1 using base R and the tidyverse package[346]. To calculate odds ratios, the odds.ratio function from the epitools package[347] was used. Plots were generated with ggplot2[348]. A p-value <0.05 was considered statistically significant.

3 Epidemiology and evolution of the gonococcal β-lactamase plasmid p*bla*

3.1 Characterisation of gonococcal p*bla*

To anticipate the functional properties of the gonococcal β-lactamase plasmid p*bla*, I started by characterising the 7.4 kb pJD4 (Genbank accession NC_002098.1). pJD4 represents the considered ancestral p*bla*, previously referred to as the Asia variant[300], and has nine ORFs that are grouped into Tn*2*-derived, replication, and mobilisation regions (Figure 8). The p*bla* resistance determinant bla_{TEM} is in a truncated Tn*2*[303], which also carries 84% of the *tnpR* resolvase gene, but lacks the *tnpA* transposase gene and the left inverted repeat[349,350].

The replication region contains NEIS2358 (*repA*) and NEIS2360 (*repB*) encoding the Rep replication initiation proteins required for initiation of replication at *ori*1 and *ori*2/*ori*3, respectively[306]. The *ori*s belong to the iteron family[306]; approximately half of each origin consists of an array of ~20 bp repeats which serve as binding sites for the Rep proteins[351].

The mobilisation region of p*bla* consists of an origin of transfer (*oriT*), flanked by NEIS2961 encoding a MobA relaxase and NEIS2962 (also annotated as *mobC*)[309]. Mob typing characterises plasmids according to their N-terminal relaxase domain[42], and classified p*bla* as a MobQ family plasmid.

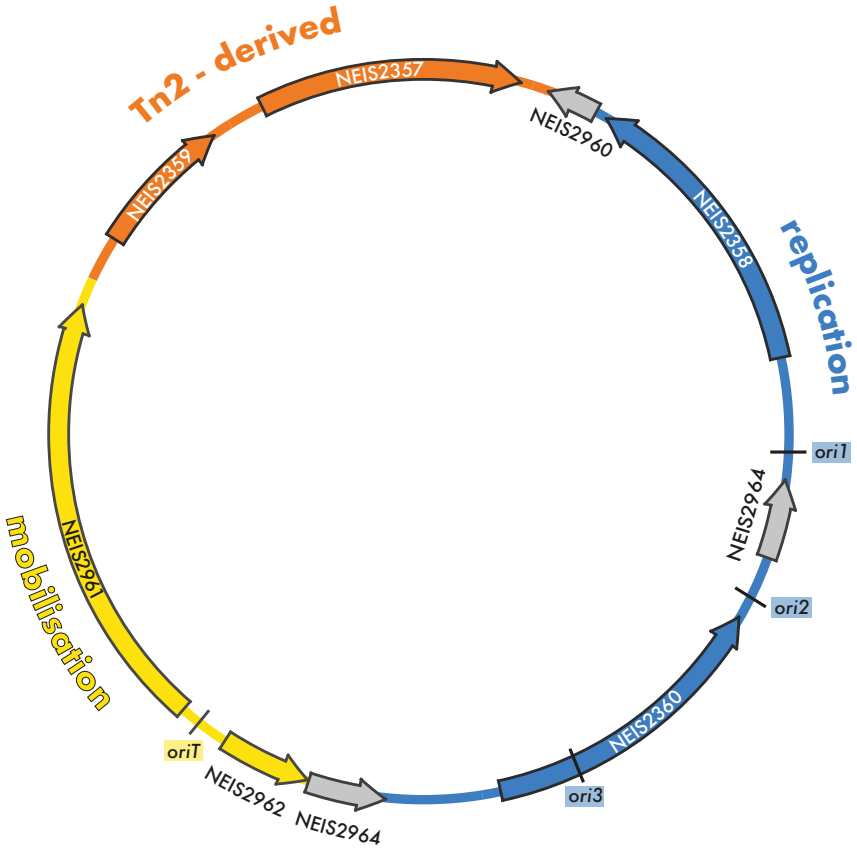

Figure 8: Gene organisation of the 7.4 kb p*bla*.
ORFs are indicated as arrows with colours reflecting their function: yellow, mobilisation; orange, Tn*2*-derived genes including bla_{TEM} (NEIS2357); blue, replication initiation; grey, unknown gene function.

Next to the mobilisation region is NEIS2964, which encodes an 86 amino acid protein of unknown function. A second copy of NEIS2964 is located between (*repA*) and NEIS2360 (*repB*). To gain insights into the function of NEIS2964, I predicted its structure using AlphaFold3 and assessed surface charge distribution and hydrophobicity using the APBS Electrostatics Plugin in PyMOL and Protscale[330,331]. NEIS2964 is predicted to contain two domains: an N-terminal hydrophobic α-helix and a charged globular C-terminal domain (Figure 9A and B). The high average hydrophobicity of the N-terminal α-helix (>1.2) predicted by Protscale, and its length (40.9 Å) matching the hydrophobic core of the lipid bilayer (30-40 Å)[352], suggests NEIS2964 is membrane-anchored. This was further supported by Phobius[353], a hidden Markov Model-based predictor for signal peptides and transmembrane segments, which identified the 33.6 Å α-helix segment between residues 6 and 26 as a transmembrane domain.

To identify structurally and functionally important sites, I investigated conserved residues between NEIS2964 homologs. BLASTp search (word size = 5, expect value = 0.05, gap costs = 11.1, BLOSUM62 matrix) of NEIS2964 against the NCBI non-redundant protein database identified 50 homologs from diverse Proteobacteria species (Appendix, Supplementary Table S5) with amino acid identity between 98.82 and 36.71% and query cover between 100 and 58%. Multiple sequence alignments with PROMALS[9] identified several residues with scores between 5 and 9, indicating medium to high conservation (Figure 9C). While the few N-terminal conserved residues had hydrophobic side-chains, conserved residues in the C-terminus are mainly positively charged and/or capable of π-stacking; non-covalent interactions between aromatic amino acids, where the electron-rich π orbitals of one aromatic group interact with those of another[354]. π -stacking of aromatic side chains of amino acids (such as phenylalanine, tyrosine and tryptophan) with the aromatic bases of DNA can facilitate protein-DNA interactions[355], suggesting the NEIS2964 C-terminal domain interacts with nucleic acids.

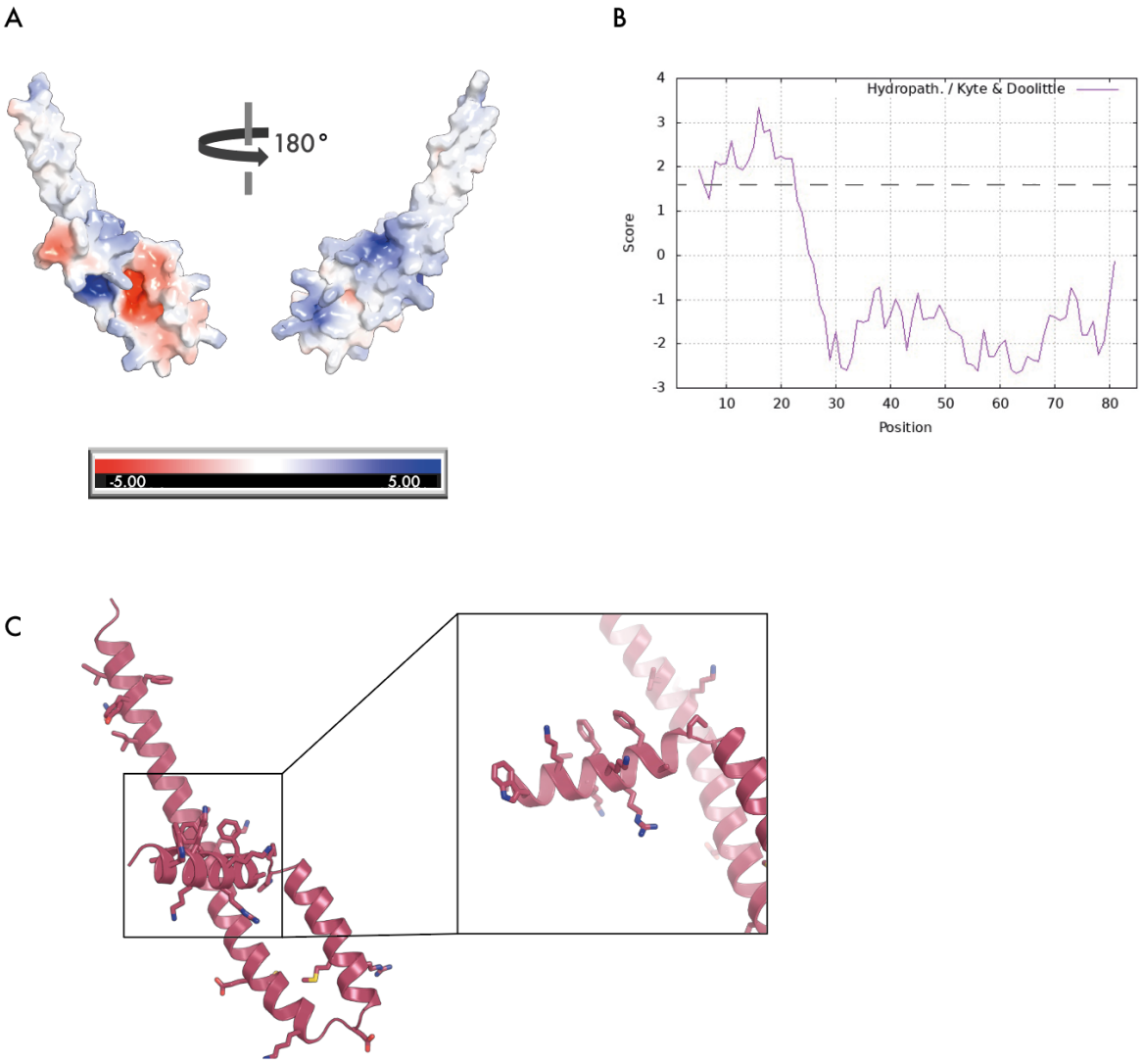

Figure 9: NEIS2964 contains a hydrophobic α-helix and a globular charged domain.
(A) AlphaFold3 structure prediction of NEIS2964 with negatively and positively charged regions indicated in red and blue, respectively. (B) Hydropathy plot of NEIS2964 indicates a N-terminal transmembrane domain. An average hydropathy score of >1.6 is suggestive of transmembrane segments and is indicated as a dashed line. (C) Conserved residues of NEIS2964 were identified with PROMALS[9] and mapped onto the AlphaFold3 structure prediction.

Conserved co-location with genes can provide further insights into gene function, and I further performed neighbourhood analysis of NEIS2964 using FlaGs (Flanking Genes) analysis[12]. The analysis revealed that NEIS2964 is often adjacent to *mob* and *rep* (Figure 10). However, using both *mobA* (WP_012881329.1)*, mobC* (WP_010904468.1) and *repB* (WP_140450222.1) as queries, I found that while *repB* is frequently found without NEIS2964-related genes, *mobA* and *mobC* show a consistent association with NEIS2964 (Figure 10). This suggests a role for NEIS2964 in plasmid mobilisation.

NEIS2960 is located between bla_{TEM} (NEIS2357) and *repA* (NEIS2358, Figure 8) and is highly conserved across p*bla* sequences (>98.2% nucleotide identity acrcross 2 758 plasmid sequences), with 97.7% of plasmids carrying NEIS2960 allele 1. NEIS2960 is predicted to be an antitoxin belonging to the VbhA family (Genbank accession: WP_164823310.1). No cognate Vbh family toxin (VbhT) is present on p*bla.* The gonococcal conjugative plasmid pConj encodes a VapD toxin, which has been indicated in forming a split TA system with a VapX antitoxin encoded by the cryptic plasmid pCryp or *vapX* on a chromosomal T4SS-encoding island[294,356]. Therefore, I also investigated whether a putative VbhT is present on the gonococcal chromosome or co-occurring plasmids. VbhT toxicity results from the inhibition of DNA replication by AMPylation of the DNA gyrase, mediated by the Fic domain of the toxin[357,358], and I identified NEIS1357 on the gonococcal chromosome as Fic domain (pfam 02661) protein, suggesting NEIS2960 and NEIS1357 could act as a split toxin-antitoxin system maintaining p*bla* in gonococci*.* However, NEIS1357 shares 99.46% amino acid identity to NmFic of *N. meningitidis* (Genbank accession: HGH6774163.1). No antitoxin gene has been described adjacent to NmFic. Instead, NmFic is regulated intramolecularly by an active site obstruction from an inhibitory α-helix at the C terminus, as well as multimerisation and self-adenylylation[359,360]. Therefore, it is unclear if NEIS2960 could contribute to p*bla* maintenance through interactions with NEIS1357.

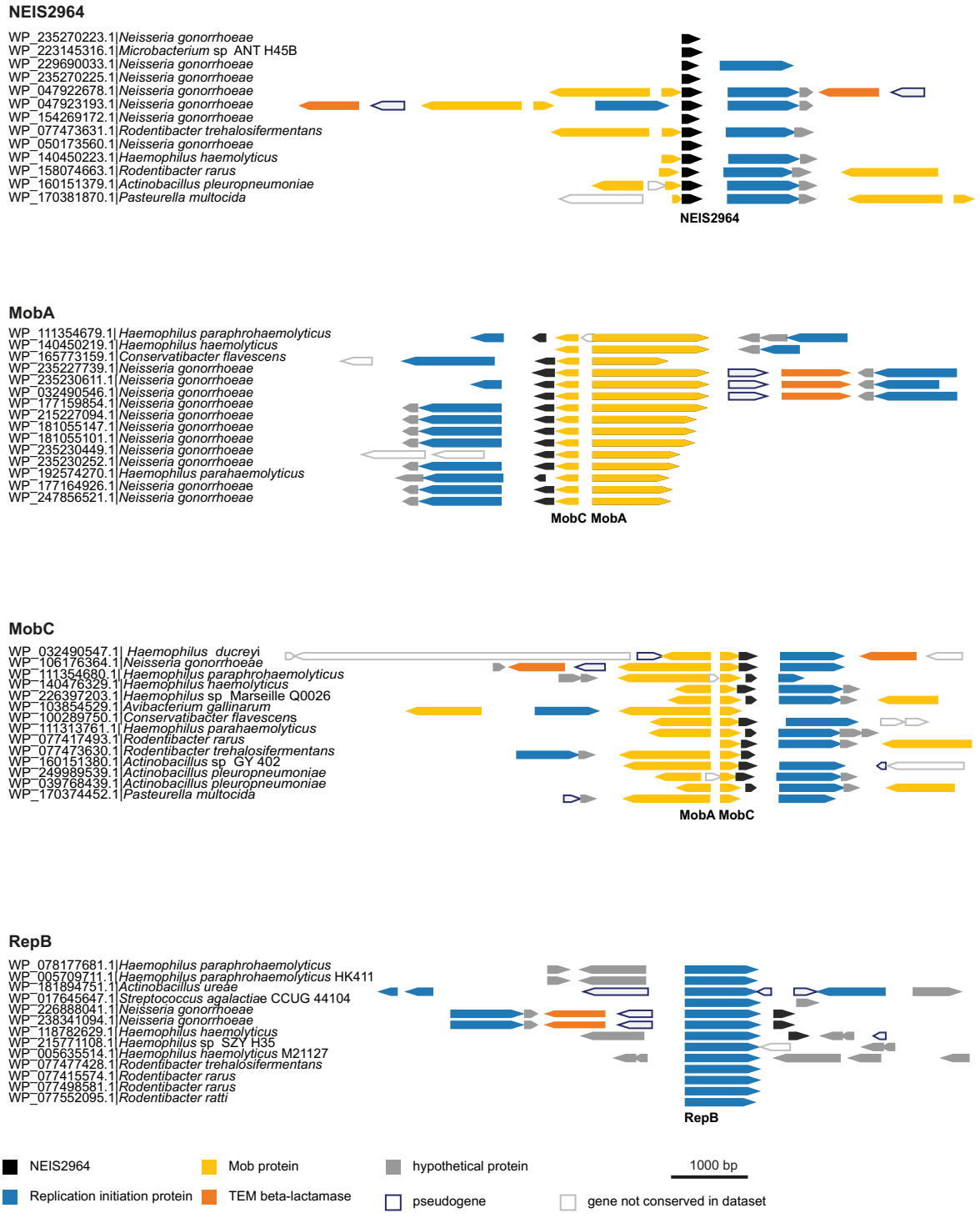

Figure 10: Neighbourhood analysis of NEIS2964, *mobA*, *mobC* and *repB*.
FlaGS queries the protein sequence against the RefSeq database[12]. The accession numbers and the species of origin of homologs are shown.

3.2 p*bla* epidemiology

3.2.1 p*bla* typing reveals three major variants circulate in gonococci

Understanding the variation and prevalence of p*bla* is essential for monitoring and predicting the spread of plasmid-mediated β-lactam resistance in the gonococcus. Seven variants of p*bla* ranging in size from 3.2 to 9.3 kb have been described previously[300,302,361]. However, *de novo* p*bla* assembly from short-read sequences is challenging due to repeat sequences on the plasmid, hindering the use of publicly available WGS to study the prevalence and distribution of p*bla* variants. Therefore, I exploited the characteristic gene presence/absence patterns of p*bla* variants to establish a typing scheme, Ng_p*bla*ST. As the WHO discourages the use of geographic regions in the naming of infectious diseases[362], I have proposed a numeric nomenclature for p*bla,* which numbers the variants in the order in which they were reported[4,233,302,361,363] (Table 3).

Initially, I analysed the available sequences of p*bla* variants to identify their differences in comparison to the 7.4 kb p*bla*.2[323]. Variants with a duplication of NEIS2358 and NEIS2964 (p*bla*.6) or an IS*5* insertion downstream of bla_{TEM} (p*bla*.7) have been reported only once[318,364]. I analysed available gonococcal isolates on PubMLST (n =15 532, Appendix, Supplementary Table S1), which includes 2 758 p*bla*-carrying isolates, for the presence of the duplicated sequence and IS*5*. I found a single p*bla*-carrying isolate (GHA-TMH-537, PubMLST id: 95801)[365] containing a duplication. GHA-TMH-537 is a hybrid assembly of Illumina and Oxford Nanopore sequences, with a 10.47 kb p*bla*. Of note, GHA-TMH-537 p*bla* has a duplication of NEIS2960, NEIS2357 (bla_{TEM}), NEIS2359 (*tnpR*), NEIS2358 (*repA*) and NEIS2360 (*repB*), and a deletion of NEIS2961 (*mobA*) and NEIS2962 (*mobC*), suggesting a novel p*bla* variant or an assembly error, as the presence of he pfour different *rep* genes in a small plasmid like p*bla* is unlikely. Additionally, IS*5* is not present in *Neisseria* spp. or in *Haemophilus* spp., but is found in the *E. coli* strain HB101 from which p*bla*.7 was isolated following

introduction of the gonococcal p*bla*[318]. Therefore, p*bla* insertion variants are rare or potential experimental artefacts[318], so were not included in the typing scheme.

p*bla*.1 (5.6 kb)[320] and p*bla*.4 (5.4 kb)[361] have deletions in the replication region. p*bla*.1 is structurally identical to p*bla*.2 except for the loss of a 1 826 bp fragment (Figure 11, Table 3), which includes NEIS2960 (*repB*), NEIS2964, *ori*2 and *ori*3. p*bla*.4 has a 2 560 bp deletion that includes *ori*2 and *ori*3. In addition to genes absent from p*bla*.1, p*bla*.4 lacks NEIS2962 (*mobC*) and the second copy of NEIS2964 (Figure 11, Table 3).

p*bla*.3 (5.1 kb)[313] and p*bla*.5 (3.2 kb)[302] have a 2 270 bp deletion spanning the *mob/oriT* region (Figure 11, Table 3). p*bla*.5 is the smallest p*bla* variant reported to date and has lost a further 1 885 bp including *ori*1 and NEIS2358 (*repA*), as well as NEIS2960 and NEIS2964.

The p*bla* typing scheme Ng_p*bla*ST characterises p*bla* variants according to their presence/absence (Table 3) and has been implemented on the PubMLST database (https://pubmlst.org/neisseria/). p*bla* loci are identified from the isolate sequence bin, with a gene considered as present when >50% of the gene with a sequence identity of >97% is identified. The low cutoff for sequence coverage was chosen to avoid misclassification of variants due to sequences at the ends of contigs being assigned as 'absent'. Although it is possible to distinguish between p*bla* variants based on the presence and absence of four genes (NEIS2961, NEIS2962, NEIS2964 and NEIS2360), plasmid variants were only assigned when the gene presence/absence pattern detected fully matched the scheme to avoid incorrect classification in isolates with low sequence quality.

Table 3: Gonococcal p*bla* variants and their defining features.

p*bla* variant	Previous name	First reported	Size (kb)	Defining gene absence	Reference
p*bla*.1	p*bla*.Af	1976	5.6	NEIS2360	233
p*bla*.2	p*bla*.As	1976	7.4		4
p*bla*.3	p*bla*.Rio	1984	5.1	NEIS2361, NEIS2362	363
p*bla*.4	p*bla*.Jo	2011	5.4	NEIS2360, NEIS2362, NEIS2964	361
p*bla*.5	p*bla*.Au	2012	3.2	NEIS2358, NEIS2361, NEIS2362, NEIS2964	302

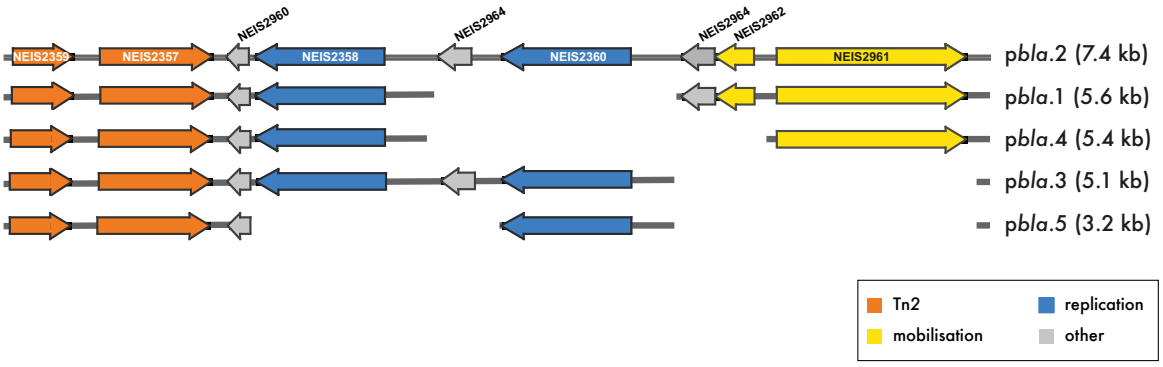

Figure 11: Schematic representation of the p*bla* deletion variants aligned to p*bla*.2.
Grey lines indicates aligned regions with arrows representing ORFs coloured according to their gene function; yellow, mobilisation proteins; orange, Tn*2*-derived genes including bla_{TEM} (NEIS2357); blue, replication initiation proteins; grey, unknown gene function.

Next, I validated Ng_p*bla*ST by examining available short-read WGS of the WHO reference strains M, N and O, which are known to harbour p*bla* and have been characterised by long-read sequencing[320,366]. Ng_p*bla*ST correctly identified the p*bla* variant in every instance from the short-read sequences alone. Additionally, I analysed short-read sequences from 16 gonococcal isolates containing p*bla* (Appendix, Supplementary Table S2) by manually extracting plasmid-loci containing contigs from the sequence bins and mapping them against the p*bla*.2 reference sequence; this also confirmed the Ng_p*bla*ST typing results.

With Ng_p*bla*ST, I characterised p*bla* variants in WGS of 2 758 p*bla*-carrying isolates from 50 countries across all six WHO regions; these isolates were recovered between 1979 and 2022 (Appendix, Supplementary Table S1). p*bla* variants were assigned in 74.6% of p*bla*-carrying isolates. The remaining sequences showed uncharacteristic gene presence/absence patterns, which could indicate novel variants or poor WGS quality. When assembling genomes from the longest to the shortest contig, the N50 is the length of the shortest contig when half the total genome has been assembled[367]; a low N50 can be indicative of low-quality genome assemblies. The sequences of isolates with uncharacterised p*bla* had a significantly lower N50 than isolates with typed p*bla* (average N50 untyped = 59578.6 *vs*. average N50 typed = 78270.6, two sample t-test p <0.001). This suggests the p*bla* variants in these isolates could not be identified due to poor sequencing quality, rather than due to the presence of novel variants.

Of the typed isolates (2 054), only six and three isolates carry p*bla*.4 and p*bla*.5, respectively. Therefore, p*bla*.1 (1 433/2 054, 69.7 %), p*bla*.3 (326/2 054, 15.8%) and p*bla*.2 (286/2 054, 13.9%) account for >99% of all typeable p*bla* in the PubMLST database. Having implemented Ng_p*bla*ST and identified the major p*bla* variants, I next analysed whether these variants are associated with distinct alleles of p*bla* genes and investigated their distribution in the gonococcus.

3.2.2 p*bla* variants are associated with distinct TEM variants

All p*bla* variants carry bla_{TEM}, conferring resistance to penicillins. There are 59 bla_{TEM} alleles in the 2 157 p*bla* sequences with assigned bla_{TEM} allele in the PubMLST database (cutoff date: 28th July 2022, 78.2% of all p*bla* sequences). TEM-1 (encoded by alleles 3, 9, 16, 18, 19, 21, 22, 25, 29, 31, 41, 44, 53, 55, 70, 80, 91, 93 and 105) is the most prevalent TEM variant, accounting for 59.6% (1 286/2 157) of sequences, followed by TEM-135 (alleles 2, 8, 26, 42, 43, 60, 65; 24.3%, 525/2,157) and allele 6 (11.1%, 240/2157). Together, these three TEM variants account for 95% of TEM encoded by p*bla*. TEM-135 differs from TEM-1 by an M182T substitution, located outside of the active site (Figure 12A and B). The M182T substitution was found to slightly reduce penicillin resistance in *E. coli*[285]. However, it is often present in ESBLs from *E. coli, K. pneumoniae* and *Salmonella* spp.[368], and compensates for the destabilising effects of mutations in the active site, so it is considered a 'stepping stone' mutation to becoming an ESBL[368,369]. Individual gonococcal isolates carry alleles with substitutions at positions P14, R61, L201, A224 and A248 in addition to M182T. These substitutions have not been characterised to date. The third most prevalent gonococcal TEM, encoded by allele 6, has a P14S substitution (Figure 12A) which is in the leader peptide, and is found in a subpopulation of p*bla*.1.

p*bla* variants are associated with distinct TEMs (Figure 12C). For example, 98.3% of p*bla*.3 encode TEM-135, while p*bla*.2 harbours TEM-1 or TEM-135 at an approximately equal frequency (44.5% and 49.5%, respectively). p*bla*.1 mainly encodes TEM-1 (76.5% of isolates with this p*bla*), TEM-1_{P14S} (17.7%) and rarely TEM-135 (1.78%). The associations of p*bla* variants with distinct TEM variants, especially p*bla*.3 with the ESBL-permissive TEM-135 (OR = 66.9, chi^2-test p <0.001), highlight the importance of understanding their global spread.

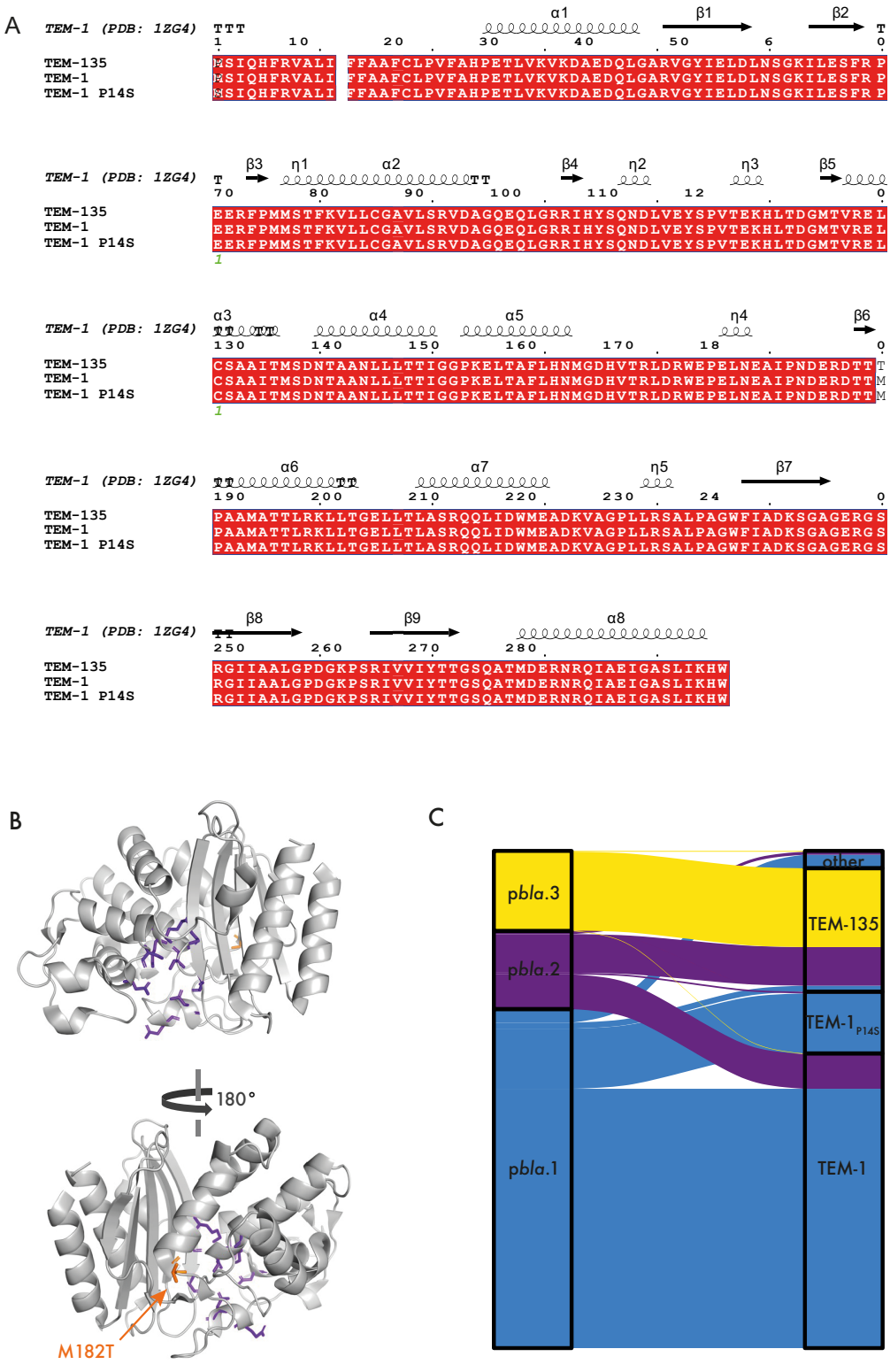

Figure 12: TEM-1, TEM-135 and TEM-1_{P14S} are the major TEMs encoded by p*bla*.
(A) Alignment of TEM-135, TEM-1 and TEM-1_{P14S}. Amino acid sequences were aligned with COBALT[3] and visualised with ESprit[5], displaying secondary structure elements (*i.e.* α-helices and β-sheets) of TEM-1 (PDB: 1ZG4) above the alignment. (B) Structure of TEM-135 (PDB: 1NY0) with key active site residues indicated in purple. The M182T substitution is shown in orange. (C) Proportion of p*bla* variants (left) and their TEMs (right). p*bla*.3 is significantly associated with TEM-135. p*bla*.2 carries TEM-1 and TEM-135 at equal frequencies, whilst p*bla*.1 mainly carries TEM-1 and TEM-1_{P14S}.

3.2.3 p*bla* variants are associated with geographic regions

Next, I analysed the distribution of p*bla* variants in a global dataset of 15 532 *N. gonorrhoeae* isolates from 66 countries and isolated from 1928 to 2022 (Appendix, Supplementary Table S1). p*bla* is present in 17.8% of the isolates (2 758/15 532) and its prevalence varies between geographic region (chi^2-test, p <0.001, Figure 13). p*bla*-carriage is highest in isolates from Africa (46.4%, 185/399; OR = 5, chi^2-test p <0.001) and lowest in North America (6.9%).

Furthermore, p*bla* variants differ in their global distribution. The most prevalent variant, p*bla*.1, is found worldwide. In contrast, p*bla*.2 is associated with isolates from China (OR = 32.0, chi^2-test p <0.001), while p*bla*.3 is more frequently found in isolates from HICs (OR = 3.0, chi^2-test p <0.001).

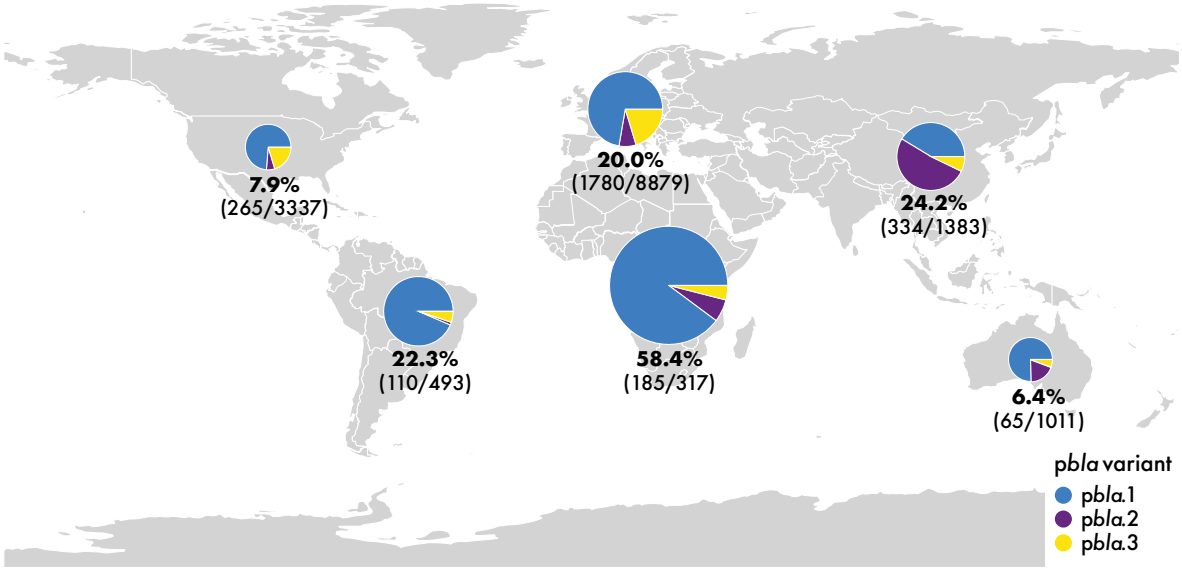

Figure 13: p*bla* prevalence in different geographic regions.
The size of pie charts depicts p*bla* prevalence in each region with p*bla* variants indicated in colours. The percentage of isolates with p*bla* and absolute numbers are given below the pie chart. p*bla*.1 is the most prevalent variant in all regions except Asia, where p*bla*.2 dominates. p*bla*.3 is more frequently found in Europe and North America.

3.2.4 p*bla* variants are associated with distinct lineages

I next assessed whether the high plasmid prevalence in certain geographical regions is driven by distinct lineages in those locations. The gonococcal population structure can be resolved by clustering isolates according to 1 668 loci that constitute the *N. gonorrhoeae* core genome (*i.e.* loci that are present in >95% of gonococci)[2]. A cut-off of 400 allelic differences has been used previously to group *N. gonorrhoeae* isolates into core genome clusters (Ng_cgc_{400}) that are stable over time[2], and was employed here. Isolates from Ng_cgc_{400} 21 and 34 are prevalent in Africa but also present in Asia, Europe and North America. Isolates from these lineages have a high p*bla* prevalence (>50%) in all geographical regions, indicating that p*bla* carriage is a feature of a Ng_cgc_{400}, rather than an isolate's country of origin.

p*bla*.3 is predominantly found in the Ng_cgc_{400}s 25, 298 and 391, which cluster together on the minimum spanning tree (Figure 14, Table 5). p*bla*.2 is mainly present in Ng_cgc_{400} 122 and 29 (Figure 14, Table 5). While p*bla*.1 is found across the gonococcal population, TEM-1_{P14S} encoding p*bla*.1 is confined to Ng_cgc_{400} 33 (Table 5), which is associated with high income countries.

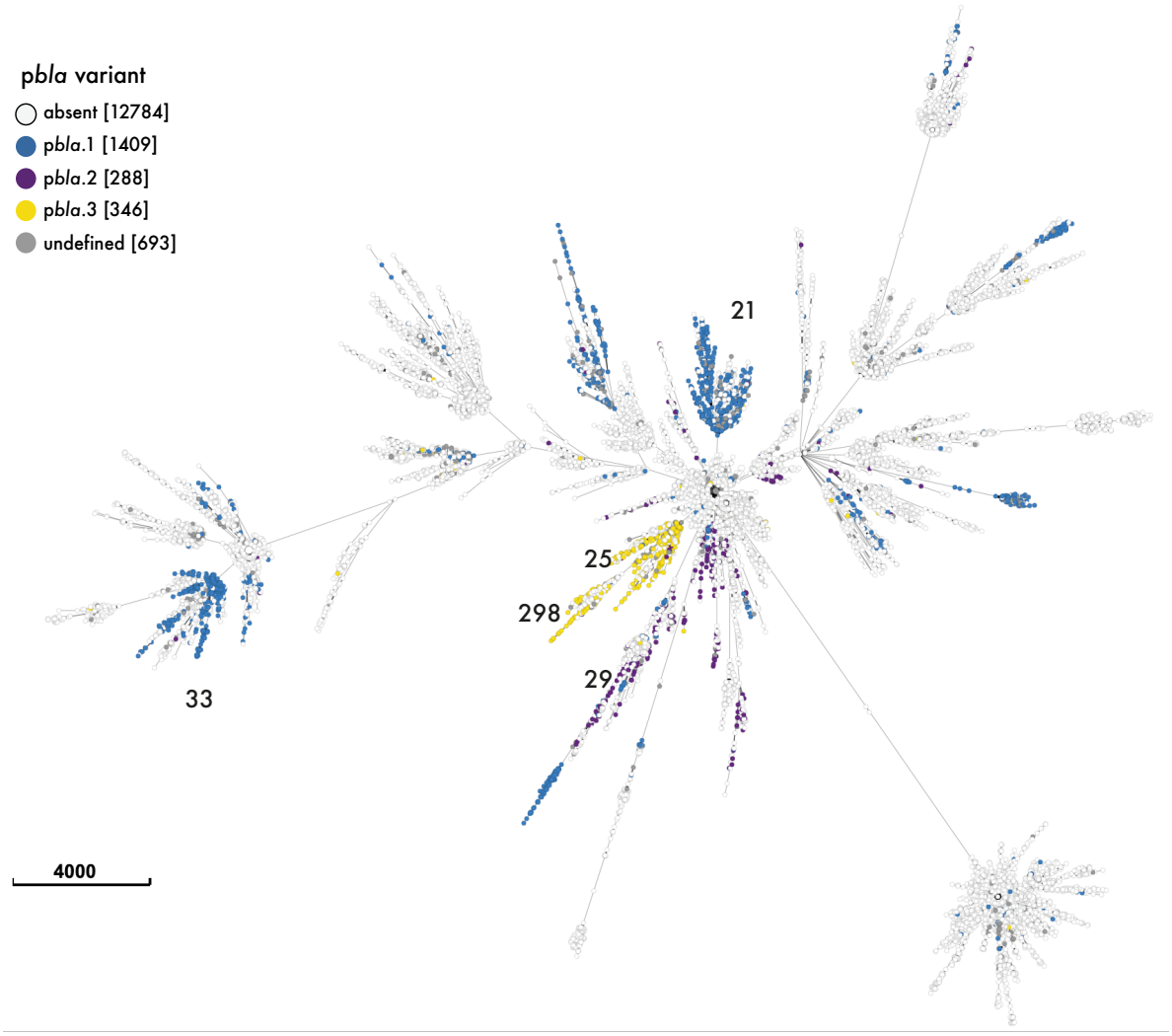

Figure 14: Minimum spanning tree of 15 532 gonococcal isolates showing the association between p*bla* variants and gonococcal lineages.
Isolates were clustered according to allelic differences in their core genome. Individual isolates are displayed as dots that are coloured according to the p*bla* variant they carry.

Table 4: Associations of p*bla* variants with distinct lineages.
The odds ratios (OR) of p*bla* variants in particular Ng_cgc$_{400}$s are given. The OR represents the odds that a *pbla*-carrying isolate within a given Ng_cgc$_{400}$ harbours the indicated variant, divided by the odds that any *pbla*-carrying isolate (regardless of Ng_cgc$_{400}$) harbours the same variant. The 95% confidence intervals (in brackets) and the p-values are given.

p*bla* variant	**lineage**		
	Ng_cgc$_{400}$ 33	Ng_cgc$_{400}$ 29, 122	Ng_cgc$_{400}$ 25, 298, 391
p*bla*.1 TEM-1$_{P14S}$	509.8 (267.0, 1083.7) p <0.001	0.2 (0.2, 0.3) p <0.001	0.004 (0.001, 0.01) p <0.001
p*bla*.2	0.02 (0.001, 0.1) p <0.001	14.0 (9.7, 19.2) p <0.001	0.1 (0.1, 0.3) p <0.001
p*bla*.3	0	0.1 (0.002, 0.03) p <0.001	92.25 (64.8, 133.3) p <0.001

3.2.5 p*bla* variants co-occur with certain pConj variants

p*bla* is not mobile on its own but can be mobilised by IncP conjugative plasmids such as pConj. Therefore, I next analysed the co-occurrence of p*bla* with the gonococcal conjugative plasmid. p*bla* is significantly associated with pConj presence (OR = 40.4, chi^2-test p <0.001), as would be expected for a mobilisable plasmid. Only 15.4% (425/2758) of all p*bla*-carrying isolates do not harbour pConj. Most of these isolates are from Ng_cgc$_{400}$s that have low (<30%) p*bla* carriage, although Ng_cgc$_{400}$ 377 has a high p*bla* prevalence (52.8%, 140/265) and does not carry pConj.

pConj can be grouped into seven variants according to differences in encoded toxin-antitoxin systems, parts of the conjugation apparatus, and the presence and allele of *tetM*[290]. pConj variants 1 and 2 carry *tetM* allele 2 (also referred to as American *tetM*[293]), while variants 3 and 4 carry *tetM* allele 1 (also referred to as Dutch *tetM*[293]). pConj variants 5, 6 and 7 lack *tetM*, and are referred to as markerless[290]. While pConj variants 1, 3, 5 and 6 are distributed across the gonococcal population, pConj.2, pConj.4 and pConj.7 are associated with distinct Ng_cgc$_{400}$s[290]. To further investigate the interplay between p*bla* and pConj, I assessed the co-occurrence of p*bla* with different pConj variants. p*bla* co-occurs most frequently with pConj.1 (30.0%), pConj.5 (29.4%) and pConj.3 (24.0%). I will examine some of the factors underlying the association of p*bla* with particular pConj variants in Chapter 4.

3.3 Origin and evolution of p*bla*

3.3.1 Tn*2* and p*bla*-related plasmids in *Haemophilus* spp. and *Neisseria* spp.

In the laboratory, p*bla* has been transferred into *E. coli*, *Salmonella enterica* serotype Minnesota*, H. influenzae* and a range of *Neisseria* spp.[370,371]. Therefore, p*bla* can replicate in a broad range of species. To examine the distribution of the plasmid in naturally occurring bacteria, I searched the NCBI non-redundant nucleotide collection[9] (BLASTn, word size = 28, expect value = 0.05, match/mismatch scores = 1/-2, gap costs = 0, 2.5) for NEIS2960, which is conserved between p*bla* variants, and verified the presence of p*bla* in hits (alignment length >50%, identity >80%) by aligning NEIS2960-harbouring contigs to p*bla*.2. This showed that the p*bla* host range is restricted to *Neisseria* and *Haemophilus* spp., so I further investigated p*bla* presence in isolates deposited in the PubMLST *Neisseria* (n = 41 129 from 37 species) and *Haemophilus* (n = 6 896 isolates from 12 species) databases[321]. Potential p*bla*-carrying isolates were identified by the presence of NEIS2960 (alignment length >50%, identity >80%), and the presence of the plasmid was verified by the presence of *repA* and bla_{TEM}.

Despite the ability of p*bla* to replicate in diverse *Neisseria* spp.[371], NEIS2960 was only detected in three out of 39 372 *N. meningitidis*, and in no non-invasive *Neisseria* spp. isolates (n = 1 757 isolates, 36 species). Further sequence analysis of the three *N. meningitidis* isolates (PubMLST ids: 26543, 54730, 54823) revealed that their plasmids were identical to gonococcal p*bla*.1. The p*bla*-carrying meningococcal strains were from patients in Chad, Burkina Faso and Norway, regions with a high prevalence of p*bla* in gonococci, and belong to distinct clonal complexes (*i.e.* CC-5, CC-11 and CC-32 complex, respectively). This suggests that p*bla* has been transferred occasionally into the meningococcus in regions where p*bla* is prevalent in the gonococcus, with no evidence of sustained p*bla* carriage by *N. meningitidis*.

Previous reports suggest p*bla* is related to small β-lactamase plasmids in *Haemophilus* spp.[372,373]. However, these studies predate available WGS and do not provide insights into the prevalence of p*bla* in *Haemophilus* spp.. I detected NEIS2960 together with *repA* in 0.3% of *H. influenzae* (19/6 403), 1.5% *H. parainfluenzae* (4/296) and 22.6% *H. ducreyi* (7/31). bla_{TEM} was present in 12.5% of *H. influenzae* (802/6 403), 19.3% *H. parainfluenzae* (52/296 isolates) and 22.6% *H. ducreyi* (7/31). However, only two *H. influenzae* (PubMLST ids: 23482 and 33361) and *H. parainfluenzae* isolates (PubMLST ids: 16289 and 34872) carried NEIS2960, *repA* and bla_{TEM}. In contrast, bla_{TEM} was present in all the NEIS2960 and *repA*-harbouring *H. ducreyi* isolates, suggesting p*bla* carriage. bla_{TEM} on gonococcal p*bla* lies within a partial Tn*2* (34% of sequence) that has a truncated TnpR resolvase and lacks the Tn*2* transposase TnpA[303]. BLASTn search (sequence identity >97%, alignment length >50%) of Tn*2* (GenBank accession: LC091537.1), against bla_{TEM} -carrying *Haemophilus* spp. isolates and subsequent confirmation of *tnpA,* and *tnpR,* revealed that all isolates carry intact Tn*2*. Taken together, p*bla* could have emerged through transposition of Tn*2* into a p*bla*-like replicon in *Haemophilus* spp..

3.3.2 Impact of host niche on p*bla* carriage

While *N. meningitidis* and *H. influenzae* rarely carry p*bla*, the related *N. gonorrhoeae* and *H. ducreyi* have a relatively high p*bla* prevalence (15.6% and 22.6%, respectively). Interestingly, *N. meningitidis* and *H. influenzae* are present in the nasopharynx and can cause meningitis, while *N. gonorrhoeae* and *H. ducreyi* are STI pathogens present in the urogenital niche. The difference in p*bla* prevalence in pathogens that typically reside in these sites suggests a benefit of p*bla* carriage in the urogenital tract. To further investigate the association of p*bla* with this niche, I assessed the prevalence of p*bla* in gonococcal isolates from different infection sites. Besides urethral infections, *N. gonorrhoeae* can also infect mucosal tissues of the uterine cervix, conjunctiva, pharynx and rectum[156]. On PubMLST, 5 585 isolates have attached metadata indicating the sites of infection. Isolates were from cervical (5.5%), rectal (18.3%), urethral (65.8%), and pharyngeal (10.1%) swabs, and 0.3% of isolates were from eye infections. Of the isolates, 20.3% and 34.7% carried p*bla* and pConj, respectively. Both p*bla* and pConj were significantly associated with isolates from the urogenital tract (OR = 3.1, chi^2-test $p < 0.001$ and OR = 4.0, chi^2-test $p < 0.001$, respectively). Taken together, the high prevalence of p*bla* in the two STI pathogens *N. gonorrhoeae* and *H. ducreyi* and the association of p*bla* with gonococcal isolates from the urethra suggest selection for p*bla* carriage in this niche.

3.3.3 Comparison of p*bla*.1 and p*bla*.2 in *H. ducreyi* and *N. gonorrhoeae*

The common infection site of *N. gonorrhoeae* and *H. ducreyi* provides opportunities for plasmid transfer, and I further characterised the *H. ducreyi* p*bla*-like sequences to assess their relationship to gonococcal p*bla*. *H. ducreyi* strains are divided into two clades, which diverged 1.9 million years ago[374]. I detected potential p*bla*.1 and p*bla*.2-like gene presence/absence patterns in Class I and Class II isolates, respectively (Appendix, Supplementary Table S6). Analysis of published closed genomes[375] suggested that p*bla* is integrated into the chromosome of these strains. To verify the chromosomal integration of p*bla* in *H. ducreyi*, I selected HD183 and DMC64, representing Class I and Class II *H. ducreyi* strains[375], respectively, and performed PCR of genomic DNA (a kind gift from Prof. S. Spinola) with primers binding to sequences within the chromosomal flanking region and p*bla*. However, these PCRs did not yield any products. In contrast, when using p*bla*-specific primers that generate overlapping fragments, I obtained PCR products indicating the presence of circular p*bla*-like plasmids in both strains (Figure 15A and B). Sequencing of the PCR products identified plasmids of 9.1 and 10.9 kb in HD183 and DMC64, respectively. I next aligned the sequences of p*bla*.1 and p*bla*.2 to the β-lactamase plasmids from *H. ducreyi* HD183 and DMC64[376]. Of note, the 9.1 and 10.9 kb *H. ducreyi* plasmids are highly related to p*bla*.1 and p*bla*.2. p*bla*.1 and the 9.1 kb *H. ducreyi* plasmid carry *repB* and one copy of NEIS2964 (Figure 15C). In contrast, the 10.9 kb *H. ducreyi* plasmid and gonococcal p*bla*.2 carry two *rep* genes, *repA* and *repB*, and two copies of NEIS2964 (Figure 15C). In contrast to the truncated Tn*2* on gonococcal p*bla*, *H. ducreyi* p*bla* have a full-length (4.95 kb) copy of Tn*2*, suggesting *H. ducreyi* p*bla* is ancestral to gonococcal p*bla*.

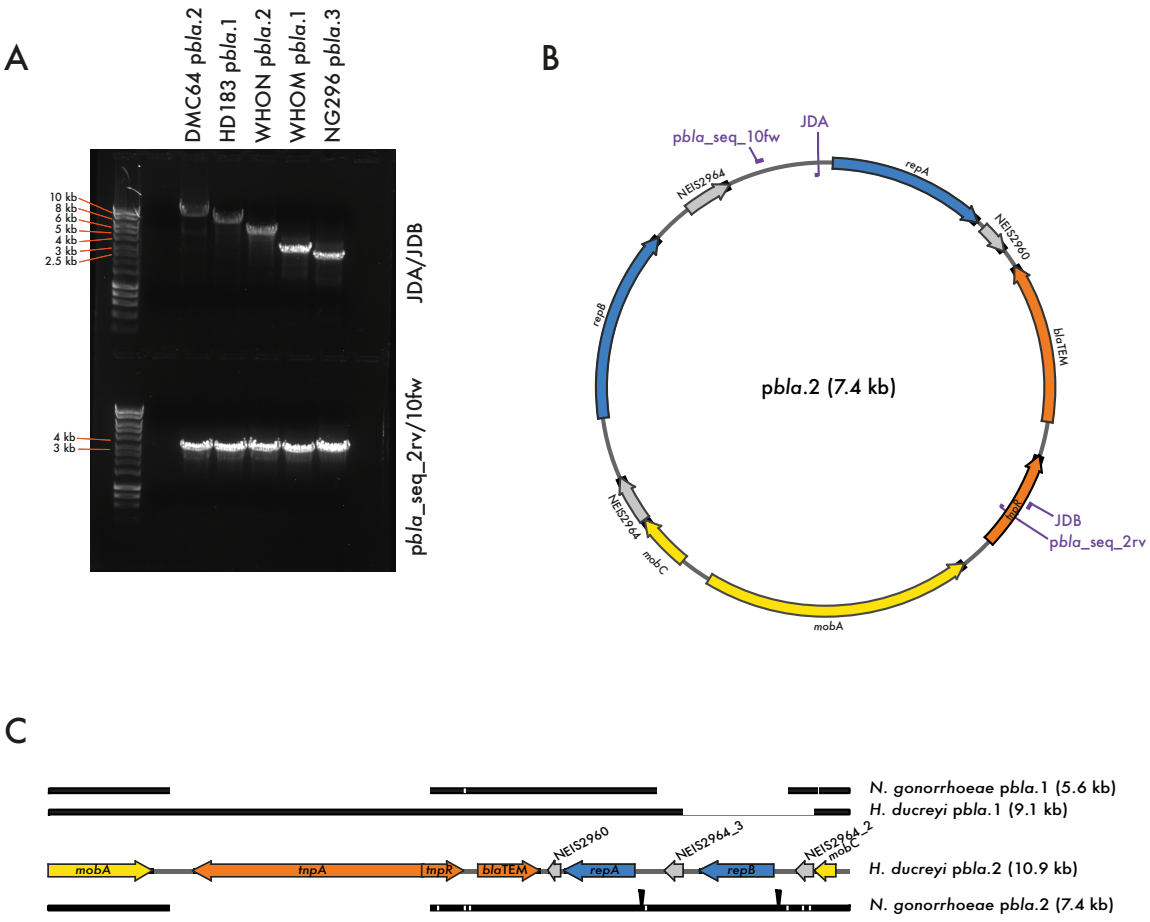

Figure 15: *H. ducreyi* DMC64 and HD183 carry two distinct p*bla* variants.
(A) Agarose gel of p*bla*-specific PCRs using *H. ducreyi* DMC64 and HD183 and *N. gonorrhoeae* WHO N, WHO M and NG296 DNA as templates. (B) Schematic of p*bla*.2 with location of p*bla*-specific primers indicated. The primer pairs generate overlapping fragments, confirming the presence of circular p*bla*. (C) Representation of alignment of gonococcal and *H. ducreyi* p*bla* variants to *H. ducreyi* p*bla*.2. Aligned regions are shown as black bars, with nucleotide polymorphisms indicated in white. Insertions are indicated as black triangles above the bars. ORFs on *H. ducreyi* DMC64 p*bla*.2 are coloured according to gene function: yellow, mobilisation proteins; orange, Tn*2*-derived genes including *bla*$_{TEM}$; blue, replication initiation proteins; grey, unknown function.

Two alternative scenarios could explain the occurrence of p*bla.*1 and p*bla.*2-like plasmids in *H. ducreyi* and *N. gonorrhoeae*: i) Independent introductions of the two variants into the gonococcus, both associated with a truncation of Tn*2*, or ii) introduction of p*bla*.2 into the gonococcus, with p*bla*.1 emerging independently in *H. ducreyi* and *N. gonorrhoeae* through deletion of *repB* and one copy of NEIS2964.

In an attempt to distinguish between the two scenarios, I first examined the similarity of the plasmid backbone sequences (*i.e.* without Tn*2* and the NEIS2964/*repB*/NEIS2964 sequence) of gonococcal and *H. ducreyi* p*bla*.1 and p*bla*.2. Higher sequence divergence between p*bla*.1 and p*bla*.2 than between *H. ducreyi* and *N. gonorrhoeae* p*bla* would support independent introductions of the variants into the gonococcus, whereas independent emergence of p*bla*.1 in both *H. ducreyi* and *N. gonorrhoeae* would be implied by a higher similarity between p*bla* sequences within a species. However, multiple sequence alignments revealed all plasmid backbones were highly similar; *H. ducreyi* plasmids were identical except for the *repB*/NEIS2964 deletion (100% nucleotide identity), and gonococcal plasmids shared 99.92% nucleotide identity. The similarity of p*bla*.1 and p*bla*.2 between *H. ducreyi* and *N. gonorrhoeae* was 99.96% and 99.92%, respectively.

I next examined the Tn*2* deletion site in gonococcal p*bla.*1 and p*bla*. 2, as differences in the truncation sites would support their independent introduction into *N. gonorrhoeae*. Sequence alignment of the p*bla* Tn*2* sequence reveals an additional nucleotide at the truncation of p*bla*.2 in comparison to p*bla*.1 (Figure 16A), resulting in two distinct *tnpR* alleles (alleles 3 and 2 in p*bla*.1 and p*bla*.2, respectively). Of note, 92.3% of gonococcal p*bla*.2 sequences (264/286) carry *tnpR* allele 2, while 92.3% p*bla*.1 (1323/1433) have allele 3.

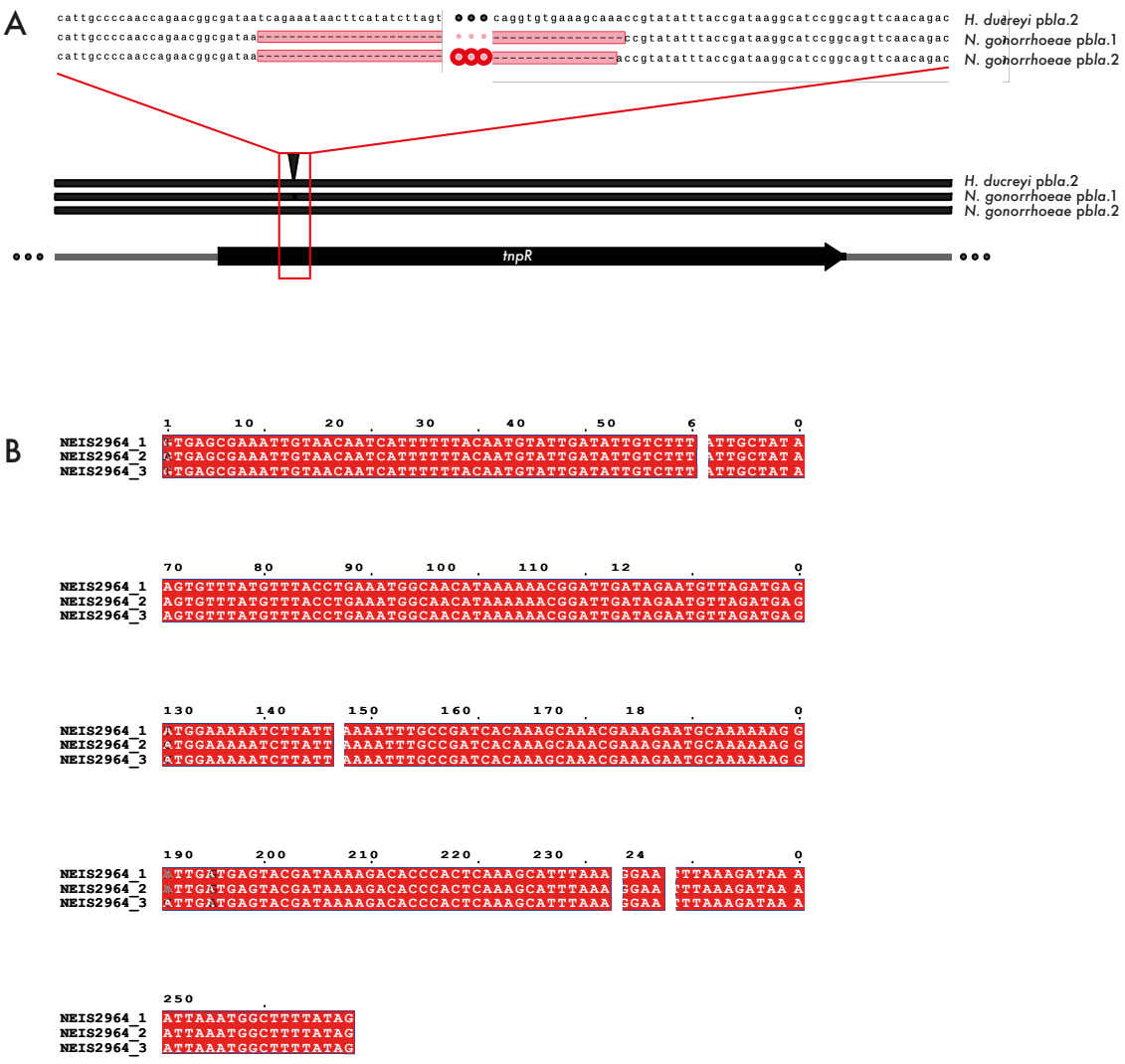

Figure 16: Comparison of *tnpR* and NEIS2964 sequences of *H. ducreyi* and *N. gonorrhoeae* p*bla*.
(A) Analysis of the Tn*2* deletion region: *tnpR* in gonococcal p*bla*.1 and p*bla*.2 differs by a single nucleotide at the site of the *tnpA*/*tnpR* deletion. Schematic representation of *tnpR* sequences of gonococcal and *H. ducreyi* p*bla*s is shown on the bottom with the SNP displayed as a white line and the site of the Tn*2* truncation in relation to *H. ducreyi* p*bla* indicated with a triangle. Displayed above is the nucleotide alignment of gonococcal p*bla* to *H. ducreyi* DMC64 p*bla*.2. (B) Sequence alignment of NEIS2964 alleles 1, 2 and 3 with the SNPs highlighted in white.

I also tested the hypothesis of two independent emergences of p*bla*.1 by investigating the p*bla*.1 deletion site spanning *repB*. Two copies of NEIS2964 flank *repB* on p*bla*.2, and p*bla*.1 has been suggested to have emerged following homologous recombination between the repeated sequences[300]. Therefore, I examined the repertoire of NEIS2964 in the different plasmids. The two copies of NEIS2964 (alleles 2 and 3) on *H. ducreyi* p*bla*.2 differ by three nucleotides (Figure 16B). Gonococcal p*bla*.2 carries alleles 1 and 2, which differ in 2 nucleotides. Of note, *H. ducreyi* p*bla*.1 carries allele 3, whereas gonococcal p*bla*.1 is associated with allele 2. As both gonococcal and *H. ducreyi* p*bla*.2 carry NEIS2964 allele 2, the difference in NEIS2964 cannot distinguish whether gonococcal p*bla*.1 emerged from *H. ducreyi* or *N. gonorrhoeae* p*bla*.2, however, the difference in NEIS2964 allele carried by *H. ducreyi* and *N. gonorrhoeae* p*bla*.1 suggests the p*bla*.1 emerged twice through independent deletions of *repB* and one copy of NEIS2964.

Taken together, based on available WGS, the presence of p*bla* with intact Tn*2* in *Haemophilus* spp. indicates p*bla* arose in *Haemophilus* through the transposition of Tn*2* into a mobilisable plasmid and was transferred from *H. ducreyi* into *N. gonorrhoeae*; the transfer is associated with a truncation of Tn*2.* Due to the high sequence conservation of p*bla* and the limited number of confirmed *H. ducreyi* p*bla* sequences, it is not possible to exclude the hypothesis of independent introductions of p*bla*.1 and p*bla*.2 into the gonococcus. However, the most parsimonious explanation for the differences in NEIS2964 alleles carried by *H. ducreyi* HD183 p*bla*.1 and *N. gonorrhoeae* p*bla*.1 is that gonococcal p*bla*.1 emerged independently following the introduction of p*bla*.2 into the gonococcus.

3.3.4 Adaptation to the gonococcus through gene loss and TEM diversification

Finally, I examined the evolution of p*bla* following its introduction into the gonococcus. I assembled p*bla* sequences from a subset of 414 p*bla*-carrying *N. gonorrhoeae* isolates on PubMLST (15% of the 2 758 isolates with p*bla*, Appendix, Supplementary Table S4) using the 10.9 kb *H. ducreyi* p*bla* as the reference and constructed a maximum likelihood phylogeny. The gonococcal plasmids in the subset include the same proportion of variants as in the database (*i.e.* 70% p*bla*.1, 14% p*bla*.2, 16% p*bla*.3) and were isolated between 1979 and 2022. The phylogeny (Figure 17) distinguishes the three p*bla* variants into distinct clades, indicating monophyletic origins of the variants.

Two TEM variants appear to have emerged in p*bla* after its introduction into the gonococcus; TEM-1 with the P14S substitution arose in p*bla*.1. TEM-135 emerged in p*bla*.2 and p*bla*.3 evolved from TEM-135 carrying p*bla*.2 following the loss of NEIS2961 and NEIS2962. Individual instances of TEM-135 are found across the tree due to synonymous amino acid changes, indicating independent appearance of TEM-135, however, without clonal expansion of strains with these plasmids.

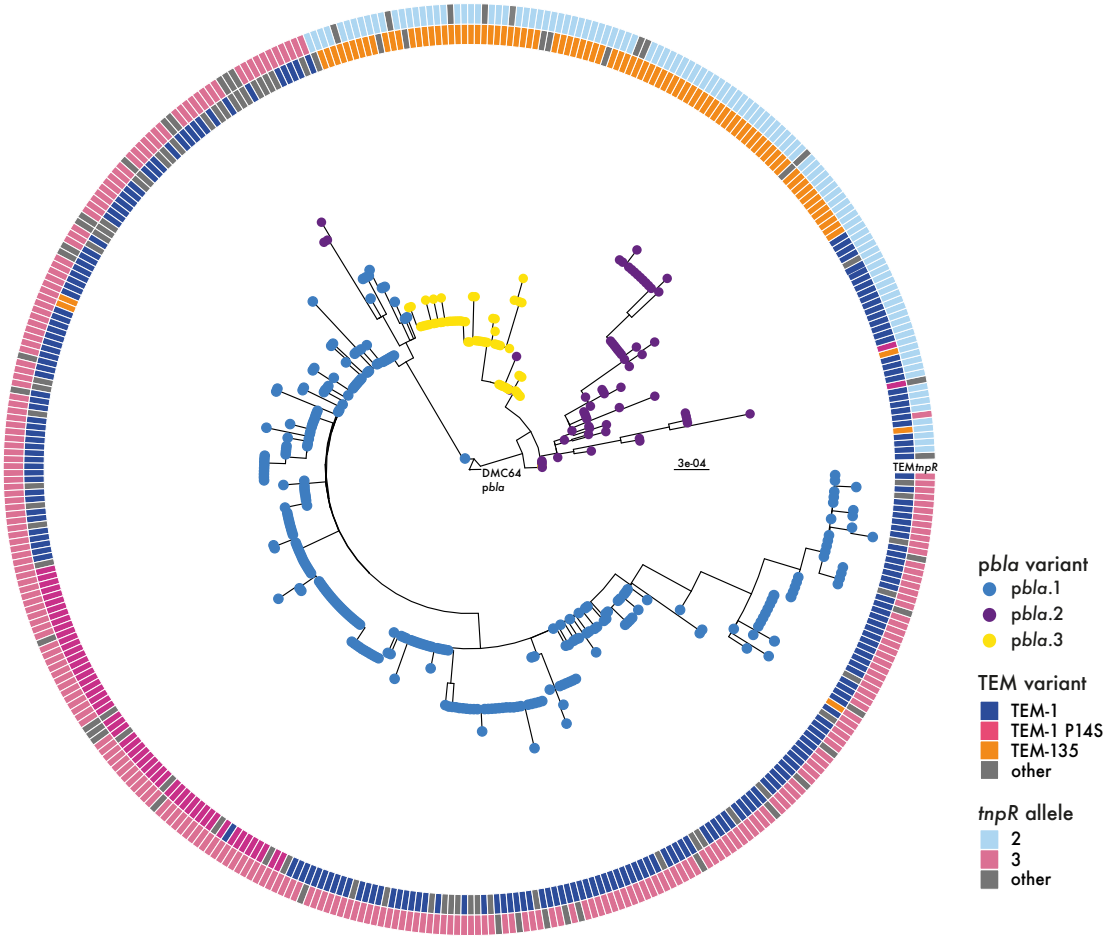

Figure 17: Maximum likelihood tree of 414 gonococcal p*bla* sequences.
The tree is rooted at the *H. ducreyi* DMC64 p*bla.* Tips are coloured according to p*bla* variant, and circles show the *tnpR* allele (outer circle) and the encoded TEM variant (inner circle). The scale bar indicates the substitutions per site.

3.4 Summary

The potential of the p*bla*-encoded TEM β-lactamase to become an ESBL highlights the importance of monitoring the spread and diversity of p*bla* in the gonococcal population. Previously, p*bla* variants have been characterised by restriction digestion patterns[300] or by PCR-based assays[317,319], which only allow small-scale analyses and lack information about sequence variation. Large amounts of WGS data are available on public databases such as PubMLST[321], offering an untapped resource to understand the epidemiology of p*bla* in gonococci. However, repeat regions on the plasmid[300] have hindered *de novo* assembly from short-read sequences. Therefore, I devised and implemented the Ng_p*bla*ST typing scheme which identifies plasmid variants from short-read WGS through their characteristic gene presence/absence and enables analysis of large datasets. I did not include the p*bla* insertion variants into the typing scheme, as I was not able to detect their insertion or duplication sequences in *N. gonorrhoeae* isolates on PubMLST. However, while the absence of IS*5* from gonococcal sequences suggests the reported IS*5* insertion p*bla* variant[318] is an experimental artefact, the inability to detect the duplication sequence of p*bla*.6[364] may also be due to issues with *de novo* assembly of repetitive sequences from short-read WGS. This could be resolved by combining short and long-read sequences to generate hybrid assemblies, however, long-read sequences of *N. gonorrhoeae* isolates are sparse. To date, the p*bla* duplication variant has only been reported in a single occasion and was indicated to be unstable[364]. Therefore, I focused my analysis on the p*bla* deletion variants.

I validated the typing scheme using short-read sequences from p*bla*-containing WHO reference strains, for which hybrid assemblies of plasmid sequences are available. As only three WHO reference strains carry p*bla*[320], I also manually extracted and aligned p*bla* contigs from 16 p*bla*-carrying isolates. This confirmed the typing result in every case. Ng_p*bla*ST is available on PubMLST, allowing further independent evaluation by the research community. The typing scheme identifies

the five reported deletion variants but will also classify novel variants as untypeable; these should be investigated by PCR or plasmid-specific long-read sequencing to monitor for the emergence of novel variants which are not included in the current scheme.

Albeit simple in itself, the implementation of Ng_p*bla*ST enabled the first population-wide analysis of the distribution of p*bla* variants. Analysis of the occurrence of p*bla* variants across 15 532 isolates demonstrated that p*bla*.1, p*bla*.2 and p*bla*.3 are the major variants, accounting for >99% of typeable p*bla* sequences; the remaining two previously described deletion variants were found in only nine isolates. My dataset is the largest quality-checked collection of publicly available isolates at the time. It includes strains from 66 countries and spans almost 100 years. However, isolates from LMICs, especially Africa, are underrepresented in this and all datasets.

Consistent with the previously reported negative correlation between a country's GDP and plasmid carriage[290], p*bla* prevalence was highest in LMICs. For example, 58.3 % of isolates from countries in Africa harbour p*bla*, compared with only 7.9 % of isolates from North America and 20 % of isolates from Europe. The high plasmid prevalence in LMICs has been suggested to result from the extensive spread of resistance plasmids in isolates[290]. However, I found that plasmid prevalence is lineage-specific and independent of the country of origin (Figure 14). This suggests p*bla* forms long-term, stable relationships with certain lineages, which could differ in their ability either to acquire and/or maintain the plasmid.

I found that NEIS2960 on p*bla* is a potential VbhA antitoxin and identified NEIS1357 as a potential VbhT toxin on the chromosome. A split toxin-antitoxin system has been indicated to be involved in the maintenance of pConj in *N. gonorrhoeae*[294]. However, NEIS1357 is highly similar to NmFic of *N. meningitidis* for which no antitoxin has been described. Instead, NmFic is tightly regulated by autoregulatory mechanisms[359,360]. Therefore, it is unclear if NEIS2960/NEIS1357 play a role in maintaining p*bla.* Future work should assess the stability of p*bla* in the presence and absence of

NEIS1357 and investigate the presence and distribution of NEIS1357 in the gonococcal population to clarify whether interplay between NEIS2960 and NEIS1357 could impact the stability and distribution of p*bla* in gonococci.

Several other factors might contribute to the association of p*bla* with certain lineages. For example, compensatory mutations that reduce the burden of plasmid carriage could occur in certain lineages[67,142]. In contrast, barriers to horizontal gene transfer could prevent plasmid uptake into other lineages. I will further explore the impact of fitness costs, mobilisation and barriers to horizontal gene transfer in Chapters 4 and 5.

As described previously[290], I found that p*bla* is significantly associated with pConj. However, my analysis revealed that p*bla* co-occurs with specific variants of pConj. p*bla* is rarely found with pConj variants 2, 4, 6 and 7 (only 17% of p*bla*-carrying isolates), which are present at lower frequencies than the pConj variants that co-occur with p*bla*[290]. Therefore, the co-occurrence between p*bla* and pConj variants could merely reflect the wider distribution of pConj variants 1, 3, and 5. Alternatively, specific interactions between p*bla* and pConj variants could explain their co-occurrence, and I will explore the interplay between p*bla* and variants of pConj in Chapter 4.

p*bla*.3 is associated with TEM-135 and is confined to three Ng_cgc$_{400}$s that cluster together on a minimum spanning tree (Figure 14), suggesting this variant might not be mobile. This matches the lack of *mob* genes on p*bla*.3, which could limit its mobilisation by pConj. However, p*bla*.3 transfer has been reported[314], and co-integration into pConj, mediated by IS*1*, was described as a transfer mechanism of p*bla*.3 in *E. coli*[312,313]. I will further investigate the mobility of this p*bla* variant in Chapter 4.

TEM-135 is the second most prevalent TEM variant encoded by p*bla* (24.3% of plasmids) and has an M182T substitution relative to TEM-1. The M182T substitution is considered a 'stepping stone'

mutation towards an ESBL[368], due to its stabilising effect[285], facilitating amino acid changes in the active site. I found TEM-135 in two of the major p*bla* variants and at almost twice the frequency described before in gonococcal p*bla*[290]. Previous reports had indicated an association of p*bla*.3 with TEM-135[315], while TEM-135 carrying p*bla*.2 has only been described on a few occasions[377,378]. My results confirm these observations but show that almost half of p*bla*.2 carry TEM-135. In contrast, p*bla*.1 encodes mainly TEM-1, with TEM-1_{P14S} present in a subpopulation of p*bla*.1 associated with Ng_cgc_{400} 33.

The host range of p*bla* is largely restricted to the two STI pathogens *N. gonorrhoeae* and *H. ducreyi*. I identified two distinct p*bla* variants in *H. ducreyi* that are highly similar to gonococcal p*bla*.1 and p*bla*.2 but carry intact Tn*2* sequences. *H. ducreyi* strains are divided into two classes[374] and p*bla*.1- and p*bla*.2-like plasmids are associated with Class I and Class II isolates, respectively. The intact Tn*2* sequence in *H. ducreyi* p*bla* indicates that p*bla* was introduced from *H. ducreyi* into the gonococcus and this was associated with a truncation of Tn*2*. Besides anecdotal reports that transposons are not active in *N. gonorrhoeae*[341], little is known about transposition in this organism. It would be interesting to address this in future studies.

In women, *N. gonorrhoeae* primarily causes cervicitis, while *H. ducreyi* causes ulcers at the vaginal entrance and cervix. In men, *N. gonorrhoeae* primarily causes urethritis and *H. ducreyi* mainly causes penile ulcers[379]. However, ~ 3.5% of men with chancroid also have urethritis[379]. Therefore, the two species can occupy the same niche, providing opportunities for gene transfer. Interestingly, p*bla* carriage is negligible in the related pathogens *H. influenzae* and *N. meningitidis* which inhabit the nasopharynx. Further, p*bla* carriage was low for *H. parainfluenzae*, which is primarily found in the oropharynx[380], and p*bla* was not detected in any non-invasive *Neisseria* spp., which are part of the nasopharyngeal microbiome. The distribution of p*bla* might reflect the renal excretion of β-lactams[381], favouring p*bla* carriage in bacteria inhabiting the urogenital tract compared with other

sites. This is supported by the association gonococcal plasmids with isolates from urethral swabs. Of note, like penicillin, tetracycline is excreted *via* the urine[382], and, similar to p*bla*, the host range of pConj is mostly limited to *N. gonorrhoeae*, with rare occurrences in *N. meningitidis*[296]. However, recently, the meningococcal urethritis clade (NmUC) evolved from ST-11 *N. meningitidis* by acquiring genetic elements from *N. gonorrhoeae*[383,384]. So far, no pConj or p*bla*-carrying NmUC isolates have been reported, however, co-infection of *N. gonorrhoeae* and NmUC could lead to the transfer of p*bla* in this environment.

There are two alternative scenarios explaining the emergence of p*bla*.1 and p*bla*.2-like plasmids in *H. ducreyi* and *N. gonorrhoeae*; i) independent introductions of p*bla*.1 and p*bla*.2 into the gonococcus, both associated with a truncation of Tn*2*, or ii) a single interspecies transfer of p*bla*.2 with independent emergence of p*bla*.1 in *H. ducreyi* and *N. gonorrhoeae.* While I cannot reject either scenario, the independent emergence of p*bla*.1 in the two organisms through the deletion of *repB*/NEIS2964 allele 2 and *repB*/NEIS2964 allele 3, is the most parsimonious explanation.

In summary, in this chapter, I have characterised p*bla* variants and analysed their evolutionary relationships and spread in the gonococcal population. The three major p*bla* variants differ in gene presence/absence patterns and are associated with distinct TEM variants. In the following chapter, I will investigate how these genomic differences affect the phenotype of the p*bla* variants and whether phenotypic differences can explain their distribution in gonococci.

4 Impact of fitness cost, resistance patterns, and mobilisation on the spread of p*bla* in gonococci

The introduction of TEM-1 encoding p*bla* in 1976[4,299] and the subsequent spread of the plasmid in the gonococcal population led to the emergence of high-level penicillin resistance in *N. gonorrhoeae* and has contributed to the cessation of penicillin treatment for gonorrhoea[385]. TEM-1 only differs in a few amino acid substitutions from ESBLs found in other pathogens[282], which would be active against ceftriaxone, the current treatment of gonorrhoea[239,297]. In the previous chapter, I have characterised the diversity and epidemiology of p*bla* in the gonococcal population and described distinct associations of p*bla* variants with TEM variants, gonococcal lineages and variants of the gonococcal conjugative plasmid pConj. Here, I will investigate the interplay between p*bla* and pConj in the transfer of β-lactamase resistance in gonococci and assess how the genotypic differences between p*bla* variants are reflected in their resistance levels, fitness costs and mobility. Linking the characteristics of p*bla* variants to their epidemiology provides insights into molecular mechanisms underlying their distribution in the gonococcal population and aids in anticipating future trends in plasmid-mediated β-lactam resistance in *N. gonorrhoeae*.

4.1 Plasmid-mediated β-lactam resistance in *N. gonorrhoeae*

4.1.1 p*bla* variants with TEM-135 confer increased resistance to penicillin

p*bla* variants have been suggested to confer different levels of resistance to penicillin[377]. However, as resistance levels were measured in a range of non-isogenic clinical isolates, the differences could be due to the associated strain background, the plasmid variant, or the TEM variant encoded by the plasmid. To distinguish between these factors, I introduced p*bla* variants into FA1090 and measured the penicillin minimal inhibitory concentrations (MICs) of the strains. For all p*bla* variants, introduction of the plasmid increased the MIC above the resistance breakpoint (1 µg/ml)[386]. However, while p*bla*.1 and 2 conferred MICs of 8 µg/ml, p*bla*.3 led to a significantly higher MIC of 32 µg/ml (Tukey multiple comparison of means, p = 0.003, Figure 18A).

In the previous chapter, I showed that the three major TEM variants (TEM-1, TEM-1_{P14S} and TEM-135) are associated with distinct p*bla* variants. Whilst the p*bla*.1 and p*bla*.2 tested carried TEM-1, p*bla*.3 harboured TEM-135. To establish whether the observed difference in MIC was due to the TEM or p*bla* variant, I modified TEM-135 on p*bla*.3 by introducing a T182M substitution, resulting in p*bla*.$3^{TEM\text{-}1}$. This reduced the MIC of p*bla*.3 to the level of p*bla*.1 and p*bla*.2 carrying TEM-1 (Figure 18B), indicating that TEM-135 is responsible for the elevated MIC seen with p*bla*.$3^{TEM\text{-}135}$.

I also compared resistance levels conferred by TEM-1, TEM-1_{P14S} and TEM-135 (which account for >95% of TEMs in gonococci) by introducing them into p*bla*.2 and measuring MICs in FA1090. Again, TEM-135 led to a significant increase in penicillin MIC (128 µg/ml compared to 8 µg/ml with TEM-1, Tukey multiple comparison of means of $\log_2$-transformed MIC values, p <0.001, Figure 18C), while TEM-1_{P14S} resulted in a minor, non-significant increase in MIC to 16 µg/ml. Therefore, TEM-135 might increase the benefit of p*bla* carriage due to elevated penicillin resistance levels.

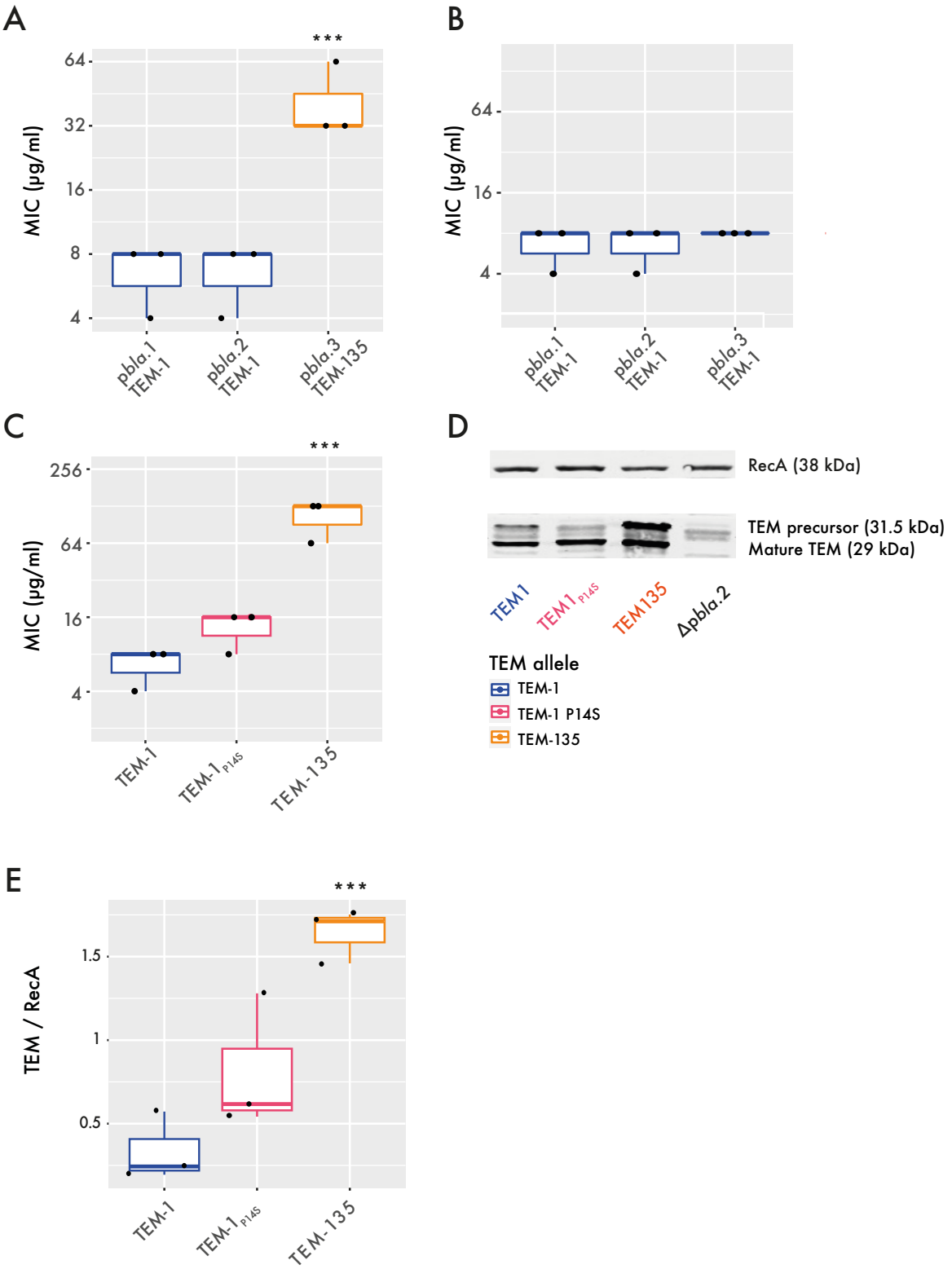

Figure 18: TEM-135 confers increased penicillin MIC.
(A) Benzylpenicillin MICs of different p*bla* variants in FA1090 (one-way ANOVA on $\log_2$-transformed MIC values with Tukey multiple comparisons of means; *** p <0.001). (B) MICs of TEM-1 in different p*bla* variants. (C) MICs of different TEMs in p*bla*.2 (one-way ANOVA on $\log_2$-transformed MIC values; *** p <0.001). (D) Western blot of cellular levels of different TEM variants with RecA included as a loading control. The Western blot shown is representative of three independent repeats. (E) TEM/RecA ratios of whole cell lysates were quantified with the LI-COR system (one-way ANOVA with Tukey multiple comparisons, n.s. p >0.05; *** p <0.001).

The M182T substitution in TEM-135 is not in the active centre of the enzyme and has no impact on enzyme activity[285]. To define the basis for the MICs conferred by different TEMs, I measured their cellular levels by Western blot analysis. This revealed that the MICs correlate with cellular levels of each TEM, with levels of TEM-135 significantly higher than of f TEM-1 and TEM-1_{P14S} (29 kDa, Figure 18D and E). TEM β-lactamases are synthesised in the cytoplasm with an N-terminal signal sequence (31.5 kDa). After translocation through the Sec secretion system, the signal sequence is cleaved off by membrane-anchored signal peptidases, resulting in the release of mature TEM (29 kDa) into the periplasm[387-389]. Changes in the signal peptide can affect β-lactamase secretion[390]. Therefore, I also assessed the levels of unprocessed TEM (31.5 kDa, Figure 18D). Relative to TEM-1, I found increased levels of unprocessed TEM-135, while there were reduced amounts of unprocessed TEM-1_{P14S}, consistent with the P14S substitution affecting secretion. However, this substitution had no obvious effect on the periplasmic TEM levels. In conclusion, MICs conferred by p*bla* variants correlate with levels of mature TEM.

4.1.2 Plasmid-mediated resistance is influenced by the strain background

Interactions between a plasmid and its strain background can modify plasmid-mediated resistance[391-393], potentially altering the benefit a plasmid confers to a particular strain. To test whether p*bla*.1-mediated penicillin resistance differs between strains, I introduced p*bla*.1^{TEM-1} into isolates from lineages with low p*bla* prevalence (*i.e.* NG015, Ng_cgc$_{400}$ 3, 4.5% p*bla* and FA1090, Ng_cgc$_{400}$ 286, 0% p*bla*) or associated with certain p*bla* variants (*i.e.* 2086_K, p*bla*.1; NG064, p*bla*.1/ p*bla*.2; NG114, p*bla*.3), and measured their MICs. p*bla*.1^{TEM-1}-mediated resistance differed significantly between strains (one-way ANOVA on $\log_2$-transformed MIC values, $p < 0.001$, Figure 19A), with significantly increased MICs for isolates NG015 and 2086_K.

I hypothesised that chromosomal resistance mutations could influence plasmid-mediated resistance and examined the genomes of the isolates for chromosomal determinants associated with penicillin resistance. ResFinder[394] identified the resistance-associated PorB G120K mutation in isolate NG015, while isolates NG064 and 2086_K have a L421P substitution in PBP1 (encoded by *ponA*). The outer membrane porin PorB forms a homotrimeric β-pleated barrel with each monomer consisting of 16 transmembrane-spanning segments and 8 extracellular loops[395]. The G102K substitution is in loop 3 (Figure 19B) and has been associated with intermediate-level penicillin resistance[396]. Previous investigations indicated slightly lower β-lactam permeation rates of PBP1$_{L421P}$ compared to the wild type; however, the effect was not statistically significant and changes in MIC were only apparent in strains that also have mutations in the multidrug efflux pump regulator MtrR and altered PBP1[263]. The L421P substitution in PBP1 is in the C-terminal transpeptidase domain and reduces the affinity of PBP1 for penicillin[267]. Of note, neither PorB$_{G120K}$ nor PBP1$_{L421P}$ co-occurred with mutations in *mtrR* or the *mtrR* promoter in the tested isolates.

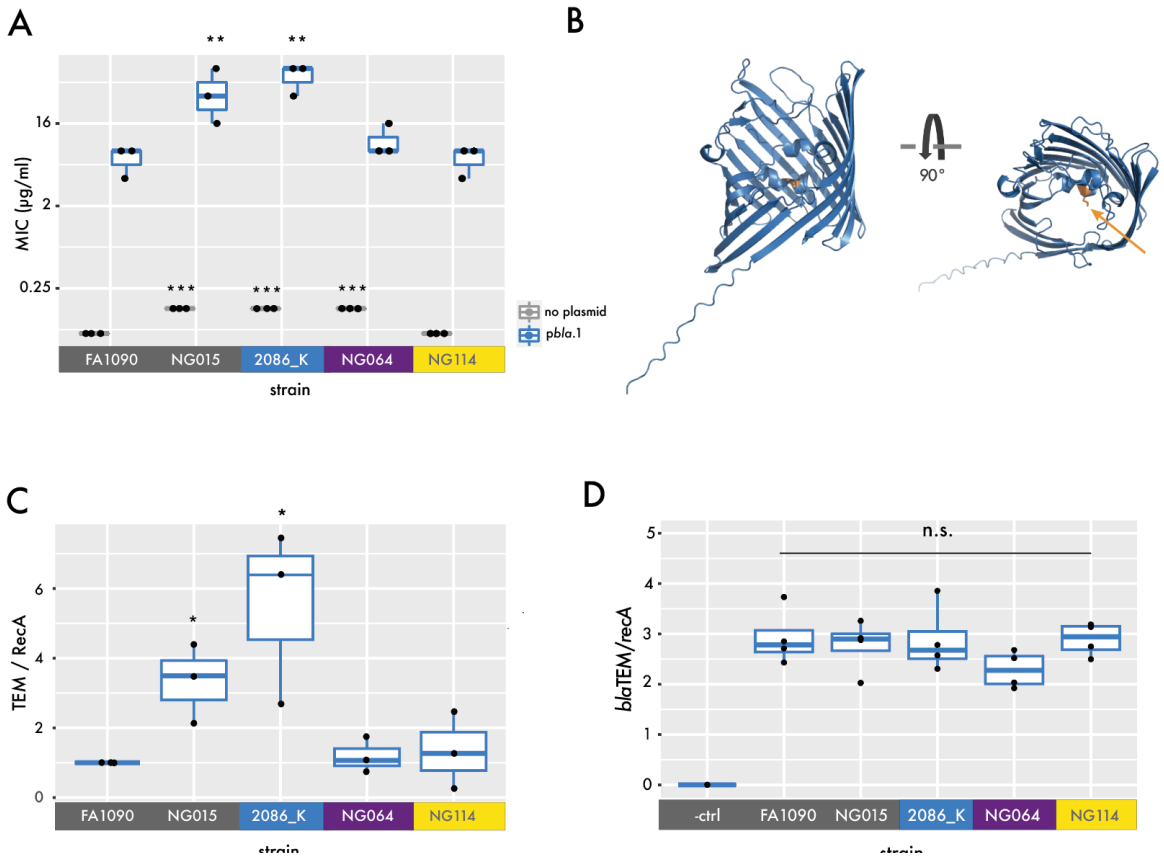

Figure 19: Impact of strain background on p*bla*-mediated resistance.
(A) Penicillin MICs of strains from plasmid-free (dark grey) and plasmid-associated lineages (light blue, p*bla*.1-associated; purple, p*bla*.2-associated; yellow, p*bla*.3-associated) without (light grey) or with p*bla*.1 (light blue). MICs of plasmid-carrying and plasmid-free strains were compared to corresponding FA1090 strains (one-way ANOVA with Tukey multiple comparisons; n.s. p >0.05, * p <0.05, ** p <0.01, *** p <0.001). (B) Alphafold3 prediction of NG015 PorB with the G120K substitution in loop 3 indicated in orange. (C) TEM levels of whole cell lysates were examined by Western blot analysis and quantified with the Li-COR system. TEM levels were measured on three independent occasions, and results were standardised to FA1090 TEM. (D) TEM mRNA levels were measured by RT-ddPCR on four occasions and standardised to *recA* mRNA levels strains.

PorB$_{G120K}$ and PBP1$_{L421P}$ were associated with a one-fold increase in penicillin MICs in the plasmid-free isolates (Figure 19A). However, only isolates NG015 and 2086_K had amplified MICs in the presence of p*bla*, suggesting that the L421P substitution in PBP1 does not amplify plasmid-mediated resistance. NG015, which has PorB$_{G102K}$, shows increased penicillin MICs both in the presence and absence of p*bla*. However, as NG015 is the only isolate with PorB$_{G102K}$, it is unclear whether the increased resistance in the presence of p*bla* is due to synergism between TEM-1 and PorB$_{G102K}$.

If plasmid and chromosomally-encoded resistance act synergistically, p*bla* might be found more often in strains harbouring these chromosomal resistance mutations. Therefore, I assessed the co-occurrence of p*bla* with the PBP1$_{L421P}$ and PorB$_{G120K}$ across the population as well as within individual p*bla*-associated Ng_cgc$_{400}$s (*i.e.* Ng_cgc$_{400}$ 21 and 29). Both on the population level and within lineages, p*bla* is less likely to be found together with PBP1$_{L421P}$ (OR <1). In contrast, p*bla* is more likely found together with PorB$_{G120K}$ in the p*bla*-associated Ng_cgc$_{400}$s 21 and 29 (OR = 2.2, chi^2-test p = 2 e-5 and 2.1, chi^2-test p = 1.6 e-4, respectively), supporting a synergistic effect of PorB$_{G120K}$ and p*bla*-encoded TEM. However, there was no signal on the population level (OR = 1, chi^2-test p = 0.65)

While synergistic effects of PorB$_{G120K}$ might account for the increased resistance provided by p*bla*.1 in NG015, they do not explain the increased MIC of 2086_K with p*bla*.1. Other factors such as differences in cellular enzyme levels could result in increased resistance, and I also measured cellular TEM of different strains by Western blot analysis. TEM-1 levels in strains correlate with their penicillin MICs (R^2 = 0.99, p <0.001, Figure 19C), with significantly elevated levels in NG015 and 2086_K. To determine whether these differences were caused by changes in transcript levels, I assessed TEM mRNA levels by RT-ddPCR. However, I did not detect differences in expression levels (Figure 19D), indicating post-transcriptional mechanisms (*e.g.* changes in enzyme stability) can modify plasmid-mediated resistance.

Taken together, plasmid-mediated resistance is modified by the strain background, potentially through synergistic effects with chromosomal resistance determinants and post-transcriptional mechanisms affecting enzyme levels.

4.2 Impact of copy number and fitness costs on the stability of p*bla* in the gonococcal population

4.2.1 p*bla* has remained in the gonococcal population after the cessation of penicillin treatment

The dynamics of chromosomally and plasmid-encoded resistance differ within a population. While plasmid-encoded resistance genes can spread rapidly within bacterial populations if the plasmid is mobile, plasmids can be unstable within individual hosts or populations, leading to the loss of the resistance gene from the population[67]. While penicillin is no longer used for treating gonorrhoea, understanding the stability of p*bla* within the gonococcal population is critical due to the potential of the encoded TEM β-lactamase to evolve into an ESBL.

I first assessed the prevalence of p*bla*-carrying isolates in PubMLST between 2010 and 2019 (n = 12 914). The dataset consists of isolates from 44 countries, although isolates from the UK and the US dominate. Results show that even 30 years after the cessation of penicillin treatment[385], p*bla* has remained at a prevalence between 10.9% and 18.3% (Figure 20). The dataset consists of isolates from different studies and is not a representative longitudinal study; therefore, it cannot resolve the prevalence of p*bla* over time. Nonetheless, the data indicate that p*bla* is maintained in the gonococcal population, which is in line with recent studies reporting p*bla*-carriage in isolates from Kenya, China and Italy[397-399].

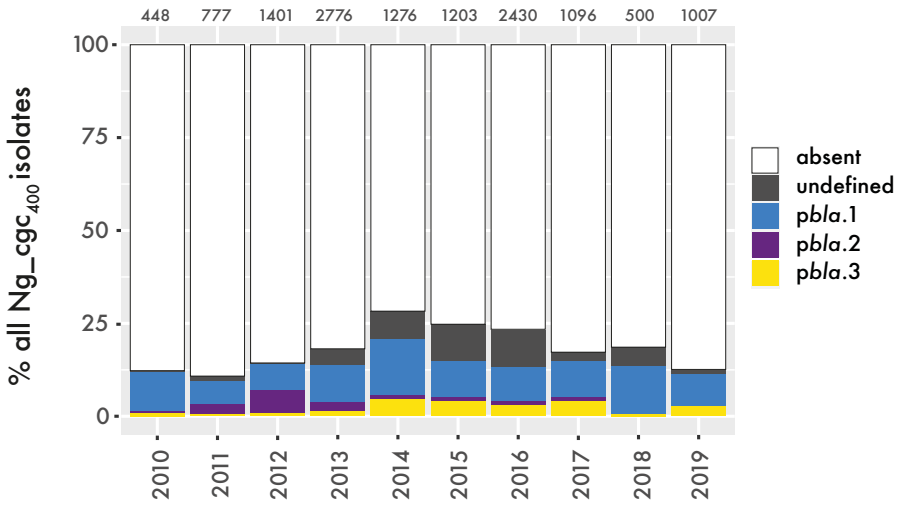

Figure 20: p*bla* prevalence in isolates on PubMLST between 2010 and 2019.
Percentage of isolates carrying p*bla* in gonococcal isolates deposited on PubMLST between 2010 and 2019 (n = 12 914 isolates) is shown. Colours indicate p*bla* variants, and the numbers of isolates each year are indicated above the bars.

4.2.2 p*bla* copy number alone cannot explain its persistence within the gonococcal population

Plasmid copy number influences the stability of a plasmid within a clonal population by affecting the likelihood that at least one plasmid copy is inherited by a daughter cell during cell division. Higher copy numbers generally increase stability by reducing the chance of plasmid loss[129], while low copy number plasmids often require active partitioning and TA systems to maintain stability[122].

To assess the probability of the emergence of a p*bla*-free daughter cell following cell division, I measured the p*bla* copy number in five strains from different lineages (*i.e.* FA1090, Ng_cgc$_{400}$ 286; NG015, Ng_cgc$_{400}$ 3; NG064, Ng_cgc$_{400}$ 29; NG114, Ng_cgc$_{400}$ 25; 2086_K, Ng_cgc$_{400}$ 21) by digital droplet PCR (ddPCR). ddPCR enables absolute quantification of nucleic acid targets without requiring standard curves[400]. PCR is partitioned into thousands of nanoliter-sized oil droplets, resulting in the random distribution of DNA; droplets can contain zero, one, or more copies of the target DNA. PCR amplification occurs independently in each droplet, producing a fluorescent signal if the droplet contains at least one target DNA. Following amplification, positive droplets are enumerated, and the DNA concentration is calculated from the number of positive droplets using a Poisson distribution. To estimate the copy number of p*bla*, I measured the copy number of *tnpR* (plasmid marker) relative to *recA* (chromosome marker). Primers were designed to produce a ~ 200 bp amplicon, and their specificity was confirmed using FA1090 gDNA (p*bla*-minus control), p*bla*.1 DNA (purified by miniprep, chromosome-minus control) and water as controls.

An average of 1.6 copies (sd = 0.27, Figure 21) of p*bla.*1 are present per chromosome. As the gonococcus is polyploid, with approximately six chromosomes per diplococcus[188], this equates ~ 10 copies of p*bla* per diplococcus. Assuming random segregation of plasmids between daughter cells, the plasmid loss frequency P_{loss} is $(1/2)^{10}$. If plasmid-carrying cells grow at the same rate, the fraction of plasmid-free cells (f) after g generations is:

$$f_{g+1} = f_g + (1 - f_g) P_{loss}$$

Starting with a single plasmid-bearing cell, the fraction of plasmid-free cells after g generations is approximately:

$$f_g = 1 - (1 - P_{loss})^g$$

If we approximate the number of plasmid-free cells after 100 generations, the expected proportion of plasmid-free cells is 9.31%. Therefore, p*bla* copy number might not be sufficient to maintain the plasmid, and other mechanisms such as plasmid transfer or sporadic antibiotic selection are required to explain the persistence of p*bla* in the gonococcal population.

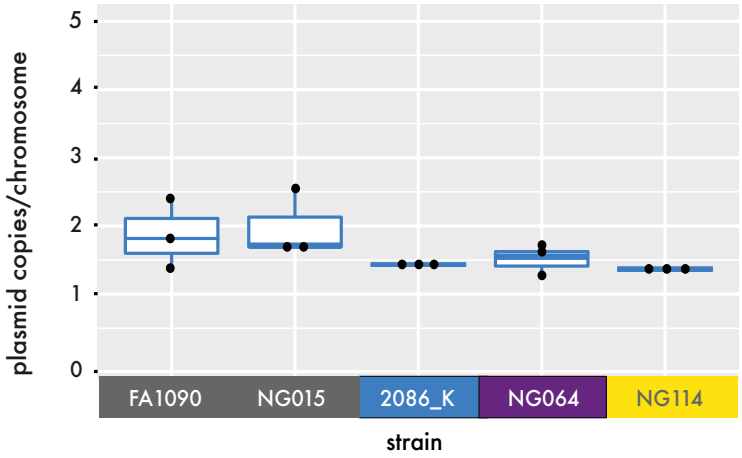

Figure 21: p*bla*.1 copy number in different strains.
The plasmid copy number was measured by ddPCR and is indicated as number of plasmids per chromosomes.

4.2.3 p*bla*.1 carriage imposes minimal fitness costs in different strains

Plasmid carriage can impose fitness costs on a bacterium, leading to a competitive disadvantage of plasmid-carrying isolates *vs.* their plasmid-free counterparts[67]. In the absence of selection for plasmid-encoded traits, costly plasmids should be eliminated from the population through purifying selection. However, plasmid-imposed costs can differ between strains, and variability in fitness costs can improve the maintenance of a plasmid within a population[132].

To assess the contribution of p*bla* fitness costs on the persistence and distribution of the plasmid in gonococci, I introduced p*bla*.1 into a range of plasmid-free isolates from plasmid-associated lineages (2086_K, Ng_cgc$_{400}$ 21, 64.3% p*bla*; NG064, Ng_cgc$_{400}$ 29, 32% p*bla*; NG114, Ng_cgc$_{400}$ 25, 56.8% p*bla*) and from lineages with low p*bla* carriage (NG015, Ng_cgc$_{400}$ 3, 4.5% p*bla* and FA1090, Ng_cgc$_{400}$ 286, 0% p*bla*) by electroporation. The number of passages after plasmid introduction was kept to one passage after plasmid introduction to limit the emergence of compensatory mutations[141,142].

I approximated fitness costs by measuring the growth rates of monocultures and competing p*bla*.1-carrying *vs*. isogenic plasmid-free strains in liquid medium. From the growth curves of monocultures, intrinsic growth rate (r) and carrying capacity (K) can be estimated by calculating the maximum growth rate (μ_{max}) and maximum optical density (OD_{max}), respectively[132]. Additionally, the area under the curve (AUC) integrates information about r and K. I compared r, K and AUC between each pair of plasmid-carrying and plasmid-free isogenic isolates, which did reveal no impact of p*bla*.1 on the growth of any of the examined strains by these parameters (Figure 22A).

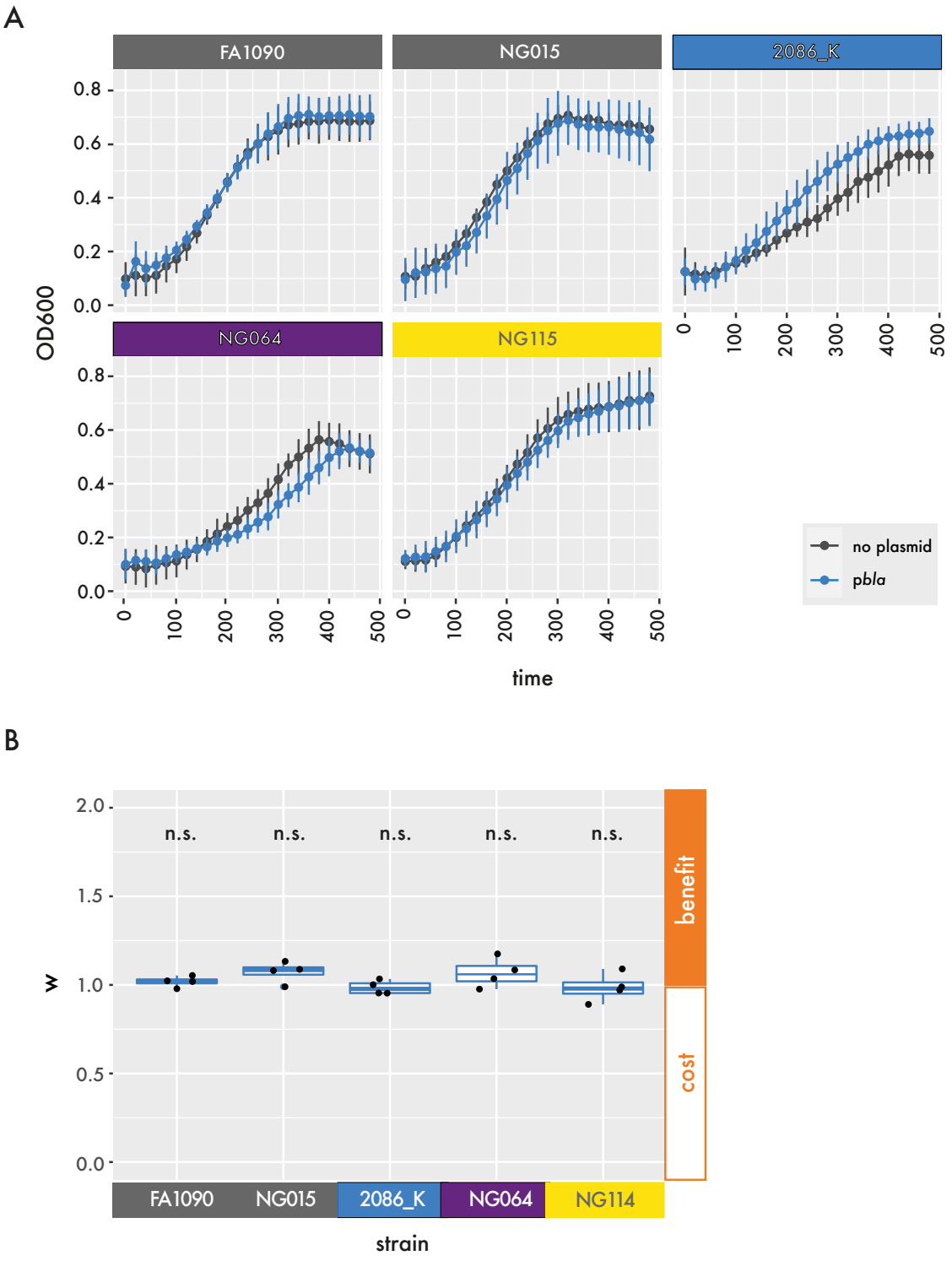

Figure 22: p*bla*.1 imposes no fitness cost in five different strains.
(A) Growth curves of plasmid-carrying (light blue) and plasmid-free (grey) isogenic strains. p*bla* was introduced into clinical isolates from different p*bla*-free (grey) or p*bla*-associated lineages (blue, p*bla*.1-associated; purple, p*bla*.1/p*bla*.2-associated; yellow, p*bla*.3-associated). Averages of three independent replicates are shown, with SD indicated as error bars. (B) Fitness cost (w) of p*bla*.1 measured in competition assays. w >1 indicates a benefit, whereas w <1 signifies a cost of a plasmid. Each dot represents a single experiment; n.s., not significantly different from 1 (t-test with Bonferroni correction for multiple comparisons).

I also performed competition assays to assess the relative fitness (w) of strains utilising shared resources[401]. In the assays, plasmid-carrying isolates with *pilD::ermC* were grown together with isogenic plasmid-free isolates with *pilD::aph* for 24 hours. The resistance marker allowed the enumeration of plasmid-carrying and plasmid-free isolates. To control for potential fitness costs of the chromosomal resistance markers, plasmid-free *pilD::ermC* and *pilD::aph* strains were also competed. In line with the results from the growth curves, w for p*bla*.1 carriage was not significantly different from 1 (t-test with Bonferroni correction for multiple comparisons, $p > 0.4$, Figure 22B), indicating that p*bla*.1 does not impose any fitness cost in any of the strains.

4.2.4 Fitness cost of p*bla*.2 correlates with its decreasing prevalence over time

p*bla*.1 did not impose a fitness cost in any of the strains tested and is the most prevalent p*bla* variant in gonococci. p*bla*.2 (7.4 kb) and p*bla*.3 (5.1 kb) differ in their size and gene content from p*bla*.1 (5.6 kb). I hypothesised that this could affect their fitness costs and introduced the p*bla* variants into isogenic FA1090 *pilD::ermC* strains. Plasmid-carrying strains were competed against FA1090 *pilD::aph(3),* and fitness costs were compared to the competition of plasmid-free FA1090 *pilD::ermC* and FA1090 *pilD::aph(3).* Like p*bla*.1, p*bla*.3 did not impose a significant fitness cost in FA1090 (Tukey multiple comparison of means, p = 0.73, Figure 23A). In contrast, p*bla*.2 inflicts a significant fitness cost in FA1090 (w = 0.7, Tukey multiple comparison of means, p = 0.02, Figure 23A).

p*bla*.2 differs from p*bla*.1 by the presence of *repB* and *ori*2/*ori*3. In *E. coli*, p*bla*.2 mostly initiates replication from *ori*2/*ori*3*,* and replication is independent of Pol I, while p*bla*.1 initiates replication from *ori*1 and is unable to replicate in a host lacking Pol I[306]. Differences in replication strategy might affect the copy number and fitness costs of variants. Therefore, I measured the copy number of p*bla* variants in FA1090 by ddPCR. Results show that p*bla*.2 has an increased copy number (>6 *vs.* 1-2 plasmids/chromosome, Figure 23B) compared to p*bla*.1, suggesting different replication strategies leading to changes in copy number could explain the fitness cost of p*bla*.2.

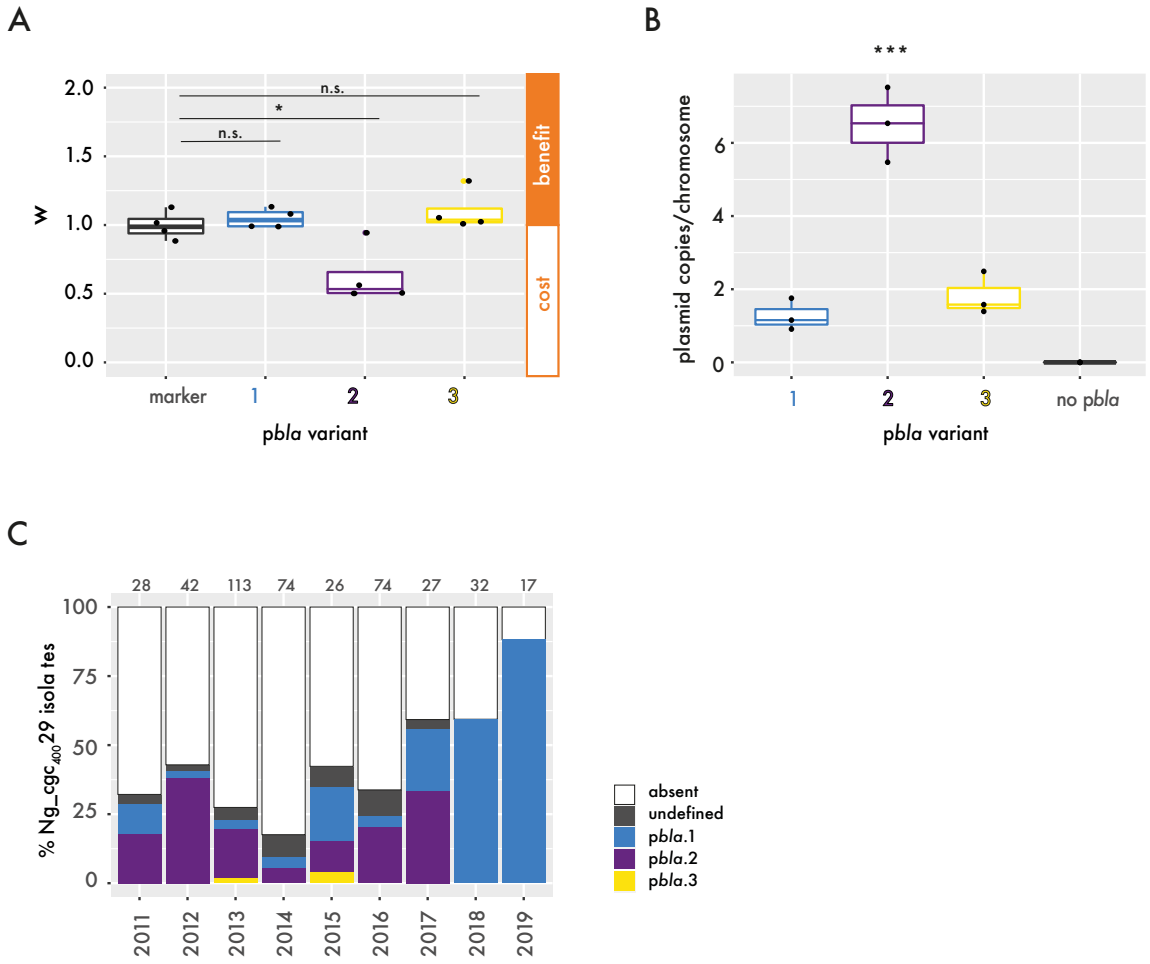

Figure 23: p*bla*.2-imposed fitness cost is reflected by its decreasing prevalence in gonococci.
(A) Fitness cost of p*bla* variants in FA1090 were assessed in four independent replicates and compared to the competition of FA1090 *pilD::ermC* vs. FA1090 *pilD::aph* (one-way ANOVA with Tukey multiple comparisons, n.s. $p > 0.05$; * $p < 0.05$). (B) Copy number of p*bla* variants in FA1090 was assessed by ddPCR (one-way ANOVA with Tukey multiple comparisons; *** $p < 0.001$). (C) p*bla*.1 and p*bla*.2 carriage in Ng_cgc_{400} 29 between 2011 and 2019 (n = 433 isolates). Bar colours indicate the p*bla* variant and numbers above the bars specify the number of isolates in each year.

I next assessed whether the competitive disadvantage of p*bla*.2 is reflected in the gonococcal population. My previous analysis of p*bla* prevalence in isolates on PubMLST between 2010 and 2019 (Figure 20), suggested a decreasing prevalence of p*bla*.2 in gonococci. However, this result could also reflect bias in the sampling of isolates or associations of plasmid variants with successful lineages. Fitness effects of a plasmid correlate with the phylogeny of a strain[132], and lower genetic diversity within a lineage should reduce the impact of strain-specific fitness, thereby increasing the relative influence of plasmid-specific fitness costs on population dynamics. Therefore, I also examined the prevalence of p*bla* variants within a single lineage, Ng_cgc$_{400}$ 29, which carries both p*bla*.2 and p*bla*.1. Between 2010 and 2020, there was a shift from p*bla*.2 to p*bla*.1, accompanied by an increase in p*bla* prevalence from <20% to >80% (Figure 23C).

Further evidence of the relative success of the p*bla* variants comes from their abundance within lineages. If a plasmid is costly, plasmid-carrying strains are outcompeted by plasmid-free strains, resulting in low plasmid prevalence. In contrast, strains harbouring a beneficial plasmid can undergo clonal expansion, increasing plasmid prevalence within a lineage. To test whether the fitness costs of p*bla*.2 correlate with a lower plasmid prevalence in p*bla*.2-associated lineages, I compared the percentage of isolates carrying p*bla* in the three largest Ng_cgc$_{400}$ that carry each p*bla* variant (Table 5). More than 50.1% and 39.0% of isolates carry p*bla* in p*bla*.1 and p*bla*.3-associated lineages, respectively. In contrast, p*bla*.2 is only present at comparably low frequency (18%, 8.5% and 0.5% in Ng_cgc$_{400}$s 29, 175 and 3, respectively) within lineages, indicating a competitive disadvantage of carrying p*bla*.2, and a lack of clonal expansion of isolates with this variant. Taken together, the fitness costs imposed by p*bla*.2 are consistent with the shift to p*bla*.1 within lineage Ng_cgc$_{400}$ 29, and its low prevalence within lineages in comparison to p*bla*.1 in the gonococcal population.

Table 5: The percentage of isolates carrying p*bla* in the three largest Ng_cgc$_{400}$ that are associated with a given variant.

p*bla* variant(s)	Ng_cgc$_{400}$	Number of isolates	p*bla* carriage (%)
1	21	574	64.3
1	33	476	51.9
1	187	94	62.8
1 / 2 / 3	3	4 545	1.2 / 0.5 / 0.3
1 / 2	29	473	14 / 18
2	175	318	8.5
3	25	346	56.8
3	298	101	39.6
3	391	31	87.1

4.3 Impact of mobilisation on the spread of p*bla* in gonococci

4.3.1 p*bla*.1 transfer in isogenic matings

Horizontal transfer of plasmids can enhance their presence within bacterial populations by compensating for plasmid loss during cell division and introducing them into novel genetic backgrounds. Therefore, I next examined p*bla* transfer by the gonococcal conjugative plasmid pConj. Previous studies reported highly variable transfer frequencies of p*bla*[308,314,402,403], which could be due to different donor and recipient strains, p*bla* and pConj variants used. To minimise the variables that could affect p*bla* transfer, I first focused on p*bla*.1 and pConj.1, the most prevalent and widely distributed p*bla*/pConj combination (Chapter 3.2.5), and assessed their transfer in matings between isogenic strains of FA1090. *ermC* and *aph(3)* were inserted into the *pilD* locus of donors and recipients, respectively, to eliminate transfer by transformation[294,340,404] and enable quantification by selective plating. pConj.1 and p*bla*.1 were introduced by conjugation and transformation, respectively.

A conjugation assay to measure pConj transfer has previously been established by Dr Wearn-Xin Yee[296], and I optimised the assay for p*bla* transfer. Initially, I determined the minimal amount of time required to detect transconjugants, as shorter mating times limit bias due to fitness effects of plasmid carriage or different growth rates of strains, and ensure the dynamics are dominated by donors and recipients rather than by transconjugants and recipients[405]. Briefly, donors and recipients were sub-cultured to mid-exponential phase, mixed at a 1:1 ratio, spotted onto agar at an inoculum of 10^6 CFU in 10 μl and incubated for 4, 6, 20 and 24 hours, after which donors, recipients and transconjugants were enumerated. Mobilisation rates were calculated as number of transconjugants / total number of recipients, and the ratio of donors to recipients was measured at the start and the end of the mating to detect differences in growth rates of donors and recipients. The mating between FA1090 *pilD::ermC* p*bla*.1 and FA1090 *pilD::aph(3)* served as a control. No

p*bla*.1 transfer was detected in the absence of pConj, confirming the dependence of p*bla* on the conjugative plasmid for its transfer. In the presence of pConj, p*bla* mobilisation was consistently observed after six hours of conjugation, with no significant difference in the proportion of transconjugants per recipients between the 6, 20 and 24 hour time points (one-way ANOVA, p = 0.33, Figure 24A). Therefore, subsequent matings were performed for 6 hours.

As the donor to recipient ratio could affect the frequency of plasmid transfer by impacting the likelihood of contact between donors and recipients, I next measured p*bla* transfer across different donor to recipient ratios (1:10, 1:2, 1:1, 2:1 and 10:1), while keeping the inoculum constant at 10^6 CFU. pConj transfer plateaued at ~ 80% at a 1:1 ratio, suggesting a saturation of the transfer due to the remarkably high conjugation frequency of pConj (Figure 24B). In contrast, p*bla* mobilisation increased from 0.08% (sd = 0.04%) to 1.2% (sd = 0.36%) when increasing the donor to recipient ratio from 1:10 to 10:1 (Figure 24B), and subsequent matings were performed at a 10:1 ratio.

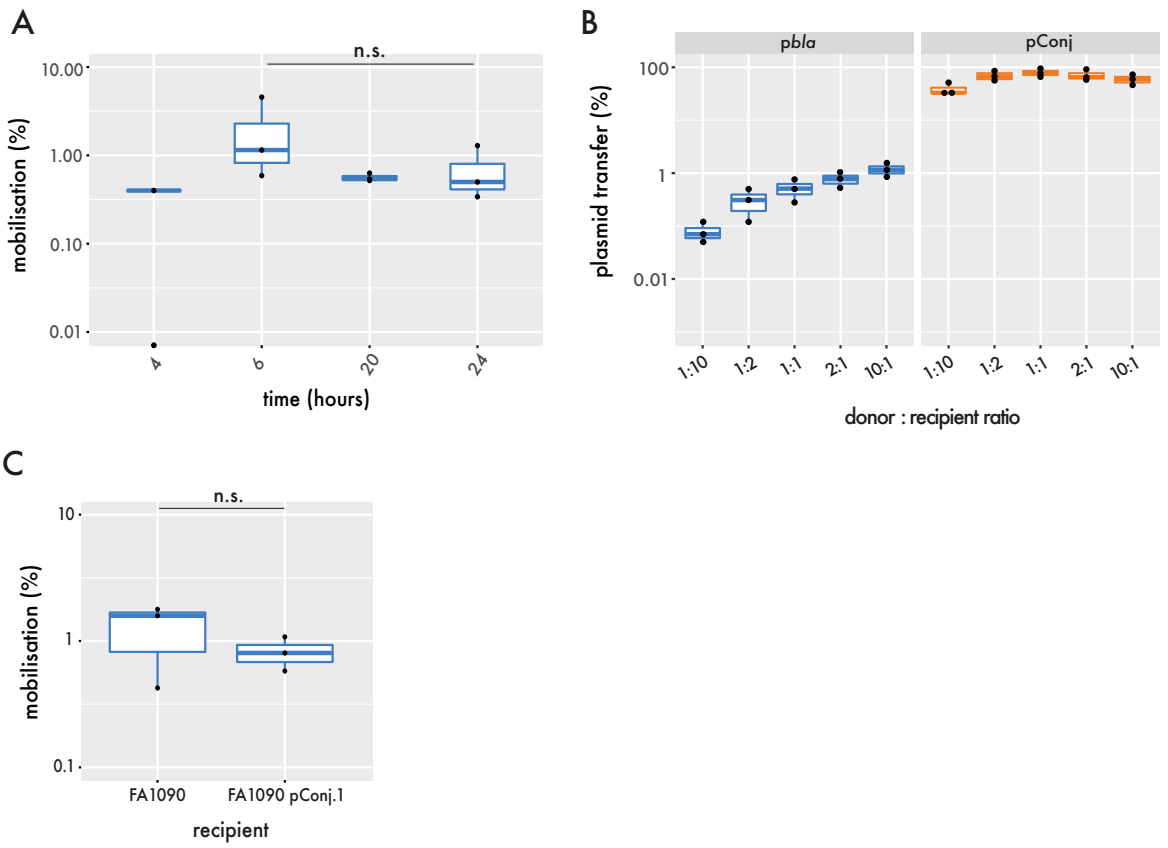

Figure 24: Mobilisation of p*bla*.1 by pConj.1 in isogenic matings.
(A) p*bla*.1 mobilisation by pConj.1 over time at a 1:1 donor to recipient ratio and an inoculum of 10^6 bacteria. The mobilisation frequency was calculated as the number of p*bla*-carrying transconjugants / recipients (one-way ANOVA of t = 6, 20 and 24 hour time points, p = 0.33). (B) p*bla*.1 and pConj.1 transfer at different donor to recipient ratios; the total number of bacteria was kept constant. (C) p*bla* mobilisation into a pConj-free and pConj-carrying recipient (Welch two-sample t-test, p = 0.87).

4.3.2 Lack of entry exclusion by pConj permits p*bla* acquisition

Conjugative plasmids can block the acquisition of other plasmids by expressing entry exclusion proteins[406]; entry exclusion could impede p*bla* mobilisation, as the initial transfer of pConj during conjugation could block subsequent acquisition of p*bla*. pConj encodes a predicted lipoprotein annotated as TrbK entry exclusion protein[293], with 21% amino acid similarity with *Agrobacterium fabrum* Ti plasmid TrbK (locus tag: ATU_RS23180, Genbank: NC_003065.3). I examined whether pConj in a recipient can impair the transfer of p*bla* by comparing the mobilisation rate of isogenic matings where the recipient either did or did not harbour pConj. Results show no difference in p*bla* transfer into pConj-free and pConj-containing recipients (1.1% and 0.9%, respectively, Welch two-sample t-test, p = 0.87, Figure 24C), indicating that surface exclusion mediated by pConj is unlikely to limit p*bla* spread in the gonococcal population.

4.3.3 Differences in p*bla* mobilisation by pConj variants explain their co-occurrence

While p*bla* is significantly associated with pConj, only isolates with pConj variants 1, 3, 4 and 5 also commonly carry p*bla* (Chapter 3.2.5 and Figure 25A). This could be due to the abundance and geographical distribution of these plasmids; pConj 1, 3 and 5 are the most prevalent variants in the gonococcal population, while pConj.4 is associated with isolates from Africa, where p*bla* is most prevalent (Chapter 3.2.3). Alternatively, the co-occurrence of plasmid variants could reflect interactions between them. For example, p*bla* MobA has a relaxase domain which nicks the *oriT* sequence on p*bla*[309], but then must interact with the pConj-encoded T4SS for its transfer[6]. Therefore, differences in the T4SS of pConj variants[286] may lead to distinct interactions with p*bla* and favour their co-transfer. Therefore, I evaluated whether pConj variants differ in their ability to mobilise p*bla*. I selected pConj variants that frequently co-occur with p*bla* (*i.e.* pConj.1, pConj.3, and pConj.4 with 59%, 37.9%, and 88.1% co-occurrence, respectively, Figure 25A) and pConj variants that do not (pConj.2 and pConj.7, with 26.3% and 9.0% co-occurrence, respectively). I then assessed the conjugation frequencies of the pConj variants and their ability to mobilise p*bla.*1. In FA1090, the conjugation rate of pConj variants differed significantly (Figure 25B, one-way ANOVA, $p < 0.001$) with pConj.1, 3 and 4 having conjugation frequencies of >79%. The conjugation frequencies of pConj.2 and pConj.7 (which are not highly associated with p*bla*) were three to four orders of magnitude lower (Figure 25B). p*bla* mobilisation mirrored the conjugation frequencies and was 1 to 2% in the presence of pConj variants 1, 3 and 4, while p*bla* mobilisation by pConj.7 was three orders of magnitude lower (Figure 25B); p*bla* transfer by pConj.2 was not detected in these assays (limit of detection = 0.001%). Therefore, results indicate that within the gonococcal population, p*bla* is particularly associated with pConj variants that can mobilise it efficiently.

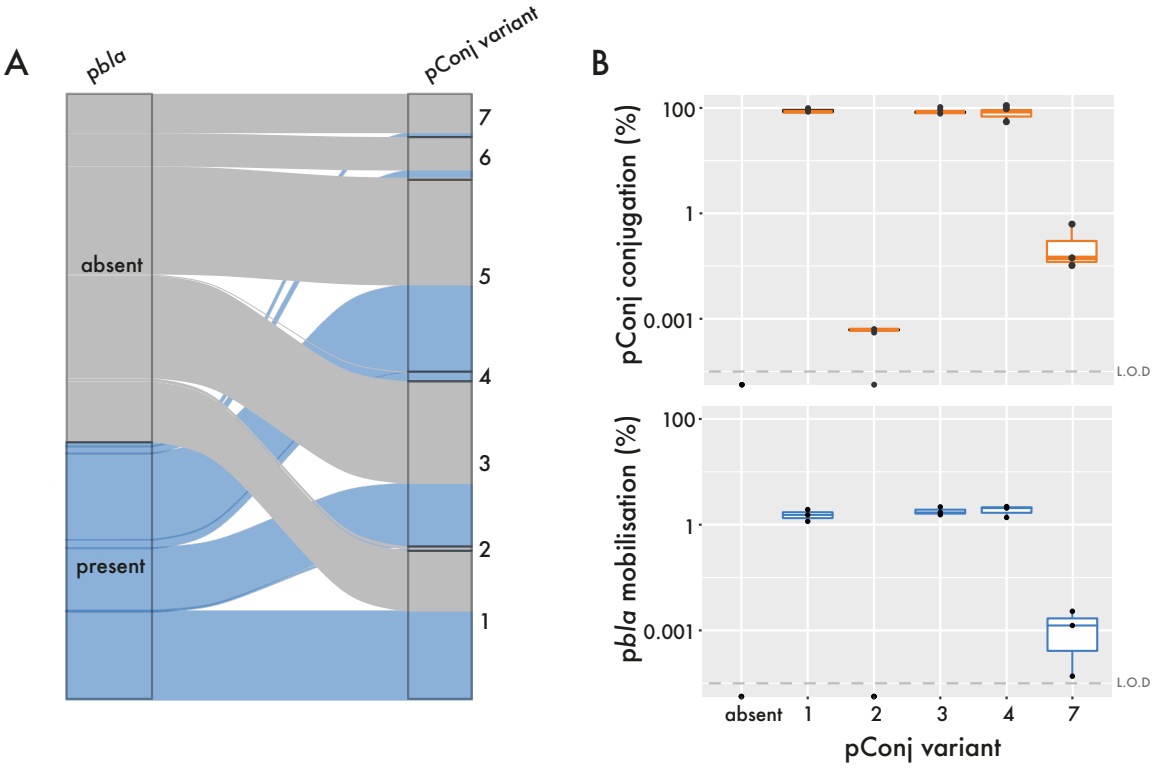

Figure 25: p*bla* co-occurrence and mobilisation by pConj variants.
(A) Sankey plot of pConj carrying isolates (n = 4 883 isolates), displaying the presence of p*bla* (left) and co-occurrence of p*bla* with individual pConj variants (right). (B) Conjugation rates of pConj variants (top) and the mobilisation rates of co-located p*bla*.1 (bottom). Plasmid transfer rates were calculated as the number of p*bla* or pConj-containing transconjugants / number of recipients; the limit of detection (L.O.D.) is indicated as a dashed line.

4.3.4 The limited distribution of p*bla*.3 correlates with its immobility

There are conflicting data about the mobility of p*bla*.3, which lacks the mobilisation region[312-314,407]. Therefore, I next assessed the mobilisation of wild-type p*bla* (p*bla*^{wt}) variants by pConj.1 in FA1090. Results demonstrate that p*bla*.1^{wt} and p*bla*.2^{wt} are mobilised efficiently with no significant difference between these variants (Figure 26A, 1.4% and 1.3%, respectively, Tukey multiple comparison of means, p = 0.99). Of note, p*bla*.3 mobilisation was not detected in any of these assays (limit of detection = 0.001%). To determine whether p*bla* variant deletions are responsible for the differences in mobilisation, I generated isogenic p*bla* variants (p*bla*.1^{iso} and p*bla*.3^{iso}) by introducing the variant-specific deletions into p*bla*.2^{wt}. The mobilisation frequency of p*bla*.1^{iso} did not differ from p*bla*.1^{wt} (Tukey multiple comparisons of means, p = 0.82). Furthermore, no transfer of p*bla*.3^{iso} was detected, showing that the variant-specific deletion is responsible for its immobility.

The inability of p*bla*.3 to be transferred by pConj correlates with its restricted distribution in the gonococcal population, with p*bla*.3 only found in the closely related Ng_cgc$_{400}$ lineages 25, 298 and 391 (Chapter 3.2.4), consistent with the clonal expansion of p*bla*.3-carrying strains.

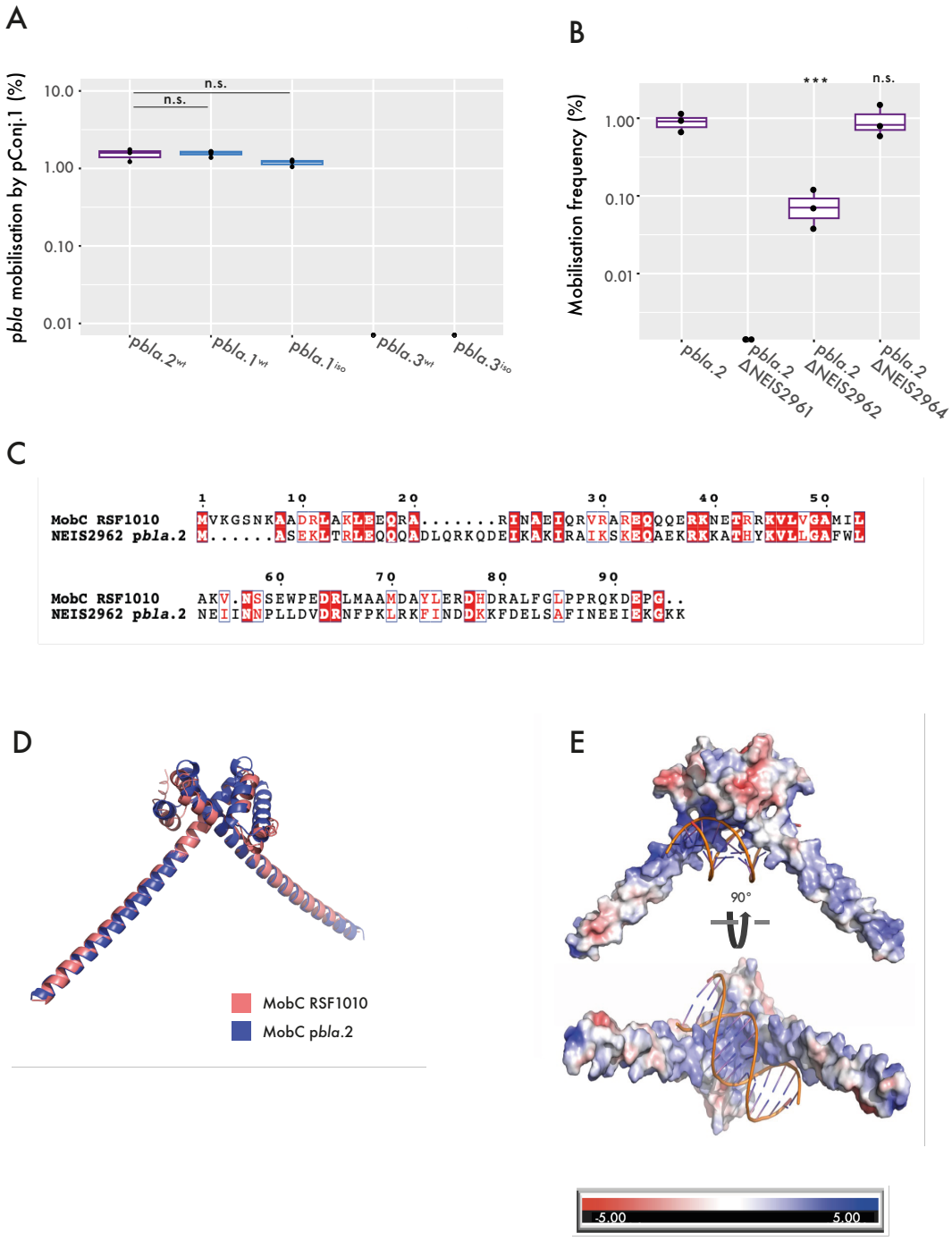

Figure 26: p*bla*.3 is immobile due to the lack of NEIS2961 (*mobA*) and NEIS2962 (*mobC*).
(A) Mobilisation rates of wild-type and isogenic p*bla* variants (p*bla*^{iso}) by pConj.1. (B) The impact of single *mob* gene knockouts in p*bla*.2 on p*bla* mobilisation frequencies. Three biological repeats were performed for all assays, and results were analysed by one-way ANOVA with Tukey multiple comparisons of means; n.s. p >0.05, *** p <0.001. (C) Alignment of MobC from *E. coli* plasmid RSF1010 (Genbank accession: S96966.1) and NEIS2962 from p*bla*.2 (Genbank accession: NZ_LT591911). Amino acid sequences were aligned with COBALT[3,4], and the alignment was visualised with ESprit[4,5]. Identical residues are shown in white on a red background, residues with a similarity score >0.7 are framed in blue, and the remaining residues are shown in black. (D) Superimposed AlphaFold3 structure prediction of MobC from the *E. coli* plasmid RSF1010 (salmon, Genbank accession: S96966.1) and NEIS2962 (blue) dimers (Match Align: 677.7, RMSD: 0.775 Å) (E) Electrostatics prediction of NEIS2962 homodimer with p*bla oriT* sequence using the APBS Electrostatics Plugin. Negatively and positively charged regions are shown in red and blue, respectively.

4.3.5 p*bla* requires its own MobA relaxase and MobC for its mobilisation

To further investigate the mechanism of p*bla* mobilisation, I deleted individual genes that are absent from p*bla*.3 (NEIS2961, NEIS2962 and NEIS2964) from p*bla*.2 and quantified the transfer of the resulting p*bla*.2$^{\Delta NEIS2961}$, p*bla*.2$^{\Delta NEIS2962}$, p*bla*.2$^{\Delta NEIS2964}$ by pConj.1. Deletion of NEIS2961, which encodes a MobA-family relaxase[309], abolished p*bla* transfer (Figure 26B), indicating that the pConj relaxase cannot recognise p*bla oriT* and compensate for the absence of the p*bla* relaxase. In the absence of NEIS2362, there was a significant reduction in p*bla* mobilisation (Tukey multiple comparisons of means, $p < 0.001$, Figure 26B). NEIS2962 encodes a protein with 26% amino acid similarity to MobC from the *E. coli* plasmid, RSF1010 (Figure 26C). *E. coli* MobC forms a homodimer that aids mobilisation by unwinding DNA at *oriT*, improving access of the relaxase to the adjacent DNA[408].

To assess whether NEIS2962 might act in a manner similar to RSF1010 MobC, I evaluated their predicted structural similarity using AlphaFold3 and characterised surface charge distributions using the APBS Electrostatics Plugin in PyMOL. RSF1010 MobC and NEIS2962 homodimers are closely related at a structural level (Figure 26D, pTM = 0.76 and pTM = 0.67, for RSF1010 MobC and NEIS2962, respectively, Match Align score: 677.704, Executive RMSD: 0.775 Å). Analysis of the distribution of electrostatic charges revealed a pronounced electropositive groove formed by RSF1010 MobC and NEIS2962 dimers, consistent with a putative DNA binding site. To evaluate the sequence specificity of the hypothesised MobC-DNA interactions, I incorporated dsDNA corresponding to p*bla oriT*, sequences of identical length and nucleotide composition ('scrambled *oriT* sequences'), and random dsDNA of identical length into the model. Alphafold3 structural predictions indicate binding of dsDNA *oriT* to the electropositive groove of NEIS2962 (Figure 26E), but not of random or scrambled *oriT* sequences. This suggests that NEIS2962 increases p*bla* mobilisation in a manner analogous to RSF1010 MobC[408].

NEIS2964 is present in two copies on p*bla*.2, yet deletion of both copies did not impact p*bla* transfer (Figure 26B), indicating that it does not contribute to p*bla* mobilisation in these assays.

4.4 Summary

In Chapter 3, I showed that three major p*bla* variants have distinct patterns of distribution in the gonococcal population, raising the question of what molecular mechanisms underlie this distribution. Here, I explored the impact of plasmid fitness costs, resistance and mobilisation patterns on the distribution of p*bla* variants in gonococci.

The spread of a plasmid in a bacterial population is shaped by the complex interplay between plasmid and strain-specific, as well as ecological factors. For example, I found that p*bla* variants carry distinct TEMs, which lead to different resistance levels in the same genetic background. However, p*bla*-mediated resistance also varies between strains, probably through the synergistic effects of chromosomal resistance mutations and differences in cellular TEM levels. This suggests that the benefit offered through the same p*bla* variant can differ between strains. However, for the small sample size of isolates tested, there was no indication that strain-specific resistance levels determine the association of p*bla* variants with certain lineages. Future studies could expand the panel of strains tested, examine the interactions between chromosomally- and plasmid-mediated resistance in an isogenic background, and determine enzyme stability in different strain backgrounds.

p*bla* is associated with pConj, which promotes the spread of the β-lactamase plasmid. Here, I showed that pConj variants differ in their conjugation rates, and I found that the p*bla* mobilisation frequency in isogenic matings correlates with the conjugation frequency of the co-resident pConj. The differences in the ability of pConj variants to mobilise p*bla* are reflected by a high p*bla* co-occurrence with pConj variants that efficiently mobilise it. Unlike many conjugative plasmids, pConj lacks entry exclusion, allowing p*bla* to enter bacteria already containing pConj. This dynamic interaction supports the spread of successful p*bla*/pConj pairs, such as p*bla*.1/pConj.1, across the gonococcal population.

Plasmid success in bacterial populations depends on their ability to spread horizontally across lineages and/or persist vertically within clonal populations. In the absence of active maintenance systems, the probability of p*bla* being lost during cell division depends on its copy number, *i.e.* the more plasmids are present in a cell, the more likely both daughter cells are to inherit at least one copy of the plasmid. p*bla*.1 and p*bla*.3 have an intermediate copy number, which should lead to a slow decline in p*bla* in gonococci over time. However, whilst no longer recommended for the treatment of gonorrhoea, penicillins are amongst the most consumed antibiotics[409]. Therefore, sporadic bystander selection due to treatment of other diseases may support the persistence of these p*bla* variants in gonococci[410].

p*bla*.2 imposes significant fitness costs which correlates with its increased copy number. p*bla*.2 encodes two distinct replication initiation proteins and origins of replication, whereas the less costly p*bla*.1 only carries one *rep* and *ori*. Previous work in *E. coli* indicates that while p*bla*.1 initiates replication from *ori1*, p*bla*.2 preferentially uses *ori*2/*ori*3, changing its dependency on PolA and incompatibility group[306]. The expression of distinct Reps might explain the differences in copy number and costs, potentially by sequestering host DNA replication machinery[67]. Of note, the replication of p*bla*.3 has not been explored to date. Compared to the equally mobile p*bla*.1, p*bla*.2 is present at a lower abundance in the gonococcal population, and p*bla*.2-associated lineages show low plasmid prevalence compared to p*bla*.1 and p*bla*.3-carrying lineages (Table 5), which could reflect the fitness disadvantage of p*bla*.2-carrying strains. The fitness cost of p*bla*.2 is further illustrated by the change from p*bla*.2 to p*bla*.1 in Ng_cgc$_{400}$ 29, and reports of an epidemic of p*bla*.1-carrying isolates in Guangdong, China[398], a region previously associated with p*bla*.2.

p*bla*.3 has undergone clonal expansion, demonstrating its successful adaptation to gonococci. TEM-135 initially arose in p*bla*.2 and confers higher resistance levels. However, the fitness cost of p*bla*.2 may have hindered its spread. Through gene loss, p*bla*.3 evolved from TEM-135 carrying p*bla*.2, eliminating mobility but concomitantly avoiding obvious fitness costs. Due to the lack of

mobility, p*bla*.3 is not widely disseminated but has promoted the expansion of related lineages, potentially due to the enhanced β-lactam resistance conferred by TEM-135.

In summary, multiple factors contribute to the distribution of p*bla* in gonococci, including strain background, co-resident pConj, and p*bla*-specific characteristics such as mobility, fitness costs and TEM variant. It would be interesting to use the established parameters for p*bla* as inputs for agent-based modelling approaches to assess contributions of fitness, mobilisation and resistance to the spread of p*bla* and test different selection scenarios to predict future trends in plasmid-mediated resistance in gonococci.

5 Impact of restriction modification systems on plasmid transfer

5.1 Distinct associations of RMSs and plasmid carriage

Restriction modification systems (RMSs) are bacterial defence modules that recognise and cleave dsDNA based on its methylation profile. The methyltransferase of an RMS protects self-DNA by methylating sequences recognised by the restriction endonuclease. Incoming DNA that lacks this modification is restricted, and RMSs can act as a barrier to phages, transformation and plasmid acquisition[411]. *N. gonorrhoeae* possesses a remarkably large number of RMSs given the size of its genome (2.2 Mb); individual strains have 13 - 16 RMSs, while only 3 - 4 are present in other organisms with a similar sized genome[220,222].

I found that p*bla* is associated with certain lineages but absent from others (Chapter 3.2.4). A similar uneven distribution of pConj is seen, although pConj is more prevalent and widely distributed than p*bla*[412] (Figure 27A and B). Plasmid variant-specific mobility patterns provide some insights into their distribution in the population. For example, the restricted spread of p*bla*.3 and pConj.2 in the population (Chapter 3.2.4 and [286]) correlates with their lack of mobility and low transfer (Chapter 4.3.4 and [296]), respectively. However, variant-specific mobility patterns do not explain the absence of plasmids from certain lineages. I hypothesised that lineage-specific RMSs could limit plasmid transfer within the gonococcal population and explain the patchy distribution of plasmids.

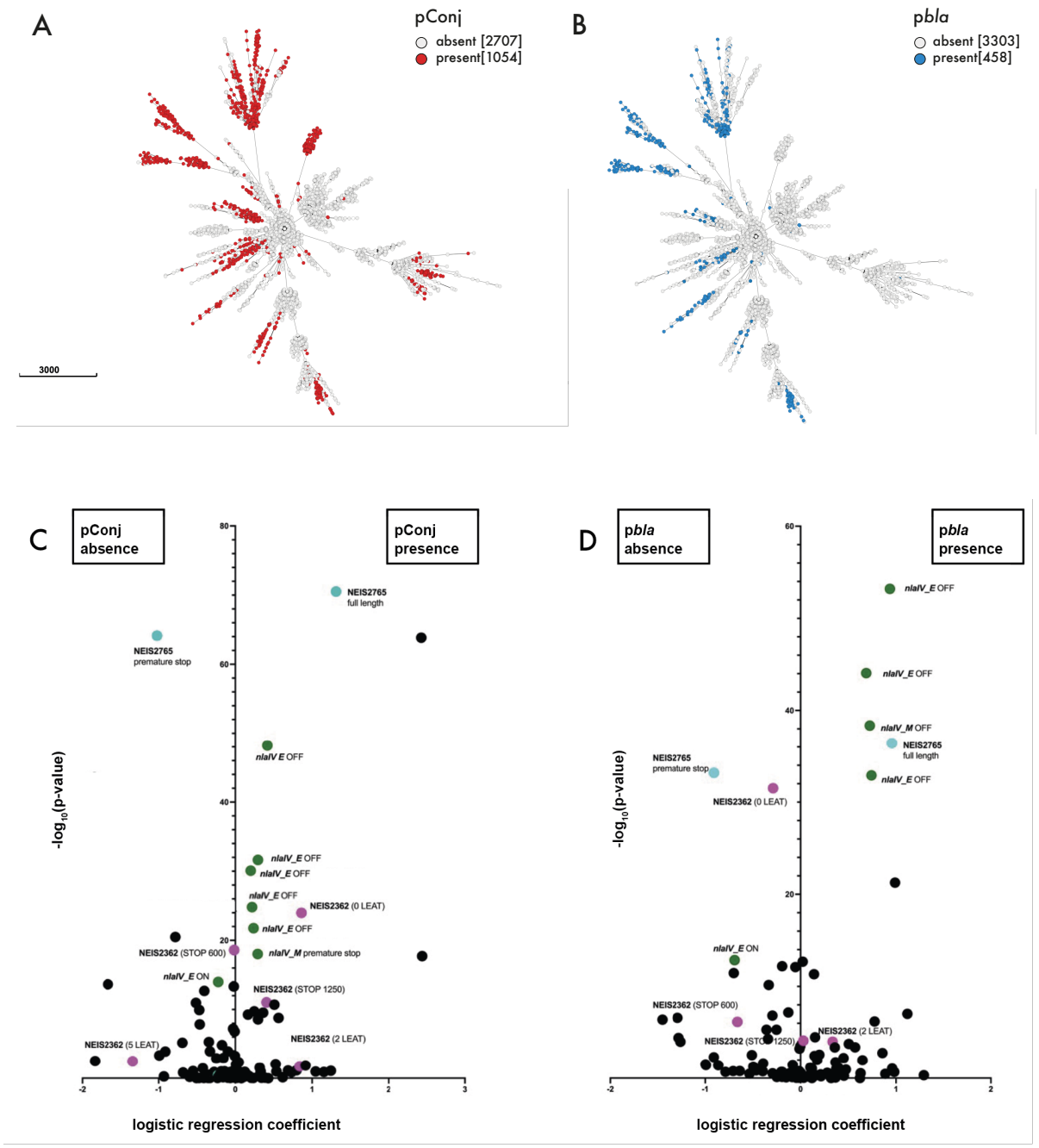

Figure 27: Association of plasmid carriage with features of RMSs.
Minimum spanning trees of 3 761 gonococcal isolates showing the distribution of pConj (A) and p*bla* (B) in gonococci. Isolates were clustered by core genomic allelic differences (cgMLST v1) using GrapeTree and coloured according to their plasmid carriage. The number of isolates carrying pConj and p*bla* is given in brackets. (C, D) Logistic regression of the correlation of individual features of RMS genes with plasmid presence (positive logistic regression coefficient) or absence (negative logistic regression coefficient). The y-axis indicates the negative logarithm of the p-value of the respective prediction, *i.e.* the higher the value, the more confident the prediction. Dots represent individual features of RMSs. Features of NEIS2765 (cyan), *nlaIV_E* and *nlaIV_M* (green) and NEIS2362 (magenta) are indicated for pConj (C) and p*bla* (D). Different poly-T tract lengths within *nlaIV_E* result in inactive NlaIV_E and are indicated as separate datapoints. The logistic regression analysis was performed by Dr Aden Forrow and Dr Sam Palmer.

To identify RMSs that potentially influence the distribution of p*bla* and pConj in gonococci, a dataset of 3 760 isolates with available WGS was used, representing 154 distinct Ng_cgc$_{400}$s. p*bla* is present in 440 (11.7%) and pConj in 1 032 (27.45%) of isolates. Dr Ana Cehovin had curated the RMS loci in these strains in PubMLST and identified a total of 16 RMSs, encoded by 33 loci (Table 6). Type II RMSs were the most frequent (12/16), with examples of type I (2/16) and type III (2/16) RMSs also present. Notably, 28/33 loci are core to the gonococcus, *i.e.*, present in more than 95% of isolates in the population. Besides the presence/absence of systems, changes in the activity or specificity of RMSs could also affect plasmid acquisition. Therefore, for each RMS locus, features such as premature stop codons and homo- or polynucleotide tracts were identified. Of the 33 RMS loci, 15 had features which could affect the activity of the RMS (Table 6).

Next, the correlation between variation in RMS loci and the presence or absence of p*bla* and pConj was examined to identify RMSs that are likely to affect plasmid transfer. For this, we collaborated with Dr Aden Forrow and Dr Sam Palmer (Mathematical Institute, University of Oxford), who conducted a logistic regression analysis, a statistical modelling approach used for predicting binary outcomes[413]. In this case, the model predicts whether a strain carries pConj or p*bla* based on the presence and features of RMS loci. Each RMS feature (*e.g.* presence of NlaIV endonuclease with a premature stop codon) was a potential predictor in the model, and the logistic regression estimated a regression coefficient for each feature that quantified how much a feature contributes to the likelihood of the plasmid being present[414]. A positive regression coefficient indicates the feature is associated with the presence of p*bla* or pConj, while a negative coefficient indicates an association with the absence of a plasmid.

The analysis suggested features of NEIS2765 (NgoAII endonuclease), NEIS1181 (NlaIV endonuclease), NEIS1180 (NlaIV methyltransferase), and NEIS2362 (*hsdS* of NgoAV) correlate with plasmid presence (Figure 27C and D). I have therefore investigated the impact of the NgoAII, NlaIV and NgoAV RMSs on the transfer of p*bla* and pConj in *N. gonorrhoeae*.

Table 6: RMS loci in the dataset. Loci present in >95% of gonococci (core) and loci with variable features that were included in the logistic regression are indicated.

Locus	Product	RMS	RMS type	Core	Variable features
NEIS0328	DpnIIB methyltransferase	NgoAXI	II	Yes	Yes
NEIS0678	NmeDIP very-short-patch-repair endonuclease	NgoAXIII	II	Yes	Yes
NEIS1158L	Methyltransferase	NgoAXVII	I	Yes	Yes
NEIS1180	BanIM methyltransferase	NgoAXV	II	Yes	Yes
NEIS1181	Restriction endonuclease NlaIV	NgoAXV	II	Yes	Yes
NEIS1193	StyLTI restriction endonuclease	NgoAX	III	No	No
NEIS1194	ModB methyltransferase	NgoAX	III	No	Yes
NEIS1310	ModA methyltransferase	NgoAXII	III	No	Yes
NEIS1311	Restriction endonuclease	NgoAXII	III	Yes	No
NEIS1990	Very short patch repair protein	NgoAXIV	II	Yes	No
NEIS1992	DNA (cytosine-5-)-methyltransferase	NgoAXIV	II	Yes	No
NEIS2361	HsdM; DNA methyltransferase subunit M	NgoAV	I	Yes	Yes
NEIS2362	HsdS; specificity subunit S	NgoAV	I	Yes	Yes
NEIS2391	HsdR; restriction enzyme EcoR124II R protein	NgoAV	I	Yes	Yes

NEIS2477	Restriction endonuclease DpnC	NgoAXI	II	Yes	Yes
NEIS2534	HsdR; RM R protein	NgoAXVII	I	Yes	Yes
NEIS2535	HsdS; specificity subunit S protein	NgoAXVII	I	Yes	No
NEIS2593	BcgIA restriction-modification enzyme	NgoAVIII	II	Yes	No
NEIS2594	BcgIB specificity unit	NgoAVIII	II	Yes	No
NEIS2596	Restriction endonuclease R.NgoVII	NgoAVII	II	Yes	No
NEIS2597	Methyltransferase BspRIM; M.NgoVII	NgoAVII	II	Yes	No
NEIS2664	HaeIII methyltransferase; M.NGOI	NgoAIV	II	Yes	No
NEIS2665	NgoMIVR restriction endonuclease; R.NGOI	NgoAIV	II	Yes	No
NEIS2691	Eco29kI restriction endonuclease; R.NgoMIII	NgoAIII	II	No	No
NEIS2692	ApIIM_2; DNA cytosine methyltransferase M.NgoMIII	NgoAIII	II	No	No
NEIS2722	Methyltransferase	NgoAII	II	Yes	No
NEIS2725	FokIM methyltransferase	NgoAXVI	II	Yes	No
NEIS2727	HhaIM methyltransferase	NgoAI	II	Yes	No
NEIS2728	HaeII restriction endonuclease	NgoAI	II	Yes	No

NEIS2765	NgoPII restriction endonuclease	NgoAII	II	Yes	Yes
NEIS2910	HaeIII methyltransferase	NgoAVI	II	Yes	No
NEIS3175	HpaII methyltransferase	NgoAIII	II	Yes	Yes
NEIS3176	Restriction endonuclease	NgoAIII	II	Yes	Yes

5.2 The type I RMS NgoAV has a minimal impact on plasmid transfer

Variation in the HsdS specificity subunit of the type I RMS NgoAV can alter the recognition motif of the system[222,227]. Logistic regression analysis showed a correlation between variation in *hsdS* and the presence/absence of pConj (Figure 27C). Type I RMS form multi-subunit complexes of the specificity (HsdS), methyltransferase (HsdM), and DNA restriction-translocation (HsdR) subunits. The methyltransferase complex is composed of two HsdM and a single HsdS (M_2S_1), and NgoAV catalyses the addition of a methyl group to the N6 position of adenosine (m6A) within its bipartite recognition sequence[222]. The addition of two HsdR subunits to the M_2S_1 complex forms the functional restriction complex ($R_2M_2S_1$). Sequence recognition by HsdS is essential for both methylation and restriction by the type I RMS[70]; therefore, changes in HsdS affect both restriction and methyltransferase activity of the system.

NgoAV *hsdS* has three variable regions (Figure 28A)[222]: i) an indel at position 186, ii) a region with different numbers of repeats of the nucleotide sequence encoding for the amino acids 'LEAT' and iii) a poly-G tract in the middle of the ORF (starting at position 612 for *hsdS* encoding 2 LEATs). Both indel and changes in the lenght of the poly-G tract alter the length of HsdS. Insertion of a T at position 186 results in a premature stop codon and an inactive HsdS of 63 amino acids ($HsdS_{63}$)[222]; different lengths of the poly-G tract translate into full-length HsdS (~ 400 amino acids, $HsdS_{400}$) or a shorter version of ~ 200 amino acids ($HsdS_{200}$) due to a premature stop codon.

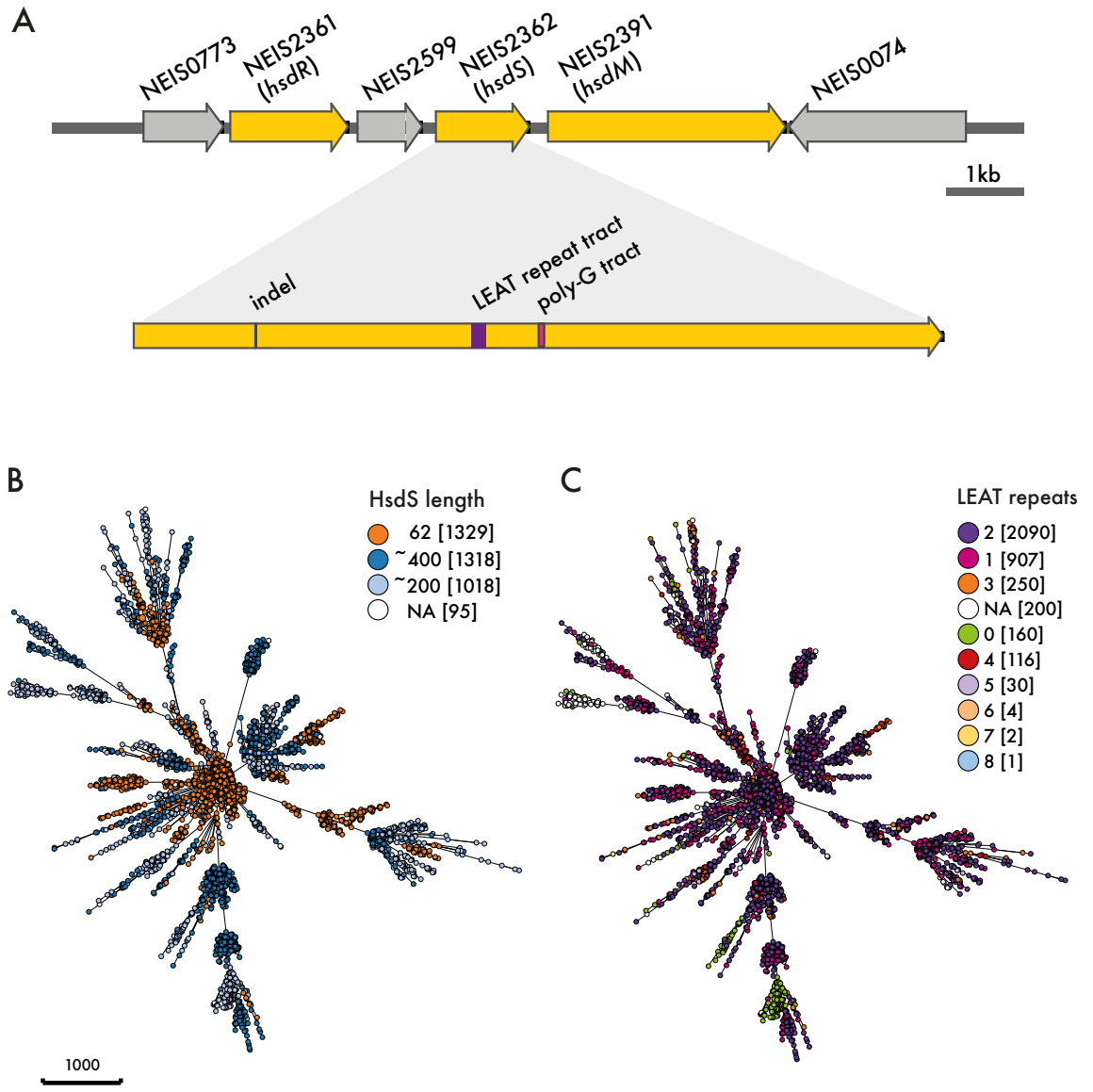

Figure 28: NgoAV *hsdS* has three regions of variability.
(A) Gene organisation of the NgoAV locus, where *hsdM* (NEIS2361), *hsdS* (NEIS2362) and hsdR (NEIS2391) are flanked by the genes encoding an ADP-D-beta-D heptose epimerase (NEIS0073) and a putative ATP-dependent protease (NEIS0074). NEIS2599 encodes the DNA damage-inducible protein D. Shown below are the three variable regions within *hsdS*: an indel at position 186 (leading to an inactive enzyme), a region with repeats of the nucleotide sequence encoding the amino acids 'LEAT' (purple rectangle) and a poly-T tract (pink rectangle). (B, C) Minimum spanning trees of 3 760 gonococcal isolates displaying HsdS length in amino acids (B) and the number of LEAT repeats (C) in the population. Incomplete *hsdS* loci, where the number of LEAT repeats and HsdS length could not be determined, are indicated as NA.

I investigated the prevalence and distribution of HsdS features in the dataset of 3 760 gonococcal isolates. Sequences encoding for $HsdS_{63}$, $HsdS_{200}$ and $HsdS_{400}$ were present in isolates at approximately equal frequency (35.3%, 27.2% and 35.0%, respectively, Figure 28B). *hsdS* in the dataset encoded for zero to eight copies of LEAT; two (55.8%) and one copy (24.0%) were the most common number of repeats (Figure 28C). Of note, isolates that cluster together on the tree encode HsdS of the same length (Figure 28B). In contrast, the number of encoded LEAT repeats varied between closely related isolates, suggesting this feature is phase-variable (Figure 28C). The only exception to this was isolates with no HsdS LEAT, which clustered together on the tree; logistic regression analysis indicated HsdS with no LEAT is associated with pConj presence (regression coefficient = 0.86, $-\log_{10}(p) = 23.98$, Figure 27C), but p*bla* absence (regression coefficient = -0.29, $-\log_{10}(p) = 31.51$, Figure 27D)

To analyse how the variation in *hsdS* affects HsdS, I predicted the structures of $HsdS_{400}$ and $HsdS_{200}$ using AlphaFold3 (Figure 29A and B, pTM = 0.66 and pTM = 0.77, respectively). Similar to other type I RMS HsdS, NgoAV $HsdS_{400}$ has two target recognition domains (TRD1 and TRD2, amino acids 18 - 153 and 219 - 356, respectively) that are separated by two α-helices (Figure 29A)[72]. $HsdS_{200}$ has a single TRD1 and one α-helix (Figure 29B). TRD1 and TRD2 share 26.45% amino acid identity, and comparison of structure predictions of individual TRDs in PyMOL indicated a Root Mean Square Deviation (RMSD) of 1.736 Å. The RMSD indicates the average distance between atoms after the structures have been aligned to minimise this distance[415]; an RMSD of 1.736 Å suggests a small to moderate level of structural difference[416]. The LEAT repeats lie within the α-helix that is present in both $HsdS_{400}$ and $HsdS_{200}$ (Figure 29A and B). Comparison of $HsdS_{400}$ with different numbers of LEAT repeats revealed that the number of LEATs alters the spacing and pitch of the TRDs (Figure 29C). For example, the spacing between the TRDs in predicted structures of $HsdS_{400}$ with 0, 1 and 2 LEAT repeats was 68.2 Å, 72.8 Å and 76.5 Å (measured between S154 and N210/214/218), respectively.

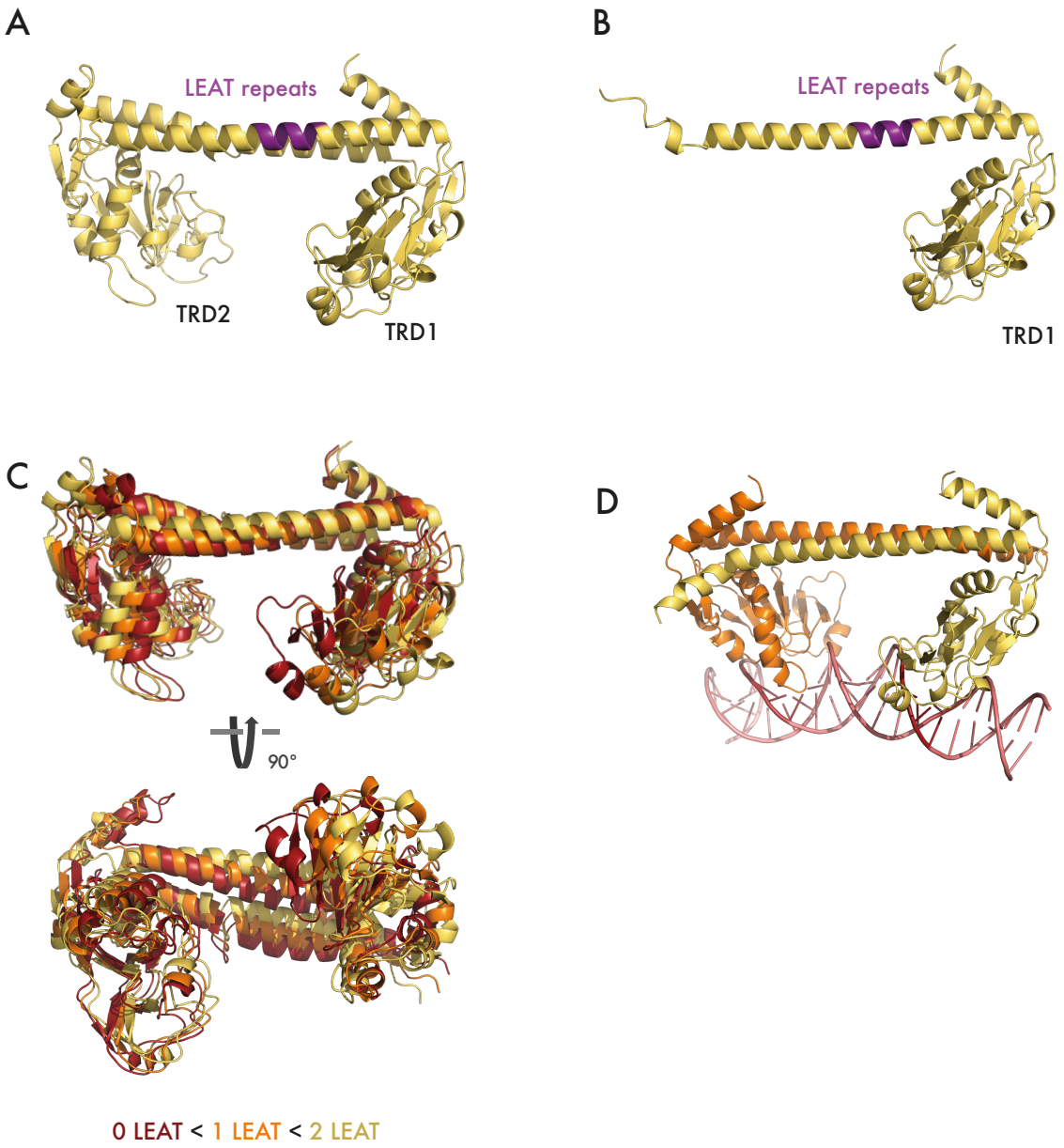

Figure 29: AlphaFold3 predictions of HsdS variants.
(A, B) AlphaFold3 predictions of $HsdS_{400}$ (A) and $HsdS_{200}$ (B). LEAT repeat regions are indicated in purple. (C) Superimposed $HsdS_{400}$ with 0 (red), 1 (orange) and 2 LEAT (yellow) repeats. (D) $HsdS_{200}$ dimer with dsDNA containing the palindromic motif $GCAN_8TGC$ (shown in red).

In the dataset, the most prevalent combination was $HsdS_{400}$ with two LEAT repeats (23.6% of isolates), followed by $HsdS_{200}$ with two LEAT repeats (13.5%) and $HsdS_{400}$ with one LEAT repeat (10.0%). No repeats were mostly found in $HsdS_{200}$ (96.9% of sequences without LEAT). To understand how these changes in HsdS affect methylation, I generated isogenic FA1090 strains with the four most prevalent HsdS variants, and with *hsdS* replaced by *aph(3)-galK*. Strains were sequenced with Nanopore, and sequencing data were processed with Dorado and Modkit to detect m6A methylation and identify motifs (Table 7). All strains showed methylation of the NgoAXVI GGTG<u>A</u> recognition sequence, as well as GCAG<u>A</u>, recognised by NgoAXII. Both RMSs are predicted to be active in FA1090. Strains encoding $HsdS_{400}$ also showed methylation of GC<u>A</u>N_xGTC and G<u>A</u>CN_xTGC motifs, with >99.5% of motifs in the genome modified. Of note, the spacer length (N_x) between the methylated motifs differed between $HsdS_{400}$ with one LEAT (six nucleotides) and two LEATs (seven nucleotides), consistent with an increase in spacing between the TRDs in the two $HsdS_{400}$ structures (Figure 29C).

In contrast, $HsdS_{200}$ with 2 LEAT repeats methylated the palindromic sequence GC<u>A</u>N_8TGC (99.3% of motifs modified). The first part of the sequence is conserved between the $HsdS_{400}$ and $HsdS_{200}$ methylation motifs, indicating TRD1 recognises GCA, whereas TRD2 (only present in $HsdS_{400}$) recognises the TGC sequence. The palindromic sequence methylated in the strain encoding $HsdS_{200}$ with 2 LEATs, suggests $HsdS_{200}$ might dimerise to recognise the bipartite sequence. $HsdS_{200}$ dimerisation is supported by AlphaFold3 predictions of $HsdS_{200}$ with dsDNA containing the GCAN_8TGC motif, indicating that two $HsdS_{200}$ reconstitute the two TRD structure of $HsdS_{400}$ (Figure 29D, ipTM = 0.55). Of note, no additional m6A methylation was detected in the strain encoding $HsdS_{200}$ without LEAT repeats, suggesting that this HsdS variant is inactive.

Table 7: HsdS of strains constructed with their methylation motifs and number of target sequences on p*bla* and pConj.

HsdS length	**# LEAT**	**motif**	**fraction of modified motifs (%)**	**# sites on pConj.1 (34 kb)**	**# sites on p*bla*.1 (5.6 kb)**
200	0	-		0	0
200	2	GC<u>A</u>N$_8$TGC	99.3	15	1
400	1	GC<u>A</u>N$_6$GTC	99.5%	6	1
		G<u>A</u>CN$_6$TGC	100%		
400	2	GC<u>A</u>N$_7$GTC	100%	21	2
		G<u>A</u>CN$_7$TGC	100%		

To examine the effect of NgoAV on conjugation, I performed isogenic matings with FA1090-based donors and recipients with different versions of HsdS (Figure 30). As in Chapter 4, donor strains contained *pilD::ermC,* p*bla*.1 and pConj.1 and recipients *pilD::aph(3)*. Results show that plasmid transfer was only slightly reduced in matings between strains with different *hsdS*; conjugation rates were reduced by less than 50% compared to matings where donor and recipient had identical *hsdS*, and all conjugations yielded >34.2% of transconjugants. Similarly, p*bla* mobilisation was only minimally affected.

The logistic regression revealed a correlation between strains encoding HsdS without LEATs and pConj carriage (Figure 27C). The methylation analysis did not reveal any NgoAV methylation in the strain with $HsdS_{200}$ without LEAT, indicating NgoAV is inactive. As expected in the absence of restriction barriers, the strain with no LEAT was an efficient recipient (conjugation rates >74.2%, mobilisation rates >2.4%). However, the absence of the NgoAV methylation pattern in the donor would be expected to result in a reduction in the transfer of plasmids into strains with an active NgoAV system. Counterintuitively, the strain with $HsdS_{200}$ and no LEAT was also an efficient donor (Figure 30). The activity of an RMS with an overlapping motif could explain the high transfer rates observed for the donor with inactive HsdS; NgoAV $HsdS_{400}$ shares a GAC in its recognition motif with the motif of NgoAVII $(GACN_5TGA)^{222}$. However, the base modified by NgoAVII remains undetermined, and I did not detect any methylation of NgoAVII motif in the strain with an inactive NgoAV system, indicating that the NgoAVII might not be active.

In summary, HsdS variants differ in their recognition motif due to changes in the number of LEAT repeats, which is predicted to alter the spacing of the TRDs, and the number of TRDs (2x TRD1 in $HsdS_{200}$ dimers *vs*. TRD1 and TRD2 in $HsdS_{400}$, Figure 29). However, isogenic matings between strains with different HsdS showed only minimal effects of NgoAV on plasmid transfer in *N. gonorrhoeae*.

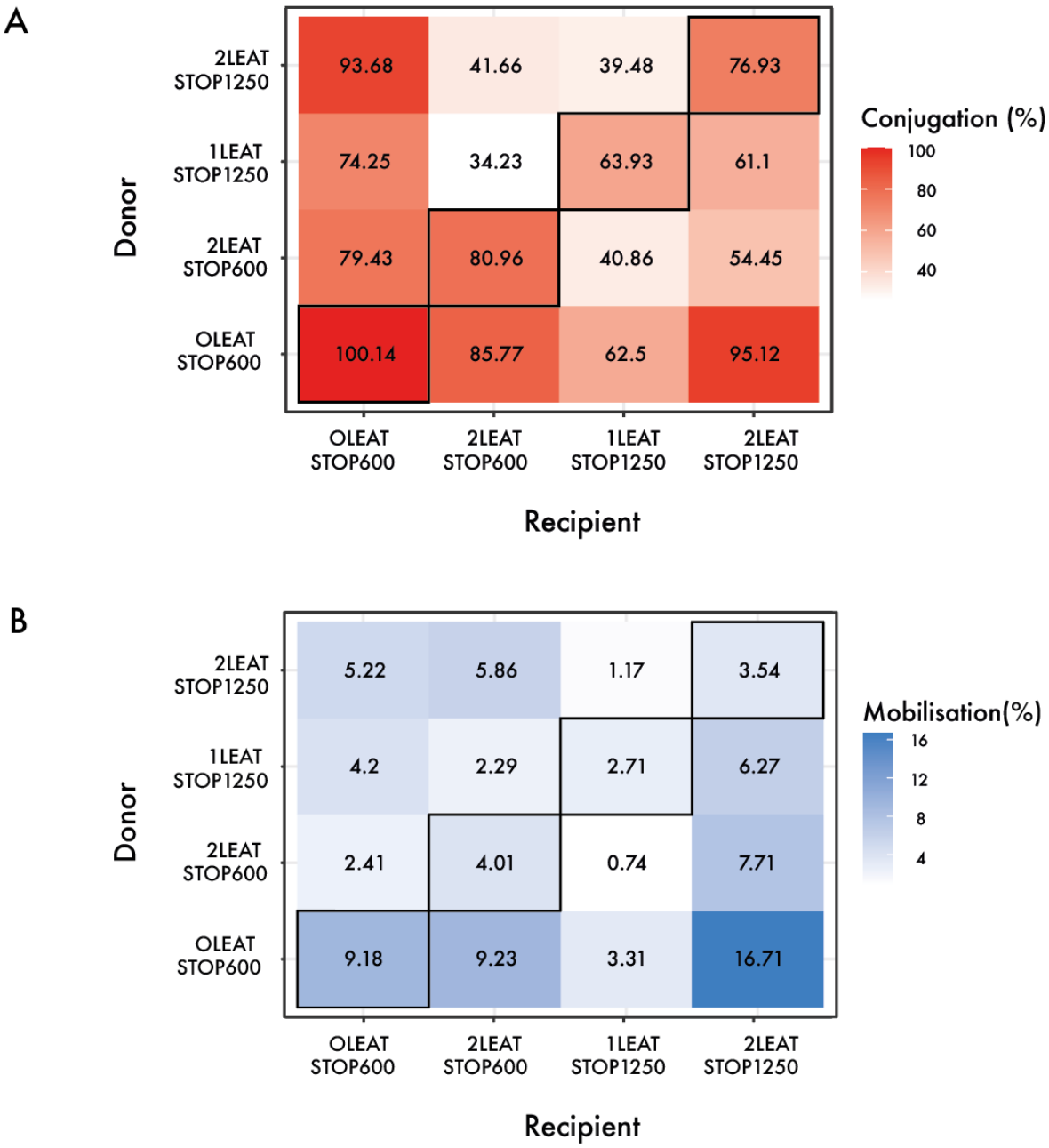

Figure 30: Heatmaps displaying the transfer rates of pConj (A) and p*bla* (B) in matings between isogenic FA1090 strains with different *hsdS*.
Darker colours indicate higher plasmid transfer, and numbers in boxes give the average of matings performed on three occasions. Isogenic matings along the diagonal are highlighted.

5.3 The NlaIV endonuclease impacts plasmid acquisition

NlaIV is a type II RMS which recognises the 5'-GGNNCC-3' motif[417]. Type II RMSs have separate enzymes for DNA methylation and restriction, and the NlaIV locus consists of NEIS1180 (*nlaIV_M*) and NEIS1181 (*nlaIV_E*, Figure 32A). Both *nlaIV_M* and *nlaIV_E* are predicted to undergo ON : OFF switching due to homopolymeric tracts within their ORFs. *nlaIV_M* has a poly-A tract starting at position 793 (Figure 31A). An active NlaIV_M (423 amino acids) is expected to be encoded by *nlaIV_M* with a poly-A tract of 9 nt. Homonucleotide tracts leading to a +1 or +2 frameshift result in truncated proteins of 273 or 291 amino acids due to premature stop codons. Furthermore, a two-base pair insertion at position 231 (GGCGC, inserted bases underlined) can result in a premature stop codon at position 271. However, only 49 of 3 760 isolates (1.3%) in the dataset have a truncated methyltransferase due to changes in poly-A tract length or the GC insertion. Therefore, most *N. gonorrhoeae* strains are predicted to be methylated by NlaIV_M, indicating that the system might not influence intra-species HGT. Notably, inactivation of the methylase alone could lead to restriction of self-DNA, and 96% of isolates with inactive NlaIV_M also have a truncated NlaIV_E.

OFF switching of NlaIV_E occurs due to a poly-T tract within the 5' end of the gene, which varies between eight and twelve nucleotides (Figure 32A). *nlaIV_E* with poly-T stretches of nine and twelve nucleotides translate to full-length NlaIV_E (424 and 425 amino acids, respectively); shorter and longer homopolymeric tracts result in +1 or +2 frameshifts, leading to truncated proteins of 75 or 78 amino acids. NlaIV_E belongs to the PD–(D/E)XK superfamily of endonucleases and acts as a dimer to cleave its palindromic recognition sequence GGNNCC[412,418]. The structure of the NlaIV_E dimer has been solved[418], and the catalytic residues D74, E87, and K89 have been confirmed by site-directed mutagenesis[412]. Truncated NlaIV_E lacks the catalytic residues E87 and K89 (Figure 31A, B), leading to the inactivation of the enzyme.

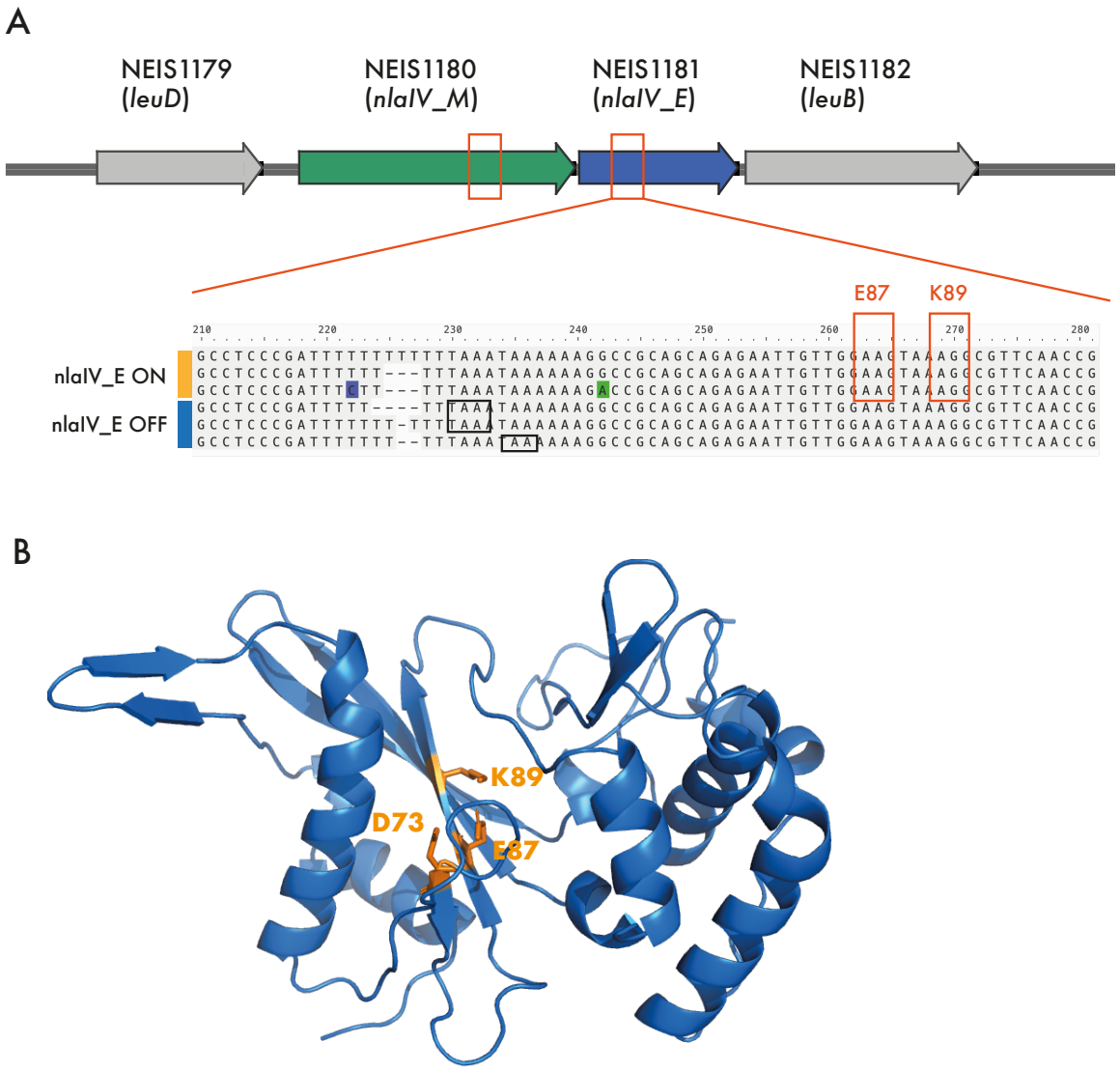

Figure 31: Impact of phase variation on NlaIV_E.
(A) Gene organisation of the NlaIV locus, where *nlaIV_M* (NEIS1180) and *nlaIV_E* (NEIS1181) are flanked by *leuD* (NEIS1179) and *leuB* (NEIS1182). Homopolymeric tracts within *nlaIV_M* and *nlaIV_E* are indicated with orange boxes. Shown below are the three types of polyT tract in *nlaIV_E.* Premature stop codons due to changes in the length of the poly-T tract are indicated in black, and codons for the active site residues E87 and K89 are highlighted in orange boxes. (B) AlphaFold3 prediction of NlaIV_E (pTM = 0.96) with active site residues D73, E87 and K89 indicated in orange.

I investigated the distribution of *nlaIV_E* poly-T tracts within the gonococcal population to gain insights into the correlation between NlaIV_E activity and plasmid presence. Despite the potential of *nlaIV_E* to undergo phase-variation, isolates with tracts that lead to *nlaIV_E* ON and *nlaIV_E* OFF cluster separately on the minimum spanning tree (Figure 32A). Furthermore, in 68.2% of isolates, the poly-T tract is interrupted by a cytosine (5'-TTTCTTTTT-3', Figure 31A and 32A), which is a silent mutation (TTT and TTC encode for phenylalanine). However, the T/C substitution reduces the length of the homonucleotide tract and could reduce or even eliminate phase variation at this locus, maintaining the endonuclease in an ON state. pConj and p*bla* are more likely to occur in isolates with inactive NlaIV_E (OR = 3.7, chi^2-test p <0.001 for pConj and OR = 4.8, chi^2-test p <0.001 for p*bla,* Figure 32B and C), suggesting active NlaIV_E hinders plasmid uptake.

To define the impact of the NlaIV RMS on plasmid transfer, I used isogenic FA1090 strains constructed by Dr Ana Cehovin and Dr Wearn Xin-Yee with active/inactive NlaIV_M (*nlaIV_M*$_{ON}$ / *nlaIV_M*$_{OFF}$) and NlaIV_E (*nlaIV_E*$_{ON}$ / *nlaIV_E*$_{OFF}$). Wild-type FA1090 carries phase-on *nlaIV_E* with an interrupted poly-T tract (5'-TTTCTTTTT-3'). For the corresponding *nlaIV_E*$_{OFF}$ strain, an additional T was introduced at the end of the *nlaIV_E* poly-T tract (5'-TTTTCTTTTT-3'); the 10 nucleotide poly-T tract results in a truncated, inactive NlaIV_E. Strains with NlaIV_M modifications were derived from FA1090 *nlaIV_E*$_{OFF}$. To limit phase variation of NlaIV_M, the poly-A tract was interrupted by a synonymous A to G substitution at position 6 of the tract (5'-AAAAAGAAA-3', both AAA and AAG encode for lysine), in the *nlaIV_M*$_{ON}$ strain; the removal of an A at the end of the tract (5'-AAAAAGAA-3'), resulted in an *nlaIV_M*$_{OFF}$ strain. As before, *pilD* was replaced by *aph(3)* to generate *nlaIV_E*$_{ON}$ / *nlaIV_E*$_{OFF}$ recipients; *nlaIV_M*$_{ON}$ / *nlaIV_M*$_{ON}$ donors have *pilD::ermC* and carry p*bla*.1 and pConj.1.

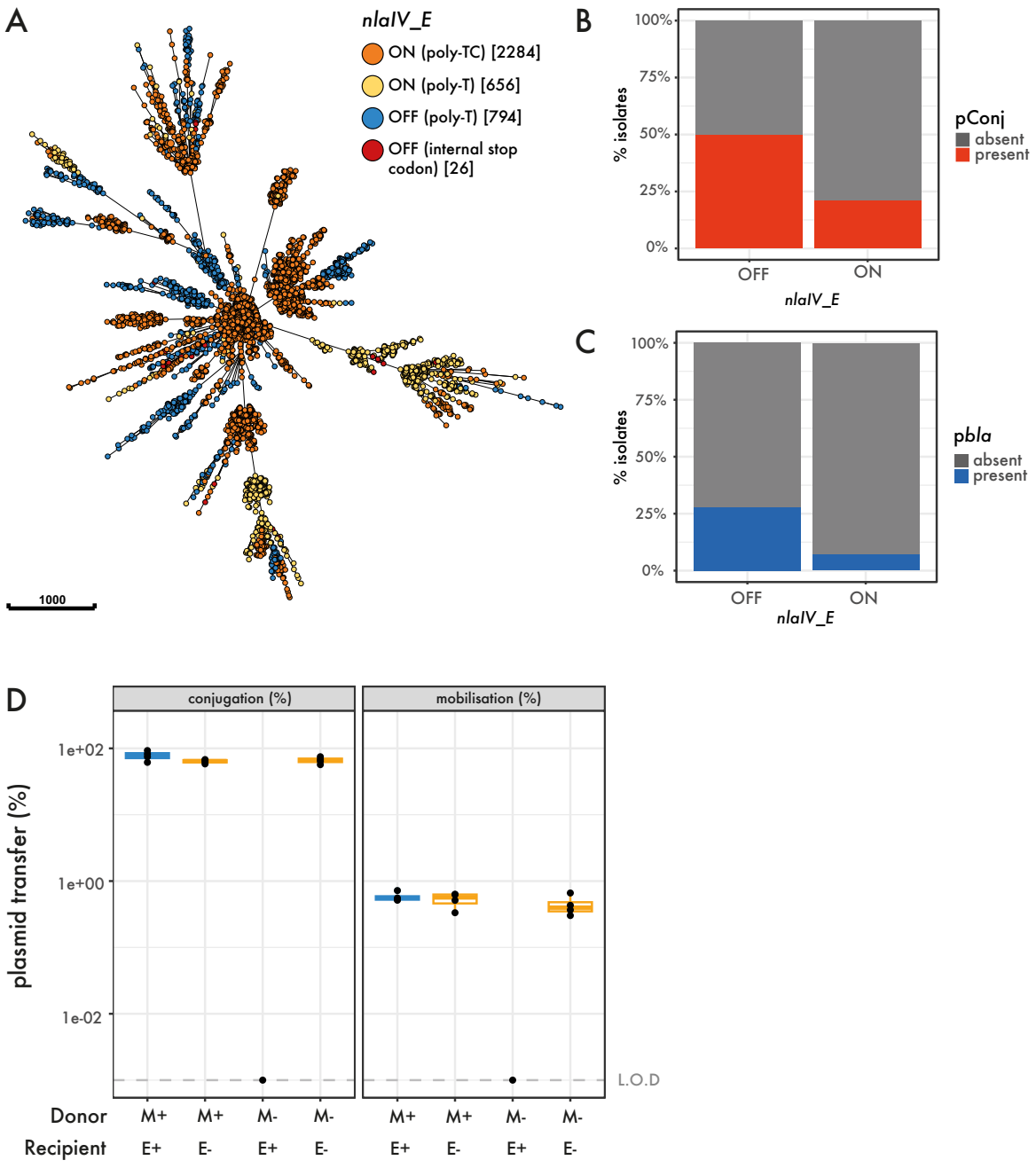

Figure 32: Presence of active NlaIV_E correlates with plasmid absence in the gonococcal population and hinders plasmid transfer in isogenic matings

(A) Minimum spanning tree depicting the distribution of *nlaIV_E* features in the population. (B, C) pConj (B) and p*bla* (C) prevalence in isolates that have *nlaIV_E* ON or OFF. (D) Plasmid transfer rates in isogenic matings between donor strains with the methyltransferase ON (M+) or OFF (M-) and a recipient carrying an ON (E+) or OFF (E-) endonuclease.

I performed matings between donors with an active or inactive methyltransferase, and recipients with the NlaIV endonuclease OFF and methyltransferase either ON or OFF (Figure 32D). In matings with an *nlaIV_M*$_{ON}$ donor, there was no difference in plasmid transfer into the *nlaIV_E*$_{ON}$ or *nlaIV_E*$_{OFF}$ recipient. However, in the absence of NlaIV methylation (*nlaIV_M*$_{OFF}$) in the donor, transfer of both p*bla* and pConj into recipients with *nlaIV_E*$_{ON}$ was reduced to below the limit of detection (<0.0001%, Figure 32D). In contrast, there was no reduction in the transfer of plasmids from the *nlaIV_M*$_{OFF}$ donor into a recipient with inactive endonuclease. These findings demonstrate that an active NlaIV_E effectively hinders the uptake of unmethylated p*bla* and pConj.

5.4 NEIS2765 has no detectable effect on plasmid transfer

The type II RMS NgoAII recognises the palindromic sequence 5'-GGCC-3' and consists of the endonuclease NgoAII_E, encoded by NEIS2765, and the methyltransferase NgoAII_M encoded by NEIS2722. NEIS2765 and NEIS2722 are arranged in tandem, with the 3' end of NEIS2765 overlapping with the 5' end of NEIS2722 (Figure 33A). The NgoAII restriction endonuclease is present in two versions in the gonococcal population: full-length (278 amino acids, NgoAII_E_{278}) or truncated (134 amino acids, NgoAII_E_{134}). The truncation of NgoAII_E occurs due to an A insertion at position 388, resulting in a premature stop codon at position 403 (Figure 33A). NgoAII_E has been classified as a class P PD-(D/E)XK phosphodiesterase based on unpublished experimental data[419], with no available structure of this enzyme. Therefore, I used AlphaFold3 to predict the structures of NgoAII_E_{278} and NgoAII_E_{134}. NgoAII_E_{278} shows the conserved folds of a mixed β-sheet flanked by two α-helices with E36, D73, E83, K85 active site residues (Figure 33B)[419,420], consistent with NgoAII_E being a member of PD-(D/E)XK phosphodiesterase superfamily of endonucleases. The truncation of NgoAII_E_{134} conserves the active site residues (Figure 33C), but results in the loss of parts of the second α-helix. Most class P PD–(D/E)XK REases act as dimers[421]. Therefore, I also investigated the impact of the NgoAII_E_{134} truncation on its ability to dimerise. AlphaFold3 predictions indicate that NgoAII_E_{278} dimerisation is facilitated by an C-terminal domain of the protein, forming a two-stranded antiparallel β-sheet and an α-helix (Figure 33D). As NgoAII_E_{134} lacks the dimerisation region, this version of the enzyme is likely inactive despite the presence of active site residues.

NgoAII_E_{278} and NgoAII_E_{134} are present at approximately equal frequency in the gonococcal population (47.8% and 52.2% of isolates, respectively, Figure 34A), with full-length NEIS2765 associated with the presence of pConj and p*bla* (Figure 27C and D; pConj regression coefficient = 1.31, $-\log_{10}(p) = 70.52$; p*bla* regression coefficient = 0.96, $-\log_{10}(p) = 36.41$).

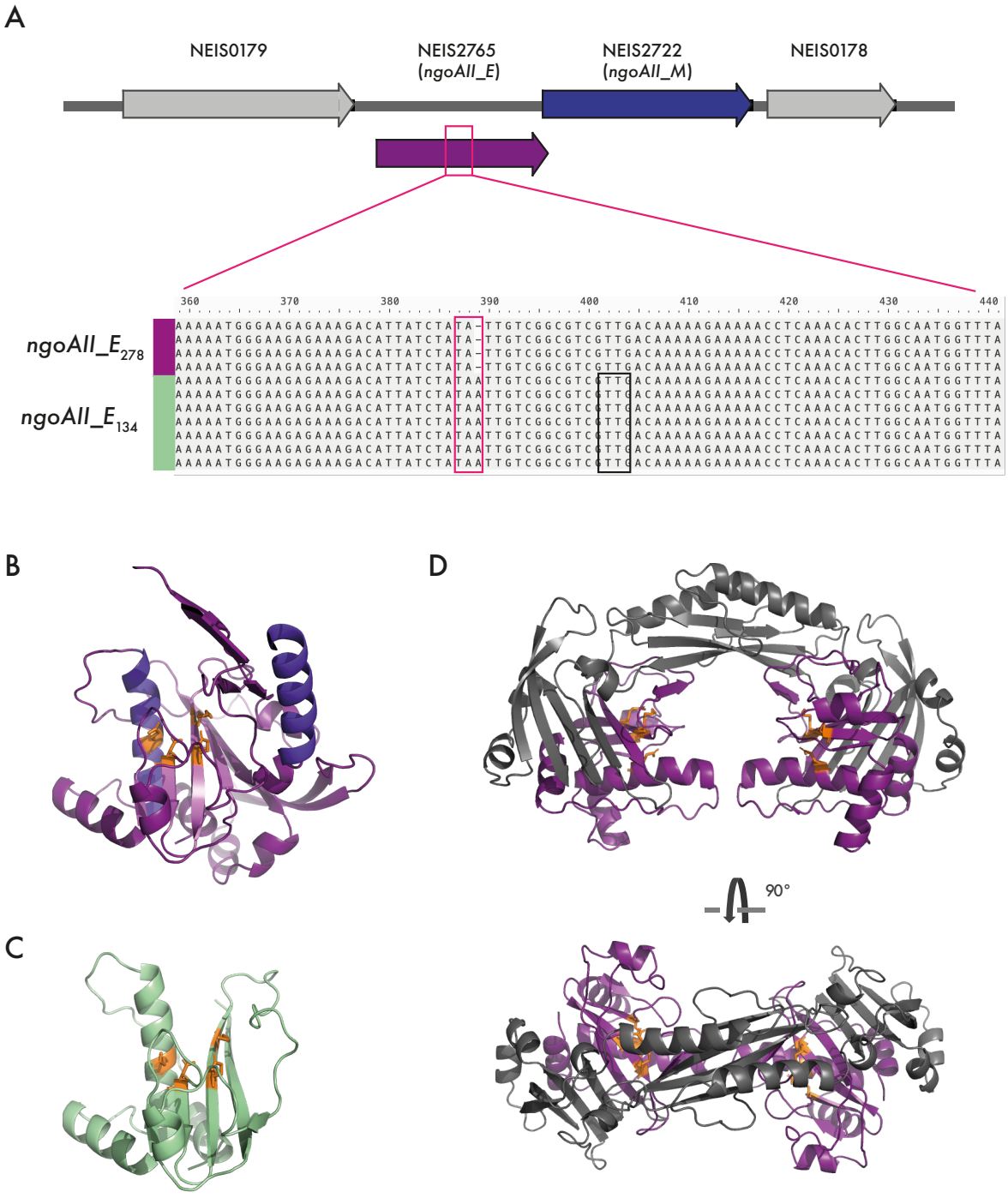

Figure 33: Two versions of NgoA_E are found in gonococci.
(A) Genetic organisation of the *ngoAII* locus. NEIS2765 (*ngoAII_E*) and NEIS2722 (*ngoAII_M*) are flanked by NEIS0179, encoding a putative inner membrane protein, and NEIS0178, encoding a ribosome recycling factor. An adenine insertion at position 388 (pink box) results in a frameshift mutation and a premature stop codon (highlighted in black). (B, C) AlphaFold3 predictions of NgoaAII_E_{278} (B) and NgoAII_E_{134} (C). The secondary structure elements of the conserved core fold of PD-(D/E)XK nucleases are shown in purple (α-helices) and violet (β-sheet), and the key active site residues E36, D73, E83, K85 are shown in orange. (D) AlphaFold3 prediction of dimeric NgoAII_E (ipTM = 0.76) with structure elements absent from NgoAII_E_{134} depicted in grey.

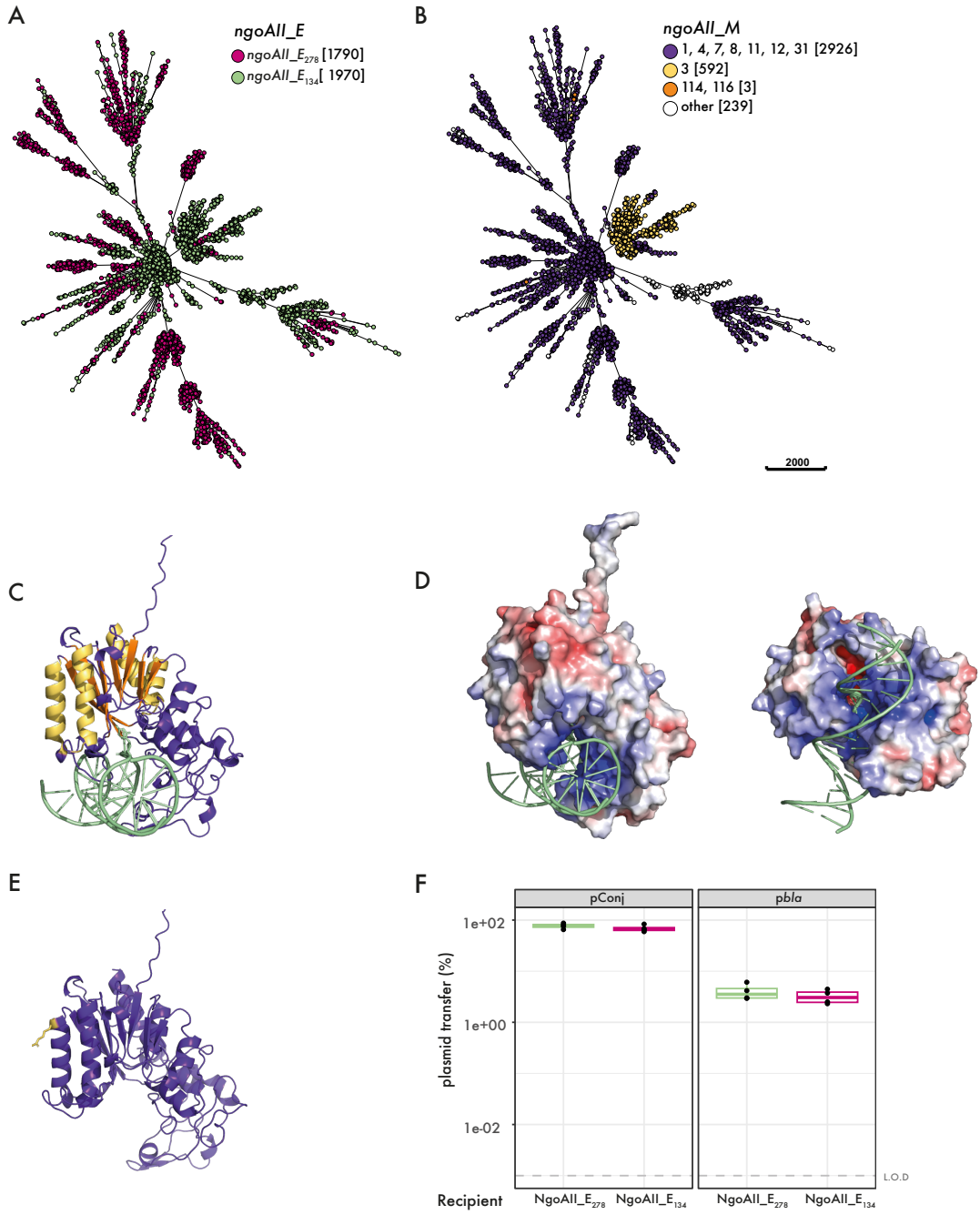

Figure 34: Characterisation of NgoAII and the RMS' impact on plasmid transfer in gonococci.
(A, B) Minimum spanning tree of 3 760 isolates that were clustered according to core genomic allelic differences (cgMLST v1). Individual isolates are represented as dots that are coloured according to the NgoAII_E variant (A), or the *ngoAII_M* (B) allele carried. *ngoAII_M* alleles encoding identical protein sequences are shown in the same colour. (C) AlphaFold3 prediction of NgoAII_M with GGCC motif-containing dsDNA. The first C of the GGCC motif is flipped into the active site of the methylase. Secondary structure elements conserved between class I MTases are indicated in yellow (α-helices) and orange (β-sheet). (D) APBS surface charge predictions of NgoAII_M. Regions with positive surface charge are indicated in blue, electronegative regions in red. (E) NgoAII_M with the G145R substitution is indicated in yellow. (F) Plasmid transfer into isogenic recipients that either harbour full-length or truncated NEIS275. Wt FA1090, which carries NEIS2722 allele 1, served as the donor. There was no significant difference in pConj or p*bla* transfer into the different donors (Welch two-sample t-test p = 0.28 and 0.41, respectively).

The NgoAII methyltransferase (NgoAII_M) is encoded by NEIS2722 and shows minimal variation in the population. The prevalent alleles 1, 4, 7, 8, 11, 12 and 31 have synonymous mutations, so they encode an identical protein, and together account for 77.8% of sequences (2 926 / 3 760, Figure 34B). Allele 3, the second most common allele, is present in 15.7% of isolates and has a G145R substitution compared with the most prevalent NgoAII_M sequence. Alleles 114 and 116 have premature stop codons resulting in inactive proteins of 46 and 67 amino acids but are rare (3 / 3 760 isolates). Of note, isolates with *ngoAII_M* with a premature stop codon also encode a truncated NgoAII_E.

As NgoAII_M has not been structurally characterised to date, I used AlphaFold to assess the potential effects of the G145R substitution. NgoAII_M shows the conserved fold of Class I MTases, consisting of a seven-stranded β-sheet flanked by α-helices forming an αβα motif (Figure 34C)[422]. APBS surface charge modelling of NgoAII_M with dsDNA containing the GGCC motif reveals an electropositive groove that is predicted to interact with the dsDNA, resulting in the flipping of the first C within the GGCC motif into the adjacent electropositive pocket (Figure 34C and D). The G145R substitution is located on the surface of the enzyme, distant from the DNA-binding groove (Figure 34E), so it is unlikely to affect the methyltransferase activity of the enzyme.

To define the effect of the NgoAII RMS on plasmid transfer, I used isogenic FA1090 strains with *ngoAII_E*$_{278}$ and *ngoAII_E*$_{134}$. Wild-type FA1090 encodes NgoAII_E$_{134}$; Dr Ana Cehovin generated an FA1090 strain encoding NgoAII_E$_{278}$ by replacing the FA1090 *ngoAII_E* with *ngoAII_E* from isolate 60755, which lacks the A388 insertion. I performed matings using FA1090 *pilD::ermC* pConj.1 and p*bla*.1, which has the dominant NEIS2722 allele 1, as the donor, and FA1090 *pilD::aph(3)* with *ngoAII_E*$_{278}$ or *ngoAII_E*$_{134}$ as the recipient. As expected from a donor with an active methyltransferase, there was no difference in pConj and p*bla* transfer rates into FA1090 expressing full-length NgoAII_E or the truncated enzyme (Figure 34F, Welch two-sample t-test p = 0.28 and

0.41, respectively). Given that 99.9% of isolates in the dataset are predicted to encode an active methylase, these results suggest that NgoAII does not limit plasmid transfer between gonococci.

5.5 Plasmid transfer occurs in most mixed-strain matings

Characterisation of NgoAV, NlaIV and NgoAII suggests that these individual RMSs have a limited impact on intraspecies transfer of pConj and p*bla*. However, this does not rule out the possibility that the strain background, either due to effects of combined RMSs or other factors, influences plasmid transfer. To investigate this, I quantified the transfer of pConj and p*bla* between clinical isolates from Ng_cgc$_{400}$s that have high (*i.e.* Ng_cgc$_{400}$s 21, 25) or low (*i.e.* Ng_cgc$_{400}$ 3) p*bla* and pConj carriage (Table 8, Figure 35). Furthermore, I included isolate NG149 from Ng_cgc$_{400}$ 377; this lineage is unusual as it has a high p*bla* (52.8%, 140/265) but low pConj (1.9%, 5/265) prevalence. For each strain, I generated a donor by introducing p*bla*.1 and pConj.1, as well as *pilD::ermC,* into a plasmid-free clinical isolate. Recipients were constructed by replacing *pilD* with *aph(3)*. Subsequently, I performed matings between all combinations of donors and recipients, including matings between isogenic strains and with FA1090, and measured the frequency of transfer of both p*bla* and pConj. This generated a matrix of plasmid transfer rates for 25 donor/recipient combinations (Figure 36A and B).

Plasmid transfer differed significantly between different pairs of donors and recipients. Isogenic matings of FA1090, NG149 and 2086_K gave high pConj (>69%) and p*bla* (>2.99%) transfer. In contrast, plasmid transfer in isogenic matings with NG015 or NG114 was an order of magnitude lower (conjugation rates <7.4% and mobilisation rates <0.38%).

Table 8: Gonococcal lineages with percentage of isolates with p*bla* and pConj indicated.

Ng_cgc$_{400}$	number of isolates	isolates with pConj (%)	isolates with p*bla* (%)	isolate
21	574	80.0%	74.0%	2086_K
25	346	99.1%	56.5%	NG114
3	4 552	0.1%	0.5%	NG015
286	8	0%	0%	FA1090
377	265	1.9%	52.8 %	NG149

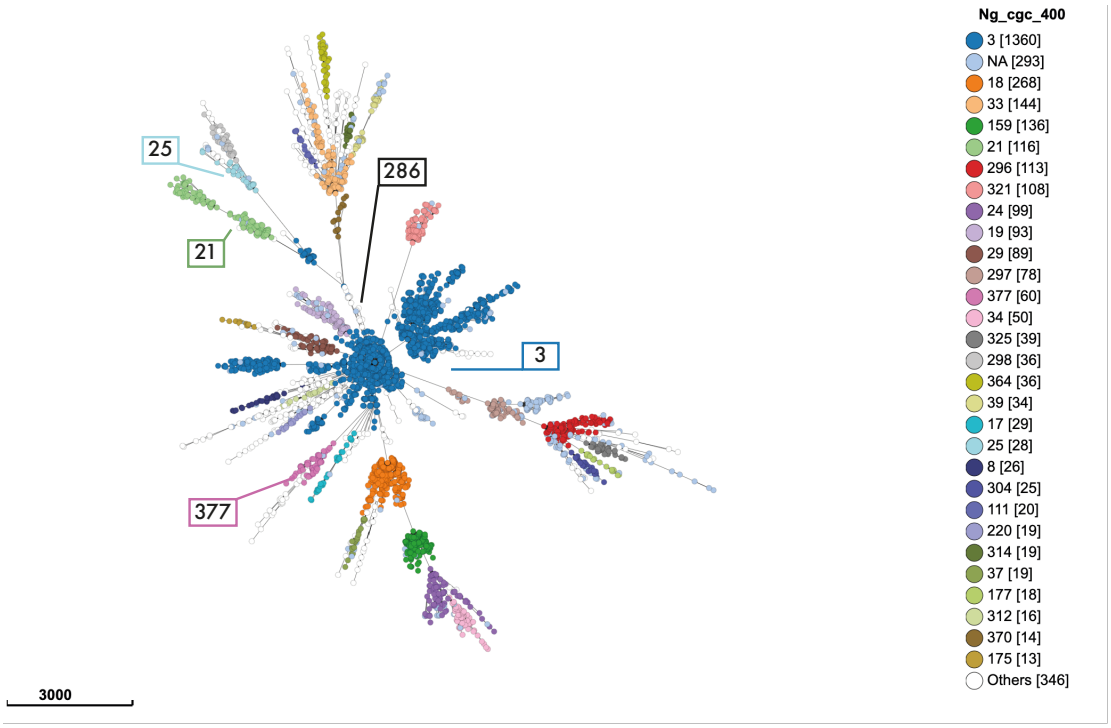

Figure 35: Minimum spanning tree of 3 760 gonococcal isolates clustered by core genome allelic differences (cgMLST v1), with isolates coloured according to their Ng_cgc$_{400}$.
Ng_cgc$_{400}$s represented by isolates in the mixed strain matings are indicated.

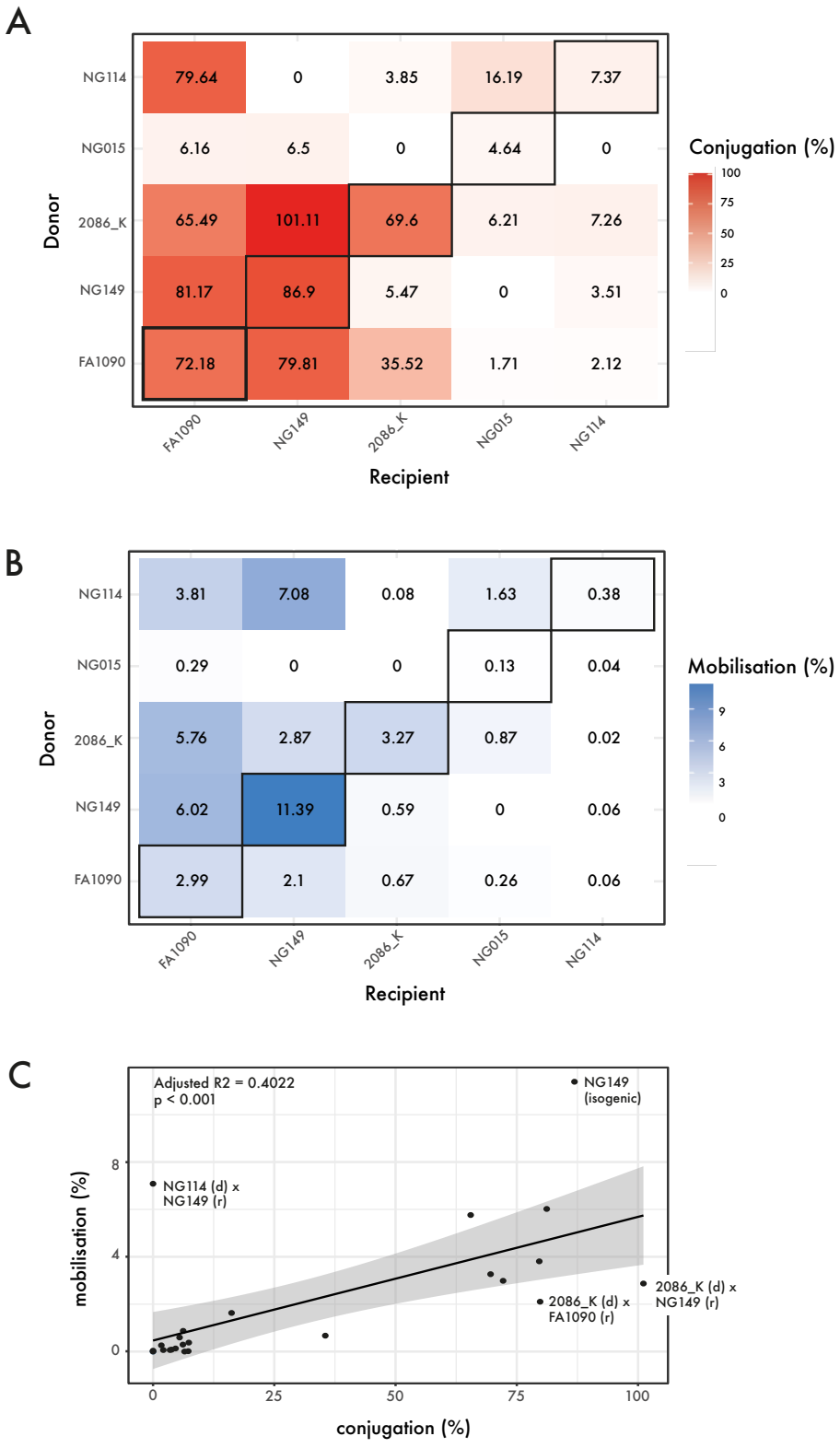

Figure 36: Plasmid transfer between strains from different lineages.
Heatmaps of the pConj conjugation (A) and p*bla* mobilisation frequency (B) between different donor and recipients. Isogenic matings along the diagonal are highlighted. Darker colours indicate higher plasmid transfer and numbers in boxes give the average of matings performed on three occasions. (C) Correlation between mobilisation and conjugation rates. Dots represent matings; donor (d) and recipient (r) are given for outliers.

If RMSs or other defence systems are the limiting factor for plasmid transfer, isogenic matings, in which the donor and recipient have the same defence systems, should produce the highest plasmid transfer rates compared with mixed-strain matings. However, several mixed-strain matings produced equivalent or even higher plasmid transfer rates than isogenic matings. Most notable, pConj and p*bla* transfer from NG114 into FA1090 was 79.6% and 3.8%, respectively, while NG114 isogenic matings resulted in conjugation and mobilisation frequencies of only 7.4% and 0.38%; overall, NG114 stood out as an inefficient recipient (pConj transfer <7.4%, p*bla* transfer <0.4, Figure 36A and B, respectively) in isogenic and in mixed-strain matings. In contrast, FA1090 was an efficient recipient, with mixed-strain matings with FA1090 as the recipient yielding comparable or higher rates of transfer compared with the mating of the donor strain with itself in isogenic matings (Figure 36A and B). This suggests other, strain-specific factors impact the ability of some strains to act as donors or recipients.

However, transfer rates also varied depending on the donor. This is illustrated by matings with FA1090 as the recipient; pConj and p*bla* transfer from 2086_K was an order of magnitude higher than from NG015 (pConj transfer = 65.5 and 6.2%, p*bla* transfer = 5.8% and 0.3, respectively, Figure 36A and B). Similarly, pConj transfer was higher from 2086_K (7.3%) than from NG015 (undetectable) with NG114 as the recipient. Indeed, in all matings (including isogenic matings), NG015 was an inefficient donor, with the lowest plasmid transfer rates with every recipient. Matings with 2086_K as the donor resulted in comparable or higher plasmid transfer to recipients as observed with their isogenic donors, indicating that 2086_K is an efficient donor. Taken together, plasmid transfer frequency in mixed-strain matings depended on both donor and recipient.

In addition, the direction of plasmid transfer also had a major effect. For example, plasmids were efficiently transferred from 2086_K to FA1090 and NG149 (pConj transfer >65%, p*bla* transfer >2.8%, Figure 36A and B), while plasmid transfer from FA1090 and NG149 into 2086_K resulted in

reduced transfer rates (pConj transfer = 5.5 and 35.5%, p*bla* transfer = 0.59 and 0.64% into NG149 and FA1090, respectively, Figure 36A and B).

Of note, of the 25 matings, only the matings between NG015 (donor) and 2086_K (recipient), and NG149 (donor) and NG015 (recipient) did not result in any transconjugants (Figure 36A and B). Furthermore, the pairing between NG015 (donor) and NG149 (recipient) yielded pConj transconjugants without p*bla*, and transconjugants from matings between NG114 (donor)/NG149 (recipient) and NG015 (donor)/NG114 (recipient) carried p*bla*, but not pConj. The latter was surprising, as pConj transfer is usually a magnitude higher than p*bla*, and p*bla* mobilisation rates correlated with conjugation rates of different pConj variants in previous assays (Chapter 4.3.3). However, the emergence of transconjugants carrying p*bla* in the absence of pConj would be consistent with the presence of an RMS that recognises sequences on pConj but not p*bla*. In line with this, pConj conjugation rates only weakly correlated with p*bla* transfer (adjusted R^2 = 0.4, $p < 0.001$, Figure 36C).

Even with the limited number of strains tested, different patterns of plasmid transfer were detected in mixed-strain matings. Comparison of isogenic and mixed-strain matings indicates the situation is complex and cannot be explained only by host-encoded barriers such as RMS. However, strain-specific patterns (with NG114 an inefficient, and FA1090 an effective recipient, and NG015 an inefficient and 2086_K an efficient donor) are observed that affect the transfer of plasmids between clinical isolates. Of note, within this limited sample size, there was no obvious correlation between plasmid transfer rates and the plasmid prevalence in the lineage of the donor or recipient strain, suggesting the ability to acquire pConj and p*bla* *via* conjugation might not be a major determinant of the distribution of plasmids in gonococci.

5.6 Summary

Plasmid carriage is lineage-specific in gonococci, consistent with barriers hindering plasmid transfer between phylogenetically distinct isolates. *N. gonorrhoeae* strains can harbour up to 16 different RMSs, and the DNA methylation of an *E. coli* donor has been shown to affect plasmid transfer into *N. gonorrhoeae*[76]. Therefore, based on correlations of features of RMS loci with the presence of p*bla* and pConj, I have characterised the effect of three RMSs, NgoAV, NlaIV and NgoAII, on the transfer of these plasmids in gonococci.

Changes in the type I RMS NgoAV *hsdS* alter the recognition sequence of this RMS, suggesting differences in *hsdS* sequences of isolates could limit plasmid transfer. The logistic regression had shown a correlation between HsdS lacking the LEAT repeat sequence and pConj carriage (Figure 27C). Methylation analysis revealed that strains with HsdS without LEAT repeats lack NgoAV methylation, indicating that the absence of a LEAT sequence inactivates the RMS. However, results with FA1090 engineered to express different versions of NgoAV HsdS show that the presence of distinct HsdS only minimally affects plasmid transfer in isogenic matings. Intriguingly, FA1090 without inactive NgoAV was an efficient recipient independent of the donor. However, this strain was also an effective donor, which was surprising as the lack of plasmid methylation should lead to their elimination from recipients with active NgoAV. The presence of a type IV RMS in the recipient degrading methylated DNA could explain the high transfer rates of the unmethylated donor. However, to date, no type IV RMS has been described in *N. gonorrhoeae*. While RMS are usually considered to limit HGT, methylation by certain RMS can also impact gene expression[223,225,226], and the absence of NgoAV methylation has been associated with transcriptional changes[228]. Therefore, expression of genes required for conjugation might differ between strains with distinct *hsdS*, resulting in increased conjugation rates. Future studies could compare the transcriptome of the

different strains using RNAseq or study the expression of distinct T4SS genes using RT-ddPCR to test this hypothesis.

Both methyltransferase and endonuclease genes of the type II RMS NlaIV have homopolymeric tracts in their gene sequences, which could allow ON : OFF switching of enzyme activity. In conjugation experiments with isogenic donors and recipients with NlaIV methyltransferase and endonuclease phase-locked ON or OFF, the NlaIV endonuclease is highly effective at preventing plasmid acquisition from a donor lacking NlaIV methylation. No effect was observed if the donor carries a functional methyltransferase. Therefore, NlaIV can efficiently block p*bla* and pConj transfer. However, while gonococcal plasmids are more frequently found in strains with *nlaIV_E* OFF, *nlaIV_M* is in the ON state in the overwhelming majority of isolates in the dataset. Therefore, while NlaIV_E could limit plasmid transfer from other species that lack the NlaIV methylation pattern, NlaIV is unlikely to limit p*bla* and pConj transfer between gonococci.

Logistic regression analysis also correlated truncated NgoAII endonuclease (NEIS2765) with the absence of plasmids, whilst the full-length version of the enzyme was associated with plasmid presence. This is counterintuitive, as a functional endonuclease should protect a strain from plasmid invasion by restricting incoming DNA. Furthermore, my analysis showed that the NgoAII methyltransferase is highly conserved across gonococci, with only three of 3 760 isolates with *ngoAII_E* with premature stop codons resulting in a truncated methyltransferase. Thus, similar to NlaIV, most plasmids circulating in gonococci should be methylated by NgoAII, and consequently, the NgoAII endonuclease should not affect plasmid transfer in the gonococcal population. This was supported by my plasmid transfer data.

A recent study showed that the number of restriction sites on the plasmid affects the efficiency of restriction enzymes in preventing plasmid acquisition[77]. Furthermore, plasmid-encoded anti-restriction systems and type of RMS affect the ability of the systems to limit HGT[77]. I found a marked

effect of the type II RMS NlaIV on plasmid transfer, while NgoAV, a type I RMS, only minimally affected plasmid transfer. Type I and II RMS not only differ in their components (REase and MTase *vs*. complex of HsdS, HsdM and HsdR), but also where and how they cleave DNA. Type II RMSs cut within the recognition sequence, whereas for type I RMSs, the DNA restriction occurs at a variable distance from the recognition site. Following binding of the type I restriction complex to the unmethylated recognition site, DNA is pulled towards the bound complex from both directions in an ATP-dependent manner. DNA is cleaved upon halting of DNA translocation due to collision with other translocating enzymes or DNA secondary structure[423,424]. These differences in the mechanisms of restriction could explain why the efficiency of inhibiting plasmid transfer varied between the two systems.

Due to the large number of RMSs in gonococci, we used a logistic regression to identify RMSs that could impact plasmid transfer. A weakness of logistic regression is that it does not take population structure into account *i.e.* it assumes independence of observations. Without correcting for population structure, the logistic regression may incorrectly attribute lineage-driven patterns to a causal association between plasmid carriage and RMS. Other population structure-aware methods, such as a genome-wide association study (GWAS), could be applied in the future to determine genetic features associated with pConj and p*bla* presence or absence.

Individual RMSs can only provide an initial barrier to HGT. Once a plasmid is established in a bacterium, it will be modified by the resident RMSs and recognised as 'self' DNA by other bacteria with the same repertoire of RMSs. As such, the timing of restriction and methylation will determine whether an RMS prevents plasmid acquisition. Modelling predicts that even in the presence of bacterial defence systems, beneficial plasmids can spread in bacterial populations, with high conjugation rates increasing the ability of a plasmid to overcome barriers imposed by RMSs[425]. Therefore, the high conjugation rates of pConj.1 (conjugation rates of up to 80% in mixed-strain

matings) might favour plasmid transfer between hosts. In contrast, the smaller p*bla*.1 (5.6 kb) may have evolved to avoid restriction sites in its sequence[80].

Of note, while *N. gonorrhoeae* strains carry several RMSs, many of these systems are present in >95% of gonococci and are part of the core genome[2]. While variation in the activity of RMSs could limit the transfer of plasmids between gonococci, most of the variation in the three RMSs I studied affects the activity of the endonuclease. This indicates that gonococcal RMSs are more likely to be effective against DNA from other bacterial species, rather than against preventing plasmid transfer within gonococci.

Other factors could prevent plasmid transfer between gonococci and explain the patchy distribution of the plasmids in the population. However, I detected transconjugants in 18 of the 20 mixed-strain matings, suggesting only limited barriers preventing plasmid transfer under laboratory conditions. Nevertheless, plasmid transfer varied significantly between strains. NG015 and NG114 emerged as inefficient donor and recipient and could be further examined to better understand factors limiting plasmid transfer. For example, the low efficiency of NG015 plasmid donation could be due to low expression of the pConj MPF, which could be investigated by RT-ddPCR of target *mpf* genes or RNAseq. Low plasmid transfer into NG114 could be due to the presence of defence systems other than RMS, or the absence of surface structures stabilising the MPF. To explore these scenarios, NG114 (inefficient donor) could be transformed with the genomic DNA of FA1090 (efficient donor), and the resulting NG114 library could be screened for clones with improved plasmid acquisition.

For the limited number of strains tested, the pConj and p*bla* transfer frequencies did not correlate with plasmid carriage in the Ng_cgc$_{400}$ the isolate belongs to. This suggests that the absence of p*bla* and pConj from certain lineages may not be due to their inability to acquire them.

6 Conclusions

This thesis describes my research on plasmid-mediated AMR in *N. gonorrhoeae*. I addressed three key aspects: i) the evolution and epidemiology of the gonococcal β-lactamase plasmid p*bla*; ii) the molecular characteristics of the three major p*bla* variants, focusing on resistance, fitness costs and mobility patterns; and iii) the impact of gonococcal RMSs on intraspecies plasmid transfer.

A major challenge in the field of plasmid biology is the inability to assemble complete plasmid sequences from short-read WGS, hindering large-scale epidemiological analyses of plasmid-mediated resistance. I addressed this issue by developing a typing scheme for p*bla* that identifies variants from WGS based on characteristic patterns of gene presence and absence (Chapter 3.2.1). The typing scheme is available on the public database PubMLST (https://pubmlst.org/neisseria/), which enables further verification of the scheme by the research community and should aid monitoring the spread of p*bla* in gonococci.

Albeit simple, the typing scheme allowed me to harness the vast amount of publicly available genomic data. By analysing a dataset of over 15 000 isolates, I attained an unprecedented view of the spread of p*bla* in the global gonococcal population (Chapter 3.2.4). However, although the dataset contains isolates from 66 countries and spans almost a century, it is heavily biased towards isolates from Europe and the US where extensive surveillance programs are in place[426,427]. Furthermore, isolates are mostly from urethral swabs from symptomatic patients from MSM communities, while samples from other body sites and cisgender women, which often present asymptomatic infections[428], are underrepresented. Therefore, the dataset cannot fully represent the *N. gonorrhoeae* species diversity.

A major finding of my analysis was that while seven variants of p*bla* have been described[302,311,429], only three commonly circulate in gonococci. Together with recent advances in resolving the

gonococcal population structure[2], my analysis further identified distinct associations of p*bla* variants with gonococcal lineages, which is important for monitoring the spread of resistant clones, as well as detecting the introduction of p*bla* into novel genetic backgrounds. Of note, throughout this thesis, I used the Ng_cgc$_{400}$ scheme[2], which was the gold standard for resolving the gonococcal population structure at the beginning of my work. However, Ng_cgc classifications may not be stable *i.e.* they can change with the addition of further isolates to a database. Recently, Life Identification Number (LIN) codes have been implemented for *N. gonorrhoeae* classification[430]. The LIN code nomenclature builds on a refined cgMLST scheme of 1 430 loci and assigns each isolate a multi-position numeric barcode. Each position in the barcode represents clustering at a different allelic mismatch threshold, allowing the LIN code to capture hierarchical relationships among strains at multiple levels of resolution. LIN codes remain stable over time and provide a consistent and scalable framework for genomic surveillance. Therefore, LIN codes should be used in further analyses.

Another discrepancy between the literature and my findings is the host range of p*bla*. p*bla* has been labelled as a 'broad host range plasmid'[431] as it can replicate in diverse bacteria including *E. coli*, *S. enterica* serotype Minnesota, *Haemophilus* spp. and *Neisseria* spp. in the laboratory[306,371]. However, analysis of p*bla* in public genome databases showed that it is restricted to the two STI pathogens *N. gonorrhoeae* and *H. ducreyi* (Chapter 3.3.1), highlighting the difference between a plasmid's host range in the laboratory and in natural populations. Interestingly, p*bla* is rarely found in the related pathogens *N. meningitidis* and *H. influenzae* despite its ability to replicate in these organisms. *N. meningitidis* and *H. influenzae* are pathogens that largely reside in the upper airways, while *N. gonorrhoeae* and *H. ducreyi* are found mostly in the urogenital tract, suggesting selective pressure for p*bla* carriage in the urogenital niche. This is further supported by the association of p*bla* with isolates from urethral swabs compared to other sites (Chapter 3.3.2). Similar patterns are also observed for pConj, which is present in 0.5% *N. meningitidis* isolates[296], but is found in around

one-third of gonococci[286]. Both penicillin and tetracycline are excreted renally[381,382], potentially explaining the association of the plasmids with the urethral niche. However, as gonococcal plasmids are associated with distinct lineages, the association of p*bla* with isolates from the urethral niche might also be driven by the adaptation of certain strains to the niche, rather than any contribution from the plasmids.

The sequence of p*bla* is remarkably conserved, and adaptation seems to occur mostly through gene loss events. The introduction of p*bla* from *H. ducreyi* into *N. gonorrhoeae* was associated with the loss of the *tnpA* transposase. Again, parallels can be drawn with pConj, where the *tetM* resistance determinant is located on a truncated Tn*916* transposon[432]. The truncation of Tn*2* drastically reduces the size of the p*bla* from 10.9 kb (p*bla*.2) and 9.1 kb (p*bla*.1) in *H. ducreyi* to 7.4 kb (p*bla*.2) and 5.6 kb (p*bla*.1) in *N. gonorrhoeae.* However, the implications of this change on p*bla* biology remain unknown. My analysis of the phylogenetic relationships of p*bla* variants in *H. ducreyi* and *N. gonorrhoeae* could not exclude the possibility of independent introduction of p*bla*.1 and p*bla*.2 into the gonococcus, with both introductions associated with the truncation of Tn*2*. However, analysis of the p*bla*.1 deletion site indicates independent emergence of p*bla*.1 from p*bla*.2 through the loss of *repB* and one copy of NEIS2964 in *H. ducreyi* and *N. gonorrhoeae* as the most parsimonious explanation. This is further supported by the reduced fitness cost of p*bla*.1 compared to p*bla*.2 in the gonococcus; however, p*bla* fitness costs in *H. ducreyi* have not been explored to date.

Previous studies have characterised p*bla* in *E. coli*[306,309,433]. However, results obtained in *E. coli* may not be relevant for *N. gonorrhoeae*. For instance, while IS*1*-mediated integration of p*bla*.3 into gonococcal pConj facilitated the co-transfer of p*bla*.3 in *E. coli*[433], IS*1* is not present in *N. gonorrhoeae*, and p*bla*.3 was not mobilised by pConj in my assays using *N. gonorrhoeae* (Chapter 4.3.4). Another study characterised the p*bla mob* genes in *E. coli* and indicated that MobC does not

affect p*bla* transfer[309]. However, using p*bla* variants lacking individual *mob* genes, I detected a 10-fold reduction in p*bla* transfer in *N. gonorrhoeae* in the absence of MobC (Chapter 4.3.5).

Further differences between *N. gonorrhoeae* and *E. coli* were apparent in my analysis of TEM-mediated resistance. While TEM-135 has been highlighted as a precursor of ESBLs due to the stabilising effect of the M182T substitution[285,368], the M182T substitution resulted in slightly reduced penicillin MICs in *E. coli*[285]. In contrast, in *N. gonorrhoeae,* TEM-135 provided significantly increased resistance levels compared to TEM-1, correlating with increased cellular TEM levels (Chapter 4.1.1).

The differences in MICs of TEM-135 and the impact of MobC on p*bla* transfer in *E. coli* and *N. gonorrhoeae* highlight the need to broaden investigations to non-*E. coli* model organisms, as results in *E. coli* may not always be representative. It is also noteworthy that studying narrow host range plasmids in the gonococcus has revealed important differences from paradigms that are based on well-characterised plasmids such as the F-plasmid. Many F-like plasmids tightly control the expression of the conjugative apparatus to reduce associated costs and minimise predation by phages targeting conjugative pili[434]. However, the pConj conjugative apparatus is constitutively expressed[402], and both pConj and p*bla* show strikingly high transfer rates in both isogenic and mixed-strain matings (Chapter 5.4)[294]. Furthermore, different from other IncP plasmids[86,94], pConj does not display entry exclusion (Chapter 4.3.2). Therefore, pConj carriage does not prevent the acquisition of p*bla*, which relies on the conjugative machinery of pConj. This allows the introduction of p*bla* into isolates with different pConj variants and the subsequent spread of successful pConj/p*bla* combinations. This is evidenced by the co-occurrence of p*bla* with pConj variants that mobilise it efficiently in gonococci (Chapter 4.3.3). Finally, while plasmid carriage is often associated with a cost to their bacterial host[67], which can promote the loss of the plasmid from a bacterial population, successful p*bla* and pConj variants impose no detectable fitness cost on their host

(Chapter 4.2.3, 4.2.4 and [294]). Both plasmids persist within the gonococcal population (Chapter 4.2.1 and [294]), endangering current treatment and prevention options including Doxy-PEP.

While I defined the molecular characteristics of the three major p*bla* variants in their native host, results obtained in the laboratory may not accurately reflect the behaviour of the plasmid and its host *in vivo*. Host niche factors such as iron limitation, the spatial organisation of bacteria and microbiota can alter plasmid fitness costs, mobility and resistance to antibiotics. Nevertheless, some characteristics of p*bla* variants are consistent with their distribution in the gonococcal population. For example, the fitness cost of p*bla*.2 matches its low prevalence in p*bla*-associated lineages and its decreasing prevalence over time. Results are also supported by a recent study from China, a region historically associated with p*bla*.2, where p*bla*.2 has been gradually replaced by p*bla*.1 between 2013 and 2022[398].

p*bla*.3 and p*bla*.1 have adapted distinct evolutionary strategies that have led to their success in the gonococcus. p*bla*.3 provides increased resistance due to TEM-135 and has reduced fitness costs compared to p*bla*.2$^{TEM-135}$, with the trade-off of immobility. The high prevalence of p*bla*.3 in associated lineages suggests clonal expansion of p*bla*.3-carrying isolates, potentially because TEM-135 increases resistance. In contrast, p*bla*.1 mostly carries TEM-1 and TEM-1$_{P14S}$ but is mobile, so might associate with lineages that carry chromosomal mutations that enhance plasmid-mediated resistance. However, it is important to consider the circumstances in which a change is adaptive. While increased levels of resistance provided by TEM-135 or combined effects of plasmid and chromosomal resistance determinants provide a benefit during antibiotic selection, mobility and the absence of fitness costs promote the p*bla* carriage in the absence of antibiotics. Furthermore, due to the co-transfer of p*bla* with pConj, selection with tetracycline might increase the prevalence of p*bla*. This has important implications for the recent implementation of Doxy-PEP against STIs after unprotected sexual intercourse. In June 2024, the US Centres for Disease Control and Prevention (CDC) issued guidelines on the use of Doxy-PEP[435], and the practice has been adopted

in different parts of the US and Europe[436-439]. The implementation of Doxy-PEP has been associated with increased tetracycline resistance in *N. gonorrhoeae*[245], likely through the selection for pConj^{tetM+}-carrying isolates. Of note, doxycycline has been used for syndromic treatment of gonorrhoea in LMICs such as Kenya, where there is a strikingly high prevalence of plasmid-mediated resistance[240,286]. Taken together, increased doxycycline use will likely further increase the prevalence of pConj and, due to their co-transfer, p*bla*-carrying strains. Higher numbers of potential plasmid donors also increase the potential of these plasmids entering new lineages.

Whilst my analysis of plasmid-mediated resistance in the gonococcal population revealed lineage-specific plasmid carriage, mixed-strain matings and investigation of the impact of gonococcal RMS on plasmid transfer suggested that there are only limited barriers to the transfer of plasmids between phylogenetically distinct strains. I only tested transfer between five gonococcal isolates and characterised the impact of three of the 16 gonococcal RMSs[221] on plasmid transfer. Therefore, I cannot exclude the possibility that other RMSs or strain combinations show stronger effects. However, RMSs generally are weak barriers to plasmid transfer, having more pronounced effects against phage infection and transformation[77]. Once overcome, plasmid methylation in a new host will allow the plasmid to spread to other hosts with the same RMS configuration. Therefore, the diversity and co-occurrence of RMSs are important to assess their impact on the spread of plasmid-mediated resistance. The more diverse the combinations, the more effective the protection should be. However, distinct from *N. meningitidis*, where the presence of distinct RMSs limit HGT between clonal complexes[440], most gonococcal RMSs are part of the core genome and for the analysed systems, variation occurred mostly in restriction endonucleases rather than the methylases. The conserved methylase activity within the population should allow HGT within the gonococcus. Nevertheless, RMSs may still limit DNA uptake from other species, and it is indeed curious that the gonococcus only has three plasmids, while other bacteria can have a plethora of such MGEs[287,441,442].

Throughout this thesis I combined bioinformatics and molecular genetics to investigate plasmid-mediated resistance in the gonococcus. Both approaches have their shortcomings: unevenly sampled datasets can bias epidemiological analyses, and observed associations between distinct RMS features and plasmid presence/absence may be due to effects of population structure rather than functional interactions. Results obtained in laboratory settings may not represent the behaviour *in vivo* and can differ between lab strains and clinical isolates. However, by combining these complementary approaches, I was able to test hypotheses generated by the bioinformatic analyses and provide further support for observed trends by offering potential underlying molecular mechanisms. For instance, my analysis of the prevalence of p*bla* variants over time indicated a decrease in p*bla*.2, which was mirrored by the fitness cost of p*bla*.2. At the same time, the bioinformatic analyses complemented my experimental data *e.g.* AlphaFold predictions of NgoAV HsdS variants provided structural insights into methylation patterns. Taken together, the combination of bioinformatic analyses and molecular microbiology provides a powerful approach to study the interplay between mobile genetic elements and their bacterial host in a public health context.

6.1 Future directions

The potential of the p*bla*-encoded TEMs to develop into ESBLs and the increased resistance levels of TEM-135, highlight the importance of monitoring p*bla* in gonococci. However, with most sampling efforts limited to high-income countries, knowledge about strains circulating in low-income countries, especially in Africa, which has the highest incidence of gonorrhoea and high levels of plasmid carriage[172,240], remains limited. Therefore, future sampling efforts should focus on this region to gain a better understanding of the global gonococcal population and plasmids in *N. gonorrhoeae*.

The gonococcus is an obligate human pathogen that infects mucosal surfaces of the urethra, uterine cervix, conjunctiva, pharynx, and rectum[178]. My analysis indicates an association of p*bla* with isolates from the urethra, potentially due to the renal excretion of penicillin[381,382]. Exposure to antibiotics may also differ between isolates circulating in distinct sexual networks, which is indicated by the association of multi-drug resistant lineages with MSM populations, while antibiotic-sensitive strains are largely associated with heterosexual populations[443]. However, many datasets lack high-quality metadata and are biased towards urethral samples from MSM. Future studies should also consider different anatomical sites and sexual networks. Knowledge about distinct resistance patterns in different populations and infection sites will aid in providing targeted treatments and improve our understanding of the spread of resistance.

My results indicate distinct patterns of p*bla* variants in the gonococcal population, and characterisation of the fitness costs, mobility and resistance of the three major variants improved our understanding of the molecular mechanisms underlying their distribution. However, several aspects of the interplay between p*bla* and its bacterial host remain unexplored. Firstly, my analysis showed that p*bla*.1-mediated resistance is modified by strain background. Strain-specific differences in plasmid-mediated resistance have been described previously in *E. coli*, with differences in copy number or expression levels correlating with resistance[391,392]. I did not detect differences in p*bla* copy number and bla_{TEM} expression in different strains. Instead, my results suggest synergistic effects with chromosomally-encoded resistance determinants and differences in cellular TEM levels modify plasmid-mediated resistance in *N. gonorrhoeae*. However, the small sample size limited the power of this analysis. Future studies should assess the MICs of p*bla* in a broader panel of isolates to identify co-occurring resistance determinants in strains with increased plasmid-mediated resistance. Furthermore, investigating the stability of TEM β-lactamases in different strains could provide insights into the differences in levels of cellular TEM (Chapter 4.1.2).

It would also be interesting to examine whether findings are generalisable to other resistance mechanisms such as *tetM*-mediated tetracycline resistance.

Secondly, my analysis of the distribution of p*bla* in the gonococcal population revealed that p*bla*-carriage is lineage-specific, consistent with barriers to HGT between gonococci from different lineages. With gonococcal RMS a potential explanation, I focused our analysis on these systems to assess whether they could impede plasmid transfer. However, the effect of the three systems I characterised on plasmid transfer was minimal. While the remaining RMSs could be tested in a similar fashion, a GWAS for plasmid carriage would provide an unbiased and population-structure aware approach, where both associations with the presence/absence of certain genes and allelic variants could be considered.

While the lineage-specific pattern of plasmid carriage in gonococci could be due to barriers to HGT, it is worth remembering that a prerequisite for conjugation is physical contact. Therefore, plasmids can only be transferred between co-infecting strains. PorB typing of cervical swabs and urine samples indicated that up to 40% of patients are infected with multiple strains[444]. However, studies characterising co-occurring strains are lacking. Investigating the co-occurrence of strains could provide insights into spread of plasmids and gene flow between gonococcal strains in general, and ultimately, enhance our understanding of the evolution of this pathogen.

Due to their impact on antibiotic treatment, most research on plasmids in the gonococcus focused on p*bla* and pConj, and the function of the third plasmid, pCryp, remains unknown. However, pCryp is present in >90% of gonococci[286], suggesting an important role of this plasmid in the gonococcus. Therefore, future work could characterise isolates that lack pCryp or attempt to cure the plasmid to assess its significance in the gonococcus.

Finally, *N. gonorrhoeae* has developed resistance against all classes of antibiotics, and the maintenance of resistance determinants prevents recycling of previously used antibiotics[445]. In recent years, phage therapy has been highlighted as a promising alternative to antibiotic treatment, but so far, has not been considered for *N. gonorrhoeae*. With pConj widespread and expected to further increase in prevalence, and p*bla* depending on pConj for its transfer, the use of phages that use conjugative pili as their receptor could be a promising approach to combat plasmid-mediated resistance in this WHO priority pathogen.

6.2 Closing remarks

This thesis addressed different aspects of plasmid-mediated resistance in *N. gonorrhoeae*, generating a tool to identify p*bla* variants from short read WGS and providing the first population-wide analysis of plasmid-mediated β-lactam resistance in the gonococcus. Complementing bioinformatic approaches with molecular microbiology, I characterised the three major p*bla* variants and investigated the interactions between the plasmid and its bacterial host, improving our understanding of mechanisms underlying the patterns observed at the population level. This knowledge should aid designing treatment and intervention strategies and highlights the importance of continued surveillance to monitor the evolution of bla_{TEM}, ensuring timely detection of potential ESBL evolution.

7 Appendices

7.1 Supplementary Tables

Seven supplementary tables are provided as separate files.

Supplementary Table S1: Dataset of 15 532 global gonococcal isolates between 1928 and 2022. WGSs are accessible on PubMLST *via* the isolate id. The Ng_cgc$_{400}$ and plasmid variants carried are specified; plasmid variants that could not be typed are indicated as NA.

Supplementary Table S2: p*bla*-carrying isolates used to verify Ng_p*bla*ST.

Supplementary Table S3: Primers used in this work.

Supplementary Table S4: Dataset of 414 p*bla*-carrying gonococcal isolates on PubMLST used for the analysis of the phylogenetic relationship of p*bla* variants. p*bla* alleles and variant are shown. Raw sequencing data is accessible on ENA using the run_accession.

Supplementary Table S5: NEIS2964 homologs on the NCBI nr protein database determined by BLASTp search.

Supplementary Table S6: p*bla* gene presence absence patterns of Class I and II *H. ducreyi* isolates carrying p*bla*-like plasmids. Gene presence is indicated as '1', absence as '0'; the p*bla* variant was assigned according to the pattern. WGSs are accessible on PubMLST *via* the isolates id.

7.2 References

1 Aitolo, G. L., Adeyemi, O. S., Afolabi, B. L. & Owolabi, A. O. *Neisseria gonorrhoeae* Antimicrobial Resistance: Past to Present to Future. *Curr Microbiol* **78**, 867-878 (2021). https://doi.org:10.1007/s00284-021-02353-8

2 Harrison, O. B. *et al. Neisseria gonorrhoeae* population genomics: Use of the gonococcal core genome to improve surveillance of antimicrobial Resistance. *J Infect Dis* **222**, 1816-1825 (2020). https://doi.org:10.1093/infdis/jiaa002

3 Papadopoulos, J. S. & Agarwala, R. COBALT: constraint-based alignment tool for multiple protein sequences. *Bioinformatics* **23**, 1073-1079 (2007). https://doi.org:10.1093/bioinformatics/btm076

4 Ashford, W. A., Golash, R. G. & Hemming, V. G. Penicillinase-producing *Neisseria gonorrhoeae*. *Lancet* **2**, 657-658 (1976). https://doi.org:10.1016/s0140-6736(76)92467-3

5 Robert, X. & Gouet, P. Deciphering key features in protein structures with the new ENDscript server. *Nucleic Acids Res* **42**, W320-324 (2014). https://doi.org:10.1093/nar/gku316

6 Ramsay, J. P. & Firth, N. Diverse mobilization strategies facilitate transfer of non-conjugative mobile genetic elements. *Current Opinion in Microbiology* **38**, 1-9 (2017). https://doi.org:10.1016/j.mib.2017.03.003

7 Smillie, C., GarcilláN-Barcia, M. P., Francia, M. V., Rocha, E. P. C. & De La Cruz, F. Mobility of Plasmids. *Microbiology and Molecular Biology Reviews* **74**, 434-452 (2010). https://doi.org:10.1128/mmbr.00020-10

8 Rotman, E. & Seifert, H. S. The genetics of Neisseria species. *Annu Rev Genet* **48**, 405-431 (2014). https://doi.org:10.1146/annurev-genet-120213-092007

9 Pei, J. & Grishin, N. V. PROMALS: towards accurate multiple sequence alignments of distantly related proteins. *Bioinformatics* **23**, 802-808 (2007). https://doi.org:10.1093/bioinformatics/btm017

10 He, Y., Lei, J., Pan, X., Huang, X. & Zhao, Y. The hydrolytic water molecule of Class A β-lactamase relies on the acyl-enzyme intermediate ES* for proper coordination and catalysis. *Scientific Reports* **10**, 10205 (2020). https://doi.org:10.1038/s41598-020-66431-w

11 Goire, N. *et al.* Molecular approaches to enhance surveillance of gonococcal antimicrobial resistance. *Nature Reviews Microbiology* **12**, 223-229 (2014). https://doi.org:10.1038/nrmicro3217

12 Saha, C. K., Sanches Pires, R., Brolin, H., Delannoy, M. & Atkinson, G. C. FlaGs and webFlaGs: discovering novel Biology through the analysis of gene neighbourhood conservation. *Bioinformatics* **37**, 1312-1314 (2021). https://doi.org:10.1093/bioinformatics/btaa788

13 Ershova, A. S., Rusinov, I. S., Spirin, S. A., Karyagina, A. S. & Alexeevski, A. V. Role of Restriction-Modification Systems in Prokaryotic Evolution and Ecology. *Biochemistry (Mosc)* **80**, 1373-1386 (2015). https://doi.org:10.1134/s0006297915100193

14 Obergfell, K. P. & Seifert, H. S. Mobile DNA in the Pathogenic *Neisseria*. *Microbiol Spectr* **3**, MDNA3-0015-2014 (2015). https://doi.org:10.1128/microbiolspec.MDNA3-0015-2014

15 Founou, L. L., Founou, R. C. & Essack, S. Y. Antimicrobial resistance in the farm-to-plate continuum: more than a food safety issue. *Future Sci OA* **7**, Fso692 (2021). https://doi.org:10.2144/fsoa-2020-0189

16 Naghavi, M. *et al.* Global burden of bacterial antimicrobial resistance 1990-2021: a systematic analysis with forecasts to 2050. *The Lancet* **404**, 1199-1226 (2024). https://doi.org:10.1016/S0140-6736(24)01867-1

17 Castañeda-Barba, S., Top, E. M. & Stalder, T. Plasmids, a molecular cornerstone of antimicrobial resistance in the One Health era. *Nat Rev Microbiol* **22**, 18-32 (2024). https://doi.org:10.1038/s41579-023-00926-x
18 Hawkey, J. *et al.* Linear plasmids in Klebsiella and other Enterobacteriaceae. *Microb Genom* **8** (2022). https://doi.org:10.1099/mgen.0.000807
19 Ravin, N. V. N15: the linear phage-plasmid. *Plasmid* **65**, 102-109 (2011). https://doi.org:10.1016/j.plasmid.2010.12.004
20 Sternberg, N. & Austin, S. The maintenance of the P1 plasmid prophage. *Plasmid* **5**, 20-31 (1981). https://doi.org:10.1016/0147-619x(81)90075-5
21 Gilcrease, E. B. & Casjens, S. R. The genome sequence of Escherichia coli tailed phage D6 and the diversity of Enterobacteriales circular plasmid prophages. *Virology* **515**, 203-214 (2018). https://doi.org:10.1016/j.virol.2017.12.019
22 Johnson, C. M. & Grossman, A. D. Integrative and Conjugative Elements (ICEs): What They Do and How They Work. *Annu Rev Genet* **49**, 577-601 (2015). https://doi.org:10.1146/annurev-genet-112414-055018
23 Brockhurst, M. A. *et al.* The Ecology and Evolution of Pangenomes. *Curr Biol* **29**, R1094-r1103 (2019). https://doi.org:10.1016/j.cub.2019.08.012
24 Chandran Darbari, V. & Waksman, G. Structural Biology of Bacterial Type IV Secretion Systems. *Annu Rev Biochem* **84**, 603-629 (2015). https://doi.org:10.1146/annurev-biochem-062911-102821
25 Virolle, C., Goldlust, K., Djermoun, S., Bigot, S. & Lesterlin, C. Plasmid Transfer by Conjugation in Gram-Negative Bacteria: From the Cellular to the Community Level. *Genes* **11**, 1239 (2020). https://doi.org:10.3390/genes11111239
26 Matson, S. W. & Morton, B. S. Escherichia coli DNA helicase I catalyzes a site- and strand-specific nicking reaction at the F plasmid oriT. *J Biol Chem* **266**, 16232-16237 (1991).
27 Everett, R. & Willetts, N. Characterisation of an in vivo system for nicking at the origin of conjugal DNA transfer of the sex factor F. *J Mol Biol* **136**, 129-150 (1980). https://doi.org:10.1016/0022-2836(80)90309-5
28 Erich, L. & Brian, M. W. DNA processing reactions in bacterial conjugation. *Annu. Rev. Biochem* **64**, 141-169 (1995).
29 Bhattacharjee, M., Rao, X. M. & Meyer, R. J. Role of the origin of transfer in termination of strand transfer during bacterial conjugation. *J Bacteriol* **174**, 6659-6665 (1992). https://doi.org:10.1128/jb.174.20.6659-6665.1992
30 Furuya, N. & Komano, T. Initiation and termination of DNA transfer during conjugation of IncI1 plasmid R64: roles of two sets of inverted repeat sequences within oriT in termination of R64 transfer. *J Bacteriol* **182**, 3191-3196 (2000). https://doi.org:10.1128/jb.182.11.3191-3196.2000
31 Lanka, E. & Wilkins, B. M. DNA processing reactions in bacterial conjugation. *Annu Rev Biochem* **64**, 141-169 (1995). https://doi.org:10.1146/annurev.bi.64.070195.001041
32 Li, Y. G. & Christie, P. J. The Agrobacterium VirB/VirD4 T4SS: Mechanism and Architecture Defined Through In Vivo Mutagenesis and Chimeric Systems. *Curr Top Microbiol Immunol* **418**, 233-260 (2018). https://doi.org:10.1007/82_2018_94
33 Chandran Darbari, V. & Waksman, G. Structural Biology of Bacterial Type IV Secretion Systems. *Annual Review of Biochemistry* **84**, 603-629 (2015). https://doi.org:10.1146/annurev-biochem-062911-102821
34 Cabezón, E., Ripoll-Rozada, J., Peña, A., De La Cruz, F. & Arechaga, I. Towards an integrated model of bacterial conjugation. *FEMS Microbiology Reviews*, n/a-n/a (2014). https://doi.org:10.1111/1574-6976.12085
35 de la Cruz, F., Frost, L. S., Meyer, R. J. & Zechner, E. L. Conjugative DNA metabolism in Gram-negative bacteria. *FEMS Microbiol Rev* **34**, 18-40 (2010). https://doi.org:10.1111/j.1574-6976.2009.00195.x

36 Dostál, L., Shao, S. & Schildbach, J. F. Tracking F plasmid TraI relaxase processing reactions provides insight into F plasmid transfer. *Nucleic Acids Res* **39**, 2658-2670 (2011). https://doi.org:10.1093/nar/gkq1137

37 Draper, O., César, C. E., Machón, C., de la Cruz, F. & Llosa, M. Site-specific recombinase and integrase activities of a conjugative relaxase in recipient cells. *Proceedings of the National Academy of Sciences* **102**, 16385-16390 (2005). https://doi.org:doi:10.1073/pnas.0506081102

38 Lorenzo-Díaz, F., Fernández-López, C., Garcillán-Barcia, M. P. & Espinosa, M. Bringing them together: plasmid pMV158 rolling circle replication and conjugation under an evolutionary perspective. *Plasmid* **74**, 15-31 (2014). https://doi.org:10.1016/j.plasmid.2014.05.004

39 Ares-Arroyo, M., Coluzzi, C. & Rocha, E. P. C. Origins of transfer establish networks of functional dependencies for plasmid transfer by conjugation. *Nucleic Acids Res* **51**, 3001-3016 (2023). https://doi.org:10.1093/nar/gkac1079

40 Kishida, K. *et al.* Chimeric systems composed of swapped Tra subunits between distantly-related F plasmids reveal striking plasticity among type IV secretion machines. *PLoS Genet* **20**, e1011088 (2024). https://doi.org:10.1371/journal.pgen.1011088

41 Cabezón, E., Sastre, J. I. & De La Cruz, F. Genetic evidence of a coupling role for the TraG protein family in bacterial conjugation. *Molecular and General Genetics MGG* **254**, 400-406 (1997). https://doi.org:10.1007/s004380050432

42 Francia, M. V. *et al.* A classification scheme for mobilization regions of bacterial plasmids. *FEMS Microbiology Reviews* **28**, 79-100 (2004). https://doi.org:10.1016/j.femsre.2003.09.001

43 O'Brien, F. G. *et al.* Origin-of-transfer sequences facilitate mobilisation of non-conjugative antimicrobial-resistance plasmids in Staphylococcus aureus. *Nucleic Acids Res* **43**, 7971-7983 (2015). https://doi.org:10.1093/nar/gkv755

44 Ramsay, J. P. *et al.* An updated view of plasmid conjugation and mobilization inStaphylococcus. *Mobile Genetic Elements* **6**, e1208317 (2016). https://doi.org:10.1080/2159256x.2016.1208317

45 Strahinic, I., Kojic, M., Tolinacki, M., Fira, D. & Topisirovic, L. Molecular characterization of plasmids pS7a and pS7b from Lactococcus lactis subsp. lactis bv. diacetylactis S50 as a base for the construction of mobilizable cloning vectors. *J Appl Microbiol* **106**, 78-88 (2009). https://doi.org:10.1111/j.1365-2672.2008.03977.x

46 Ares-Arroyo, M., Coluzzi, C., Moura de Sousa, J. A. & Rocha, E. P. C. Hijackers, hitchhikers, or co-drivers? The mysteries of mobilizable genetic elements. *PLoS Biol* **22**, e3002796 (2024). https://doi.org:10.1371/journal.pbio.3002796

47 Lee, C. A., Thomas, J. & Grossman, A. D. The Bacillus subtilis Conjugative Transposon ICE Bs1 Mobilizes Plasmids Lacking Dedicated Mobilization Functions. *Journal of Bacteriology* **194**, 3165-3172 (2012). https://doi.org:10.1128/jb.00301-12

48 Fernández-López, C. *et al.* Mobilizable Rolling-Circle Replicating Plasmids from Gram-Positive Bacteria: A Low-Cost Conjugative Transfer. *Microbiol Spectr* **2** (2014). https://doi.org:10.1128/microbiolspec.PLAS-0008-2013

49 Ceccarelli, D., Daccord, A., René, M. & Burrus, V. Identification of the origin of transfer (oriT) and a new gene required for mobilization of the SXT/R391 family of integrating conjugative elements. *J Bacteriol* **190**, 5328-5338 (2008). https://doi.org:10.1128/jb.00150-08

50 Cabezón, E., Lanka, E. & de la Cruz, F. Requirements for mobilization of plasmids RSF1010 and ColE1 by the IncW plasmid R388: trwB and RP4 traG are interchangeable. *J Bacteriol* **176**, 4455-4458 (1994). https://doi.org:10.1128/jb.176.14.4455-4458.1994

51 Werbowy, O. & Kaczorowski, T. Plasmid pEC156, a Naturally Occurring Escherichia coli Genetic Element That Carries Genes of the EcoVIII Restriction-Modification System, Is

Mobilizable among Enterobacteria. *PLoS One* **11**, e0148355 (2016). https://doi.org:10.1371/journal.pone.0148355
52 Meyer, R. Replication and conjugative mobilization of broad host-range IncQ plasmids. *Plasmid* **62**, 57-70 (2009). https://doi.org:10.1016/j.plasmid.2009.05.001
53 Puyet, A., del Solar, G. H. & Espinosa, M. Identification of the origin and direction of replication of the broad-host-range plasmid pLS1. *Nucleic Acids Res* **16**, 115-133 (1988). https://doi.org:10.1093/nar/16.1.115
54 Fogarty, E. C. *et al.* A cryptic plasmid is among the most numerous genetic elements in the human gut. *Cell* **187**, 1206-1222.e1216 (2024). https://doi.org:10.1016/j.cell.2024.01.039
55 Touchon, M., Moura de Sousa, J. A. & Rocha, E. P. Embracing the enemy: the diversification of microbial gene repertoires by phage-mediated horizontal gene transfer. *Curr Opin Microbiol* **38**, 66-73 (2017). https://doi.org:10.1016/j.mib.2017.04.010
56 Humphrey, S. *et al.* Staphylococcal phages and pathogenicity islands drive plasmid evolution. *Nat Commun* **12**, 5845 (2021). https://doi.org:10.1038/s41467-021-26101-5
57 Quiles-Puchalt, N., Martínez-Rubio, R., Ram, G., Lasa, I. & Penadés, J. R. Unravelling bacteriophage φ11 requirements for packaging and transfer of mobile genetic elements in Staphylococcus aureus. *Mol Microbiol* **91**, 423-437 (2014). https://doi.org:10.1111/mmi.12445
58 Coluzzi, C. & Rocha, E. P. C. The Spread of Antibiotic Resistance Is Driven by Plasmids Among the Fastest Evolving and of Broadest Host Range. *Molecular Biology and Evolution* **42** (2025). https://doi.org:10.1093/molbev/msaf060
59 Rodríguez-Rubio, L. *et al.* Extensive antimicrobial resistance mobilization via multicopy plasmid encapsidation mediated by temperate phages. *Journal of Antimicrobial Chemotherapy* **75**, 3173-3180 (2020). https://doi.org:10.1093/jac/dkaa311
60 Matsumoto, A. *et al.* Natural Escherichia coli strains undergo cell-to-cell plasmid transformation. *Biochem Biophys Res Commun* **481**, 59-62 (2016). https://doi.org:10.1016/j.bbrc.2016.11.018
61 Lorenz, M. G. & Wackernagel, W. Bacterial gene transfer by natural genetic transformation in the environment. *Microbiol Rev* **58**, 563-602 (1994). https://doi.org:10.1128/mr.58.3.563-602.1994
62 Chen, I. & Dubnau, D. DNA uptake during bacterial transformation. *Nature Reviews Microbiology* **2**, 241-249 (2004). https://doi.org:10.1038/nrmicro844
63 Chaussee, M. S. & Hill, S. A. Formation of single-stranded DNA during DNA transformation of Neisseria gonorrhoeae. *J Bacteriol* **180**, 5117-5122 (1998). https://doi.org:10.1128/jb.180.19.5117-5122.1998
64 Barany, F., Kahn, M. E. & Smith, H. O. Directional transport and integration of donor DNA in Haemophilus influenzae transformation. *Proceedings of the National Academy of Sciences* **80**, 7274-7278 (1983). https://doi.org:doi:10.1073/pnas.80.23.7274
65 Nielsen, K. M. *et al.* Natural transformation and availability of transforming DNA to Acinetobacter calcoaceticus in soil microcosms. *Appl Environ Microbiol* **63**, 1945-1952 (1997). https://doi.org:10.1128/aem.63.5.1945-1952.1997
66 Li, Y. H., Lau, P. C., Lee, J. H., Ellen, R. P. & Cvitkovitch, D. G. Natural genetic transformation of Streptococcus mutans growing in biofilms. *J Bacteriol* **183**, 897-908 (2001). https://doi.org:10.1128/jb.183.3.897-908.2001
67 San Millan, A. & MacLean, R. C. Fitness costs of plasmids: a limit to plasmid transmission. *Microbiol Spectr* **5** (2017). https://doi.org:10.1128/microbiolspec.MTBP-0016-2017
68 Bernheim, A. & Sorek, R. The pan-immune system of bacteria: antiviral defence as a community resource. *Nature Reviews Microbiology* **18**, 113-119 (2020). https://doi.org:10.1038/s41579-019-0278-2
69 Tesson, F. *et al.* Systematic and quantitative view of the antiviral arsenal of prokaryotes. *Nat Commun* **13**, 2561 (2022). https://doi.org:10.1038/s41467-022-30269-9

70 Roberts, R. J. *et al.* A nomenclature for restriction enzymes, DNA methyltransferases, homing endonucleases and their genes. *Nucleic Acids Research* **31**, 1805-1812 (2003). https://doi.org:10.1093/nar/gkg274

71 Horiuchi, K. & Zinder, N. D. Cleavage of bacteriophage fl DNA by the restriction enzyme of Escherichia coli B. *Proc Natl Acad Sci U S A* **69**, 3220-3224 (1972). https://doi.org:10.1073/pnas.69.11.3220

72 Gao, Y. *et al.* Structural insights into assembly, operation and inhibition of a type I restriction-modification system. *Nat Microbiol* **5**, 1107-1118 (2020). https://doi.org:10.1038/s41564-020-0731-z

73 Moser, D. P., Zarka, D. & Kallas, T. Characterization of a restriction barrier and electrotransformation of the cyanobacterium Nostoc PCC 7121. *Arch Microbiol* **160**, 229-237 (1993). https://doi.org:10.1007/bf00249129

74 Purdy, D. *et al.* Conjugative transfer of clostridial shuttle vectors from Escherichia coli to Clostridium difficile through circumvention of the restriction barrier. *Mol Microbiol* **46**, 439-452 (2002). https://doi.org:10.1046/j.1365-2958.2002.03134.x

75 Pinedo, C. A. & Smets, B. F. Conjugal TOL transfer from Pseudomonas putida to Pseudomonas aeruginosa: effects of restriction proficiency, toxicant exposure, cell density ratios, and conjugation detection method on observed transfer efficiencies. *Appl Environ Microbiol* **71**, 51-57 (2005). https://doi.org:10.1128/aem.71.1.51-57.2005

76 Butler, C. A. & Gotschlich, E. C. High-frequency mobilization of broad-host-range plasmids into Neisseria gonorrhoeae requires methylation in the donor. *J Bacteriol* **173**, 5793-5799 (1991). https://doi.org:10.1128/jb.173.18.5793-5799.1991

77 Dimitriu, T., Szczelkun, Mark D. & Westra, Edze R. Various plasmid strategies limit the effect of bacterial restriction–modification systems against conjugation. *Nucleic Acids Research* **52**, 12976-12986 (2024). https://doi.org:10.1093/nar/gkae896

78 Wilkins, B. M., Chilley, P. M., Thomas, A. T. & Pocklington, M. J. Distribution of restriction enzyme recognition sequences on broad host range plasmid RP4: molecular and evolutionary implications. *J Mol Biol* **258**, 447-456 (1996). https://doi.org:10.1006/jmbi.1996.0261

79 Stein, D. C., Gregoire, S. & Piekarowicz, A. Restriction of plasmid DNA during transformation but not conjugation in Neisseria gonorrhoeae. *Infect Immun* **56**, 112-116 (1988). https://doi.org:10.1128/iai.56.1.112-116.1988

80 Shaw, L. P., Rocha, E. P. C. & MacLean, R. C. Restriction-modification systems have shaped the evolution and distribution of plasmids across bacteria. *Nucleic Acids Res* **51**, 6806-6818 (2023). https://doi.org:10.1093/nar/gkad452

81 Sorek, R. *et al.* Genome-wide experimental determination of barriers to horizontal gene transfer. *Science* **318**, 1449-1452 (2007). https://doi.org:10.1126/science.1147112

82 Rath, D., Amlinger, L., Rath, A. & Lundgren, M. The CRISPR-Cas immune system: Biology, mechanisms and applications. *Biochimie* **117**, 119-128 (2015). https://doi.org:https://doi.org/10.1016/j.biochi.2015.03.025

83 Goldfarb, T. *et al.* BREX is a novel phage resistance system widespread in microbial genomes. *Embo j* **34**, 169-183 (2015). https://doi.org:10.15252/embj.201489455

84 Duncan-Lowey, B. & Kranzusch, P. J. CBASS phage defense and evolution of antiviral nucleotide signaling. *Current Opinion in Immunology* **74**, 156-163 (2022). https://doi.org:https://doi.org/10.1016/j.coi.2022.01.002

85 Shmakov, S. A. *et al.* The CRISPR Spacer Space Is Dominated by Sequences from Species-Specific Mobilomes. *mBio* **8**, 10.1128/mbio.01397-01317 (2017). https://doi.org:doi:10.1128/mbio.01397-17

86 Garcillán-Barcia, M. P. & de la Cruz, F. Why is entry exclusion an essential feature of conjugative plasmids? *Plasmid* **60**, 1-18 (2008). https://doi.org:https://doi.org/10.1016/j.plasmid.2008.03.002

87 Achtman, M., Kennedy, N. & Skurray, R. Cell--cell interactions in conjugating Escherichia coli: role of traT protein in surface exclusion. *Proc Natl Acad Sci U S A* **74**, 5104-5108 (1977). https://doi.org:10.1073/pnas.74.11.5104
88 Lederberg, J., Cavalli, L. L. & Lederberg, E. M. Sex Compatibility in Escherichia Coli. *Genetics* **37**, 720-730 (1952). https://doi.org:10.1093/genetics/37.6.720
89 Gunton, J. E. *et al.* Entry exclusion in the IncHI1 plasmid R27 is mediated by EexA and EexB. *Plasmid* **59**, 86-101 (2008). https://doi.org:10.1016/j.plasmid.2007.11.004
90 Kamruzzaman, M., Mathers, A. J. & Iredell, J. R. A Novel Plasmid Entry Exclusion System in pKPC_UVA01, a Promiscuous Conjugative Plasmid Carrying the bla(KPC) Carbapenemase Gene. *Antimicrob Agents Chemother* **66**, e0232221 (2022). https://doi.org:10.1128/aac.02322-21
91 Marrero, J. & Waldor, M. K. Determinants of entry exclusion within Eex and TraG are cytoplasmic. *J Bacteriol* **189**, 6469-6473 (2007). https://doi.org:10.1128/jb.00522-07
92 Rivard, N. *et al.* Surface exclusion of IncC conjugative plasmids and their relatives. *PLoS Genet* **20**, e1011442 (2024). https://doi.org:10.1371/journal.pgen.1011442
93 Seddon, C. *et al.* Cryo-EM structure and evolutionary history of the conjugation surface exclusion protein TraT. *Nature Communications* **16**, 659 (2025). https://doi.org:10.1038/s41467-025-55834-w
94 Haase, J., Kalkum, M. & Lanka, E. TrbK, a small cytoplasmic membrane lipoprotein, functions in entry exclusion of the IncP alpha plasmid RP4. *J Bacteriol* **178**, 6720-6729 (1996). https://doi.org:10.1128/jb.178.23.6720-6729.1996
95 Novick, R. P. Plasmid incompatibility. *Microbiological Reviews* **51**, 381-395 (1987). https://doi.org:10.1128/mr.51.4.381-395.1987
96 Carattoli, A. *et al.* Identification of plasmids by PCR-based replicon typing. *Journal of Microbiological Methods* **63**, 219-228 (2005). https://doi.org:10.1016/j.mimet.2005.03.018
97 Carattoli, A. *et al.* In Silico Detection and Typing of Plasmids using PlasmidFinder and Plasmid Multilocus Sequence Typing. *Antimicrobial Agents and Chemotherapy* **58**, 3895-3903 (2014). https://doi.org:10.1128/aac.02412-14
98 Velappan, N., Sblattero, D., Chasteen, L., Pavlik, P. & Bradbury, A. R. Plasmid incompatibility: more compatible than previously thought? *Protein Eng Des Sel* **20**, 309-313 (2007). https://doi.org:10.1093/protein/gzm005
99 Baltrus, D. A. Exploring the costs of horizontal gene transfer. *Trends Ecol Evol* **28**, 489-495 (2013). https://doi.org:10.1016/j.tree.2013.04.002
100 Vogwill, T. & MacLean, R. C. The genetic basis of the fitness costs of antimicrobial resistance: a meta-analysis approach. *Evol Appl* **8**, 284-295 (2015). https://doi.org:10.1111/eva.12202
101 Prensky, H., Gomez-Simmonds, A., Uhlemann, A. C. & Lopatkin, A. J. Conjugation dynamics depend on both the plasmid acquisition cost and the fitness cost. *Mol Syst Biol* **17**, e9913 (2021). https://doi.org:10.15252/msb.20209913
102 Baharoglu, Z., Bikard, D. & Mazel, D. Conjugative DNA transfer induces the bacterial SOS response and promotes antibiotic resistance development through integron activation. *PLoS Genet* **6**, e1001165 (2010). https://doi.org:10.1371/journal.pgen.1001165
103 Fernandez-Lopez, R., Del Campo, I., Revilla, C., Cuevas, A. & de la Cruz, F. Negative feedback and transcriptional overshooting in a regulatory network for horizontal gene transfer. *PLoS Genet* **10**, e1004171 (2014). https://doi.org:10.1371/journal.pgen.1004171
104 Fernandez-Lopez, R. & de la Cruz, F. Rebooting the genome: The role of negative feedback in horizontal gene transfer. *Mob Genet Elements* **4**, 1-6 (2014). https://doi.org:10.4161/2159256x.2014.988069

105 San Millan, A., Toll-Riera, M., Qi, Q. & MacLean, R. C. Interactions between horizontally acquired genes create a fitness cost in *Pseudomonas aeruginosa*. *Nat Commun* **6**, 6845 (2015). https://doi.org:10.1038/ncomms7845
106 Ingmer, H., Miller, C. & Cohen, S. N. The RepA protein of plasmid pSC101 controls *Escherichia coli* cell division through the SOS response. *Mol Microbiol* **42**, 519-526 (2001). https://doi.org:10.1046/j.1365-2958.2001.02661.x
107 Del Solar, G., Giraldo, R., Ruiz-EchevarríA, M. A. J. S., Espinosa, M. & DíAz-Orejas, R. N. Replication and Control of Circular Bacterial Plasmids. *Microbiology and Molecular Biology Reviews* **62**, 434-464 (1998). https://doi.org:10.1128/mmbr.62.2.434-464.1998
108 Plotkin, J. B. & Kudla, G. Synonymous but not the same: the causes and consequences of codon bias. *Nat Rev Genet* **12**, 32-42 (2011). https://doi.org:10.1038/nrg2899
109 Tuller, T. *et al.* Association between translation efficiency and horizontal gene transfer within microbial communities. *Nucleic Acids Res* **39**, 4743-4755 (2011). https://doi.org:10.1093/nar/gkr054
110 Medrano-Soto, A., Moreno-Hagelsieb, G., Vinuesa, P., Christen, J. A. & Collado-Vides, J. Successful lateral transfer requires codon usage compatibility between foreign genes and recipient genomes. *Mol Biol Evol* **21**, 1884-1894 (2004). https://doi.org:10.1093/molbev/msh202
111 Loftie-Eaton, W. *et al.* Evolutionary Paths That Expand Plasmid Host-Range: Implications for Spread of Antibiotic Resistance. *Mol Biol Evol* **33**, 885-897 (2016). https://doi.org:10.1093/molbev/msv339
112 Sota, M. *et al.* Shifts in the host range of a promiscuous plasmid through parallel evolution of its replication initiation protein. *Isme j* **4**, 1568-1580 (2010). https://doi.org:10.1038/ismej.2010.72
113 Caro, L. G. & Schnös, M. The attachment of the male-specific bacteriophage F1 to sensitive strains of Escherichia coli. *Proc Natl Acad Sci U S A* **56**, 126-132 (1966). https://doi.org:10.1073/pnas.56.1.126
114 Novotny, C., Knight, W. S. & Brinton, C. C., Jr. Inhibition of bacterial conjugation by ribonucleic acid and deoxyribonucleic acid male-specific bacteriophages. *J Bacteriol* **95**, 314-326 (1968). https://doi.org:10.1128/jb.95.2.314-326.1968
115 Kozlowicz, B. K. *et al.* Molecular basis for control of conjugation by bacterial pheromone and inhibitor peptides. *Mol Microbiol* **62**, 958-969 (2006). https://doi.org:10.1111/j.1365-2958.2006.05434.x
116 McAnulla, C., Edwards, A., Sanchez-Contreras, M., Sawers, R. G. & Downie, J. A. Quorum-sensing-regulated transcriptional initiation of plasmid transfer and replication genes in Rhizobium leguminosarum biovar viciae. *Microbiology (Reading)* **153**, 2074-2082 (2007). https://doi.org:10.1099/mic.0.2007/007153-0
117 Koraimann, G. & Wagner, M. A. Social behavior and decision making in bacterial conjugation. *Front Cell Infect Microbiol* **4**, 54 (2014). https://doi.org:10.3389/fcimb.2014.00054
118 Bergstrom, C. T., Lipsitch, M. & Levin, B. R. Natural selection, infectious transfer and the existence conditions for bacterial plasmids. *Genetics* **155**, 1505-1519 (2000). https://doi.org:10.1093/genetics/155.4.1505
119 Harrison, E. & Brockhurst, M. A. Plasmid-mediated horizontal gene transfer is a coevolutionary process. *Trends Microbiol* **20**, 262-267 (2012). https://doi.org:10.1016/j.tim.2012.04.003
120 Stewart, F. M. & Levin, B. R. The Population Biology of Bacterial Plasmids: A PRIORI Conditions for the Existence of Conjugationally Transmitted Factors. *Genetics* **87**, 209-228 (1977). https://doi.org:10.1093/genetics/87.2.209
121 Brockhurst, M. A. & Harrison, E. Ecological and evolutionary solutions to the plasmid paradox. *Trends Microbiol* **30**, 534-543 (2022). https://doi.org:10.1016/j.tim.2021.11.001

122 Sengupta, M. & Austin, S. Prevalence and significance of plasmid maintenance functions in the virulence plasmids of pathogenic bacteria. *Infect Immun* **79**, 2502-2509 (2011). https://doi.org:10.1128/iai.00127-11
123 Stark, W. M., Boocock, M. R. & Sherratt, D. J. Catalysis by site-specific recombinases. *Trends Genet* **8**, 432-439 (1992).
124 Austin, S., Ziese, M. & Sternberg, N. A novel role for site-specific recombination in maintenance of bacterial replicons. *Cell* **25**, 729-736 (1981). https://doi.org:10.1016/0092-8674(81)90180-x
125 Ebersbach, G. & Gerdes, K. Plasmid segregation mechanisms. *Annu Rev Genet* **39**, 453-479 (2005). https://doi.org:10.1146/annurev.genet.38.072902.091252
126 Møller-Jensen, J. *et al.* Bacterial mitosis: ParM of plasmid R1 moves plasmid DNA by an actin-like insertional polymerization mechanism. *Mol Cell* **12**, 1477-1487 (2003). https://doi.org:10.1016/s1097-2765(03)00451-9
127 Yarmolinsky, M. B. Programmed cell death in bacterial populations. *Science* **267**, 836-837 (1995). https://doi.org:10.1126/science.7846528
128 Jurėnas, D., Fraikin, N., Goormaghtigh, F. & Van Melderen, L. Biology and evolution of bacterial toxin-antitoxin systems. *Nat Rev Microbiol* **20**, 335-350 (2022). https://doi.org:10.1038/s41579-021-00661-1
129 Million-Weaver, S. & Camps, M. Mechanisms of plasmid segregation: have multicopy plasmids been overlooked? *Plasmid* **75**, 27-36 (2014). https://doi.org:10.1016/j.plasmid.2014.07.002
130 Simonsen, L. The existence conditions for bacterial plasmids: Theory and reality. *Microbial Ecology* **22**, 187-205 (1991). https://doi.org:10.1007/BF02540223
131 Dunn, S., Carrilero, L., Brockhurst, M. & McNally, A. Limited and Strain-Specific Transcriptional and Growth Responses to Acquisition of a Multidrug Resistance Plasmid in Genetically Diverse Escherichia coli Lineages. *mSystems* **6** (2021). https://doi.org:10.1128/mSystems.00083-21
132 Alonso-Del Valle, A. *et al.* Variability of plasmid fitness effects contributes to plasmid persistence in bacterial communities. *Nat Commun* **12**, 2653 (2021). https://doi.org:10.1038/s41467-021-22849-y
133 Kottara, A., Hall, J. P. J., Harrison, E. & Brockhurst, M. A. Variable plasmid fitness effects and mobile genetic element dynamics across Pseudomonas species. *FEMS Microbiology Ecology* **94** (2017). https://doi.org:10.1093/femsec/fix172
134 Sheppard, R. J., Beddis, A. E. & Barraclough, T. G. The role of hosts, plasmids and environment in determining plasmid transfer rates: A meta-analysis. *Plasmid* **108**, 102489 (2020). https://doi.org:10.1016/j.plasmid.2020.102489
135 Alderliesten, J. B. *et al.* Effect of donor-recipient relatedness on the plasmid conjugation frequency: a meta-analysis. *BMC Microbiology* **20**, 135 (2020). https://doi.org:10.1186/s12866-020-01825-4
136 Sakuda, A., Suzuki-Minakuchi, C., Okada, K. & Nojiri, H. Conjugative Selectivity of Plasmids Is Affected by Coexisting Recipient Candidates. *mSphere* **3** (2018). https://doi.org:10.1128/mSphere.00490-18
137 San Millan, A., Heilbron, K. & MacLean, R. C. Positive epistasis between co-infecting plasmids promotes plasmid survival in bacterial populations. *Isme j* **8**, 601-612 (2014). https://doi.org:10.1038/ismej.2013.182
138 Gama, J. A., Zilhão, R. & Dionisio, F. Plasmid Interactions Can Improve Plasmid Persistence in Bacterial Populations. *Front Microbiol* **11**, 2033 (2020). https://doi.org:10.3389/fmicb.2020.02033
139 Vogwill, T., Kojadinovic, M. & MacLean, R. C. Epistasis between antibiotic resistance mutations and genetic background shape the fitness effect of resistance across species of *Pseudomonas*. *Proc Biol Sci* **283** (2016). https://doi.org:10.1098/rspb.2016.0151

140 Dionisio, F., Zilhão, R. & Gama, J. A. Interactions between plasmids and other mobile genetic elements affect their transmission and persistence. *Plasmid* **102**, 29-36 (2019). https://doi.org:10.1016/j.plasmid.2019.01.003

141 San Millan, A. *et al.* Positive selection and compensatory adaptation interact to stabilize non-transmissible plasmids. *Nat Commun* **5**, 5208 (2014). https://doi.org:10.1038/ncomms6208

142 Hall, J. P. J. *et al.* Plasmid fitness costs are caused by specific genetic conflicts enabling resolution by compensatory mutation. *PLoS Biol* **19**, e3001225 (2021). https://doi.org:10.1371/journal.pbio.3001225

143 Loftie-Eaton, W. *et al.* Compensatory mutations improve general permissiveness to antibiotic resistance plasmids. *Nature Ecology & Evolution* **1**, 1354-1363 (2017). https://doi.org:10.1038/s41559-017-0243-2

144 Hall, J. P. J., Wright, R. C. T., Guymer, D., Harrison, E. & Brockhurst, M. A. Extremely fast amelioration of plasmid fitness costs by multiple functionally diverse pathways. *Microbiology (Reading)* **166**, 56-62 (2020). https://doi.org:10.1099/mic.0.000862

145 San Millan, A., Escudero, J. A., Gifford, D. R., Mazel, D. & Maclean, R. C. Multicopy plasmids potentiate the evolution of antibiotic resistance in bacteria. *Nature Ecology & Evolution* **1**, 0010 (2017). https://doi.org:10.1038/s41559-016-0010

146 Hernandez-Beltran, J. C. R. *et al.* Plasmid-mediated phenotypic noise leads to transient antibiotic resistance in bacteria. *Nat Commun* **15**, 2610 (2024). https://doi.org:10.1038/s41467-024-45045-0

147 Tønjum, T. & van Putten, J. in *Infectious Diseases (Fourth Edition)* (eds Jonathan Cohen, William G. Powderly, & Steven M. Opal) 1553-1564.e1551 (Elsevier, 2017).

148 Liu, G., Tang, C. M. & Exley, R. M. Non-pathogenic Neisseria: members of an abundant, multi-habitat, diverse genus. *Microbiology (Reading)* **161**, 1297-1312 (2015). https://doi.org:10.1099/mic.0.000086

149 Humbert, M. V. & Christodoulides, M. Atypical, Yet Not Infrequent, Infections with Neisseria Species. *Pathogens* **9**, 10 (2020). https://doi.org:10.3390/pathogens9010010

150 Claus, H. *et al.* Genetic analysis of meningococci carried by children and young adults. *J Infect Dis* **191**, 1263-1271 (2005). https://doi.org:10.1086/428590

151 Tzeng, Y. L. *et al.* Emergence of a new Neisseria meningitidis clonal complex 11 lineage 11.2 clade as an effective urogenital pathogen. *Proc Natl Acad Sci U S A* **114**, 4237-4242 (2017). https://doi.org:10.1073/pnas.1620971114

152 Toh, E. *et al.* Neisseria meningitidis ST11 Complex Isolates Associated with Nongonococcal Urethritis, Indiana, USA, 2015-2016. *Emerg Infect Dis* **23**, 336-339 (2017). https://doi.org:10.3201/eid2302.161434

153 Vanbaelen, T. *et al.* Global epidemiology of antimicrobial resistance in commensal Neisseria species: A systematic review. *International Journal of Medical Microbiology* **312**, 151551 (2022). https://doi.org:https://doi.org/10.1016/j.ijmm.2022.151551

154 Unemo, M. *et al.* WHO global antimicrobial resistance surveillance for *Neisseria gonorrhoeae* 2017-18: a retrospective observational study. *Lancet Microbe* **2**, e627-e636 (2021). https://doi.org:10.1016/s2666-5247(21)00171-3

155 Merrick, R. *et al.* Antimicrobial-resistant gonorrhoea: the national public health response, England, 2013 to 2020. *Euro Surveill* **27** (2022). https://doi.org:10.2807/1560-7917.Es.2022.27.40.2200057

156 Quillin, S. J. & Seifert, H. S. *Neisseria gonorrhoeae* host adaptation and pathogenesis. *Nat Rev Microbiol* **16**, 226-240 (2018). https://doi.org:10.1038/nrmicro.2017.169

157 Higashi, D. L. *et al.* Dynamics of Neisseria gonorrhoeae attachment: microcolony development, cortical plaque formation, and cytoprotection. *Infect Immun* **75**, 4743-4753 (2007). https://doi.org:10.1128/iai.00687-07

158 Merz, A. J. & So, M. Interactions of pathogenic neisseriae with epithelial cell membranes. *Annu Rev Cell Dev Biol* **16**, 423-457 (2000). https://doi.org:10.1146/annurev.cellbio.16.1.423
159 Cohen, M. S. *et al.* Human experimentation with Neisseria gonorrhoeae: rationale, methods, and implications for the biology of infection and vaccine development. *J Infect Dis* **169**, 532-537 (1994). https://doi.org:10.1093/infdis/169.3.532
160 Jerse, A. E. *et al.* Multiple gonococcal opacity proteins are expressed during experimental urethral infection in the male. *J Exp Med* **179**, 911-920 (1994). https://doi.org:10.1084/jem.179.3.911
161 Virji, M., Makepeace, K., Ferguson, D. J. & Watt, S. M. Carcinoembryonic antigens (CD66) on epithelial cells and neutrophils are receptors for Opa proteins of pathogenic neisseriae. *Mol Microbiol* **22**, 941-950 (1996). https://doi.org:10.1046/j.1365-2958.1996.01551.x
162 Simms, A. N. & Jerse, A. E. In vivo selection for Neisseria gonorrhoeae opacity protein expression in the absence of human carcinoembryonic antigen cell adhesion molecules. *Infect Immun* **74**, 2965-2974 (2006). https://doi.org:10.1128/iai.74.5.2965-2974.2006
163 Hagblom, P., Segal, E., Billyard, E. & So, M. Intragenic recombination leads to pilus antigenic variation in Neisseria gonorrhoeae. *Nature* **315**, 156-158 (1985). https://doi.org:10.1038/315156a0
164 Seifert, H. S., Wright, C. J., Jerse, A. E., Cohen, M. S. & Cannon, J. G. Multiple gonococcal pilin antigenic variants are produced during experimental human infections. *J Clin Invest* **93**, 2744-2749 (1994). https://doi.org:10.1172/JCI117290
165 Rice, P. A., Vayo, H. E., Tam, M. R. & Blake, M. S. Immunoglobulin G antibodies directed against protein III block killing of serum-resistant Neisseria gonorrhoeae by immune serum. *J Exp Med* **164**, 1735-1748 (1986). https://doi.org:10.1084/jem.164.5.1735
166 Virji, M. & Heckels, J. E. Nonbactericidal antibodies against Neisseria gonorrhoeae: evaluation of their blocking effect on bactericidal antibodies directed against outer membrane antigens. *J Gen Microbiol* **134**, 2703-2711 (1988). https://doi.org:10.1099/00221287-134-10-2703
167 Liu, Y., Feinen, B. & Russell, M. W. New concepts in immunity to Neisseria gonorrhoeae: innate responses and suppression of adaptive immunity favor the pathogen, not the host. *Front Microbiol* **2**, 52 (2011). https://doi.org:10.3389/fmicb.2011.00052
168 Liu, Y., Islam, E. A., Jarvis, G. A., Gray-Owen, S. D. & Russell, M. W. Neisseria gonorrhoeae selectively suppresses the development of Th1 and Th2 cells, and enhances Th17 cell responses, through TGF-beta-dependent mechanisms. *Mucosal Immunol* **5**, 320-331 (2012). https://doi.org:10.1038/mi.2012.12
169 Jerse, A. E. & Deal, C. D. Vaccine research for gonococcal infections: where are we? *Sex Transm Infect* **89 Suppl 4**, iv63-68 (2013). https://doi.org:10.1136/sextrans-2013-051225
170 Platt, R., Rice, P. A. & McCormack, W. M. Risk of acquiring gonorrhea and prevalence of abnormal adnexal findings among women recently exposed to gonorrhea. *Jama* **250**, 3205-3209 (1983). https://doi.org:10.1001/jama.1983.03340230057031
171 Fox, K. K. *et al.* Longitudinal evaluation of serovar-specific immunity to Neisseria gonorrhoeae. *Am J Epidemiol* **149**, 353-358 (1999). https://doi.org:10.1093/oxfordjournals.aje.a009820
172 Kirkcaldy, R. D., Weston, E., Segurado, A. C. & Hughes, G. Epidemiology of gonorrhoea: a global perspective. *Sex Health* **16**, 401-411 (2019). https://doi.org:10.1071/SH19061
173 Adamson, P. C. & Klausner, J. D. The Staying Power of Pharyngeal Gonorrhea: Implications for Public Health and Antimicrobial Resistance. *Clin Infect Dis* **73**, 583-585 (2021). https://doi.org:10.1093/cid/ciab074
174 Kerle, K. K., Mascola, J. R. & Miller, T. A. Disseminated gonococcal infection. *Am Fam Physician* **45**, 209-214 (1992).

175 Desenclos, J. C., Garrity, D., Scaggs, M. & Wroten, J. E. Gonococcal infection of the newborn in Florida, 1984-1989. *Sex Transm Dis* **19**, 105-110 (1992).
176 Fleming, D. T. & Wasserheit, J. N. From epidemiological synergy to public health policy and practice: the contribution of other sexually transmitted diseases to sexual transmission of HIV infection. *Sex Transm Infect* **75**, 3-17 (1999). https://doi.org:10.1136/sti.75.1.3
177 World Health Organization. *Multi-drug resistant gonorrhoea*, <https://www.who.int/news-room/fact-sheets/detail/multi-drug-resistant-gonorrhoea> (2021).
178 Unemo, M. *et al.* Gonorrhoea. *Nature Reviews Disease Primers* **5** (2019). https://doi.org:10.1038/s41572-019-0128-6
179 Kojima, N., Davey, D. J. & Klausner, J. D. Pre-exposure prophylaxis for HIV infection and new sexually transmitted infections among men who have sex with men. *Aids* **30**, 2251-2252 (2016). https://doi.org:10.1097/qad.0000000000001185
180 Traeger, M. W. *et al.* Association of HIV Preexposure Prophylaxis With Incidence of Sexually Transmitted Infections Among Individuals at High Risk of HIV Infection. *Jama* **321**, 1380-1390 (2019). https://doi.org:10.1001/jama.2019.2947
181 O'Rourke, M. & Stevens, E. Genetic structure of Neisseria gonorrhoeae populations: a non-clonal pathogen. *J Gen Microbiol* **139**, 2603-2611 (1993). https://doi.org:10.1099/00221287-139-11-2603
182 Unitt, A., Maiden, M. & Harrison, O. Characterizing the diversity and commensal origins of penA mosaicism in the genus Neisseria. *Microb Genom* **10** (2024). https://doi.org:10.1099/mgen.0.001209
183 O'Rourke, M. & Spratt, B. G. Further evidence for the non-clonal population structure of Neisseria gonorrhoeae: extensive genetic diversity within isolates of the same electrophoretic type. *Microbiology (Reading)* **140 (Pt 6)**, 1285-1290 (1994). https://doi.org:10.1099/00221287-140-6-1285
184 Maiden, M. C. J. *et al.* MLST revisited: the gene-by-gene approach to bacterial genomics. *Nature Reviews Microbiology* **11**, 728-736 (2013). https://doi.org:10.1038/nrmicro3093
185 Martin, I. M. C., Ison, C. A., Aanensen, D. M., Fenton, K. A. & Spratt, B. G. Rapid Sequence-Based Identification of Gonococcal Transmission Clusters in a Large Metropolitan Area. *The Journal of Infectious Diseases* **189**, 1497-1505 (2004). https://doi.org:10.1086/383047
186 Demczuk, W. *et al. Neisseria gonorrhoeae* Sequence Typing for Antimicrobial Resistance, a Novel Antimicrobial Resistance Multilocus Typing Scheme for Tracking Global Dissemination of N. gonorrhoeae Strains. *Journal of Clinical Microbiology* **55**, 1454-1468 (2017). https://doi.org:10.1128/jcm.00100-17
187 Viscidi, R. P. & Demma, J. C. Genetic diversity of *Neisseria gonorrhoeae* housekeeping genes. *J Clin Microbiol* **41**, 197-204 (2003). https://doi.org:10.1128/jcm.41.1.197-204.2003
188 Tobiason, D. M. & Seifert, H. S. The obligate human pathogen, Neisseria gonorrhoeae, is polyploid. *PLoS Biol* **4**, e185 (2006). https://doi.org:10.1371/journal.pbio.0040185
189 Tobiason, D. M. & Seifert, H. S. Genomic content of Neisseria species. *J Bacteriol* **192**, 2160-2168 (2010). https://doi.org:10.1128/jb.01593-09
190 Spencer-Smith, R., Varkey, E. M., Fielder, M. D. & Snyder, L. A. S. Sequence Features Contributing to Chromosomal Rearrangements in Neisseria gonorrhoeae. *PLoS ONE* **7**, e46023 (2012). https://doi.org:10.1371/journal.pone.0046023
191 Goodman, S. D. & Scocca, J. J. Identification and arrangement of the DNA sequence recognized in specific transformation of Neisseria gonorrhoeae. *Proc Natl Acad Sci U S A* **85**, 6982-6986 (1988). https://doi.org:10.1073/pnas.85.18.6982
192 Frye, S. A., Nilsen, M., Tønjum, T. & Ambur, O. H. Dialects of the DNA uptake sequence in Neisseriaceae. *PLoS Genet* **9**, e1003458 (2013). https://doi.org:10.1371/journal.pgen.1003458

193 Marri, P. R. *et al.* Genome sequencing reveals widespread virulence gene exchange among human Neisseria species. *PLoS One* **5**, e11835 (2010). https://doi.org:10.1371/journal.pone.0011835
194 Davidsen, T. *et al.* Biased distribution of DNA uptake sequences towards genome maintenance genes. *Nucleic Acids Res* **32**, 1050-1058 (2004). https://doi.org:10.1093/nar/gkh255
195 Snyder, L. A. *et al.* The repertoire of minimal mobile elements in the Neisseria species and evidence that these are involved in horizontal gene transfer in other bacteria. *Mol Biol Evol* **24**, 2802-2815 (2007). https://doi.org:https://doi.org:10.1093/molbev/msm215
196 Roberts, S. B. *et al.* Correia Repeat Enclosed Elements and Non-Coding RNAs in the Neisseria Species. *Microorganisms* **4** (2016). https://doi.org:10.3390/microorganisms4030031
197 Callaghan, M. M., Heilers, J. H., van der Does, C. & Dillard, J. P. Secretion of Chromosomal DNA by the Neisseria gonorrhoeae Type IV Secretion System. *Curr Top Microbiol Immunol* **413**, 323-345 (2017). https://doi.org:10.1007/978-3-319-75241-9_13
198 Dillard, J. P. & Seifert, H. S. A variable genetic island specific for Neisseria gonorrhoeae is involved in providing DNA for natural transformation and is found more often in disseminated infection isolates. *Mol Microbiol* **41**, 263-277 (2001). https://doi.org:10.1046/j.1365-2958.2001.02520.x
199 Phelps, L. N. Isolation and characterization of bacteriophages for Neisseria. *J Gen Virol* **1**, 529-536 (1967). https://doi.org:10.1099/0022-1317-1-4-529
200 Steinberg, V. I., Hart, E. J., Handley, J. & Goldberg, I. D. Isolation and characterization of a bacteriophage specific for Neisseria perflava. *J Clin Microbiol* **4**, 87-91 (1976). https://doi.org:10.1128/jcm.4.1.87-91.1976
201 Stone, R. L., Culbertson, C. G. & Powell, H. M. Studies of a bacteriophage active against a chromogenic Neisseria. *J Bacteriol* **71**, 516-520 (1956). https://doi.org:10.1128/jb.71.5.516-520.1956
202 Cehovin, A. & Lewis, S. B. Mobile genetic elements in *Neisseria gonorrhoeae*: movement for change. *Pathog Dis* **75** (2017). https://doi.org:10.1093/femspd/ftx071
203 Piekarowicz, A. *et al.* Neisseria gonorrhoeae filamentous phage NgoΦ6 is capable of infecting a variety of Gram-negative bacteria. *J Virol* **88**, 1002-1010 (2014). https://doi.org:10.1128/jvi.02707-13
204 van der Woude, M. W. & Bäumler, A. J. Phase and antigenic variation in bacteria. *Clin Microbiol Rev* **17**, 581-611, table of contents (2004). https://doi.org:10.1128/cmr.17.3.581-611.2004
205 Levinson, G. & Gutman, G. A. Slipped-strand mispairing: a major mechanism for DNA sequence evolution. *Mol Biol Evol* **4**, 203-221 (1987). https://doi.org:10.1093/oxfordjournals.molbev.a040442
206 Mayer, L. W. Rates in vitro changes of gonococcal colony opacity phenotypes. *Infect Immun* **37**, 481-485 (1982). https://doi.org:10.1128/iai.37.2.481-485.1982
207 Richardson, A. R. & Stojiljkovic, I. Mismatch repair and the regulation of phase variation in Neisseria meningitidis. *Mol Microbiol* **40**, 645-655 (2001). https://doi.org:10.1046/j.1365-2958.2001.02408.x
208 Jordan, P. W., Snyder, L. A. S. & Saunders, N. J. Strain-specific differences in Neisseria gonorrhoeae associated with the phase variable gene repertoire. *BMC Microbiology* **5**, 21 (2005). https://doi.org:10.1186/1471-2180-5-21
209 Snyder, L. A. S., Butcher, S. A. & Saunders, N. J. Comparative whole-genome analyses reveal over 100 putative phase-variable genes in the pathogenic Neisseria spp. *Microbiology (Reading)* **147**, 2321-2332 (2001). https://doi.org:10.1099/00221287-147-8-2321

210 Gibbs, C. P. *et al.* Reassortment of pilin genes in Neisseria gonorrhoeae occurs by two distinct mechanisms. *Nature* **338**, 651-652 (1989). https://doi.org:10.1038/338651a0
211 Haas, R. & Meyer, T. F. The repertoire of silent pilus genes in Neisseria gonorrhoeae: evidence for gene conversion. *Cell* **44**, 107-115 (1986). https://doi.org:10.1016/0092-8674(86)90489-7
212 Hamrick, T. S., Dempsey, J. A. F., Cohen, M. S. & Cannon, J. G. Antigenic variation of gonococcal pilin expression in vivo: analysis of the strain FA1090 pilin repertoire and identification of the pilS gene copies recombining with pilE during experimental human infection. *Microbiology (Reading)* **147**, 839-849 (2001). https://doi.org:10.1099/00221287-147-4-839
213 Biswas, G. D., Sox, T., Blackman, E. & Sparling, P. F. Factors affecting genetic transformation of Neisseria gonorrhoeae. *J Bacteriol* **129**, 983-992 (1977). https://doi.org:10.1128/jb.129.2.983-992.1977
214 Sparling, P. F. Genetic transformation of Neisseria gonorrhoeae to streptomycin resistance. *J Bacteriol* **92**, 1364-1371 (1966). https://doi.org:10.1128/jb.92.5.1364-1371.1966
215 Unemo, M. & Shafer, W. M. Antimicrobial resistance in *Neisseria gonorrhoeae* in the 21st Century: Past, evolution, and future. *Clinical Microbiology Reviews* **27**, 587-613 (2014). https://doi.org:10.1128/cmr.00010-14
216 Berry, J. L., Cehovin, A., McDowell, M. A., Lea, S. M. & Pelicic, V. Functional Analysis of the Interdependence between DNA Uptake Sequence and Its Cognate ComP Receptor during Natural Transformation in Neisseria Species. *Plos Genetics* **9** (2013). https://doi.org:https://doi.org:10.1371/journal.pgen.1004014
217 Ambur, O. H., Frye, S. A. & Tonjum, T. New functional identity for the DNA uptake sequence in transformation and its presence in transcriptional terminators. *J Bacteriol* **189**, 2077-2085 (2007). https://doi.org:10.1128/JB.01408-06
218 Koomey, J. M. & Falkow, S. Cloning of the recA gene of Neisseria gonorrhoeae and construction of gonococcal recA mutants. *J Bacteriol* **169**, 790-795 (1987). https://doi.org:10.1128/jb.169.2.790-795.1987
219 Mehr, I. J. & Seifert, H. S. Differential roles of homologous recombination pathways in *Neisseria gonorrhoeae* pilin antigenic variation, DNA transformation and DNA repair. *Molecular Microbiology* **30**, 697-710 (1998). https://doi.org:10.1046/j.1365-2958.1998.01089.x
220 Vasu, K. & Nagaraja, V. Diverse functions of restriction-modification systems in addition to cellular defense. *Microbiol Mol Biol Rev* **77**, 53-72 (2013). https://doi.org:10.1128/MMBR.00044-12
221 Stein, D. C., Gunn, J. S., Radlinska, M. & Piekarowicz, A. Restriction and modification systems of Neisseria gonorrhoeae. *Gene* **157**, 19-22 (1995). https://doi.org:10.1016/0378-1119(94)00649-d
222 Sanchez-Buso, L., Golparian, D., Parkhill, J., Unemo, M. & Harris, S. R. Genetic variation regulates the activation and specificity of Restriction-Modification systems in Neisseria gonorrhoeae. *Sci Rep* **9**, 14685 (2019). https://doi.org:10.1038/s41598-019-51102-2
223 Srikhanta, Y. N. *et al.* Phasevarions mediate random switching of gene expression in pathogenic Neisseria. *PLoS Pathog* **5**, e1000400 (2009). https://doi.org:10.1371/journal.ppat.1000400
224 Srikhanta, Y. N., Fox, K. L. & Jennings, M. P. The phasevarion: phase variation of type III DNA methyltransferases controls coordinated switching in multiple genes. *Nat Rev Microbiol* **8**, 196-206 (2010). https://doi.org:10.1038/nrmicro2283
225 Phillips, Z. N., Husna, A. U., Jennings, M. P., Seib, K. L. & Atack, J. M. Phasevarions of bacterial pathogens - phase-variable epigenetic regulators evolving from restriction-

modification systems. *Microbiology (Reading)* **165**, 917-928 (2019). https://doi.org:10.1099/mic.0.000805

226 Atack, J. M., Tan, A., Bakaletz, L. O., Jennings, M. P. & Seib, K. L. Phasevarions of Bacterial Pathogens: Methylomics Sheds New Light on Old Enemies. *Trends Microbiol* **26**, 715-726 (2018). https://doi.org:10.1016/j.tim.2018.01.008

227 Adamczyk-Poplawska, M., Lower, M. & Piekarowicz, A. Deletion of one nucleotide within the homonucleotide tract present in the hsdS gene alters the DNA sequence specificity of type I restriction-modification system NgoAV. *J Bacteriol* **193**, 6750-6759 (2011). https://doi.org:10.1128/JB.05672-11

228 Adamczyk-Poplawska, M. *et al.* Phase-variable Type I methyltransferase M.NgoAV from Neisseria gonorrhoeae FA1090 regulates phasevarion expression and gonococcal phenotype. *Front Microbiol* **13**, 917639 (2022). https://doi.org:10.3389/fmicb.2022.917639

229 Elsener, T. A. *et al.* The origin and evolution of the gonococcal beta-lactamase plasmid, and implications for public health. *bioRxiv*, 2025.2001.2003.631176 (2025). https://doi.org:10.1101/2025.01.03.631176

230 Dunlop, E. M. Gonorrhoea and the sulphonamides. *Br J Vener Dis* **25**, 81-83 (1949). https://doi.org:10.1136/sti.25.2.81

231 Van Slyke, C. J., Arnold, R. C. & Buchholtz, M. Penicillin Therapy in Sulfonamide-Resistant Gonorrhea in Men. *Am J Public Health Nations Health* **33**, 1392-1394 (1943). https://doi.org:10.2105/ajph.33.12.1392

232 Unemo, M. & Shafer, W. M. Antibiotic resistance in *Neisseria gonorrhoeae*: origin, evolution, and lessons learned for the future. *Annals of the New York Academy of Sciences* **1230**, E19-E28 (2011). https://doi.org:10.1111/j.1749-6632.2011.06215.x

233 Phillips, I. β-lactamase-producing, penicillin-resistant gonococcus. *Lancet* **2**, 656-657 (1976). https://doi.org:10.1016/s0140-6736(76)92466-1

234 CDC. Sexually transmitted diseases treatment guidelines 1982. *MMWR Morb Mortal Wkly Rep* **31 Suppl 2**, 33s-60s (1982).

235 Morse, S. A., Johnson, S. R., Biddle, J. W. & Roberts, M. C. High-level tetracycline resistance in Neisseria gonorrhoeae is result of acquisition of streptococcal tetM determinant. *Antimicrob Agents Chemother* **30**, 664-670 (1986). https://doi.org:10.1128/aac.30.5.664

236 Starnino, S. *et al.* Trend of ciprofloxacin resistance in Neisseria gonorrhoeae strains isolated in Italy and analysis of the molecular determinants. *Diagn Microbiol Infect Dis* **67**, 350-354 (2010). https://doi.org:10.1016/j.diagmicrobio.2010.03.001

237 Belland, R. J., Morrison, S. G., Ison, C. & Huang, W. M. Neisseria gonorrhoeae acquires mutations in analogous regions of gyrA and parC in fluoroquinolone-resistant isolates. *Mol Microbiol* **14**, 371-380 (1994). https://doi.org:10.1111/j.1365-2958.1994.tb01297.x

238 Hazra, A., Collison, M. W. & Davis, A. M. CDC Sexually transmitted infections treatment guidelines, 2021. *JAMA* **327**, 870 (2022). https://doi.org:10.1001/jama.2022.1246

239 Workowski, K. A. *et al.* Sexually Transmitted Infections Treatment Guidelines, 2021. *MMWR. Recommendations and Reports* **70**, 1-187 (2021). https://doi.org:10.15585/mmwr.rr7004a1

240 Cehovin, A. *et al.* Identification of Novel Neisseria gonorrhoeae Lineages Harboring Resistance Plasmids in Coastal Kenya. *J Infect Dis* **218**, 801-808 (2018). https://doi.org:10.1093/infdis/jiy240

241 Luetkemeyer, A. F. *et al.* Postexposure doxycycline to prevent bacterial sexually transmitted infections. *N Engl J Med* **388**, 1296-1306 (2023). https://doi.org:10.1056/NEJMoa2211934

242 Molina, J. M. *et al.* Post-exposure prophylaxis with doxycycline to prevent sexually transmitted infections in men who have sex with men: an open-label randomised

substudy of the ANRS IPERGAY trial. *Lancet Infect Dis* **18**, 308-317 (2018). https://doi.org:10.1016/s1473-3099(17)30725-9

243 Ohnishi, M. *et al.* Is Neisseria gonorrhoeae initiating a future era of untreatable gonorrhea?: detailed characterization of the first strain with high-level resistance to ceftriaxone. *Antimicrob Agents Chemother* **55**, 3538-3545 (2011). https://doi.org:10.1128/aac.00325-11

244 Fifer, H. *et al.* Ceftriaxone-resistant Neisseria gonorrhoeae detected in England, 2015-24: an observational analysis. *J Antimicrob Chemother* (2024). https://doi.org:10.1093/jac/dkae369

245 Soge, O. O. *et al.* Potential Impact of Doxycycline Post-Exposure Prophylaxis on Tetracycline Resistance in Neisseria gonorrhoeae and Colonization with Tetracycline-Resistant Staphylococcus aureus and Group A Streptococcus. *Clin Infect Dis* (2025). https://doi.org:10.1093/cid/ciaf089

246 Unemo, M., Cole, M. J., Kodmon, C., Day, M. & Jacobsson, S. High tetracycline resistance percentages in Neisseria gonorrhoeae in Europe: is doxycycline post-exposure prophylaxis unlikely to reduce the incident gonorrhoea cases? *Lancet Reg Health Eur* **38**, 100871 (2024). https://doi.org:10.1016/j.lanepe.2024.100871

247 Stewart, J. *et al.* Doxycycline Prophylaxis to Prevent Sexually Transmitted Infections in Women. *N Engl J Med* **389**, 2331-2340 (2023). https://doi.org:10.1056/NEJMoa2304007

248 Jesudason, T. WHO publishes updated list of bacterial priority pathogens. *The Lancet Microbe* **5** (2024). https://doi.org:10.1016/j.lanmic.2024.07.003

249 Franco, S. & Hammerschlag, M. R. Alternative drugs for the treatment of gonococcal infections: old and new. *Expert Rev Anti Infect Ther*, 1-7 (2024). https://doi.org:10.1080/14787210.2024.2401560

250 Ross, J. D. C. *et al.* Oral gepotidacin for the treatment of uncomplicated urogenital gonorrhoea (EAGLE-1): a phase 3 randomised, open-label, non-inferiority, multicentre study. *The Lancet* https://doi.org:10.1016/S0140-6736(25)00628-2

251 Taylor, S. N. *et al.* Single-Dose Zoliflodacin (ETX0914) for Treatment of Urogenital Gonorrhea. *N Engl J Med* **379**, 1835-1845 (2018). https://doi.org:10.1056/NEJMoa1706988

252 Bradford, P. A., Miller, A. A., O'Donnell, J. & Mueller, J. P. Zoliflodacin: An Oral Spiropyrimidinetrione Antibiotic for the Treatment of Neisseria gonorrheae, Including Multi-Drug-Resistant Isolates. *ACS Infect Dis* **6**, 1332-1345 (2020). https://doi.org:10.1021/acsinfecdis.0c00021

253 Gibson, E. G., Bax, B., Chan, P. F. & Osheroff, N. Mechanistic and Structural Basis for the Actions of the Antibacterial Gepotidacin against Staphylococcus aureus Gyrase. *ACS Infect Dis* **5**, 570-581 (2019). https://doi.org:10.1021/acsinfecdis.8b00315

254 Farrell, D. J., Sader, H. S., Rhomberg, P. R., Scangarella-Oman, N. E. & Flamm, R. K. In Vitro Activity of Gepotidacin (GSK2140944) against Neisseria gonorrhoeae. *Antimicrobial Agents and Chemotherapy* **61**, 10.1128/aac.02047-02016 (2017). https://doi.org:doi:10.1128/aac.02047-16

255 Adamson, P. C., Lin, E. Y., Ha, S. M. & Klausner, J. D. Using a public database of Neisseria gonorrhoeae genomes to detect mutations associated with zoliflodacin resistance. *J Antimicrob Chemother* **76**, 2847-2849 (2021). https://doi.org:10.1093/jac/dkab262

256 Abdellati, S. *et al.* Gonococcal resistance to zoliflodacin could emerge via transformation from commensal Neisseria species. An in-vitro transformation study. *Sci Rep* **14**, 1179 (2024). https://doi.org:10.1038/s41598-023-49943-z

257 Robinson, L. R., McDevitt, C. J., Regan, M. R., Quail, S. L. & Wadsworth, C. B. In vitro evolution of ciprofloxacin resistance in Neisseria commensals and derived mutation population dynamics in natural Neisseria populations. *bioRxiv* (2024). https://doi.org:10.1101/2024.07.16.603762

258 Sparling, P. F., Sarubbi, F. A. & Blackman, E. Inheritance of low-level resistance to penicillin, tetracycline, and chloramphenicol in Neisseria gonorrhoeae. *Journal of Bacteriology* **124**, 740-749 (1975). https://doi.org:doi:10.1128/jb.124.2.740-749.1975

259 Wise, E. M., Jr. & Park, J. T. Penicillin: its basic site of action as an inhibitor of a peptide cross-linking reaction in cell wall mucopeptide synthesis. *Proc Natl Acad Sci U S A* **54**, 75-81 (1965). https://doi.org:10.1073/pnas.54.1.75

260 Yocum, R. R., Rasmussen, J. R. & Strominger, J. L. The mechanism of action of penicillin. Penicillin acylates the active site of Bacillus stearothermophilus D-alanine carboxypeptidase. *J Biol Chem* **255**, 3977-3986 (1980).

261 Brannigan, J. A., Tirodimos, I. A., Zhang, Q. Y., Dowson, C. G. & Spratt, B. G. Insertion of an extra amino acid is the main cause of the low affinity of penicillin-binding protein 2 in penicillin-resistant strains of Neisseria gonorrhoeae. *Mol Microbiol* **4**, 913-919 (1990). https://doi.org:10.1111/j.1365-2958.1990.tb00664.x

262 Spratt, B. G. in *Microbial Resistance to Drug* (ed Lawrence E. Bryan) 77-100 (Springer Berlin Heidelberg, 1989).

263 Olesky, M., Zhao, S., Rosenberg, R. L. & Nicholas, R. A. Porin-mediated antibiotic resistance in Neisseria gonorrhoeae: ion, solute, and antibiotic permeation through PIB proteins with penB mutations. *J Bacteriol* **188**, 2300-2308 (2006). https://doi.org:10.1128/jb.188.7.2300-2308.2006

264 Shafer, W. M. & Folster, J. P. Towards an understanding of chromosomally mediated penicillin resistance in Neisseria gonorrhoeae: evidence for a porin-efflux pump collaboration. *J Bacteriol* **188**, 2297-2299 (2006). https://doi.org:10.1128/jb.188.7.2297-2299.2006

265 Barrera, O. & Swanson, J. Proteins IA and IB exhibit different surface exposures and orientations in the outer membranes of Neisseria gonorrhoeae. *Infect Immun* **44**, 565-568 (1984). https://doi.org:10.1128/iai.44.3.565-568.1984

266 Gill, M. J. *et al.* Gonococcal resistance to beta-lactams and tetracycline involves mutation in loop 3 of the porin encoded at the penB locus. *Antimicrob Agents Chemother* **42**, 2799-2803 (1998). https://doi.org:10.1128/aac.42.11.2799

267 Ropp, P. A., Hu, M., Olesky, M. & Nicholas, R. A. Mutations in ponA, the gene encoding penicillin-binding protein 1, and a novel locus, penC, are required for high-level chromosomally mediated penicillin resistance in Neisseria gonorrhoeae. *Antimicrob Agents Chemother* **46**, 769-777 (2002). https://doi.org:10.1128/aac.46.3.769-777.2002

268 Zhao, S., Tobiason, D. M., Hu, M., Seifert, H. S. & Nicholas, R. A. The penC mutation conferring antibiotic resistance in Neisseria gonorrhoeae arises from a mutation in the PilQ secretin that interferes with multimer stability. *Mol Microbiol* **57**, 1238-1251 (2005). https://doi.org:10.1111/j.1365-2958.2005.04752.x

269 Ito, M. *et al.* Emergence and spread of Neisseria gonorrhoeae clinical isolates harboring mosaic-like structure of penicillin-binding protein 2 in Central Japan. *Antimicrob Agents Chemother* **49**, 137-143 (2005). https://doi.org:10.1128/aac.49.1.137-143.2005

270 Lindberg, R., Fredlund, H., Nicholas, R. & Unemo, M. *Neisseria gonorrhoeae* isolates with reduced susceptibility to cefixime and ceftriaxone: association with genetic polymorphisms in *penA*, *mtrR*, *porB*1b, and *ponA*. *Antimicrob Agents Chemother* **51**, 2117-2122 (2007). https://doi.org:10.1128/aac.01604-06

271 Vincent, L. R. *et al.* In Vivo-Selected Compensatory Mutations Restore the Fitness Cost of Mosaic penA Alleles That Confer Ceftriaxone Resistance in Neisseria gonorrhoeae. *mBio* **9** (2018). https://doi.org:10.1128/mBio.01905-17

272 Bush, K. & Jacoby, G. Nomenclature of TEM β-lactamases. *J Antimicrob Chemother* **39**, 1-3 (1997). https://doi.org:10.1093/jac/39.1.1

273 Christensen, H., Martin, M. T. & Waley, S. G. Beta-lactamases as fully efficient enzymes. Determination of all the rate constants in the acyl-enzyme mechanism. *Biochem J* **266**, 853-861 (1990).
274 Chen, C. C. *et al.* Structure and kinetics of the beta-lactamase mutants S70A and K73H from Staphylococcus aureus PC1. *Biochemistry* **35**, 12251-12258 (1996). https://doi.org:10.1021/bi961153v
275 Strynadka, N. C. *et al.* Molecular structure of the acyl-enzyme intermediate in beta-lactam hydrolysis at 1.7 A resolution. *Nature* **359**, 700-705 (1992). https://doi.org:10.1038/359700a0
276 Herzberg, O. & Moult, J. Bacterial resistance to beta-lactam antibiotics: crystal structure of beta-lactamase from Staphylococcus aureus PC1 at 2.5 A resolution. *Science* **236**, 694-701 (1987). https://doi.org:10.1126/science.3107125
277 Adachi, H., Ohta, T. & Matsuzawa, H. Site-directed mutants, at position 166, of RTEM-1 beta-lactamase that form a stable acyl-enzyme intermediate with penicillin. *J Biol Chem* **266**, 3186-3191 (1991).
278 Jelsch, C., Mourey, L., Masson, J. M. & Samama, J. P. Crystal structure of Escherichia coli TEM1 beta-lactamase at 1.8 A resolution. *Proteins* **16**, 364-383 (1993). https://doi.org:10.1002/prot.340160406
279 Matagne, A., Lamotte-Brasseur, J. & Frère, J. M. Catalytic properties of class A beta-lactamases: efficiency and diversity. *Biochem J* **330 (Pt 2)**, 581-598 (1998). https://doi.org:10.1042/bj3300581
280 Walther-Rasmussen, J. & Høiby, N. Class A carbapenemases. *J Antimicrob Chemother* **60**, 470-482 (2007). https://doi.org:10.1093/jac/dkm226
281 Cantu, C., 3rd, Huang, W. & Palzkill, T. Cephalosporin substrate specificity determinants of TEM-1 beta-lactamase. *J Biol Chem* **272**, 29144-29150 (1997). https://doi.org:10.1074/jbc.272.46.29144
282 Salverda, M. L. M., De Visser, J. A. G. M. & Barlow, M. Natural evolution of TEM-1 β-lactamase: experimental reconstruction and clinical relevance. *FEMS Microbiology Reviews* **34**, 1015-1036 (2010). https://doi.org:10.1111/j.1574-6976.2010.00222.x
283 Ambler, R. P. *et al.* A standard numbering scheme for the class A β-lactamase. *Biochem J* **276 (Pt 1)**, 269-270 (1991). https://doi.org:10.1042/bj2760269
284 Brown, N. G., Pennington, J. M., Huang, W., Ayvaz, T. & Palzkill, T. Multiple Global Suppressors of Protein Stability Defects Facilitate the Evolution of Extended-Spectrum TEM β-Lactamases. *Journal of Molecular Biology* **404**, 832-846 (2010). https://doi.org:https://doi.org/10.1016/j.jmb.2010.10.008
285 Huang, W. & Palzkill, T. A natural polymorphism in β-lactamase is a global suppressor. *Proc Natl Acad Sci U S A* **94**, 8801-8806 (1997). https://doi.org:10.1073/pnas.94.16.8801
286 Cehovin, A., Jolley, K. A., Maiden, M. C. J., Harrison, O. B. & Tang, C. M. Association of Neisseria gonorrhoeae Plasmids With Distinct Lineages and The Economic Status of Their Country of Origin. *J Infect Dis* **222**, 1826-1836 (2020). https://doi.org:10.1093/infdis/jiaa003
287 Snaith, A. E. *et al.* The highly diverse plasmid population found in Escherichia coli colonizing travellers to Laos and its role in antimicrobial resistance gene carriage. *Microb Genom* **9** (2023). https://doi.org:10.1099/mgen.0.001000
288 Coluzzi, C. & Rocha, E. P. The spread of antibiotic resistance is driven by plasmids amongst the fastest evolving and of broadest host range. *BioRxiv* (2024). https://doi.org:https://doi.org/10.1101/2024.07.23.604842
289 Haudiquet, M., de Sousa, J. M., Touchon, M. & Rocha, E. P. C. Selfish, promiscuous and sometimes useful: how mobile genetic elements drive horizontal gene transfer in microbial populations. *Philos Trans R Soc Lond B Biol Sci* **377**, 20210234 (2022). https://doi.org:10.1098/rstb.2021.0234

290 Cehovin, A., Jolley, K. A., Maiden, M. C. J., Harrison, O. B. & Tang, C. M. Association of *Neisseria gonorrhoeae* plasmids with distinct lineages and the economic status of their country of origin. *The Journal of Infectious Diseases* **222**, 1826-1836 (2020). https://doi.org:10.1093/infdis/jiaa003

291 Engelkirk, P. G. & Schoenhard, D. E. Physical evidence of a plasmid in Neisseria gonorrhoeae. *J Infect Dis* **127**, 197-200 (1973). https://doi.org:10.1093/infdis/127.2.197

292 Mayer, L. W., Holmes, K. K. & Falkow, S. Characterization of plasmid deoxyribonucleic acid from Neisseria gonorrhoeae. *Infect Immun* **10**, 712-717 (1974). https://doi.org:10.1128/iai.10.4.712-717.1974

293 Pachulec, E. & Van Der Does, C. Conjugative Plasmids of *Neisseria gonorrhoeae*. *PLoS ONE* **5**, e9962 (2010). https://doi.org:10.1371/journal.pone.0009962

294 Yee, W. X. *et al.* Evolution, persistence, and host adaption of a gonococcal AMR plasmid that emerged in the pre-antibiotic era. *PLoS Genet* **19**, e1010743 (2023). https://doi.org:10.1371/journal.pgen.1010743

295 Dönhöfer, A. *et al.* Structural basis for TetM-mediated tetracycline resistance. *Proc Natl Acad Sci U S A* **109**, 16900-16905 (2012). https://doi.org:10.1073/pnas.1208037109

296 Yee, W. X., Elsener, T., Cehovin, A., Maiden, M. C. J. & Tang, C. M. Evolution and exchange of plasmids in pathogenic Neisseria. *mSphere* **8**, e0044123 (2023). https://doi.org:10.1128/msphere.00441-23

297 St Cyr, S. *et al.* Update to CDC's Treatment Guidelines for Gonococcal Infection, 2020. *MMWR Morb Mortal Wkly Rep* **69**, 1911-1916 (2020). https://doi.org:10.15585/mmwr.mm6950a6

298 Helekal, D., Mortimer, T. D. & Grad, Y. H. Expansion of tetM-Carrying Neisseria gonorrhoeae in the United States, 2018–2024. *New England Journal of Medicine* **393**, 198-200 (2025). https://doi.org:doi:10.1056/NEJMc2504010

299 Phillips, I. Beta-lactamase-producing, penicillin-resistant gonococcus. *Lancet* **2**, 656-657 (1976). https://doi.org:10.1016/s0140-6736(76)92466-1

300 Pagotto, F. *et al.* Sequence analysis of the family of penicillinase-producing plasmids of *Neisseria gonorrhoeae*. *Plasmid* **43**, 24-34 (2000). https://doi.org:10.1006/plas.1999.1431

301 Muller, E. E., Fayemiwo, S. A. & Lewis, D. A. Characterization of a novel β-lactamase-producing plasmid in *Neisseria gonorrhoeae*: sequence analysis and molecular typing of host gonococci. *Journal of Antimicrobial Chemotherapy* **66**, 1514-1517 (2011). https://doi.org:10.1093/jac/dkr162

302 Trembizki, E., Buckley, C., Lawrence, A., Lahra, M. & Whiley, D. Characterization of a novel *Neisseria gonorrhoeae* penicillinase-producing plasmid isolated in Australia in 2012. *Antimicrobial Agents and Chemotherapy* **58**, 4984-4985 (2014). https://doi.org:10.1128/aac.02993-14

303 Roberts, M., Elwell, L. P. & Falkow, S. Molecular characterization of two β-lactamase-specifying plasmids isolated from *Neisseria gonorrhoeae*. *J Bacteriol* **131**, 557-563 (1977). https://doi.org:10.1128/jb.131.2.557-563.1977

304 Sox, T. E., Mohammed, W. & Sparling, P. F. Transformation-derived Neisseria gonorrhoeae plasmids with altered structure and function. *J Bacteriol* **138**, 510-518 (1979). https://doi.org:10.1128/jb.138.2.510-518.1979

305 Jain, A. Y. & Srivastava, P. Broad host range plasmids. *FEMS microbiology letters* **348 2**, 87-96 (2013). https://doi.org:10.1111/1574-6968.12241

306 Pagotto, F. & Dillon, J.-A. R. Multiple origins and replication proteins influence biological properties of β-lactamase-producing plasmids from *Neisseria gonorrhoeae*. *Journal of Bacteriology* **183**, 5472-5481 (2001). https://doi.org:10.1128/jb.183.19.5472-5481.2001

307 Dillon, J.-A. R. & Yeung, K. H. β-lactamase plasmids and chromosomally mediated antibiotic resistance in pathogenic *Neisseria* species. *Clinical Microbiology Reviews* **2**, S125 - S133 (1989). https://doi.org:10.1128/CMR.2.Suppl.S125

308 Roberts, M. C. & Falkow, S. Conjugal transfer of R plasmids in Neisseria gonorrhoeae. *Nature* **266**, 630-631 (1977). https://doi.org:10.1038/266630a0
309 Rodriguez-Bonano, N. M. & Torres-Bauza, L. J. Molecular analysis of *oriT* and MobA protein in the 7.4 kb mobilizable β-lactamase plasmid pSJ7.4 from *Neisseria gonorrhoeae*. *Plasmid* **52**, 89-101 (2004). https://doi.org:10.1016/j.plasmid.2004.05.002
310 Simon, R., Priefer, U. & Pühler, A. A Broad Host Range Mobilization System for In Vivo Genetic Engineering: Transposon Mutagenesis in Gram Negative Bacteria. *Bio/Technology* **1**, 784-791 (1983). https://doi.org:10.1038/nbt1183-784
311 Muller, E. E., Fayemiwo, S. A. & Lewis, D. A. Characterization of a novel beta-lactamase-producing plasmid in Neisseria gonorrhoeae: sequence analysis and molecular typing of host gonococci. *J Antimicrob Chemother* **66**, 1514-1517 (2011). https://doi.org:10.1093/jac/dkr162
312 Scharbaai-Vázquez, R., González-Caraballo, A. L. & Torres-Bauzá, L. J. Four different integrative recombination events involved in the mobilization of the gonococcal 5.2kb β-lactamase plasmid pSJ5.2 in *Escherichia coli*. *Plasmid* **60**, 200-211 (2008). https://doi.org:10.1016/j.plasmid.2008.07.004
313 Scharbaai-Vázquez, R., Candelas, T. & Torres-Bauzá, L. J. Mobilization of the gonococcal 5.2kb β-lactamase plasmid pSJ5.2 into Escherichia coli by cointegration with several gram-conjugative plasmids. *Plasmid* **57**, 156-164 (2007). https://doi.org:10.1016/j.plasmid.2006.07.006
314 Marquez, C., Xia, M., Borthagaray, G. & Roberts, M. C. Conjugal transfer of the 3.05 β-lactamase plasmid by the 25.2 Mda plasmid in *Neisseria gonorrhoeae*. *Sex Transm Dis* **26**, 157-159 (1999). https://doi.org:10.1097/00007435-199903000-00006
315 Muhammad, I. *et al.* Characterisation of *bla*TEM genes and types of β-lactamase plasmids in *Neisseria gonorrhoeae* – the prevalent and conserved *bla*TEM-135 has not recently evolved and existed in the Toronto plasmid from the origin. *BMC Infectious Diseases* **14**, 454 (2014). https://doi.org:10.1186/1471-2334-14-454
316 Orencia, M. C., Yoon, J. S., Ness, J. E., Stemmer, W. P. C. & Stevens, R. C. Predicting the emergence of antibiotic resistance by directed evolution and structural analysis. *Nature Structural Biology* **8**, 238-242 (2001). https://doi.org:10.1038/84981
317 Dillon, J. R., Li, H., Yeung, K. & Aman, T. A. A PCR assay for discriminating *Neisseria gonorrhoeae* β-lactamase-producing plasmids. *Mol Cell Probes* **13**, 89-92 (1999). https://doi.org:10.1006/mcpr.1998.0216
318 Gouby, A., Bourg, G. & Ramuz, M. Previously undescribed 6.6-kilobase R plasmid in penicillinase-producing *Neisseria gonorrhoeae*. *Antimicrob Agents Chemother* **29**, 1095-1097 (1986). https://doi.org:10.1128/aac.29.6.1095
319 Palmer, H. M., Leeming, J. P. & Turner, A. A multiplex polymerase chain reaction to differentiate β-lactamase plasmids of *Neisseria gonorrhoeae*. *J Antimicrob Chemother* **45**, 777-782 (2000). https://doi.org:10.1093/jac/45.6.777
320 Unemo, M. *et al.* The novel 2016 WHO *Neisseria gonorrhoeae* reference strains for global quality assurance of laboratory investigations: Phenotypic, genetic and reference genome characterization. *Journal of Antimicrobial Chemotherapy* **71**, 3096-3108 (2016). https://doi.org:10.1093/jac/dkw288
321 Jolley, K. A., Bray, J. E. & Maiden, M. C. J. Open-access bacterial population genomics: BIGSdb software, the PubMLST.org website and their applications. *Wellcome Open Research* **3**, 124 (2018). https://doi.org:10.12688/wellcomeopenres.14826.1
322 Jolley, K. A. *et al.* Ribosomal multilocus sequence typing: Universal characterization of bacteria from domain to strain. *Microbiology (Reading)* **158**, 1005-1015 (2012). https://doi.org:10.1099/mic.0.055459-0

323 Pagotto, F. J., Salimnia, H., Totten, P. A. & Dillon, J. R. Stable shuttle vectors for *Neisseria gonorrhoeae*, *Haemophilus* spp. and other bacteria based on a single origin of replication. *Gene* **244**, 13-19 (2000). https://doi.org:10.1016/s0378-1119(99)00557-0
324 Sayers, E. W. *et al.* Database resources of the National Center for Biotechnology Information. *Nucleic Acids Res* **50**, D20-d26 (2022). https://doi.org:10.1093/nar/gkab1112
325 Cox, K. E. L. & Schildbach, J. F. Sequence of the R1 plasmid and comparison to F and R100. *Plasmid* **91**, 53-60 (2017). https://doi.org:10.1016/j.plasmid.2017.03.007
326 Fernández-López, R. *et al.* Dynamics of the IncW genetic backbone imply general trends in conjugative plasmid evolution. *FEMS Microbiology Reviews* **30**, 942-966 (2006). https://doi.org:10.1111/j.1574-6976.2006.00042.x
327 Madeira, F. *et al.* Search and sequence analysis tools services from EMBL-EBI in 2022. *Nucleic Acids Res* **50**, W276-279 (2022). https://doi.org:10.1093/nar/gkac240
328 Abramson, J. *et al.* Accurate structure prediction of biomolecular interactions with AlphaFold 3. *Nature* **630**, 493-500 (2024). https://doi.org:10.1038/s41586-024-07487-w
329 DeLano, W. L. The PyMOL molecular graphics system. *http://www. pymol. org/* (2002).
330 Jurrus, E. *et al.* Improvements to the APBS biomolecular solvation software suite. *Protein Sci* **27**, 112-128 (2018). https://doi.org:10.1002/pro.3280
331 Wilkins, M. R. *et al.* Protein identification and analysis tools in the ExPASy server. *Methods Mol Biol* **112**, 531-552 (1999). https://doi.org:10.1385/1-59259-584-7:531
332 Zhou, Z. *et al.* GrapeTree: Visualization of core genomic relationships among 100,000 bacterial pathogens. *Genome Research* **28**, 1395-1404 (2018). https://doi.org:10.1101/gr.232397.117
333 Kozlov, A. M., Darriba, D., Flouri, T., Morel, B. & Stamatakis, A. RAxML-NG: a fast, scalable and user-friendly tool for maximum likelihood phylogenetic inference. *Bioinformatics* **35**, 4453-4455 (2019). https://doi.org:10.1093/bioinformatics/btz305
334 Paradis, E. & Schliep, K. ape 5.0: an environment for modern phylogenetics and evolutionary analyses in R. *Bioinformatics* **35**, 526-528 (2019). https://doi.org:10.1093/bioinformatics/bty633
335 Yu, G., Smith, D. K., Zhu, H., Guan, Y. & Lam, T. T. Y. ggtree: an r package for visualization and annotation of phylogenetic trees with their covariates and other associated data. *Methods in Ecology and Evolution* **8**, 28-36 (2017). https://doi.org:10.1111/2041-210x.12628
336 Dorado: Oxford Nanopore's Basecaller (Github, 2025).
337 Danecek, P. *et al.* Twelve years of SAMtools and BCFtools. *GigaScience* **10** (2021). https://doi.org:10.1093/gigascience/giab008
338 Modkit (Github, 2024).
339 Cartwright, C. P., Stock, F. & Gill, V. J. Improved enrichment broth for cultivation of fastidious organisms. *J Clin Microbiol* **32**, 1825-1826 (1994). https://doi.org:10.1128/jcm.32.7.1825-1826.1994
340 Jones, R. A., Yee, W. X., Mader, K., Tang, C. M. & Cehovin, A. Markerless gene editing in *Neisseria gonorrhoeae*. *Microbiology (Reading)* **168** (2022). https://doi.org:10.1099/mic.0.001201
341 Dillard, J. P. Genetic Manipulation of *Neisseria gonorrhoeae*. *Curr Protoc Microbiol* **Chapter 4**, Unit4A.2 (2011). https://doi.org:10.1002/9780471729259.mc04a02s23
342 Elkins, C., Thomas, C. E., Seifert, H. S. & Sparling, P. F. Species-specific uptake of DNA by gonococci is mediated by a 10-base-pair sequence. *J Bacteriol* **173**, 3911-3913 (1991).
343 Watson, J. F. & García-Nafría, J. In vivo DNA assembly using common laboratory bacteria: A re-emerging tool to simplify molecular cloning. *J Biol Chem* **294**, 15271-15281 (2019). https://doi.org:10.1074/jbc.REV119.009109
344 growthrates: Estimate Growth Rates from Experimental Data (Comprehensive R Archive Network (CRAN), 2022).

345 Magnus Unemo, R. B., Catherine Ison, David Lewis, Francis Ndowa, Rosanna Peeling. (World Health Organization, https://iris.who.int/bitstream/handle/10665/85343/9789241505840_eng.pdf?sequence=1, 2013).
346 Wickham, H. *et al.* Welcome to the Tidyverse. *Journal of Open Source Software* **4**, 1686 (2019). https://doi.org:10.21105/joss.01686
347 Epitools epidemiological calculators (Ausvet, 2018).
348 Wickham, H. *Elegant graphics for data analysis*. 2 edn, (Springer-Verlag, New York, 2016).
349 Chen, S. T. & Clowes, R. C. Nucleotide sequence comparisons of plasmids pHD131, pJB1, pFA3, and pFA7 and β-lactamase expression in *Escherichia coli, Haemophilus influenzae*, and *Neisseria gonorrhoeae*. *J Bacteriol* **169**, 3124-3130 (1987). https://doi.org:10.1128/jb.169.7.3124-3130.1987
350 Fayet, O., Froment, Y. & Piffaretti, J. C. β-lactamase-specifying plasmids isolated from *Neisseria gonorrhoeae* have retained an intact right part of a Tn3-like transposon. *Journal of Bacteriology* **149**, 136-144 (1982). https://doi.org:10.1128/jb.149.1.136-144.1982
351 Wegrzyn, K. E., Gross, M., Uciechowska, U. & Konieczny, I. Replisome assembly at bacterial chromosomes and iteron plasmids. *Front Mol Biosci* **3**, 39 (2016). https://doi.org:10.3389/fmolb.2016.00039
352 Lewis, B. A. & Engelman, D. M. Lipid bilayer thickness varies linearly with acyl chain length in fluid phosphatidylcholine vesicles. *Journal of Molecular Biology* **166**, 211-217 (1983). https://doi.org:https://doi.org/10.1016/S0022-2836(83)80007-2
353 Käll, L., Krogh, A. & Sonnhammer, E. L. A combined transmembrane topology and signal peptide prediction method. *J Mol Biol* **338**, 1027-1036 (2004). https://doi.org:10.1016/j.jmb.2004.03.016
354 Smith, M. B. *Advanced Organic Chemistry: Reactions, Mechanisms and Structure*. 6th ed. edn, (Whiley-Interscience, 2007).
355 Wilson, K. A., Kellie, J. L. & Wetmore, S. D. DNA-protein π-interactions in nature: abundance, structure, composition and strength of contacts between aromatic amino acids and DNA nucleobases or deoxyribose sugar. *Nucleic Acids Res* **42**, 6726-6741 (2014). https://doi.org:10.1093/nar/gku269
356 Hook, E. W., 3rd & Kirkcaldy, R. D. A Brief History of Evolving Diagnostics and Therapy for Gonorrhea: Lessons Learned. *Clin Infect Dis* **67**, 1294-1299 (2018). https://doi.org:10.1093/cid/ciy271
357 Lu, C., Nakayasu, E. S., Zhang, L. Q. & Luo, Z. Q. Identification of Fic-1 as an enzyme that inhibits bacterial DNA replication by AMPylating GyrB, promoting filament formation. *Sci Signal* **9**, ra11 (2016). https://doi.org:10.1126/scisignal.aad0446
358 Harms, A. *et al.* Adenylylation of Gyrase and Topo IV by FicT Toxins Disrupts Bacterial DNA Topology. *Cell Rep* **12**, 1497-1507 (2015). https://doi.org:10.1016/j.celrep.2015.07.056
359 Stanger, F. V. *et al.* Intrinsic regulation of FIC-domain AMP-transferases by oligomerization and automodification. *Proceedings of the National Academy of Sciences* **113**, E529-E537 (2016). https://doi.org:doi:10.1073/pnas.1516930113
360 Engel, P. *et al.* Adenylylation control by intra- or intermolecular active-site obstruction in Fic proteins. *Nature* **482**, 107-110 (2012). https://doi.org:10.1038/nature10729
361 Muller, E. E., Fayemiwo, S. A. & Lewis, D. A. Characterization of a novel β-lactamase-producing plasmid in *Neisseria gonorrhoeae*: sequence analysis and molecular typing of host gonococci. *Journal of Antimicrobial Chemotherapy* **66**, 1514-1517 (2011). https://doi.org:10.1093/jac/dkr162
362 World Health Organization. *World Health Organization best practices for the naming of new human infectious diseases*, <https://www.who.int/publications/i/item/WHO-HSE-FOS-15.1> (2015).

363 Van Embden, J. D., Dessens-Kroon, M. & Van Klingeren, B. A new β-lactamase plasmid in *Neisseria gonorrhoeae*. *J Antimicrob Chemother* **15**, 247-250 (1985). https://doi.org:10.1093/jac/15.2.247
364 Brett, M. A novel gonococcal β-lactamase plasmid. *J Antimicrob Chemother* **23**, 653-654 (1989). https://doi.org:10.1093/jac/23.4.653
365 Agbodzi, B. *et al.* Whole genome analysis and antimicrobial resistance of Neisseria gonorrhoeae isolates from Ghana. *Frontiers in Microbiology* **Volume 14 - 2023** (2023). https://doi.org:10.3389/fmicb.2023.1163450
366 Unemo, M. *et al.* The novel 2024 WHO Neisseria gonorrhoeae reference strains for global quality assurance of laboratory investigations and superseded WHO N. gonorrhoeae reference strains-phenotypic, genetic and reference genome characterization. *J Antimicrob Chemother* **79**, 1885-1899 (2024). https://doi.org:10.1093/jac/dkae176
367 Miller, J. R., Koren, S. & Sutton, G. Assembly algorithms for next-generation sequencing data. *Genomics* **95**, 315-327 (2010). https://doi.org:10.1016/j.ygeno.2010.03.001
368 Salverda, M. L., De Visser, J. A. & Barlow, M. Natural evolution of TEM-1 β-lactamase: experimental reconstruction and clinical relevance. *FEMS Microbiol Rev* **34**, 1015-1036 (2010). https://doi.org:10.1111/j.1574-6976.2010.00222.x
369 Kather, I., Jakob, R. P., Dobbek, H. & Schmid, F. X. Increased folding stability of TEM-1 β-lactamase by in vitro selection. *J Mol Biol* **383**, 238-251 (2008). https://doi.org:10.1016/j.jmb.2008.07.082
370 Guiney, D. G., Jr. & Ito, J. I., Jr. Transfer of the gonococcal penicillinase plasmid: mobilization in Escherichia coli by IncP plasmids and isolation as a DNA-protein relaxation complex. *J Bacteriol* **150**, 298-302 (1982). https://doi.org:10.1128/jb.150.1.298-302.1982
371 Genco, C. A., Knapp, J. S. & Clark, V. L. Conjugation of plasmids of Neisseria gonorrhoeae to other Neisseria species: potential reservoirs for the beta-lactamase plasmid. *J Infect Dis* **150**, 397-401 (1984). https://doi.org:10.1093/infdis/150.3.397
372 Laufs, R. & Kaulfers, P. M. Molecular characterization of a plasmid specifying ampicillin resistance and its relationship to other R factors from Haemophilus influenzae. *J Gen Microbiol* **103**, 277-286 (1977). https://doi.org:10.1099/00221287-103-2-277
373 Heffron, F., Sublett, R., Hedges, R. W., Jacob, A. & Falkow, S. Origin of the TEM-beta-lactamase gene found on plasmids. *J Bacteriol* **122**, 250-256 (1975). https://doi.org:10.1128/jb.122.1.250-256.1975
374 Al-Tawfiq, J. A. & Spinola, S. M. Infections caused by Haemophilus ducreyi: one organism, two stories. *Clin Microbiol Rev*, e0013524 (2024). https://doi.org:10.1128/cmr.00135-24
375 Gangaiah, D. *et al. Haemophilus ducreyi* cutaneous ulcer strains are nearly identical to class I genital ulcer strains. *PLOS Neglected Tropical Diseases* **9**, e0003918 (2015). https://doi.org:10.1371/journal.pntd.0003918
376 Gangaiah, D. *et al. Haemophilus ducreyi* cutaneous ulcer strains are nearly identical to class I genital ulcer strains. *PLoS Negl Trop Dis* **9**, e0003918 (2015). https://doi.org:10.1371/journal.pntd.0003918
377 Yan, J., Zhang, J. & van der Veen, S. High prevalence of TEM-135 expression from the Asian plasmid in penicillinase-producing *Neisseria gonorrhoeae* from Hangzhou, China. *Int J Antimicrob Agents* **54**, 361-366 (2019). https://doi.org:10.1016/j.ijantimicag.2019.06.012
378 Micaëlo, M. *et al.* Molecular epidemiology of penicillinase-producing *Neisseria gonorrhoeae* isolates in France. *Clin Microbiol Infect* **23**, 968-973 (2017). https://doi.org:10.1016/j.cmi.2017.04.010
379 Kunimoto, D. Y. *et al.* Urethral infection with Haemophilus ducreyi in men. *Sex Transm Dis* **15**, 37-39 (1988).
380 Utter, D. R., Borisy, G. G., Eren, A. M., Cavanaugh, C. M. & Mark Welch, J. L. Metapangenomics of the oral microbiome provides insights into habitat adaptation and

cultivar diversity. *Genome Biol* **21**, 293 (2020). https://doi.org:10.1186/s13059-020-02200-2

381 Barza, M. & Weinstein, L. Pharmacokinetics of the penicillins in man. *Clin Pharmacokinet* **1**, 297-308 (1976). https://doi.org:10.2165/00003088-197601040-00004

382 Engelund, A., Terp, P. & Trolle-Lassen, C. Studies on renal excretion of tetracycline. *Acta Pharmacol Toxicol (Copenh)* **12**, 227-232 (1956). https://doi.org:10.1111/j.1600-0773.1956.tb01381.x

383 Retchless, A. C. *et al.* Expansion of a urethritis-associated Neisseria meningitidis clade in the United States with concurrent acquisition of N. gonorrhoeae alleles. *BMC Genomics* **19**, 176 (2018). https://doi.org:10.1186/s12864-018-4560-x

384 Bazan, J. A. *et al.* Antibiotic Susceptibility Profile for the US Neisseria meningitidis Urethritis Clade. *Open Forum Infect Dis* **10**, ofac661 (2023). https://doi.org:10.1093/ofid/ofac661

385 Statement on treatment of gonorrhea--penicillin is passe. Committee on Public Health. The New York Academy of Medicine. *Bull N Y Acad Med* **65**, 243-246 (1989).

386 EUCAST. *Breakpoint tables for interpretation of MICs and zone diameters. Version 14.0*, <http://www.eucast.org.> (2024).

387 von Heijne, G. The signal peptide. *J Membr Biol* **115**, 195-201 (1990). https://doi.org:10.1007/bf01868635

388 Paetzel, M. Structure and mechanism of Escherichia coli type I signal peptidase. *Biochim Biophys Acta* **1843**, 1497-1508 (2014). https://doi.org:10.1016/j.bbamcr.2013.12.003

389 Kaderabkova, N. *et al.* The biogenesis of β-lactamase enzymes. *Microbiology (Reading)* **168** (2022). https://doi.org:10.1099/mic.0.001217

390 Inouye, S. *et al.* Role of positive charge on the amino-terminal region of the signal peptide in protein secretion across the membrane. *Proc Natl Acad Sci U S A* **79**, 3438-3441 (1982). https://doi.org:10.1073/pnas.79.11.3438

391 Dimitriu, T., Matthews, A. C. & Buckling, A. Increased copy number couples the evolution of plasmid horizontal transmission and plasmid-encoded antibiotic resistance. *Proc Natl Acad Sci U S A* **118** (2021). https://doi.org:10.1073/pnas.2107818118

392 Matlock, W. *et al.* E. coli phylogeny drives co-amoxiclav resistance through variable expression of blaTEM-1. *bioRxiv*, 2024.2008.2012.607562 (2024). https://doi.org:10.1101/2024.08.12.607562

393 DelaFuente, J., Diaz-Colunga, J., Sanchez, A. & San Millan, A. Global epistasis in plasmid-mediated antimicrobial resistance. *Mol Syst Biol* (2024). https://doi.org:10.1038/s44320-024-00012-1

394 Florensa, A. F., Kaas, R. S., Clausen, P., Aytan-Aktug, D. & Aarestrup, F. M. ResFinder - an open online resource for identification of antimicrobial resistance genes in next-generation sequencing data and prediction of phenotypes from genotypes. *Microb Genom* **8** (2022). https://doi.org:10.1099/mgen.0.000748

395 Gotschlich, E. C., Seiff, M. E., Blake, M. S. & Koomey, M. Porin protein of Neisseria gonorrhoeae: cloning and gene structure. *Proc Natl Acad Sci U S A* **84**, 8135-8139 (1987). https://doi.org:10.1073/pnas.84.22.8135

396 Olesky, M., Hobbs, M. & Nicholas, R. A. Identification and analysis of amino acid mutations in porin IB that mediate intermediate-level resistance to penicillin and tetracycline in Neisseria gonorrhoeae. *Antimicrob Agents Chemother* **46**, 2811-2820 (2002). https://doi.org:10.1128/aac.46.9.2811-2820.2002

397 Kivata, M. W. *et al.* Plasmid mediated penicillin and tetracycline resistance among *Neisseria gonorrhoeae* isolates from Kenya. *BMC Infectious Diseases* **20** (2020). https://doi.org:10.1186/s12879-020-05398-5

398 Qin, X. L. *et al.* Emerging epidemic of the Africa-type plasmid in penicillinase-producing Neisseria gonorrhoeae in Guangdong, China, 2013-2022. *Emerg Microbes Infect* **14**, 2440489 (2025). https://doi.org:10.1080/22221751.2024.2440489
399 Carannante, A. *et al.* Seven Years of Culture Collection of Neisseria gonorrhoeae: Antimicrobial Resistance and Molecular Epidemiology. *Microbial Drug Resistance* **29**, 85-95 (2023). https://doi.org:10.1089/mdr.2021.0483
400 Taylor, S. C., Laperriere, G. & Germain, H. Droplet Digital PCR versus qPCR for gene expression analysis with low abundant targets: from variable nonsense to publication quality data. *Scientific Reports* **7**, 2409 (2017). https://doi.org:10.1038/s41598-017-02217-x
401 Lenski, R. E., Rose, M. R., Simpson, S. C. & Tadler, S. C. Long-Term Experimental Evolution in Escherichia coli. I. Adaptation and Divergence During 2,000 Generations. *The American Naturalist* **138**, 1315-1341 (1991). https://doi.org:10.1086/285289
402 Biswas, G. D., Blackman, E. Y. & Sparling, P. F. High-frequency conjugal transfer of a gonococcal penicillinase plasmid. *J Bacteriol* **143**, 1318-1324 (1980). https://doi.org:10.1128/jb.143.3.1318-1324.1980
403 Baron, E. S., Saz, A. K., Kopecko, D. J. & Wohlhieter, J. A. Transfer of plasmid-borne β-lactamase in *Neisseria gonorrhoeae*. *Antimicrobial Agents and Chemotherapy* **12**, 270-280 (1977). https://doi.org:10.1128/aac.12.2.270
404 Freitag, N. E., Seifert, H. S. & Koomey, M. Characterization of the pilF-pilD pilus-assembly locus of Neisseria gonorrhoeae. *Mol Microbiol* **16**, 575-586 (1995). https://doi.org:10.1111/j.1365-2958.1995.tb02420.x
405 Huisman, J. S. *et al.* Estimating plasmid conjugation rates: A new computational tool and a critical comparison of methods. *Plasmid* **121**, 102627 (2022). https://doi.org:10.1016/j.plasmid.2022.102627
406 Getino, M. & de la Cruz, F. Natural and Artificial Strategies To Control the Conjugative Transmission of Plasmids. *Microbiol Spectr* **6** (2018). https://doi.org:10.1128/microbiolspec.MTBP-0015-2016
407 Sarafian, S. K., Genco, C. A., Roberts, M. C. & Knapp, J. S. Acquisition of beta-lactamase and TetM-containing conjugative plasmids by phenotypically different strains of Neisseria gonorrhoeae. *Sex Transm Dis* **17**, 67-71 (1990). https://doi.org:10.1097/00007435-199004000-00004
408 Zhang, S. & Meyer, R. The relaxosome protein MobC promotes conjugal plasmid mobilization by extending DNA strand separation to the nick site at the origin of transfer. *Mol Microbiol* **25**, 509-516 (1997). https://doi.org:10.1046/j.1365-2958.1997.4861849.x
409 Klein, E. Y. *et al.* Global trends in antibiotic consumption during 2016-2023 and future projections through 2030. *Proc Natl Acad Sci U S A* **121**, e2411919121 (2024). https://doi.org:10.1073/pnas.2411919121
410 Peña-Miller, R., Rodríguez-González, R., MacLean, R. C. & San Millan, A. Evaluating the effect of horizontal transmission on the stability of plasmids under different selection regimes. *Mob Genet Elements* **5**, 1-5 (2015). https://doi.org:10.1080/2159256x.2015.1045115
411 Arber, W. & Morse, M. L. Host specificity of DNA produced by Escherichia Coli. VI. Effects on bacterial conjugation. *Genetics* **51**, 137-148 (1965). https://doi.org:10.1093/genetics/51.1.137
412 Chmiel, A. A. *et al.* A theoretical model of restriction endonuclease NlaIV in complex with DNA, predicted by fold recognition and validated by site-directed mutagenesis and circular dichroism spectroscopy. *Protein Engineering, Design and Selection* **18**, 181-189 (2005). https://doi.org:10.1093/protein/gzi019
413 Stoltzfus, J. C. Logistic regression: a brief primer. *Acad Emerg Med* **18**, 1099-1104 (2011). https://doi.org:10.1111/j.1553-2712.2011.01185.x

414 Sperandei, S. Understanding logistic regression analysis. *Biochem Med (Zagreb)* **24**, 12-18 (2014). https://doi.org:10.11613/bm.2014.003
415 Carugo, O. & Pongor, S. A normalized root-mean-spuare distance for comparing protein three-dimensional structures. *Protein Science* **10**, 1470-1473 (2001). https://doi.org:https://doi.org/10.1110/ps.690101
416 Maiorov, V. N. & Crippen, G. M. Significance of root-mean-square deviation in comparing three-dimensional structures of globular proteins. *J Mol Biol* **235**, 625-634 (1994). https://doi.org:10.1006/jmbi.1994.1017
417 Qiang, B. Q. & Schildkraut, I. Two unique restriction endonucleases from Neisseria lactamica. *Nucleic Acids Res* **14**, 1991-1999 (1986). https://doi.org:10.1093/nar/14.5.1991
418 Czapinska, H. *et al.* Crystal Structure and Directed Evolution of Specificity of NlaIV Restriction Endonuclease. *J Mol Biol* **431**, 2082-2094 (2019). https://doi.org:10.1016/j.jmb.2019.04.010
419 Orlowski, J. & Bujnicki, J. M. Structural and evolutionary classification of Type II restriction enzymes based on theoretical and experimental analyses. *Nucleic Acids Research* **36**, 3552-3569 (2008). https://doi.org:10.1093/nar/gkn175
420 Steczkiewicz, K., Muszewska, A., Knizewski, L., Rychlewski, L. & Ginalski, K. Sequence, structure and functional diversity of PD-(D/E)XK phosphodiesterase superfamily. *Nucleic Acids Res* **40**, 7016-7045 (2012). https://doi.org:10.1093/nar/gks382
421 Pingoud, A. & Jeltsch, A. Structure and function of type II restriction endonucleases. *Nucleic Acids Research* **29**, 3705-3727 (2001). https://doi.org:10.1093/nar/29.18.3705
422 Schubert, H. L., Blumenthal, R. M. & Cheng, X. Many paths to methyltransfer: a chronicle of convergence. *Trends Biochem Sci* **28**, 329-335 (2003). https://doi.org:10.1016/s0968-0004(03)00090-2
423 Rao, D. N., Saha, S. & Krishnamurthy, V. ATP-dependent restriction enzymes. *Prog Nucleic Acid Res Mol Biol* **64**, 1-63 (2000). https://doi.org:10.1016/s0079-6603(00)64001-1
424 Murray, N. E. Type I restriction systems: sophisticated molecular machines (a legacy of Bertani and Weigle). *Microbiol Mol Biol Rev* **64**, 412-434 (2000). https://doi.org:10.1128/mmbr.64.2.412-434.2000
425 Siedentop, B., Losa Mediavilla, C., Kouyos, R. D., Bonhoeffer, S. & Chabas, H. Assessing the Role of Bacterial Innate and Adaptive Immunity as Barriers to Conjugative Plasmids. *Molecular Biology and Evolution* **41** (2024). https://doi.org:10.1093/molbev/msae207
426 Cole, M. J. *et al.* The European gonococcal antimicrobial surveillance programme (Euro-GASP) appropriately reflects the antimicrobial resistance situation for Neisseria gonorrhoeae in the European Union/European Economic Area. *BMC Infect Dis* **19**, 1040 (2019). https://doi.org:10.1186/s12879-019-4631-x
427 Kersh, E. N. *et al.* Expanding U.S. Laboratory Capacity for Neisseria gonorrhoeae Antimicrobial Susceptibility Testing and Whole-Genome Sequencing through the CDC's Antibiotic Resistance Laboratory Network. *J Clin Microbiol* **58** (2020). https://doi.org:10.1128/jcm.01461-19
428 Martín-Sánchez, M. *et al.* Clinical presentation of asymptomatic and symptomatic women who tested positive for genital gonorrhoea at a sexual health service in Melbourne, Australia. *Epidemiology and Infection* **148**, 1-18 (2020). https://doi.org:10.1017/s0950268820002265
429 Pagotto, F. *et al.* Sequence analysis of the family of penicillinase-producing plasmids of Neisseria gonorrhoeae. *Plasmid* **43**, 24-34 (2000). https://doi.org:10.1006/plas.1999.1431
430 Unitt, A. *et al. Neisseria gonorrhoeae* LIN codes: a Robust, Multi-Resolution Lineage Nomenclature. *bioRxiv*, 2025.2003.2028.646058 (2025). https://doi.org:10.1101/2025.03.28.646058
431 Jain, A. & Srivastava, P. Broad host range plasmids. *FEMS Microbiol Lett* **348**, 87-96 (2013). https://doi.org:10.1111/1574-6968.12241

432 Swartley, J. S., McAllister, C. F., Hajjeh, R. A., Heinrich, D. W. & Stephens, D. S. Deletions of Tn916-like transposons are implicated in tetM-mediated resistance in pathogenic Neisseria. *Mol Microbiol* **10**, 299-310 (1993). https://doi.org:10.1111/j.1365-2958.1993.tb01956.x

433 Scharbaai-Vazquez, R., Gonzalez-Caraballo, A. L. & Torres-Bauza, L. J. Four different integrative recombination events involved in the mobilization of the gonococcal 5.2 kb beta-lactamase plasmid pSJ5.2 in Escherichia coli. *Plasmid* **60**, 200-211 (2008). https://doi.org:10.1016/j.plasmid.2008.07.004

434 Zatyka, M. & Thomas, C. M. Control of genes for conjugative transfer of plasmids and other mobile elements. *FEMS Microbiology Reviews* **21**, 291-319 (1998). https://doi.org:10.1111/j.1574-6976.1998.tb00355.x

435 Bachmann, L. H. *et al.* CDC Clinical Guidelines on the Use of Doxycycline Postexposure Prophylaxis for Bacterial Sexually Transmitted Infection Prevention, United States, 2024. *MMWR Recomm Rep* **73**, 1-8 (2024). https://doi.org:10.15585/mmwr.rr7302a1

436 Hornuss, D. *et al.* Already current practice? A snapshot survey on doxycycline use for prevention of sexually transmitted infections in parts of the German MSM community. *Infection* **51**, 1831-1834 (2023). https://doi.org:10.1007/s15010-023-02086-9

437 Chan, P. A. *et al.* Early adopters of doxycycline as post-exposure prophylaxis to prevent bacterial sexually transmitted infections in a real-world clinical setting. *Sex Transm Infect* **100**, 339-342 (2024). https://doi.org:10.1136/sextrans-2024-056152

438 Holt, M. *et al.* Acceptability of Doxycycline Prophylaxis, Prior Antibiotic Use, and Knowledge of Antimicrobial Resistance Among Australian Gay and Bisexual Men and Nonbinary People. *Sex Transm Dis* **52**, 73-80 (2025). https://doi.org:10.1097/olq.0000000000002079

439 Traeger, M. W., Krakower, D. S., Mayer, K. H., Jenness, S. M. & Marcus, J. L. Use of Doxycycline and Other Antibiotics as Bacterial Sexually Transmitted Infection Prophylaxis in a US Sample of Primarily Gay and Bisexual Men. *Sex Transm Dis* **51**, 763-771 (2024). https://doi.org:10.1097/olq.0000000000002061

440 Budroni, S. *et al.* Neisseria meningitidis is structured in clades associated with restriction modification systems that modulate homologous recombination. *Proc Natl Acad Sci U S A* **108**, 4494-4499 (2011). https://doi.org:10.1073/pnas.1019751108

441 Wang, X. *et al.* Multiple-Replicon Resistance Plasmids of Klebsiella Mediate Extensive Dissemination of Antimicrobial Genes. *Front Microbiol* **12**, 754931 (2021). https://doi.org:10.3389/fmicb.2021.754931

442 Firth, N., Jensen, S. O., Kwong, S. M., Skurray, R. A. & Ramsay, J. P. Staphylococcal Plasmids, Transposable and Integrative Elements. *Microbiology Spectrum* **6**, 10.1128/microbiolspec.gpp1123-0030-2018 (2018). https://doi.org:doi:10.1128/microbiolspec.gpp3-0030-2018

443 Sánchez-Busó, L. *et al.* The impact of antimicrobials on gonococcal evolution. *Nat Microbiol* **4**, 1941-1950 (2019). https://doi.org:10.1038/s41564-019-0501-y

444 Lynn, F. *et al.* Genetic typing of the porin protein of Neisseria gonorrhoeae from clinical noncultured samples for strain characterization and identification of mixed gonococcal infections. *J Clin Microbiol* **43**, 368-375 (2005). https://doi.org:10.1128/jcm.43.1.368-375.2005

445 Unemo, M. & Shafer, W. M. Antibiotic resistance in Neisseria gonorrhoeae: origin, evolution, and lessons learned for the future. *Ann N Y Acad Sci* **1230**, E19-28 (2011). https://doi.org:10.1111/j.1749-6632.2011.06215.x